DTU Library

New approaches to [^{18}F]fluoride recovery and radiofluorination

Mathiessen, Bente Ingemann; Zhuravlev, Fedor; Jensen, Mikael
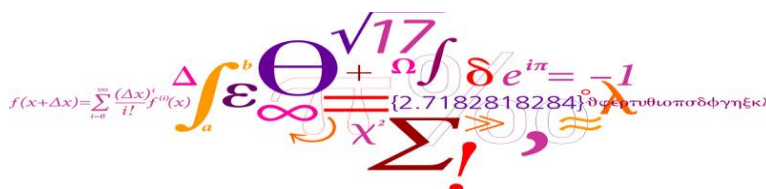
Link back to DTU Orbit

New approaches to [^{18}F]fluoride recovery and radiofluorination

Ph.D. Thesis by

Bente Ingemann Mathiessen

April 2015

The Hevesy Laboratory, Center for Nuclear Technologies, DTU

Preface

This thesis covers the work conducted through my three years as a Ph.D. student at the Hevesy Laboratory, DTU Nutech (Center for Nuclear Technologies, Technical University of Denmark), Risø Campus under the supervision of Dr. Fedor Zhuravlev and Professor Mikael Jensen at the Hevesy Laboratory. My work has focused on the development of new radiofluorination methodologies aiming at *simplification* and *versatility*.

This work is presented here, in four individual chapters. Chapter 2 is a general introduction to PET imaging and PET radiochemistry. Chapter 3 describes the advances in radiofluorination and thereby some solutions to the challenges facing radiochemists when working with radiofluorination. Chapters 2 and 3 constitute the foundation of chapters 4 and 5, which contain descriptions of our work concerning the development of a homogeneous and heterogeneous radiofluorination methodology, respectively.

Acknowledgements

When thinking of the people, who have assisted, supported and guided me through the Ph.D. years at Hevesy a great number of people comes to mind. The first and foremost is Fedor Zhuravlev, my main supervisor. It has been a privilege to work together with a person who is so driven and such a formidable chemist. His ambitions on my behalf were as inspiring as they were overwhelming. Prof. Mikael Jensen has served as a constant source of encouragement and his comprehensive knowledge of everything that is radiochemistry and PET has greatly facilitated my work.

I also wish to thank the production team at Hevesy for meeting my unquenchable thirst for target water and for assisting me whenever necessary, be it in terms of either chemicals or equipment knowledge, and for always providing a positive working atmosphere. Dr. Sorin Aburel deserves special credit for helping me on all matters related to [^{18}F]FDG, and laboratory technician Mette Munch for assisting me in a period where my own two hands were not enough; you have helped me tremendously!

Moreover, I am incredibly grateful to my fellow Ph.D. students with emphasis on Martin H. F. Pedersen, Evgeny Revunov and Pil Fredericia for always supporting me in scientific matters as well as making our often long hard days at work so much more enjoyable.

And Hedi Sønneland Pedersen, the slip saying "It will work out just fine", which you gave me when dealing with a troublesome week of [^{18}F]FDG productions has ever since attached to my monitor, serving as my mantra. I thank you for that and for several very enjoyable evenings with you, the two of us splitting a beer in the prospect of a FDG shift together the following day.

During the first half of my time at Hevesy, this place was more or less my home, and that was only passable because of the wonderful people working here. There is always someone to go to, be it for personal talks or professional discussions. The warm and welcoming atmosphere at this place is incredible! It became clearer than ever when I suffered a great loss in my family. The support I experienced from Hevesy is the main reason why I was able to continue and may now present this paper. I thank you all!

Finally, I want to thank my family and friends for believing in me and especially my husband Michael I. Hansen for stepping into my life and showing me what the meaning of it all is, for the interest in my work, for constant encouragement and for keeping me focused. I hope I can someday repay you!

Publications

Article I:

Mathiessen, B.; Jensen, M.; Zhuravlev, F. [^{18}F]Fluoride Recovery via Gaseous [18F]HF. *J. Label. Compd. Radiopharm.* **2011**, *54* (13), 816–818

Article II:

Mathiessen, B.; Jensen, A. T. I.; Zhuravlev, F. Homogeneous Nucleophilic Radiofluorination and Fluorination with Phosphazene Hydrofluorides. *Chemistry A European Journal* **2011**, *17* (28), 7796–7805

Article III:

Mathiessen, B.; Zhuravlev, F. Automated Solid-Phase Radiofluorination Using Polymer-Supported Phosphazenes. *Molecules* **2013**, *18* (9), 10531–10547

Article IV:

Mathiessen, B.; Severin, G.; Zhuravlev, F. Towards Automated Solid Phase Radiofluorination for Dose-on-Demand PET: Retention of Activity by Solid Support. *Radiochim. Acta* **2015**, *103* (3), 227–232

Patent:

Zhuravlev, F.; **Mathiessen, B.** Radiofluorination Method. PCT Patent application: WO2014020035A1, pp. 39, 16 claims, 3 drawings.

List of abbreviations and acronyms

AMPS	Aminomethyl polystyrene
ATSM	Diacetyl-bis[N^4-methylthiosemicarbazone
BEMP	2-*tert*-Butylimino-2-diethylamino-1,3-dimethylperhydro-1,3,2-diazaphosphorine
BGO	Bismuth germinate
BTMG	N-*t*butyl-*N,N,N ,N* -tetramethylguanidine
CA	Carrier added
DBN	1,5-Diazabicyclo[4.3.0]non-5-ene
DBU	1,8-Diazabicycloundec-7-ene
DC	Decay corrected
DCM	Dichloromethane
DMF	Dimethylformamide
DMSO	Dimethylsulphoxide
DoD	Dose-on-demand
DOTA	1,4,7,10-tetraazacyclododecane-1,4,7,10-tetraacetic acid
EF5	2-(2-nitro-[1]H-imidazol-1-yl)-*N*-(2,2,3,3,3-pentafluoropropyl)-acetamide
EWG	Electron-withdrawing group
FAZA	1-(5-fluoro-5-deoxy-α-D-arabinofuranosyl)-2-nitroimidazole
FDG	Fluorodeoxyglucose
FDOPA	3,4-dihydroxy-6-fluoro-L-phenylalanine
FES	16α-Fluorestradiol
FLM	Flutemetamol
FLT	3′-deoxy-3′-fluorothymidine
FMISO	Fluoromisonidazole
GMP	Good manufacturing practice
GW	Glass wool
HF	Hydrogen fluoride
HPLC	High Performance Liquid Chromatography
IL	Ionic liquid
K222	Kryptofix 2.2.2
LG	Leaving group
LOR	Line of response
LSO	Lutetium oxy-orthosilicate
MeCN	Acetonitrile
Mes	Mesitylene
Min	Minutes

MTBD	7-Methyl-1,5,7-triazabicyclo(4.4.0)dec-5-ene
NCA	Non carrier added
PE	Polyethylene
PEG	Polyethylene glycol
PET	Positron Emission Tomography
PMT	Photomultiplier tube
PS	Polymer-supported
PTSM	Pyruvaldehyde bis(N^4-methylthiosemicarbazone)
QC	Quality control
RCP	Radiochemical purity
RCY	Radiochemical yield
RGD	Arginine-glycine-aspartic acid
rt	Room temperature
rTLC	Radiolabeled thin-layer chromatography
SA	Specific activity
Sec	Seconds
SPE	Solid-phase extraction
SPOS	Solid-phase organic synthesis
SPPS	Solid-phase peptide synthesis
TA	Trapping agent
TBAB	Tetrabutylammonium bicarbonate
TBG	Triazabicyclodecene
THF	Tetrahydrofurane
tmeu	Tetramethulurea
TMGN	1,8-bis(tetramethylguanidino)naphthalene
TOC	[Tyr^3]-Octreotide
TREAT-HF	Triethylamine tris(hydrogen fluoride)
uDC	Un-decay corrected
VBA	Vinylbenzylamine
VBAH	Vinylbenzylamine hydrochloride

Abstract and outline

Positron Emission Tomography (PET) imaging is a technique for visualization of physiological processes in the body, which finds applications in more and more medical fields as well as in the area of drug development. The development of new radiopharmaceuticals to meet this demand is significant. It seems, however, that a bottleneck has formed in the shape of the radiochemistry providing these radiopharmaceuticals. Especially within radiofluorination the conventional methods used today are not very versatile, which results in extensive synthetic procedures and low radiochemical yields (RCY). The purpose of this Ph.D. project was to develop new radiofluorination methods that are not only simple when it comes to setup and purifications but also versatile with regard to both substrates and reaction conditions. The work towards achieving this is described in this thesis.

Chapter 1 presents an outline of PET radiochemistry including my personal reflection on the subject. **Chapter 2** is a general description of PET imaging and PET radiochemistry. In this chapter, the standard radiofluorination procedures are described from the production of ^{18}F, restoration of its intrinsic nucleophilicity to the labeling processes of both aliphatic and aromatic substrates. The challenges faced when working with radiofluorination are also described. **Chapter 3** covers the work that has and is being done in order to overcome these challenges and achieve greater substrate versatility and a more expeditious process. It reflects how ionic liquid or tertiary alcohols as well as complexation to aluminum or mediation through transition-metal catalysts have all shown to be beneficial when it comes to radiofluorination. **Chapter 4** deals with our development of a homogeneous fluorination and radiofluorination protocol based on phosphazene hydrofluorides. Phosphazene bases are some of the strongest organic non-ionic bases available and the complexation between them and hydrogen fluoride has proved to be a very efficient source of nucleophilic fluoride. We demonstrate how the azeotropic evaporation step can be obviated as [^{18}F]F$^-$ is extracted from aqueous solution as gaseous [^{18}F]HF and then trapped by the Schwesinger base as [^{18}F]phosphazenium hydrofluorides. Subsequently we have shown how this complex is able to label a wide variety of substrates in both a short time and in both polar and nonpolar solvents. It performed on par with conventional labeling systems when it came to pseudohalides, but when it came to lipophilic substrates this procedure resulted in significantly better RCYs.

With this knowledge in hand we turned to solid-phase radiofluorination based on polymer-supported phosphazene bases. You will find this described in **Chapter 5**. In this we demonstrate how polymer-supported phosphazene bases efficiently extract $[^{18}F]F^-$ from the aqueous solution and how radiofluorination can be carried out directly on the resin. The advantage of this approach is two-fold. One, you benefit from the general advantages of solid-phase synthesis, which are that all additives and solvents can readily be washed away with resulting simplification of the product purification step. Two, the resin can be reused several times with the same or different substrates, which may be advantageous with regard to the development of single-dose radiotracer production. One obstacle we faced was a difficulty in achieving RCYs much higher than 60%, and the reason for that was further analyzed. It appeared that we were facing a physical entrapment of nucleophilically active $[^{18}F]$fluoride within the polymer matrix. The first steps towards solving this by working with different kinds of solid support have been done with mixed results.

Resume (Dansk)

Positron Emissions Tomografi (PET) er en teknik til visualisering af fysiologiske processer i kroppen, som finder anvendelse indenfor et voksende antal lægevidenskabelige felter samt indenfor udviklingen af nye lægemidler. For at imødekomme denne stigende interesse er udviklingen af radioaktive sporstoffer til PET undersøgelser inde i en rivende udvikling. Desværre er radiokemien af og til en hæmsko for udviklingen af disse sporstoffer. Især indenfor radiofluorering er der store udfordringer, da standardmetoderne sætter begrænsninger for udvalget af solventer og substrater, hvormed resultatet er meget omfattende syntetiske procedurer, der ofte resulterer i et lavt radiokemisk udbytte. Formålet med dette Ph.D. projekt var at udvikle nye radiofluoreringsmetoder, der er simple med hensyn til udstyr og oprensning og alsidig når det kommer til udgangsstoffer og reaktionsbetingelser. Arbejdet, der har været udført i forbindelse med dette projekt, er beskrevet i denne afhandling.

Kapitel 1 er et hurtigt indblik i PET radiokemien inklusive mine personlige refleksioner i den forbindelse. **Kapitel 2** er en generel beskrivelse af PET imaging og PET radiokemi. De klassiske radiofluoreringsmetoder bliver gennemgået herunder ^{18}F produktion, gendannelse af isotopens nukleofilicitet samt mærkning af både alifatiske og aromatiske stoffer. Sideløbende beskrives de udfordringer som den klassiske teknik resulterer i. **Kapitel 3** dækker den udvikling, der sker indenfor radiofluorering, for at imødekomme netop de udfordringer og derved opnå en hurtigere proces, der kan anvendes til en væsentligt bredere vifte af udgangsstoffer. Ioniske væsker eller tertiære alkoholer samt aluminiumkomplekser eller overgangsmetalkatalyse har alle vist sig at være brugbare værktøjer. **Kapitel 4** er en beskrivelse af udviklingen af vores homogene fluorerings- og radiofluoreringsmetode der er baseret på phosphazen hydrofluorider. Schwesingers phosphazen baser er blandt de stærkeste non-ioniske baser der findes og vores studier viser at komplekset med hydrogenfluorid er en kilde til yderst reaktivt nucleofil fluorid. Vi illustrerer, hvordan azeotrop destillation kan undgås ved at ekstrahere $[^{18}F]F^-$ fra den vandige opløsning som gasformig $[^{18}F]HF$, som bliver fanget af Schwesinger basen som $[^{18}F]$phosphazen hydrofluorid. Dette kompleks, påviser vi, er i stand til at mærke en bred vifte af udgangsstoffer både på kort tid og i både polære og upolære solventer. Mærkningsgraden for pseudohalider var på niveau med de konventionelle metoder, mens den for lipofile udgangsstoffer var

væsentligt bedre. Med denne viden i baghånden vendte vi os mod udviklingen af en fastfase radiofluoreringsmetode baseret på polymer-bundne phosphazen baser. Dette arbejde er beskrevet i **kapitel 5**. Her viser vi, hvordan polymer-bundne phosphazen baser effektivt ekstraherer $[^{18}F]F^-$ fra vandig opløsning, samt hvordan mærkning af udgangsstoffer kan foretages direkte på polymeren med rigtigt gode radiokemiske udbytter. Fordelen ved denne metode er todelt. Dels opnås de fordele, som ses ved konventionel fastfasesyntese, hvilket er at alle additiver og solventer let kan vaskes af søjlen. Dette resulterer i kraftig forenkling af oprensningen af produktet. Dels kan polymeren genbruges flere gange med samme eller andre udgangsstoffer, hvilket kan være en fordel i udviklingen af enkelt-dosis sporstofproduktion. Under arbejdet med fastfase radiofluoreringen måtte vi til stadighed erkende, at vi ikke var i stand til at få mærkningsgraden meget over 60%. Grunden til dette analyserede vi yderligere for at afgøre, om der var en løsningsmulighed. Det viste sig at $[^{18}F]F^-$ er fysisk fanget i en nucleofil reaktiv tilstand i den polymere matrix. Dette er med blandede resultater forsøgt løst ved at anvende andre polymerer.

Table of Contents

Chapter 1   Outlook

1.1 PET radiochemistry

Positron Emission Tomography (PET) imaging is a medical field that experiences an exceptional progress in both research and clinical use. The number of scans performed in the USA in 2004 was about 900,000 and has grown to 1.74 million by 2010. It is very similar in Denmark where the increase was from about 5,000 scans in 2004 to around 17,000 in 2010. A vast majority of these scans are performed with tracers labeled with the radionuclide fluorine-18 $[^{18}F]$, due to its many desirable properties that lead to excellent PET scan resolution and sensitivity. At the same time the half-life of fluorine-18 (110min) allows for production, synthesis and purification of the radiotracer and subsequent delivery from the production site (the radiopharmacy) to nearby PET centers, where the PET tracer is administered to the patients.

2-Deoxy-2-$[^{18}F]$fluoro-D-glucose ($[^{18}F]$FDG) is the work horse in PET as more than 90% of all PET scans are performed with this molecule. The history of $[^{18}F]$FDG illustrates very well the development that has happened in the field of PET radiochemistry. The first dose of $[^{18}F]$FDG was synthesized in Brookhaven in 1976 through an electrophilic addition of $[^{18}F]F_2$ to triacetylglucal. The reaction and following workup took two hours and the radiochemical yield (RCY)was about 8%. Over the years the development of an approach based on nucleophilic substitution of a "good leaving group" using nucleophilically active $[^{18}F]F^-$ as well as the shift from HPLC to solid phase extraction purification has now provided us with a synthetic protocol that gives $[^{18}F]$FDG in less than 30 minutes and with RCY above 50%. The brilliance of $[^{18}F]$FDG is that it is included in the glucose metabolism until it is inside the cell and phosphorylated by hexokinase. At this stage the molecule is trapped inside the cell as the next enzyme in the metabolic pathway (1,6-phosphoglucose isomerase) distinguishes between glucose and 2-deoxyglucose. This trapping effect combined with the increased need for glucose of

proliferating cells has made $[^{18}F]$FDG highly applicable within the fields of neurology and - especially - oncology.

The outcome from a single standard production of $[^{18}F]$FDG, now called the "molecule of the millennium", can supply doses for as many as 15 patients. The benefit of making multiple doses at a time is that the extensive cost of establishing and running a PET radiopharmacy, which has huge equipment requirements and highly trained personnel, can be spread over as many costumers as possible, making the price for one dose affordable. The downside, however, is that the radiotracer production is very inflexible. It is not financially advantageous to produce the small batches of tracers that is used for research and development of new products. The outcome is that the number of tracers that are available is not even close in matching the diversity of disciplines or biological problems for which a PET tracer could be relevant.

A huge effort is put into improving and simplifying the production of radiofluorinated radiotracers in order to speed up the production and make it more versatile. Automated cassette-based synthesizers are achieving just that. These systems require a disposable cassette that contains the fluid path (tubings, valves, vessels) and a set of reagents for both synthesis and purification. The cassette and reagents are mounted on a platform that carries out the synthesis in a robot-like manner. This setup ensures a standardized and reliable production at a low price due to the mass-manufacturable design of the cassettes. Another improvement for the speed-up of the PET tracer production is the change from HPLC to solid-phase extraction (SPE) cartridges for the purification of the tracers, which reduces workup time considerably. An example of an entirely different approach is miniaturized kit-based systems based on microfluidics, where the manufacturing cost is reduced by integrating all needed components on chips as small as a coin. This microscale system provides patient-size doses in a benchtop-size solution that offer the same integrated radiochemistry possibilities as the automated macroscale setup does.

The chemistry also has to accommodate the requirements for an expeditious synthetic strategy that can be implemented in microscale systems and a major obstacle in achieving this is the conventional $[^{18}F]F^-$ drying process. Many methods that aim at avoiding this drying step have been described, which include electrochemical separation, radiofluorination in ionic liquid and inorganic or transition-metal-

mediated approaches. But several of these struggle with the removal of additives or residual solvents, limited solvent options, harsh reaction conditions or long reaction times.

1.2 Personal outlook

I learned about radiochemistry and nuclear imaging during my third year as a medicinal chemistry student at Aarhus University. I was allowed to do my bachelor project at the PET Center at Aarhus Hospital, where I worked with the synthesis of a possible α_2 adrenoreceptor ligand. I was hooked, which resulted in a project carried out at the Department of Nuclear Medicine at Aarhus Hospital regarding the synthesis of ^{99m}Tc-EDDA/HYNIC-TOC and later my Master Thesis, which aimed at the radiolabeling and PEGylation of a protein with affinity for apoptotic cells. I returned to PET radiochemistry when I got employed at the Hevesy Laboratory, DTU Risø Campus and started working with radiofluorination, the work that has resulted in this PhD thesis. The thing that intrigues me in radiochemistry and radiofluorination in particular is that the work scopes and criteria for success are totally different compared to standard organic chemistry. The synthetic tool box is very different as you have a stoichiometric mismatch as well as a strict timeline due to the half-life of ^{18}F. The toolbox, however, does not seem to match the interest in new radiofluorinated tracers and you are often left with long multistep synthetic approaches, low RCYs and finally a radiotracer that has to go through an extensive purification step due to additives, products from side-reactions and solvents that do not comply with human administration. During this study I have worked with promising new tools for the toolbox, which has already been beneficial for the daily work with radiotracers at the laboratory. Also the possibility that this work can be a step towards increased accessibility of PET radiotracer production due to simplification of the procedure is very rewarding.

Chapter 2   PET imaging and PET radiochemistry

2.1 Introduction

Since Michael E. Phelps and Edward J. Hoffman in 1973 began working on the first PET scanner, PET imaging has marked the change from anatomical imaging to imaging of biological processes in the body. It has thereby become the fastest growing diagnostic specialty and in the field of oncology in particular, it is no longer possible to practice the "highest standard" without access to PET[1,2]. PET imaging is routinely used in three areas of clinical diagnostics and management (Figure 2-1)[2]:

1. Cancer diagnostics

   - Diagnosis of malignancy

   - Grading malignancy

   - Staging disease

   - Residual disease

   - Detection of recurrences

   - Measuring response to therapy

2. Cardiology and cardiac surgery

   - Measuring myocardial perfusion

   - Measuring myocardial viability

3. Neurology and psychiatry

   - Pre-surgical evaluation of epilepsy

   - Early diagnosis of dementias

The PET imaging agent, also called the radiopharmaceutical or radiotracer, is a molecule with a specific biological activity, which is labeled with a positron-emitting nuclide. The radiotracer is then administered, often intravenously, to the patient. The distribution and accumulation of the tracer in tissues can then be visualized as 3D images due to external detection of the emission by a PET scanner.

Thus PET images allow the spatial distribution of the radiopharmaceutical to be mapped quantitatively in the human body.
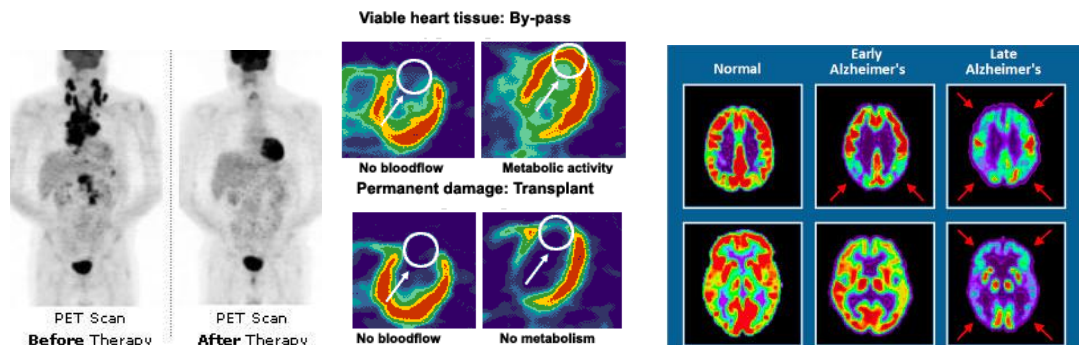
Figure 2-1
Left: Oncology PET scan (http://www.studiobin.net/positron-emission-tomography-scan.html)
Middle: Cardiac PET scan (http://www.petscaninfo.com/zportal/portals/pat/heart/heart_old)
Right: Neurology PET scan (http://www.ahrmemory.com/memory-baseline/)
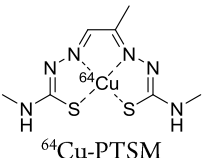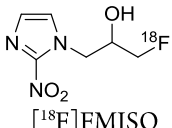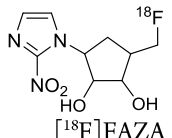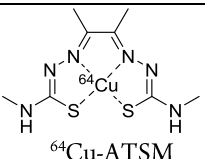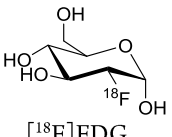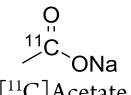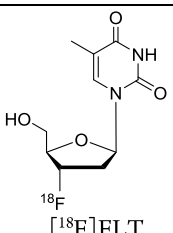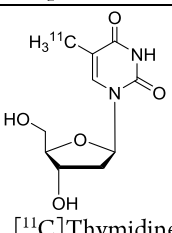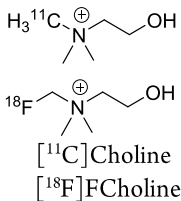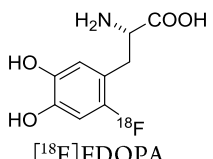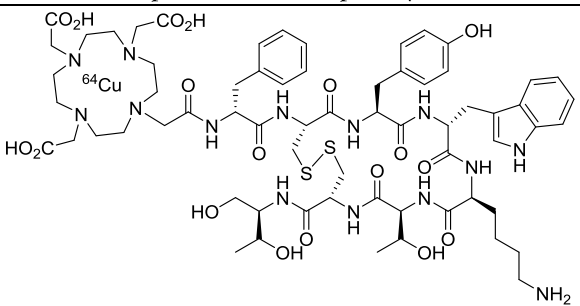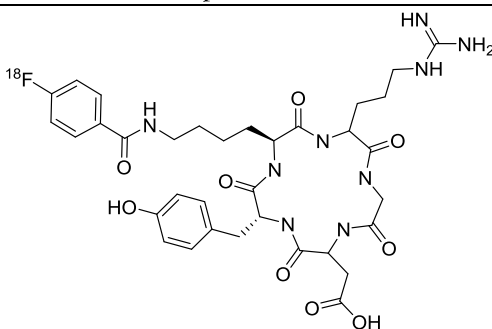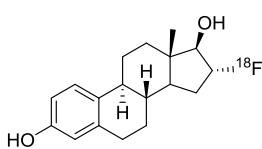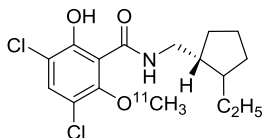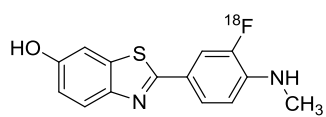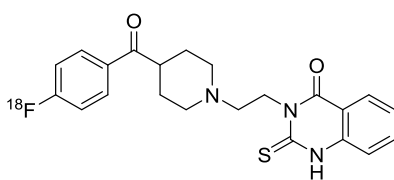
2.2 The radiopharmaceutical

For a PET radiotracer to be useful a number of criteria have to be met. These criteria vary depending on the target of the tracer. By definition, affinity of the tracer is ideally very high for the target to be imaged in order to achieve a high target to non-target ratio. A quick clearance from the blood as well as non-target areas are critical for the reduction of background signal, which means that low plasma protein binding together with high membrane permeability is important. The tracer must only be involved in a single or very few steps of a biochemical pathway in order to ensure that the measured data only represent the kinetics specific for this specific tracer. It is essential that the radiotracer does not undergo rapid metabolism over the period of the PET measurements as the PET scanner cannot discriminate between signals from the parent radiotracer and radiolabeled metabolites. Specific activity (SA) of the tracer should be as high as possible in order to trace the process under investigation without exerting significant mass effects on the target molecule[3,4].

A selected number of the main PET radiopharmaceuticals are represented in Table 2-1, where they are listed based on the biological entity/process they target[5,6].

Table 2-1. PET radiopharmaceuticals

Target	Radiopharmaceutical
Blood volume [7]	$[^{11}C]CO, [^{15}O]CO$ Evaluation used in both oncology, cardiology and several other fields
Blood flow [8,9]	$[^{15}O]H_2O, [^{13}N]NH_3$ ^{64}Cu-PTSM Evaluation of myocardial perfusion
Hypoxia [10]	 $[^{18}F]$FMISO $[^{18}F]$FAZA ^{64}Cu-ATSM The ability to detect hypoxia in tumors has a great impact on management and therapy
Substrate metabolism [11 12]	$[^{18}F]$NaF $[^{18}F]$FDG $[^{11}C]$Acetate Metabolic processes. Used extensively in oncology
Proliferation/ DNA synthesis [13 14 15]	 $[^{18}F]$FLT $[^{11}C]$Thymidine $[^{11}C]$Choline $[^{18}F]$FDOPA $[^{18}F]$FCholine Uncontrolled cell proliferation is the primary hallmark of cancer
Enzyme/ transporter/ receptor interaction [16 17 18 19 20]	 ^{64}Cu-DOTATOC – somatostatin receptor overexpression on neuroendocrine tumors

Target	Radiopharmaceutical
	$[^{18}F]$RGD - $\alpha_V\beta_3$ receptor overexpression on glioma cells
	$[^{18}F]$FES – estrogen receptor overexpression in breast cancer
	$[^{11}C]$Raclopride – dopamine D_2 receptors
	$[^{18}F]$FLM - Aβ deposition in Alzheimer´s disease
	$[^{18}F]$Altanserin - imaging of serotonin S_2 receptors

2.3 PET imaging

After administration of the radiotracer the patient is placed in a PET scanner for the visualization of the tracer distribution. This happens by external detection of the emission originating from the radionuclide.

2.3.1 Positron emission

A positron emission or β^+ decay happens when a proton in a neutron-deficient nucleus transforms into a neutron and a positron, which together with a neutrino, is ejected from the nucleus:

$$^A_Z X \; \rightarrow \; ^{\;\;A}_{Z-1} X' + e^+ + \; \nu_e$$
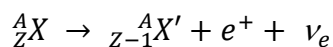
The positron will then deposit its energy in the surrounding matter and, when it comes to rest, annihilates with an electron. This happens within a few millimeters from its origin in soft tissue. In this annihilation reaction, two 511keV photons are formed. These leave the site of the annihilation event in a back-to-back emission with paths almost exactly 180° apart as shown in Figure 2-2. These two photons lay the basics for PET imaging[21].
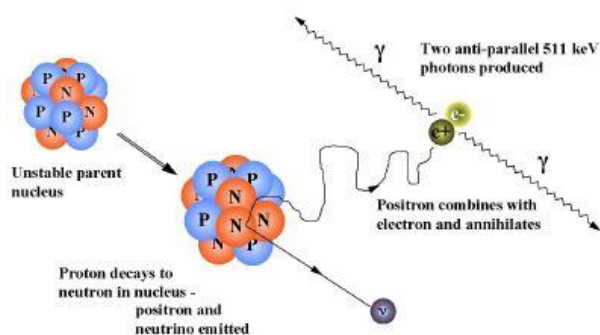
Figure 2-2. The annihilation reaction forming two 511keV photons
(http://depts.washington.edu/nucmed/IRL/pet_intro/intro_src/section2.html)

2.3.2 The PET scanner and image creation

Most PET scanners are typically made of rings of position-sensitive scintillation detectors, which consist of a scintillator coupled to a photo-detector[2,22,23].

2.3.2.1 The scintillator

The scintillator is a crystal with the property of absorbing the 511keV annihilation photons, and converts the energy into a burst of visible light photons. There are three properties of the scintillator that are crucial for the resulting PET image.

The first is the density of the crystal, which affects the detection efficiency. The sensitivity of the detector depends on a high number of annihilation photon incidents. This means that the crystal must be able to stop as many of the photons as possible, which requires a very dense crystal material. The second property is the decay constant. The time interval required by the scintillator to separate two individual photon events depends on how brief the scintillation photon pulse is. For good coincidence timing (the simultaneous detection of the two photons from one annihilation event) and high count-rate capability (the ability to process each pulse individually), a short decay time is desirable. The third is light output. The number of light photons produced per interaction between a 511keV photon and the crystal – also known as the brightness of the scintillator – is important. This is because the integrated light signal is used in the following data processing to achieve optimal energy as well as spatial resolution. High energy resolution is achieved by identification of full energy events and subtraction of measurement noise caused by Compton-scattered photons. These Compton-scattered photons can be identified as their energy – and thereby the resulting number of light photons - are lower. Good spatial resolution is achieved when the relative amplitudes of the light photons seen by adjacent light sensors are used to determine the exact location of the initial interaction.

NaI crystals doped with thallium have been used for many years for both PET and SPECT scanners because of a high light output and a reasonably fast decay time. But because NaI suffers from low detection efficiency for photons above 200keV due to low density, most of the scanners produced in the last century were built with bismuth germinate (BGO) crystals. The advantage of this crystal is its high density, resulting in drastically higher detection efficiency. This compensates for a low light output and only moderately fast decay time. Now crystals having the light output of NaI, the density of BGO, and even faster decay times are developed. A material that meets these requirements is lutetium oxy-orthosilicate (LSO) doped with cerium, as is seen in Table 2-2, and a widespread use of this scintillator is expected in the future.

Table 2-2. Properties of different scintillator material

Scintillator	Density (g/cc)	Light output (photons pr 511keV)	Decay time (ns)
NaI:Tl	3.67	19400	230
BGO	7.13	4200	300
LSO:Ce	7.40	~13000	~47

2.3.2.2   The photomultiplier tube

Most PET scanners use photomultiplier tubes (PMTs) to convert the light photons from the scintillator into an electrical current. This is shown in Figure 2-3.
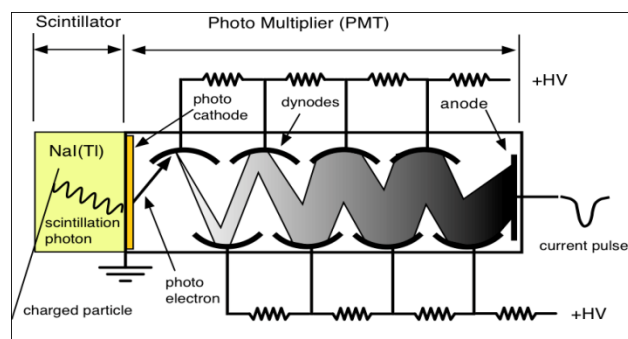
Figure 2-3. Conversion of a 511keV photon to an electric pulse by PMT
(http://wanda.fiu.edu/teaching/courses/Modern_lab_manual/scintillator.html)

The light photon liberates an electron from a photocathode. A high potential difference accelerates the electron onto a series of dynodes where each impact releases even more electrons, resulting in an avalanche of photoelectrons in the magnitude of 10^6 electrons from one photon after ten stages of amplification. This large number of electrons finally reaches an anode, where they lead to an easily detectable pulse in the milliamp scale signaling the arrival of the light photon at the photocathode a few nanoseconds earlier.

2.3.2.3   The detector

The block detector design (Figure 2-4) is used by most modern PET scanners. It consists of a 4x4 cm in area by 3cm deep block of scintillator material that is coupled to four PMTs. The block is segmented into an array of smaller detector elements (often 8 x 8), and the gaps are filled with reflective material that helps isolating the individual elements optically. The cuts are of varying depth with the deepest cuts at the detectors edge. This allows for the light to be shared to different extent, between the four PMTs, depending on the position of the crystal in which the interaction takes place. Thereby, the interaction in each detector element will produce a unique distribution of scintillation light, and thus the signal from the four PMTs is translated into an X and Y coordinate. The advantage of the block detector design is a significantly reduced detector dead-time due to restricted light spread.
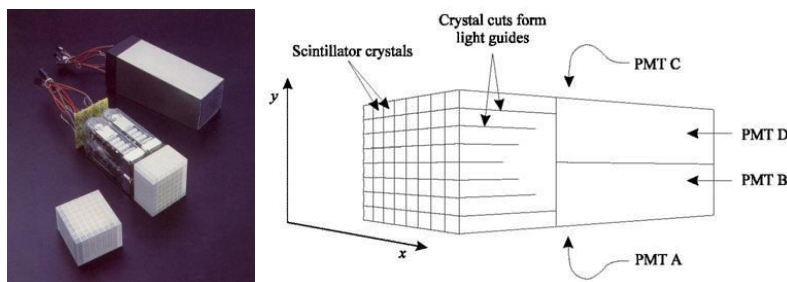
Figure 2-4. The block detector
(http://depts.washington.edu/nucmed/IRL/pet_intro/intro_src/section5.html)

2.3.2.4   The image

A coincidence event is when the two photons from an annihilation are detected by a pair of detectors with good coincidence timing, an acceptable angle (~180°) and with a proper energy deposition. Such a coincidence event is recorded by a coincidence detection system consisting of the block detector pair with associated electronics (amplifiers, pulse height analyzers etc.) and a coincidence circuit (Figure 2-5).
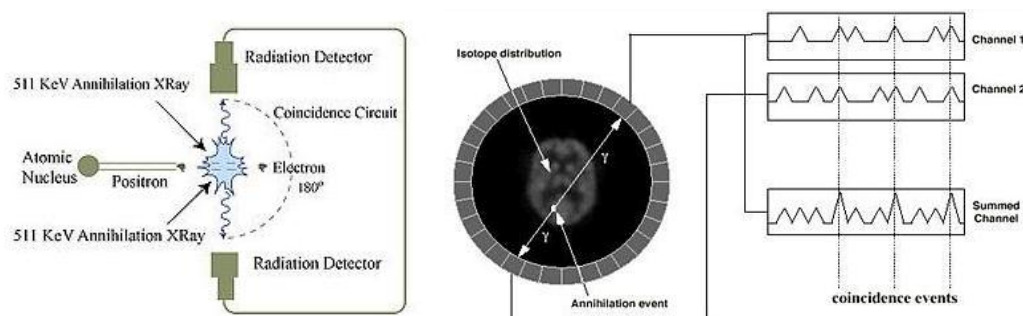
Figure 2-5. Detection of a coincidence event
(https://www.flickr.com/photos/mitopencourseware/4478628199/ and
http://www.assignmentpoint.com/science/eee/noise-equivalent-count-rate-nuclear-camera.html)

This event is assigned to a line of response (LOR) joining the two detectors. During the course of the PET scan, the total number of events measured by a particular detector pair will be proportional to the integrated radioactivity along the LOR. This data is referred to as line integral data. During the PET scan many different line integrals are measured at the same time due to the construction of the PET scanner with a large number of block detectors placed around the body to be imaged, often in ring geometry. To improve the efficiency of modern PET scanners several rings are stacked next to each other. The role of image reconstruction is to convert these line integrals into a 3D image that

quantitatively reflects the distribution of the positron-emitting atoms and, thereby, the molecule attached to it. The entire process is shown in Figure 2-6.
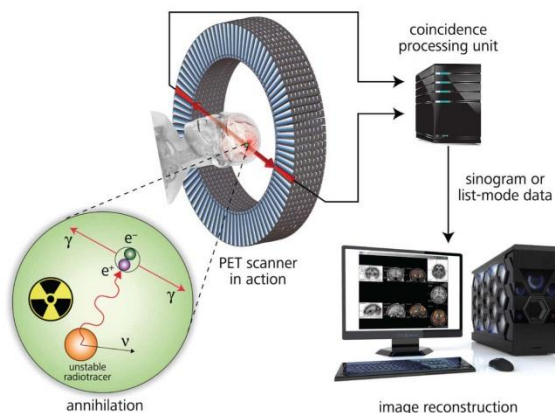
Figure 2-6. PET imaging from annihilation to image
(http://www.sepscience.com/Sectors/Pharma/Articles/429-/Radio-IC-for-Quality-Control-in-PET-Diagnostics)

2.4 The radionuclide

When choosing which radionuclides to use for PET imaging, certain considerations must be made. The physical half-life should preferably be within minutes to hours. A short half-life decreases the time the patient is exposed to unnecessary radiation after the scanning has been performed. At the same time it has to be long enough to allow for synthesis, purification, delivery and administration. The chemical properties of the radionuclide are also important. Radionuclides that are easily incorporated into biomolecules without altering the biochemical properties are desirable. Radionuclides that may easily produce useful precursors, which may be utilized in a wide range of chemical synthetic strategies are also preferred[24]. The emission energy is another critical factor. As previously stated, the positron travels a certain distance in the tissue after emission before coming to rest, and annihilates with an electron. This distance is called the positron range and is determined by the energy of the emitted positron. An energy that is characteristic for each nuclide. If the emission energy is high the resulting position range is large. That causes a loss in spatial resolution of the PET image. Early research showed that the positron range of high-energy positron-emitting radionuclides with $E_{max} \geq 1.5MeV$ was the limit for good resolution. However, as the spatial-resolution capabilities of the imaging devices has been

significantly improved, this limit is becoming less critical[3,22,25]. In Table 2-3 the most commonly used PET isotopes are presented[3].

Table 2-3. Commonly used positron-emitting radioisotopes and their physical properties

Nuclide	Half-life	E_{max} (β^+) (MeV)
^{18}F	110 min	0.64 (97 %)
^{11}C	20.3 min	0.97 (99 %)
^{13}N	10 min	1.20 (100 %)
^{15}O	122 sec	1.74 (100 %)
^{64}Cu	12.7 h	0.655 (19 %)
^{68}Ga	68 min	1.90 (89 %)

The advantage of ^{11}C, ^{13}N and ^{15}O is that they are isotopes of the main constituents of bioorganic molecules. That makes the resulting radiopharmaceuticals chemically indistinguishable from their non-radioactive counterparts, and they also possess the same physiochemical and biochemical properties as those. This is one of the key strengths of PET. The half-lives of these isotopes are, however, very short, which limits the labeling strategy possibilities and requires on-site production[3].

The radiometals ^{64}Cu and ^{68}Ga requires a chelator, most often a bifunctional kind, that both complexes the metal and couples to the biomolecule. This is mainly possible for molecules of high molecular masses (proteins, peptides, antibodies), where insertion of artificial moieties does not affect the properties of the molecule significantly. A high stability of the radiometal-chelator complex is also essential in achieving a high uptake in the target organ or tissue compared to non-specific radiometal uptake[26].

Fluorinated pharmaceuticals, including radiopharmaceuticals, often display altered electronic properties, lipophilicity and biological characteristics because of the strong withdrawing properties of fluorine and the fact that the atom rarely is a constituent of the biomolecule. The substitution of a hydrogen atom or a hydroxyl group by fluorine is, however, a very well-known bioisosteric replacement that induces minimum steric chances. ^{18}F also has the most favorable decay properties. It has low positron energy, resulting in high resolution PET images. The optimal half-life of 110min allows enough time for complex radiosynthesis, longer in-vivo investigation and, most importantly, the possibility for "satellite" distribution of ^{18}F-labeled radiopharmaceuticals[3]. ^{18}F will be described in much more detail later.

2.4.1 Radionuclide production

The majority of radionuclides used in PET imaging are produced by cyclotrons. Of the previously mentioned radionuclides ^{68}Ga is an exception, as this radionuclide is primarily produced by the ^{68}Ge/^{68}Ga generator[27], but the radionuclide can also be produced by cyclotron[28]. As some of the challenges one faces when working with ^{18}F arise from the production process, this process is described in the following pages.

2.4.1.1 The cyclotron

A cyclotron consists of a pair of semicircular hollow electrodes called dees (D's) because of their shape, placed in a flat vacuum chamber. This so-called acceleration chamber is positioned between the two poles of a homogeneous magnetic field. Near the center of the small gap between the two dees is the ion source that is used to generate charged particles. The schematics of the cyclotron are shown in Figure 2-7.
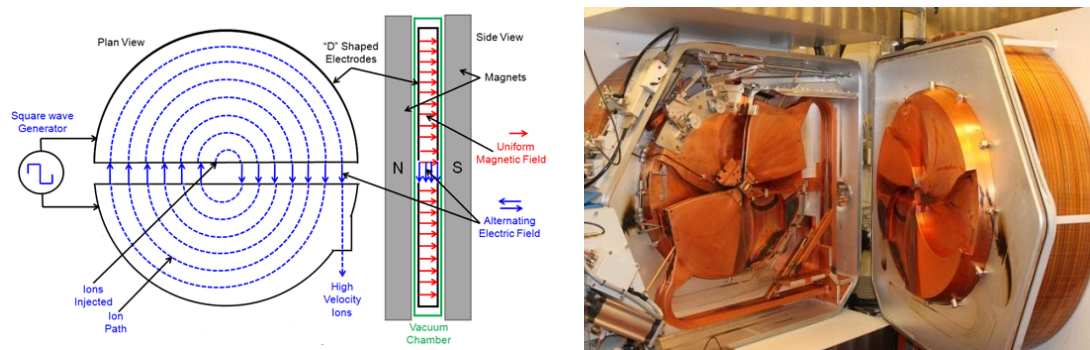
Figure 2-7.
Left: Schematics of the cyclotron (from https://mpoweruk.com/figs/cyclotron.htm).
Right: The GE PETtrace cyclotron installed at the Hevesy Laboratory

When in operation, a high-frequency alternating current voltage is applied across the dees by which an electric field is generated. When the ions are injected into the gap, they are immediately accelerated towards one of the dees by this electric field. Simultaneously, the magnetic field causes the ions to follow a curved circular path inside the dee. The ions reach the gap exactly when the voltage across the dees reaches its maximum in the opposite direction and the ions are accelerated towards the other dee, causing an increase in the radius of the circular path. In conjunction with the ions increasing in energy when they increase in velocity, the result is an ion beam that spiral outward, gaining a constant

increase in energy each time it passes the gap. When the beam reaches the outer edge of the dees, it is extracted and directed onto a target.

The ion source can either be positive or negative, meaning that they produce positively or negatively charged ions, respectively. For extraction of the positive ions electrostatic reflection is used. This is, however, not a very efficient strategy as up to 30% of the beam is lost due to collisions with the deflector or surrounding materials. Instead nearly all modern cyclotrons use a negative ion source. Here the extraction is done by stripper foils. A stripper foil is an ultra-thin foil that strips the electrons from the ions, resulting in a change in the electric charge of the beam from negative to positive, causing the beam to rotate in the opposite direction[24,29,30].

2.4.1.2   The nuclear reaction

The extracted beam is directed onto a target of either gas, liquid or solid material, depending on the desired radionuclide. Here the nuclear reaction takes place. Commonly one of the following two nuclear reactions takes place, depending on the beam particle. In the (p,n) reaction, the target nucleus is bombarded with a proton and instantly releases a neutron. This reaction is represented as

$$_{Z}^{A}X(p,n)_{Z+1}^{A}Y$$
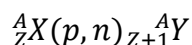
The other is the bombardment of the target using deuterons causing a neutron to be released. This reaction is represented as

$$_{Z}^{A}X(d,n)_{Z+1}^{A+1}Y$$
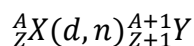
There are variations of these, depending on which particle or number of particles that are expelled from the target nucleus following the proton or deuteron bombardment, and which particle that is used for the bombardment[24]. The standard reactions of the common cyclotron-produced radioisotopes are presented in Table 2-4. As this table shows, ^{18}F is either produced in a gas or liquid target, which has significant influence on the next step in the production of ^{18}F-labeled radiotracers.

Table 2-4. Production reactions of common cyclotron-produced radionuclides

Nuclide	Production reaction	Target material
^{18}F	$^{18}O(p,n)^{18}F$	$[^{18}O]H_2O$ enriched water
	$^{20}Ne(d,\alpha)^{18}F$	Ne gas
^{11}C	$^{14}N(p,\alpha)^{11}C$	N_2 gas
	$^{10}B(d,n)^{11}C$	^{10}B powder
^{13}N	$^{16}O(p,\alpha)^{13}N$	H_2O
	$^{12}C(d,n)^{13}N$	CO_2
^{15}O	$^{14}N(d,n)^{15}O$	N_2 gas
	$^{15}N(p,n)^{15}O$	$[^{15}N]N_2$ enriched gas
^{64}Cu	$^{64}Ni(p,n)^{64}Cu$	Electroplated ^{64}Ni
^{68}Ga	$^{68}Zn(p,n)^{68}Ga$	Electroplated enriched ^{68}Zn

2.5 Traditional chemistry with ^{18}F

In order to set the stage for the description of my work regarding new radiofluorination approaches, the next pages will describe the conventional radiofluorination methodologies.

2.5.1 Production of ^{18}F

^{18}F is produced by one of the two nuclear reactions $^{20}Ne(d, \alpha)^{18}F$ or $^{18}O(p, n)^{18}F$ and used either as $[^{18}F]F_2$ for electrophilic radiofluorination or as $[^{18}F]F^-$ for nucleophilic radiofluorination.

Today two processes are employed to generate $[^{18}F]F_2$. The first one utilizes the bombardment of high pressure ^{20}Ne gas containing a low percentage (0.1-0.2%) of "cold" F_2 in a passivated nickel target using 8-18MeV deuterons. The result is carrier-added (CA) $[^{18}F]F_2$ with a relatively low specific activity (~ 12 Ci/mmol), depending on the amount of added carrier F_2. The second method is the double-shoot method, where the passivated target is loaded with $[^{18}O]O_2$ gas. Irradiation of the target produces ^{18}F, which adheres to the target walls. Following cryogenic recovery of $[^{18}O]O_2$ a noble gas plus carrier F_2 mixture is added. A second short irradiation forces a fluorine exchange that results in recoverable CA $[^{18}F]F_2$. Both these procedures are relatively low-yielding (<1 Ci) and the products from the subsequent electrophilic radiofluorination reactions also suffer from low specific activities due to the added carrier F_2[31–33].

The production of $[^{18}F]F^-$ by the $^{18}O(p, n)^{18}F$ nuclear reaction of enriched $[^{18}O]H_2O$ for nucleophilic radiofluorination is the most common method utilized. The advantages of this procedure is that $[^{18}F]F^-$ is obtained as non-carrier added (NCA) with specific activities around 10^4 Ci/mmol[31].

2.5.2 Electrophilic radiofluorination

Historically, most early PET tracers were first synthesized via the electrophilic radiofluorination pathway. In electrophilic radiofluorination strategies $[^{18}F]F_2$ is used either directly or is incorporated in reagents that work as sources of electrophilic fluorine. The reactivity of $[^{18}F]F_2$ is extraordinarily high, which results in a rather low selectivity of the labeling reactions and the oxidizing strength often leads to undesired radical side reactions and reactions with the solvents. As a solution incorporation of $[^{18}F]F_2$ into other less reactive radiofluorination reagents has been carried out in order to minimize these problems. In these reagents fluorine is highly polarized with a partial positive charge, which is reactive toward electron-donating reagents such as alkenes, aromatic molecules or carbanions[34,35].

As all these reagents are carrier added, RCY of electrophilic radiofluorination can never be more than 50%, as only one of the two fluorine atoms participate in the labeling reaction. At the same time the specific activity of the product is low to moderate at best, which limits the tracers to be used only if specific activity is not a critical factor or if they are not too toxic, as the amount of product injected into the patient needs to be relatively large.

The standard reagents and their production strategies are:

1. *molecular fluorine ($[^{18}F]F_2$)*, produced in the cyclotron target as described previously

2. *trifluoromethyl hypofluorite ($[^{18}F]CF_3OF$)*, formed in the cyclotron target by reaction between $[^{18}F]F_2$ trapped by CsF, fluorine and carbonyl fluoride at 100°C. RCY is about 30%

3. *Acetyl hypofluorite ($[^{18}F]CH_3COOF$)*, synthesized by passing $[^{18}F]F_2$ through a column containing a potassium acetate-acetic acid complex at rt. The yield is only 50% as half of the activity is converted to $[^{18}F]KF$

4. *Perchloryl fluoride ($[^{18}F]FClO_3$)*, produced by passing $[^{18}F]F_2$ through a column containing $KClO_3$ at 90°C with a radiochemical yield at about 23%

5. *Xenon difluoride ($[^{18}F]XeF_2$)*, commonly produced in a sealed nickel vessel by reaction between $[^{18}F]F_2$ and Xe gas at 390°C with RCY at 70%

6. *N-$[^{18}F]$Fluoropyridinium triflate*, produced by reacting $[^{18}F]F_2$ with N-trimethylsilylpyridinium triflate at -40°C.

2.5.2.1 Electrophilic aromatic radiofluorination

$[^{18}F]F_2$ and $[^{18}F]CH_3COOF$ react well with arenes, but the regioselectivity is often low, resulting in mixtures of fluorinated products. To increase the regioselectivity demetallation reactions of organometallic precursors are applied instead. This can be demonstrated by the synthesis of 6-$[^{18}F]$FDOPA, where the formation of the undesired 2- and 5- region isomer may be suppressed when using a mercury-labeled precursor. A tin precursor has provided same efficiency, and this synthetic procedure is much safer with regard to metal contamination in the final product. The only issue is the difficulty in synthesizing the tin precursor. The development of these regioselective strategies has been a crucial step in turning 6-$[^{18}F]$FDOPA into one of the most frequently used PET tracers[36–38]. The synthetic strategies of 6-$[^{18}F]$FDOPA is shown in Scheme 2-1.
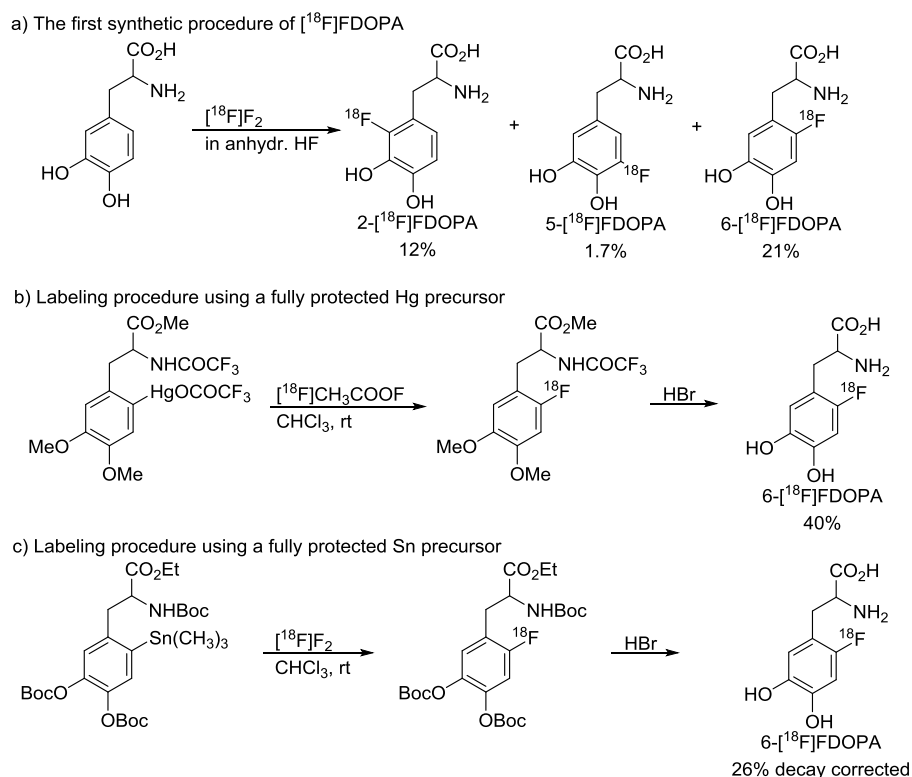
Scheme 2-1. Three synthetic procedures of 6-$[^{18}F]$FDOPA, demonstrating the improved regioselectivity when using demetallation strategies.

2.5.2.2   Fluorination of alkenes

Fluorination of a carbon-carbon double bond was utilized in the first $[^{18}F]$FDG synthetic strategies, which made it an important type of reaction in the 1980s. Syn-addition is often exclusively seen as the outcome of $[^{18}F]F_2$ addition to an alkene. It seems that this type of reaction does not share the same mechanism as seen for chlorine, bromine and iodine (bimolecular electrophilic addition AdE2). Instead the mechanism may involve the formation of an unstable tightly ion-paired α-fluorocation after the nucleophilic attack at the double bond. The fluorocation then collapses before any rotation around the carbon-carbon bond can take place.

Not many PET tracers based on addition to double bonds exist, but an exception is $[^{18}F]$EF5 (Scheme 2-2), a tracer for the detection of hypoxia. The yield of the $[^{18}F]F_2$ addition to the tri-fluoro-alkene is low, due to the low electron density of the double bond caused by the electron withdrawing fluoride atoms. The tracer is, however, routinely used at some PET centers.

$[^{18}F]$EF5
Chemically identical compounds, RCY about 10%
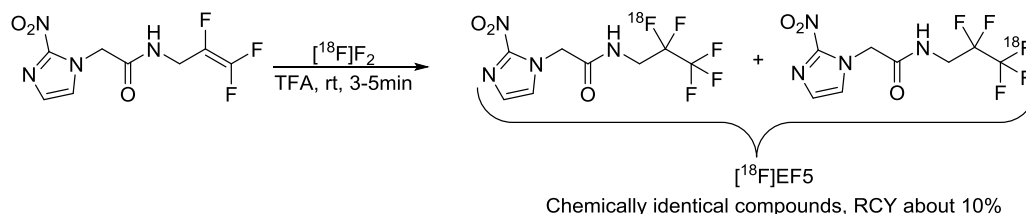
Scheme 2-2. Synthesis of $[^{18}F]$EF5

2.5.2.3 $[^{18}F]F_2$ with higher SA

A procedure for the production of $[^{18}F]F_2$ based on NCA $[^{18}F]F^-$ from the bombardment of $[^{18}O]H_2O$ has been described by Bergman and Solin[39]. $[^{18}F]F^-$ is converted into $[^{18}F]CH_3F$. This is then converted into $[^{18}F]F_2$ by an isotopic $^{18}F/^{19}F$ exchange in an electrical discharge chamber containing a small amount of F_2 carrier gas. The SA of the resulting $[^{18}F]F_2$ is 55 GBq/μmol, which is significantly better compared to the previously highest reported SA of 2 GBq/μmol. But as long as this strategy has not been translated into a commercially available synthesis platform, and the standard strategies is affected by low specific activity, selectivity and RCY, PET tracers synthesized by an electrophilic radiofluorination strategy will remain a minority.

2.5.3 Nucleophilic radiofluorination

2.5.3.1 Fluoride recovery and processing

One major issue related to the production of $[^{18}F]F^-$ by irradiation on enriched $[^{18}O]H_2O$ is that $[^{18}F]F^-$ is delivered from the cyclotron in an aqueous solution. Due to its high degree and strength of hydration at -104.3 kcal/mol, resulting in coordination with up to 15 molecules of H_2O, $[^{18}F]F^-$ is nucleophilically inert[40,41]. The consequence is that nucleophilic radiofluorination has to happen under anhydrous conditions, which means that the first step of most radiofluorination procedures has to be removal of bulk $[^{18}O]H_2O$ and the resolubilization of $[^{18}F]F^-$ in an organic solvent.

The procedure applied most often is by application of the Waters SepPak QMA ion exchange cartridge to which $[^{18}F]F^-$ is adsorbed. A great advantage of this procedure is that the expensive $[^{18}O]H_2O$ can be recovered. At the same time ionic contaminants from the target body, introduced as a result of the bombardment of the enriched water, are either removed together with the recovered water or trapped by the resin and thereby removed from the subsequent synthesis[42]. Trapped $[^{18}F]F^-$ is then eluted into a reactor vial by potassium carbonate dissolved in acetonitrile. Next, residual water is removed by three successive cycles of azeotropic evaporation with acetonitrile. In this process the carbonate ion prevents evaporation of $[^{18}F]F^-$ in form of $[^{18}F]HF(g)$. Despite of this evaporation procedure, a completely anhydrous fluoride ion is hardly ever achieved, as the removal of each water molecule is successively more difficult. However, each step renders the fluoride ion increasingly nucleophilic despite of a small degree of hydration. The nucleophilicity is enhanced even further by Kryptofix 2.2.2 (K222), a kryptand, which is also present in the potassium carbonate/acetonitrile solution. K222 complexes to the potassium ion and thereby separates the charge from $[^{18}F]F^-$, resulting in a very "naked" and thereby very reactive fluoride ion. K222 also enables the subsequent resolubilization of $[^{18}F]F^-$ in a polar aprotic solvent, such as acetonitrile, for the following radiofluorination step[35,43]. This processing of $[^{18}F]F^-$ is depicted in Scheme 2-3.

$^{18}O(n,p)^{18}F$ on $[^{18}O]H_2O \longrightarrow \ ^{18}F^-(H_2{}^{18}O)_n$ in $[^{18}O]H_2O$ $\quad$ 1: Adsorption on QMA column
$\qquad\qquad\qquad\qquad\qquad\qquad\qquad\qquad\qquad\qquad\qquad\qquad\qquad$ 2: Elution using K_2CO_3/K222 solution

3 x azeotropic evaporation steps

$^{18}F^-(H_2{}^{18}O)_n$ in $[^{18}O]H_2O$ $\qquad\qquad\qquad\qquad\qquad\qquad$ $^{18}F^-(H_2{}^{18}O)_m$
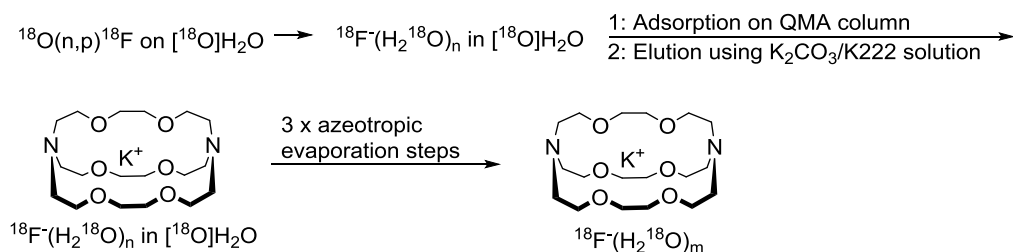
Scheme 2-3. Drying of $[^{18}F]F^-$ using the QMA/kryptofix strategy. $n \leq 15$, $m < n$.

Other kryptands, bases or counterions can also be used depending on specific considerations regarding the labeling step. Carbonate can be substituted for oxalate if the labeling substrate is base-labile. The use of quarternary ammonium salts instead of K222 is now recommended due to increased $[^{18}F]F^-$ reactivity, solubility in a wider range of solvents and their non-toxicity. But they are more difficult to make and achieve in an anhydrous state, which is the reason why most people still use K222[34].

2.5.3.2   The labeling step

The labeling step is in most cases very simple. The precursor dissolved in a suitable solvent is added to the drying vial and the reaction mixture is heated for a given period. Polar aprotic solvents are almost always used, as they enhance the ionic dissociation of the K222/$[^{18}F]$KF complex and, thereby, enhance the nucleophilicity of the fluoride ion. However, it appears that the solubility of the reactants plays a larger role than the solvent effects on reaction rates. Another reason for this choice of solvents is that they are inert toward the strong basicity of $[^{18}F]F^-$. MeCN is a standard solvent for nucleophile radiofluorination as it is easily removed. Alternatives can be DMSO or DMF. The reaction temperature is often above 90°C as lower temperature can be too low to obtain high RCYs. The reaction time is preferably only a few minutes, as the radioactive decay offsets the gain in RCY[35].

2.5.4   Nucleophilic radiofluorination pathways

2.5.4.1   Radiofluorination by nucleophilic aliphatic substitution

The nucleophilic aliphatic substitution with $[^{18}F]F^-$ happens primarily by the S_N2 mechanism where the nucleophile attacks the substrate from the backside relative to the leaving group. The result is substitution with inversion of configuration at the carbon center. Reactivity of the precursors for the aliphatic nucleophilic substitution follows the standard S_N2 pattern, where substitution at a primary

carbon is typically high-yielding, while substitution at secondary carbon may lead to alkene byproducts due to elimination reaction. The main requirement for this type of reaction is a good leaving group, such as a sulfonate or halide except fluoride. Table 2-5 shows the reactivity towards solvolysis of 1-phenylethyl esters and halides and thereby the ability of the leaving groups to stabilize the negative charge resulting from a substitution reaction[44].

Table 2-5. Leaving group ability demonstrated by a solvolysis reaction. K_{rel} = relative reaction rate

R		K_{rel}
Triflate (OTf)	$F_3C-\overset{O}{\underset{O}{S}}-O-$	1.4×10^8
Nosylate (ONs)	$O_2N--\overset{O}{\underset{O}{S}}-O-$	4.4×10^5
Tosylate (OTs)	$--\overset{O}{\underset{O}{S}}-O-$	3.7×10^4
Mesylate (OMs)	$H_3C-\overset{O}{\underset{O}{S}}-O-$	3.0×10^4
I⁻		91
Br⁻		14
Cl⁻		1
F⁻		9×10^{-6}

The triflate is by far the best leaving group, but it is also problematic with regard to the precursor synthesis, as the precursors are not always stable during purification due to the reactivity of the triflate group. This issue is solved by using the lesser reactive mesylate and tosylate leaving groups. Tosylate and mesylate have about the same reactivity, but tosylate is the most widely used leaving group. The reason is the fact that tosylate has the advantage compared to mesylate that it is UV active, which is an advantage when it comes to HPLC purification or QC analysis of the final product.

The major drawback of the substitution reaction is the need to protect acidic moieties due to the strong basicity of [18F]F⁻, as well as other nucleophilic moieties that may act as competing sites for a nucleophilic attack. This complicates of the precursor synthesis and requires additional deprotection and purification steps during the radiofluorination procedure[26,35].

2.5.4.2 Radiofluorination by nucleophilic aromatic substitution

The requirement for the nucleophilic aromatic substitution is an activated aromatic system, which, due to the electron deficiency, is attractive for nucleophilic attack. An activated aromatic system is achieved by at least one strong electron-withdrawing group (EWG) in the *o-* or *p*-position to the leaving group. The reason is that EWGs can stabilize the intermediate Meisenheimer complex resulting from the $[^{18}F]F^-$ attack and thereby lower the transition state energy. Examples of useful EWGs are nitro, cyano and carbonyl functionalities as well as halogens in the order $3\text{-}NO_2 < 4\text{-}Ac < 4\text{-}CHO < 4\text{-}CN \approx 4\text{-}CF_3 < 4\text{-}NO_2$. The mechanism is shown in Scheme 2-4.
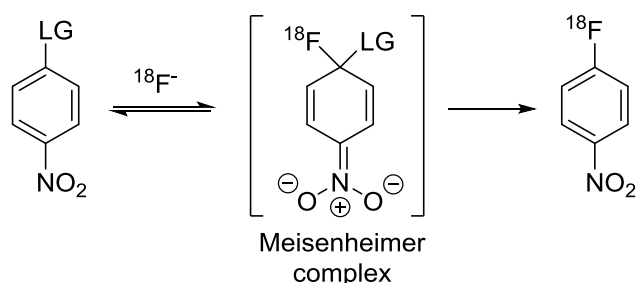
Scheme 2-4. The nucleophilic aromatic substitution mechanism

Like in the aliphatic substitution reaction the leaving group plays a crucial role. Suitable LGs are the nitro group, halogens and trimethylammonium salts in the order $I < Br < Cl < F < NO_2 \approx N^+Me_3$. However, the reason is not based on their leaving group activity directly, as is the case for nucleophilic aliphatic substitution. Instead it is in their ability to stabilize the Meisenheimer complex. As this type of reaction requires higher energy to proceed, the reaction conditions are often quite harsh. High temperatures make polar aprotic solvents with higher boiling points such as DMSO and dimethylacetamide a preferred choice. Heteroarenes, such as pyridines, are receiving increasingly more attention, as they have "built-in" electron-deficient centers due to the heteroatoms. Especially the 2-position of pyridine is highly susceptible for nucleophile attack of $[^{18}F]F^-$ with resultingly high RCY[26,45].

2.6 The PET radiopharmacy

The production of PET radiopharmaceuticals is very comprehensive and requires a large investment in equipment and infrastructure. The essentials for a PET radiopharmacy are the cyclotron

for production of the PET radionuclides, radiochemistry facilities and finally QC equipment. But these do not do it alone. Due to the heavy radiation (511 keV photons together with neutron flux) both during bombardment and after, the cyclotron has to be shielded. Cyclotrons without self-shielding require a very thick concrete vault in order to reduce neutron exposure. Today most compact cyclotrons are self-shielded, which allow for a reduction in required vault shielding, as the neutron flux is reduced by five orders of magnitude. As a result the activation of the surrounding material by the neutrons are also reduced, thereby decreasing the residual activity[46]. But either way the floor loading is significant. The weight of the magnet of the cyclotron can reach 10 tons and due to the lead blocks of the self-shielded cyclotrons these can reach 16 tons. That added up with the weight of the concrete walls requires the cyclotron to be installed on ground floor or in the basement and the soil and underground condition has to be assessed, as additional support may be needed.

Radiochemistry facilities most often include synthesizers that work either manually or automatically. They have to be placed either in hot cells or dedicated isotope fume hoods. If the tracers are for human use they have to be produced in clean rooms with LAF benches. Again the equipment weight and radiation shielding increase the requirements to the floors that have to be reinforced. The entire area has to be covered by an extensive air filtration system with both HEPA and carbon filters. At the same time the rooms have to be pressurized such that a negative pressure exists in the radiochemistry laboratories to prevent release of radioactive compounds to the surroundings, while the clean room has positive pressure in order to ensure a clean environment. QC equipment includes among other things HPLC, radioTLC scanner, GC and dose calibrator. A staff of highly trained personnel such as physicists, chemists and lab technicians is needed to operate such a facility. On top of that is added the expensive target materials, chemicals and precursors produced under GMP regulations. The result is that a PET radiopharmacy is a very costly operation[47].

2.6.1 Centralized production

Today PET radiopharmaceuticals are primarily produced in a centralized manner by commercial PET radiopharmacies and transported to PET centers within a certain radius. In this way the significant costs are spread over many costumers and the result is affordable and readily accessible PET tracers. The primary tracers produced and distributed in this way are $[^{18}F]$FDG and $[^{18}F]$F-. Due to

the half-life of $[^{18}F]$FDG the maximum distance by ground transport is about 300 km. Air transport can be employed for longer distances, but this solution is much more expensive[47]. As $[^{18}F]$FDG in commercial production for the PET centers are made in macroscale with several milligrams of precursor, there is almost no addition cost in increasing the batch size of the production to accommodate more costumers. One just have to increase the amount of $[^{18}F]F^-$ produced by the cyclotron. No change in the synthesis itself, purification or QC protocol is needed. The result is a significantly higher financial advantage in producing a large batch of a few numbers of tracers than the other way around[48].

2.7 Conclusion to Chapter 2

This chapter has described the concept of Positron Emission Tomography and the radiochemistry that lay the foundation for the synthesis of PET radiotracers. The challenges posed by the conventional radiofluorination procedures are presented together with the restraints they set on the possibilities for the development of new PET tracers. In the next chapter different strategies to circumvent these issues are presented.

Chapter 3   Advances in radiofluorination

3.1 Simplification of PET tracer production

The disadvantage of the centralization of PET tracer production is the limited availability of the wide range of tracers that is needed in order to match the diversity of disciplines and medical challenges that are under investigation. Either research centers must invest in production facilities of their own or obtain the desired tracer from centralized facilities at high cost. This has been one of the reasons for the envisioning of a decentralized production approach. With a decentralized production researchers are able, at a reduced cost, to produce desired tracers whenever they need them. This, however, requires that each batch of PET tracer is produced economically. Some of the changes that have to take place for this to be achieved are simplification (miniaturization) of equipment, which means minimal infrastructure requirements, together with simple - and preferably automated - synthesis, purification, as well as formulation strategies[48].

3.1.1 The "Dose on Demand" concept

If miniaturization and simplification are achieved it will facilitate a route to the emerging Dose-on-Demand (DoD) approach, where a single dose of tracer is produced, when it is needed for a specific PET scan. And where requests for another dose can be met, as the production line can be promptly restarted, maybe even from the same batch of starting radionuclide. This will provide a high flexibility for the users as well as low dose exposure to the personnel. A joined effort from both chemists, physicists and engineers are however needed, as development of benchtop-size microscale systems with fully integrated radiochemistry systems are ultimately a necessity[49].

An area of miniaturization that receives a lot of attention in radiochemistry is microfluidics. It is a technology that has the potential to increase the synthetic output in terms of higher RCY, shorter reaction times and reduced precursor consumption in addition to the advantages of DoD already

mentioned. This is due to precise control of reaction conditions including fast mixing and rapid heat transport. Microreactors for microfluidics consist of a network of micron-sized channels (typically 10-300 μm) together with filters, separation columns, electrodes and/or reaction loops/chambers edged onto a solid base at a size as small as a coin[50]. Microfluidics can be divided into continuous-flow and stop-flow (batch-mode) design. Continuous-flow design works by performing all synthetic steps such as mixing, heating and cooling continuously along a predefined fluid path (Figure 3-1). Batch-mode microfluidics can be described as a "micro-vessel system", where mixing or heating happens within one or more functional elements in a discontinuous flow[51].
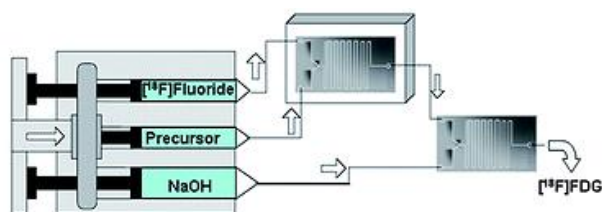
Figure 3-1. $[^{18}F]$**FDG synthesis by continuous-flow design**[52]

3.2 New radiofluorination approaches

The interest in improving the tracer production in a way that can comply with the tracer demand as well as miniaturization needs has triggered much investigation in the modification of conventional radiochemistry, as it limits the possibilities as it is right now. The primary predicament is reactivation of $[^{18}F]F^-$. The standard procedure with the kryptand elution from an anion-exchange resin and subsequent azeotropic evaporations described previously is very time-consuming and require complex automation. Consequently, significant efforts are done to eliminate this step. But also the limits set by standard reaction conditions such as solvent choice are under investigation.

3.2.1 Ionic liquids

Ionic liquids (ILs) are salts of very lipophilic cations and their counter ion. Room temperature ILs (rt ILs) have melting points below ambient temperatures and either one or both components are organic. The most common cations for rt ILs are alkylammonium, alkylphosphonium, *N-*

alkylpyridinium and N-alkylimidazolium ions (Scheme 3-1) while the anions can be BF_4, PF_6, SbF_6, triflate or tosylate[53].

$$[NR_xH_{4-x}]^+ \quad [PR_xH_{4-x}]^+$$
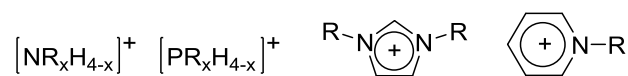
Scheme 3-1. Alkylammonium, alkylphosphonium, N,N′-dialkylimidazolium, and N-alkylpyridinium cations.

The properties that make them useful synthetic solvents are:

1. They solvate both organic and inorganic compounds and unusual combinations of reagents can be brought into same phase

2. The ions can be poorly coordinated which make them highly polar but noncoordinating to the reagents

3. They are immiscible with a range of organic solvents, thereby providing a non-aqueous polar alternative for two-phase systems

4. They are non-volatile, which eliminate containment issues

ILs has been used for the synthesis of [18F]FDG rapidly and with good yield and without the azeotropic drying step in a study by Kim and his coworkers[54]. Instead [18F]F⁻ was eluted from a QMA cartridge using 40% tetrabutylammonium bicarbonate (TBAB). The optimized conditions developed are shown in Table 3-1.
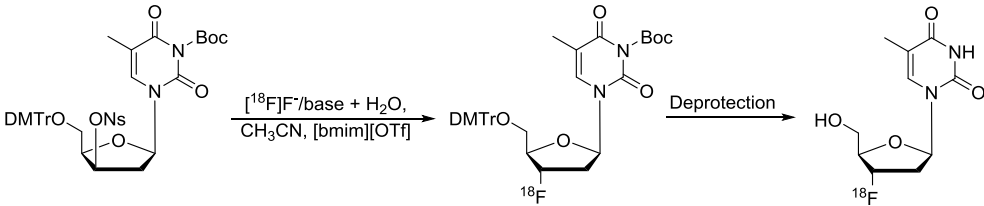
Table 3-1. [18F]FDG synthesis using IL.

Entry	[18F]F⁻/TBAB_aq (µL)	[bmim][OTf] (µL)	MeCN (µL)	Reaction time (min)	Temp (°C)	rTLC conversion (%)	RCY (%)
1	50	300	1000	5.5	100	75	49-59[a]

m(precursor) = 25 mg. [a]Depending on hydrolysis procedure

[18F]FLT has also been synthesized using IL as described in a study by Moon et al.[55]. Normally RCY of [18F]FLT is below 15% unless a substantial amount of precursor is used[56]. But in this study [18F]FLT was produced with reasonable yield with reduced amount of precursor. Also here [18F]F⁻ was eluted from a QMA cartridge, using aqueous K_2CO_3 for large amounts of trapped [18F]F⁻ or $KHCO_3$ for small amounts of trapped [18F]F⁻(Table 3-2).

Table 3-2. [^{18}F]FLT synthesis using IL.

Entry	[^{18}F]F$^-$/base+H$_2$O (μL)	IL (μL)	MeCN (μL)	Base	Reaction time (min)	Temp (°C)	rTLC conversion (%)	RCY (%)
1	5+75	200	250	KHCO$_3$	15	120	62	30
2	20+60	200	250	K$_2$CO$_3$	15	120	48	25

m(precursor) = 5 mg

3.2.2 Tertiary alcohols

A solution to the solvent limitations of the standard strategy can be the more recently developed nucleophilic aliphatic radiofluorination approach using tertiary alcohols as reaction media and fluoride sources such as [^{18}F]CsF[57,58]. Normally alcohols are not used for these reactions because of their solvation of [^{18}F]F$^-$, thereby retarding its nucleophilicity. But the tertiary alcohols enhance the radiofluorination in four significant ways (see Figure 3-2):

1. Hydrogen bonding to [^{18}F]F$^-$, thereby weakening the ionic bond between [^{18}F]F$^-$ and the counter cation

2. The bulk of the alcohol ensures that the hydrogen bond is not too strong, which provide a more "flexible" fluoride anion with the nucleophilicity still intact, but with reduced basicity

3. The *tert*-alcohol enhances the leaving-group activity of sulfonates by hydrogen bonding

4. Hydrogen bonding between substrate and the alcohol enhances selectivity by preventing side reactions such as elimination and intramolecular alkylation
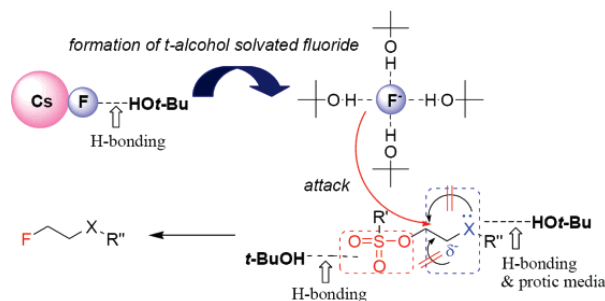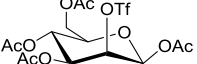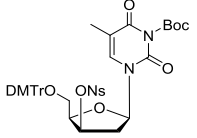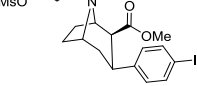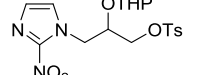
Figure 3-2. The effect of *tert*-alcohol on nucleophile radiofluorination

The PET tracers [18F]FLT, [18F]FP-CIT, and [18F]FMISO are produced with low yields, when applying the standard reaction conditions. However, the tertiary alcohol strategy has proved very useful for the radiofluorination of these PET tracers as is shown in Table 3-3[57].

Table 3-3. Improved RCY due to tertiary alcohol

Compound	Fluoride source	Alcohol	Product	RCY using *tert*-alcohols (%)	RCY using standard reaction conditions (%)
	[18F]CsF/K$_{222}$	*t*BuOH	[18F]FDG	85	60
	[18F]TBAF	*t*BuOH	[18F]FLT	66	15
	[18F]TBAF	*t*BuOH	[18F]FP-CIT	36	1
	[18F]TBAF	*t*AmOH	[18F]FMISO	70	15

3.2.3 Simplification mediated by solid support

The elution step is avoided in a procedure described by Voccia *et al.*[59] where they used a solid phase resin comprised of a non-ionic extraction or liquid chromatography resin of either polar or non-polar material. The resin was loaded with a trapping agent (TA) able to trap [18F]F- by an anion exchange process while remaining absorbed on the resin. The trapping agent was either a phase transfer catalyst (such as kryptofixes or crown ethers) complexed with a metal salt (alkali metal cation; halide, carbonate, carboxylate etc. as anion), a quaternary ammonium or phosphonium salt or an ionic liquid. The [18F]F-/[18O]H$_2$O solution was then passed through the resin and [18F]F- was extracted. After removal of most of the remaining water by a non-eluting solvent, the TA-[18F]F- complex was eluted with a solvent suitable for the subsequent radiofluorination step such as polar aprotic solvents or alcohols (primary and tertiary). The process is shown in Figure 3-3. Trapping efficiency was between 25% and 100% while elution efficiency was between 55% and 100% depending on the solid phase-SA-solvent combination. [18F]FDG synthesis based on this procedure had a striking RCY at 98% and the labeling efficiencies in general resulting from reaction between the TA-[18F]F- complex and either

aliphatic or aromatic precursors resulted in RCY above 63% with the exception of a piperonal precursor (42% RCY).

[18F] Fluoride
Water Solution

Extraction

Water

Organic Solvent and/or Gas

Purging/Drying

Organic Medium

Elution

[18F] Fluoride
Organic Solution

⬤ Solid Support ◯ Trapping Agent ▪ [18F] fluorides
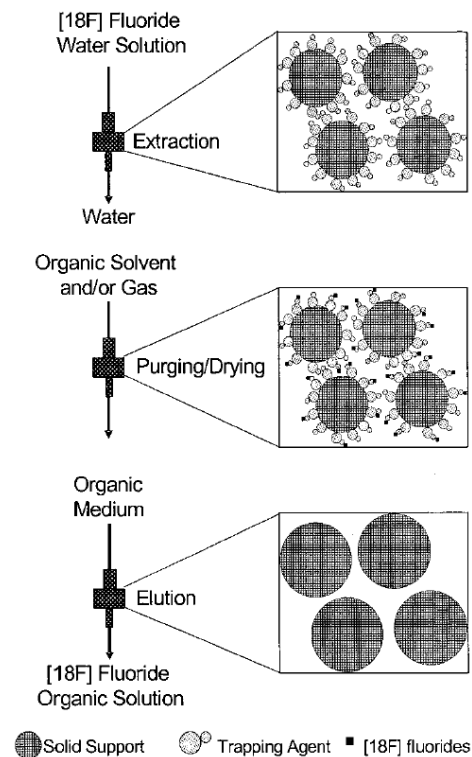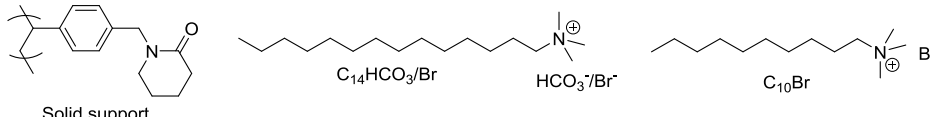
Figure 3-3. Trapping and subsequent elution of $[^{18}F]F^-$.

The same group[60] has also developed a similar method, but they used an ion exchange column (QMA and similar) onto which they extracted $[^{18}F]F^-$ from the $[^{18}F]F^-/[^{18}O]H_2O$ solution. They then eluted $[^{18}F]F^-$ from the column using an eluent containing a compound bearing a tertiary alcohol, diol or phenol functionality that enhances the solubility of the different components as well as a phase transfer agent able to mediate the release of $[^{18}F]F^-$ from the solid phase. The phase transfer catalyst was of the same compound groups as the TAs described above. Also here most of the water was removed by either a solvent (non-polar organic) or gas flush between trapping and elution. However, up to 3% water content in the eluted solution was tolerated in the subsequent radiofluorination step due to the presence of the tertiary alcohol or phenol functionalities in the mixture.

A method has also been described[61] where a water-wettable macroporous N-vinyl lactame/divinylbenzene copolymer (like Waters Oasis HBL) was functionalized with either N-

tetradecyltrimethylammonium bicarbonate ($C_{14}HCO_3$), N-tetradecyltrimethylammonium bromide ($C_{14}Br$) or N-decyltrimethylammonium bromide ($C_{10}Br$). This modification allowed for quantitative [^{18}F]F$^-$ trapping. After nitrogen purge of the column more than 90% of the trapped activity was eluted using dry aprotic solvents such as MeCN as the alkylammonium [^{18}F]fluoride in a solution containing up to 4850 ppm residual water. Nucleophilic radiofluorination using this solution resulted in efficient labeling of both aliphatic and aromatic precursors (Table 3-4), which meant that azeotropic evaporation was avoided. Labeling temperature could even be as low as 25°C (entry 4), which is beneficial for temperature-sensitive precursors. Addition of a basic additive (K_2CO_3+K222 or tetraethylammonium bicarbonate) was, however, sometimes necessary to achieve (entry 5, 7 and 8) or enhance (comparison of entries 1 and 2) radiofluorination.

Table 3-4. Radiofluorination using long-chain quaternary ammonium modified SPE cartridge

Entry	Support	Precursor	Additive	Solvent	Labeling °C/min	RCY %
1	$C_{10}Br$	FDG	-	MeCN	95/10	49
2	$C_{10}Br$	FDG	K_2CO_3/K222	MeCN	95/10	89
3	$C_{14}HCO_3$	FDG	-	MeCN	95/5	71
4	$C_{14}Br$	FDG	-	MeCN	25/20	66
5	$C_{10}Br$	Fallypride	K_2CO_3/K222	MeCN	95/10	55
6	$C_{10}Br$	Veratraldehyde	-	DMSO	190/20	68
7	$C_{14}Br$	Fluorobenzaldehyde	$(C_2H_5)_4N \cdot CO_3H$	DMSO	110/10	84
8	$C_{10}Br$	MPPF	K_2CO_3/K222	DMSO	170/20	57

3.2.4 Radiofluorination using [^{18}F]AlF

Complex molecules such as oligonucleotides, proteins, peptides and antibodies cannot be labeled by the standard radiofluorination protocol due to denaturation of the molecules because of the harsh reaction conditions. At the same time a lot of acidic functionalities are present, which would result in the destruction of the nucleophilicity of [^{18}F]F$^-$. Instead this type of compounds has been radiofluorinated using small organic prosthetic groups. These are labeled by the standard protocol and then purified. Afterwards they are coupled to the macromolecule. Acylation, alkylation and photochemical protocols are used as well as oxime, thiol/maleimide and click linkages. A second

purification step is then needed. This entire process is very cumbersome and takes 1-3 hours, which is too long for practical use, and the RCYs are often below 40%[62]. Normally these macromolecules are labeled using radiometals such as ^{68}Ga or ^{64}Cu through the application of a bifunctional chelator. Since ^{18}F form a very strong bond with Al^{3+} (670 kJ/mol) and this complex can coordinate strongly with such chelators[63] it was considered to use the same radiometal-labeling protocol with an [^{18}F]AlF complex, which would both eliminate the azeotropic drying step and add to the range of radiofluorination approaches.

This was indeed possible, which was first demonstrated by McBride et al.[64], who used [^{18}F]AlF to label the antibody pretargeting peptide IMP449 coupled with the NCS-derivatized chelator NOTA (NOTA-p-Bn-CS-D-Ala-D-Lys(HSG)-D-Tyr- D-Lys(HSG)-NH2, Scheme 3-2).
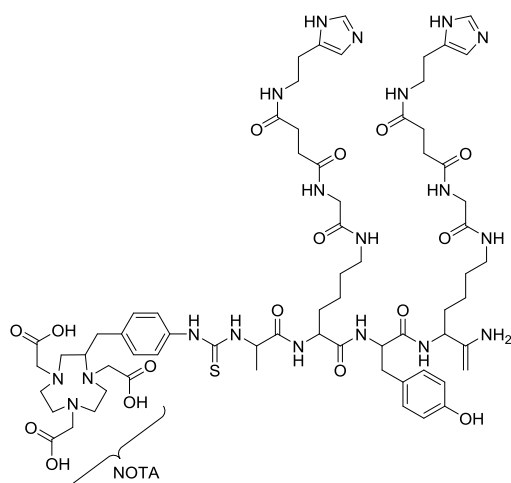
Scheme 3-2. IMP449 with the NOTA chelator

In this study [^{18}F]F- was trapped on a QMA cartridge, which was eluted using KHCO$_3$ (200 μL) and mixed with a solution of AlCl$_3$ in a pH 4 sodium acetate buffer (3 μL, 6 nmol Al(OAc)$_3$). This solution was added to a kit containing IMP449 (~ 0.8 mg) and heated at 100°C for 15 min. The crude reaction mixture was then purified by HPLC and a hydrophilic-lipophilic-balanced (HLB) column. The outcome was the desired radiolabeled peptide in 5-20%, without a drying step and with a total duration of 60 min.

With this in hand Laverman et.al.[65] turned to the labeling of the NOTA-coupled octreotide analogue designated IMP466 (NOTA-D-Phe-*cyclo*[Cys-Phe-D-Trp-Lys-Thr-Cys]-Throl, Scheme 3-3).

The procedure was very similar to the one described above and resulted in labeling of IMP466 with 50% RCY in 45 min.
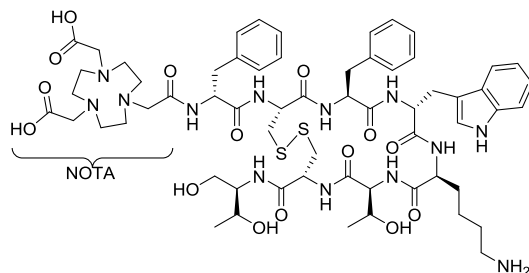
Scheme 3-3. NOTA-IMP466

The difference in RCY between these two procedures was suggested to be caused by participation of all three *N*-acetate arms in the complexation of NCS derivatized NOTA. The result is a restricted coordination site for binding ^{18}F compared to the more flexible coordination by directly-coupled NOTA because of the only two available *N*-acetate arms. To test this theory D'Souza *et al.*[66] synthesized the pentadentate chelator NODA-MPAA (methyl phenyl acetic acid spacer, Scheme 3-4), which was coupled to a pretargeting hapten-peptide (IMP485). In addition it was decided to elute [18F]F- using saline, thereby producing [18F]NaF. This eliminated the need to neutralize the very basic solution, resulting from $KHCO_3$ mediated elution, as complexation requires pH ~ 4. As [18F]NaF is produced routinely at most radiopharmacies it is readily available. The result was efficient radiofluorination when reacting IMP485 (10 µL, 20 nmol), $AlCl_3$ (10 nmol), [18F]NaF (100 µL) and EtOH (110 µL) at 105°C for 15 min with RCY at 79%. However, RCYs as high as 90% could be achieved when varying the amount of ethanol and [18F]NaF.
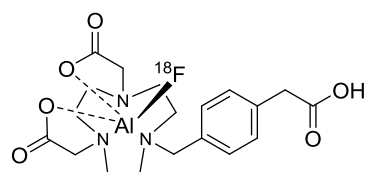
Scheme 3-4. NODA-MPAA structure

3.2.5 B-^{18}F and Si-^{18}F bond formation

Boron-fluorine as well as silicon-fluorine bonds are very strong (760 kJ/mol and 540 kJ/mol respectively[67]), which means that formation of those bonds could be another tool in the radiofluorination toolbox. Aqueous ^{18}F-labeling of a biotinylated p-aminophenylboronylpinacolate and a biotinylated (aminopropyl)-triethoxysilane was described by Ting *et al.*[68,69]. The procedure is shown in Scheme 3-5.

Dissolved in either DMF, MeOH, MeCN, DMSO or H$_2$O (5 μL, 60 mM)

Radioactive solution A1 (5 μL):
- 200 mM acetic acid pH 4.5
- 3.3 eq fluoride from a mixture of
  [^{18}F]F$^-$/[^{18}O]H$_2$O and 100 mM KHF$_2$
OR
Radioactive solution B1 (5 μL):
- 200 mM HEPES buffer pH 7.5
- 3.3 eq fluoride from a mixture of
  [^{18}F]F$^-$/[^{18}O]H$_2$O and 100 mM KHF$_2$

Radioactive solution A2 (5 μL):
- 200 mM acetic acid pH 4.5
- 3.3 eq fluoride from a mixture of
  [^{18}F]F$^-$/[^{18}O]H$_2$O and 130 mM KHF$_2$
OR
Radioactive solution B2 (5 μL):
- 200 mM HEPES buffer pH 7.5
- 3.3 eq fluoride from a mixture of
  [^{18}F]F$^-$/[^{18}O]H$_2$O and 130 mM KHF$_2$

Scheme 3-5. Radiofluorination by B-F or Si-F bond formation

Fluorination efficiencies were exceptionally high with almost 100% for the borate and 80% for the silicate. Carrier ^{19}F$^-$ was added in order to ensure stoichiometric addition of fluoride without having to work with significant amounts of activity. It was claimed, however, that the specific activity was high enough for PET imaging. These prosthetic groups could then serve as labeling precursors for labeling of proteins and peptides.

3.2.6 Electrochemical separation of [^{18}F]F$^-$ from [^{18}O]H$_2$O

It was realized by Saiki and coworkers[70] that electrochemical separation of [^{18}F]F$^-$ from [^{18}O]H$_2$O could be used for the concentration of [^{18}F]F$^-$ in a microfluidic cell. They designed a flow cell

where the surface of the upper plate was covered with platinum, while the bottom plate was covered with glassy carbon (GC). The inner flow channel between those plates was 100 μL high, 4 mm wide and 40 mm long with a volume of 16 μL. $[^{18}F]F^-/[^{18}O]H_2O$ was passed through this channel while a constant electrical potential was applied between the Pt cathode and GC anode (Figure 3-4).
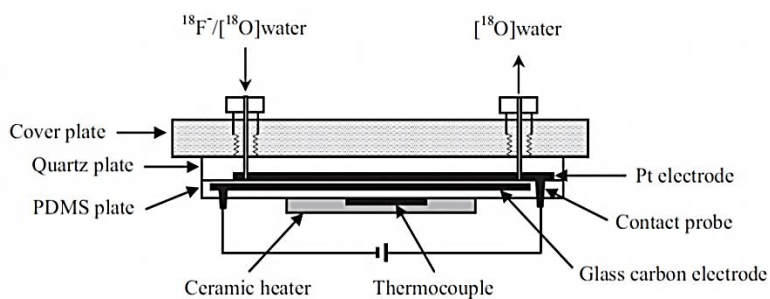
Figure 3-4. The microfluidic flow cell[71]

The short distance between the two electrodes allowed $[^{18}F]F^-$ to rapidly move to the GC surface from the flowing water. $[^{18}F]F^-$ deposition reached 90% at 10 V and the efficiency did not decrease with increased flow rate through the cell. The optimal parameters was determined to be 10 V and 700 μL/min. Release of deposited $[^{18}F]F^-$ was done into a MeCN solution containing K222/KHCO₃ and the optimum release at 70% happened at 80°C and -2 V for 1 min. A stop-flow method was applied where the flow of the solution was temporarily stopped and the release carried out. The result was a much more concentrated $[^{18}F]F^-$ solution than if release was carried out during constant solvent flow. The total time for deposition and release was only 6 min and the overall efficiency was above 60%. Subsequent microfluidic $[^{18}F]FDG$ synthesis was carried out and after 30 sec the ^{18}F-substitution was over 90%, due to the efficient mixing and heat transfer of the microfluidic reactions. The reaction was completed within 2 min.

3.2.7 Transition-metal mediated radiofluorination

Arene fluorination is a difficult reaction that requires harsh reaction conditions due to a substantial kinetic barrier to C-F bond formation. On the other hand, the C-F bond is also very strong (536 kJ/mol[67]), which makes especially the fluorination of aryl halides thermodynamically favorable. This means that the reaction can be improved by the use of catalysts and the search for appropriate

catalysts has been intense in recent years. Transition-metal catalysts have been a great part of this research. Both palladium- and copper-mediated radiofluorination procedures have been described with very good RCYs. Most of these procedures, however, also require extensive [18F]F⁻ drying before the reaction, which makes the procedures very comprehensive[72].

One of the exceptions to this drying strategy is described by Lee et al.[73], where they have used organometallic nickel complexes for a practical, one-step synthesis of aryl and alkenyl fluorides. A solution of [18F]F⁻/[18O]H₂O (2-5 μL) containing 18-cr-6 (2 mg) in MeCN (200-500 μL) was added to a mixture of nickel(II) complex **1** (1 mg) and the hypervalent iodine oxidant **2** (1.0 eq.) and the reaction was carried out at room temperature and ambient atmosphere in less than 1 min. In Scheme 3-6 the procedure is exemplified with the nickel complex **1a** for the synthesis of 4-[18F]fluorobiphenyl.
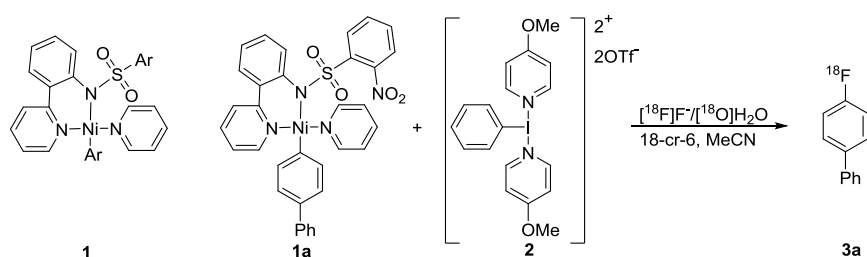
Scheme 3-6. Nickel-mediated radiofluorination using aqueous [¹⁸F]F⁻

RCY for this reaction was 42% in average after 1 min. The transformation was successful for the synthesis of alkenyl fluorides as well as electron-rich, electron-poor, ortho-, meta-, or parasubstituted as well as densely functionalized aryl fluorides as shown in Scheme 3-7.
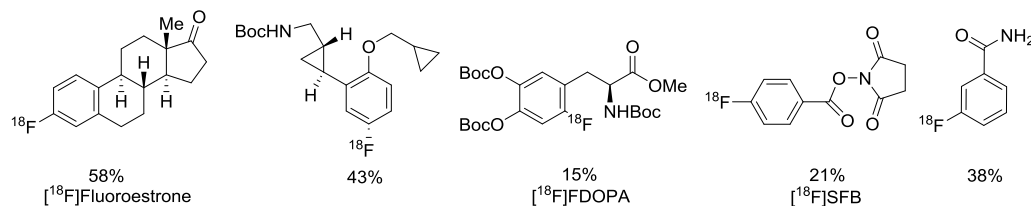
Scheme 3-7. Products from nickel-mediated radiofluorination with average RCYs

Benzylic C-H bonds were efficiently labeled by [18F]F⁻ by utilization of a manganese-salen catalyst in a procedure developed by Huang et al.[74]. The procedure involved elution of [18F]F⁻ from a Chromafix PS-HCO₃ IEX cartridge. This was done in one of two ways. Either by using K₂CO₃ in Milli-Q

water, which then was diluted with acetone and a portion was added to a reaction vial containing Mn(III)salen-OTs (17 mg, 22 μmol) and substrate (250 μmol). Or the activity was eluted directly using Mn(III)salen-OTs (15 mg, 30 μmol) in acetone and added to a vial containing the substrate. After stirring for 1 min the oxidant iodosylbenzene (PhIO, 55 mg, 250 μmol) was added and the mixture was stirred for 10 min at 50°C. Radiochemical yields from these procedures showed that no drying procedure was required, as labeling of benzylic C-H bonds in a wide range of substrates happened very efficiently with RCYs from 20% to 68%. As the reaction conditions were very mild the method could be used for late-stage labeling of a variety of well-known biologically active molecules or their protected analogues with RCYs from 22% to 72%. The procedure and some of the labeled biomolecules are shown in Scheme 3-8.
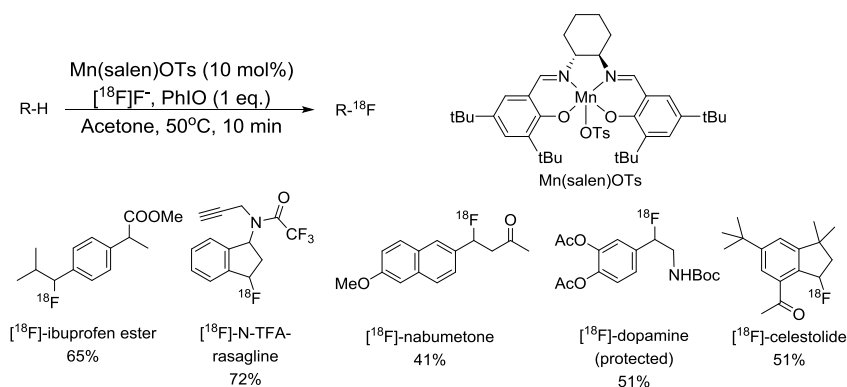
Scheme 3-8. Mn(salen)-mediated radiofluorination with resulting PET tracers (average RCYs)

An interesting transition metal-mediated approach was developed by Revunov and Zhuravlev[75] at our laboratory. They have, through the reaction of gaseous [18F]HF[76] combined with (-)tetramisole and (R,R)-Co(salen), accomplished the first enantioselective, single-step radiosynthesis of [18F]FMISO in 81% RCC and 55% enantioselectivity (Scheme 3-8). As the formation of gaseous [18F]HF results in up to 5000 ppm of water in the reaction vial it shows that this procedure is tolerant towards water to a certain degree. And as the RCY of [18F]FMISO is rarely very high as described previously, this procedure is another useful tool in the tool box.
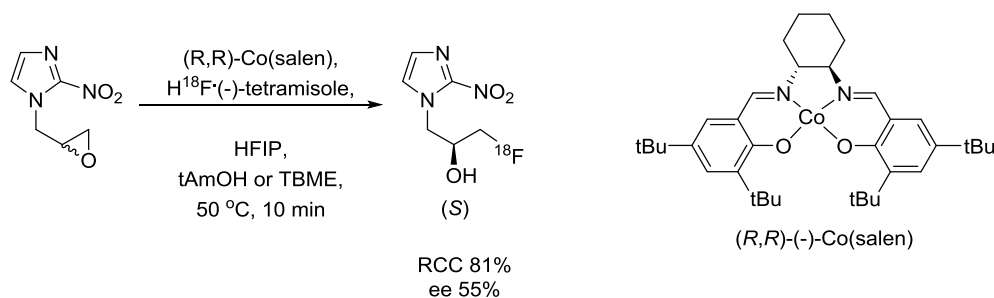
Scheme 3-9. Co(salen) mediated synthesis of [^{18}F]FMISO

3.3 Conclusion to Chapter 3

Extensive work has been carried out to simplify and speed up the process of radiofluorination. The primary approach has been to avoid the azeotropic evaporation step as this is both complex and time-consuming. And by the applications of alternative solvents or additives this has indeed been accomplished. Our approach, which is described in the following chapter, goes along this line of strategies as well.

Chapter 4 Homogeneous nucleophilic radiofluorination with phosphazene hydrofluorides

As described there are many ways to simplify and improve the conventional radiofluorination methodology. Our strategy was to achieve an almost naked and thereby very nucleophilically active [18F]fluoride ion, due to a significant cation/anion mismatch by complexation with phosphazene bases as phosphazene [18F]hydrofluorides. The work towards the development of a radiofluorination methodology based on these phosphazene [18F]hydrofluorides is described in this chapter.

4.1 Fluorination with organic base-hydrogen fluoride adducts

Anhydrous hydrogen fluoride is one of the most inexpensive fluorinating agents and has been widely used. However, working with HF is difficult due to the low boiling point (19.5°C). The very corrosive nature of HF also requires the reactions to be carried out in special equipment. In order to solve these issues less volatile complexes of HF with different bases have been studied.

In 1956 Hirshmann *et al.*[77] was the first to describe the fluorination with a base-HF complex as he discovered that epoxides could be fluorinated by HF in the presence of pyridine or THF. Since then stable solutions of HF with amines, amides, carbamic acids and esters as well as trialkyl phosphines have been described, but these seemed limited to specific fluorination reactions. In 1979 Olah *et al.*[78] described the use of a stable pyridinium poly(hydrofluoride) (30% pyridine, 70% HF) regent as a general purpose fluorinating agent for additions to alkenes and alkynes, deaminative and dediazonative halogenations as well as halogen substitutions of hydroxyl groups and halogen exchange reactions carried out at atmospheric pressure and with very good yields. The complex is now known as Olah's reagent and is a widely used fluorination reagent, but the application is still troublesome due to corrosion. A much less corrosive option is triethylamine tris(hydrogen fluoride) (also known as TREAT-HF or Franz reagent, Scheme 4-1), which can be used in borosilicate glassware without

significant etching. Both for addition and substitution reactions as well as desilylations TREAT-HF has proven useful as fluorination reagent. Also electrochemical fluorinations and aliphatic fluorine-chlorine exchange reactions under high-temperature microwave conditions proceed well with TREAT-HF[79,80].
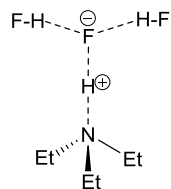
Scheme 4-1. TREAT-HF

The proton sponge (PS, 1,8-bis(dimethylamino)naphthalene) is a strong base (pK$_a$ 12.34) due to the strong N--H--N hydrogen bonds formed on monoprotonation. At the same time there is a significant strain in the system and a destabilizing effect of the overlap between the lone pairs of the diamines, which is released upon protonation. The "sponge effect", which is a very low rate of proton absorption, is caused by the hydrophobic shielding of the basic centers[81]. Due to these properties it was hypothesized that PS could bind the HF proton and thereby release fluoride for the labeling reaction as shown in Scheme 4-2.
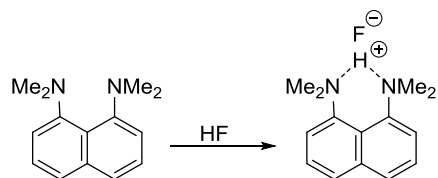
Scheme 4-2. PS-HF

It was indeed established by Chambers *et al.*[82,83] that PS-HF exists as shown above and not as free base plus dihydrofluoride and that the compound is useful as a fluoride ion donor in a range of fluorination processes with the advantage that is can be recycled. Later it was shown that PS-HF created in situ from PS and TREAT-HF not only resulted in increased fluorination ability, but it also increased regioselective and chemoselective chlorine replacement of dichlorodiazines[84]. No etching was reported for this complex due to the strength of the base. The only challenge was relatively long reaction times (>> 2 hours).

A method employing [^{18}F]PS-HF was described by Pascali *et al.*[85]. The method was rather limited in scope as ^{18}F incorporation only happened through halogen exchange with good radiochemical yields. However, the interesting thing was that when the reaction worked, the yields were comparable or better than the standard K222/K$_2$CO$_3$ radiofluorination protocol. And even more interesting was the fact that these reactions required 10% water as cosolvent. With [^{18}F]F$^-$ concentration by azeotropic evaporation prior to the labeling step no radiofluorination occurred.

4.2 Schwezinger's phosphazene bases

Based on the diminished HF dissociation with increased base strength seen in the studies above it is very likely that even stronger bases would effectively suppress dissociation completely.

While developing new base systems Schwezinger came across a group of neutral, peralkylated triaminoiminophosphoranes where no basicity, no synthetic procedure and no application were reported. It was found that the so-called phosphazenes surpassed the guanidine and amidine derivatives with regard to basicity[86]. A phosphazene base is made up of units consisting of a phosphorous atom [P(V)] bonded to four nitrogen atoms with the functionalities of three amines and one imine. They are classified as P$_n$ bases where n indicates the number of phosphorous atoms and thereby the number of units in the molecule as shown in Scheme 4-3.
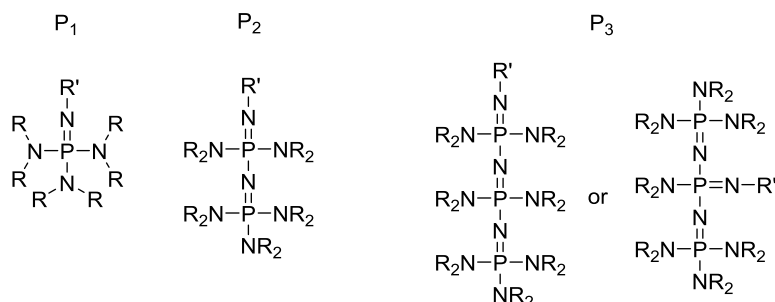
Scheme 4-3. Structure and classification of phosphazene bases

The basicity is reflected by the number of phosphorane units because of better charge delocalization in the conjugate cation. This also explains why phosphazene bases are stronger than guanidine and amidine bases, the number of isoelectronic forms being higher (Scheme 4-4).
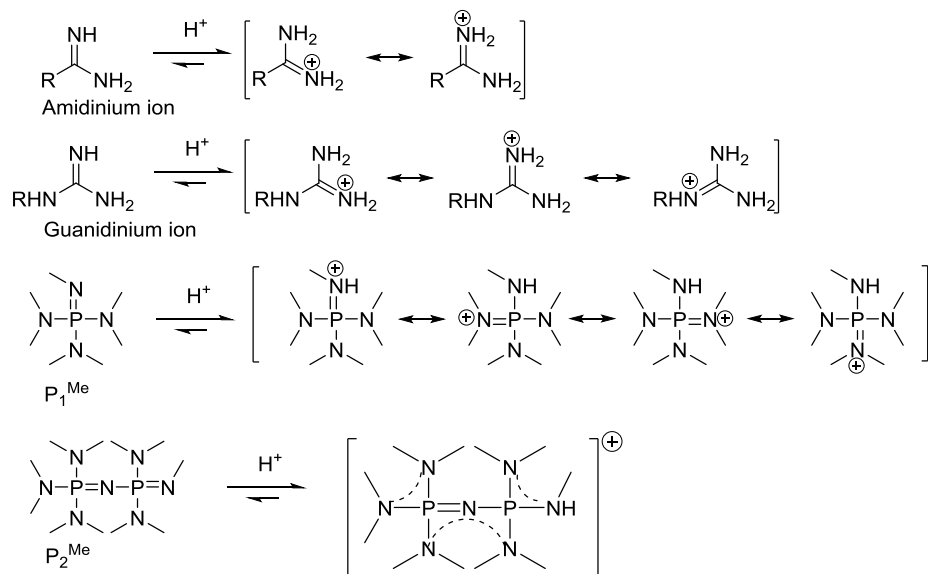
Scheme 4-4. Stabilization of cation by charge delocalization

The pK_a values for different phosphazenes as well as the classic amidines and guanidines for comparison are seen in Table 4-1.

Table 4-1. pK_a values of different phosphazene bases together with amidines and guanidines[87,88]
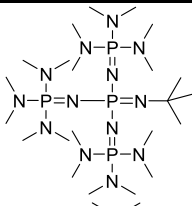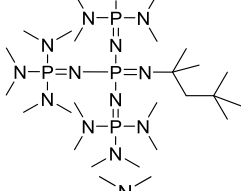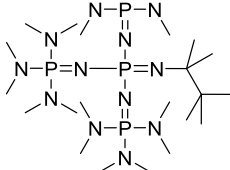
Entry	Base	pK_a (MeCN)	Structure
1	DBN	23.79	
2	DBU	24.33	
3	TBG	25.96	
4	MTBD	25.44	
5	P_1^{Me}	27.58	
6	P_1^{tBu}	26.88	
7	P_1 BEMP	27.5	

Entry	Base	pK$_a$ (MeCN)	Structure
8	P$_2^{Et}$	32.94	N–P=N–P=NEt
9	P$_2^{tBu}$	33.49	N–P=N–P=NtBu
10	P$_2^{tBu}$ cyclic	33.08	N–P=N–P–N (NtBu)
11	P$_3^{tBu}$ linear	36.6	N–P=N–P=N–P=NtBu
12	P$_3^{tBu}$ branched	38.6	N–P=N–P–N=P–N (NtBu)
13	P$_4^{tBu}$ branched	42.7	N–P=N–P–N=P–N (NtBu), N–P–N
14	P$_4^{tBu}$ branched NR$_2$ = pyrr	44.0	N–P=N–P–N=P–N (NtBu), Npyrr, pyrrolidine substituents
15	P$_5^{tBu}$ branched	45.3	N–P=N–P–N=P–N=P–N (NtBu), N–P–N
16	P$_7^{tBu}$ branched	45.3	N–P=N–P=N–P–N=P–N=P–N (NtBu), N–P–N, N–P–N

This table shows the trend of increasing basicity with the number of phosphorous units. However, the effect is biggest when going from P_1 to P_2 (entry 6 vs. entry 9) and for every additional phosphorous unit decreasing basicity increments were found. The limit to the homologation concept is P_7, which has the same basicity as P_5 (entry 15 vs. entry 16). This leveling effect indicates that resonance saturation exists in the cations of the larger systems. Branching of the phosphazenes also results in increased basicity (entry 11 vs. entry 12). This has been ascribed to stability differences of the free bases, rather than the cations, as linear conjugation in the neutral phosphazenes is more effective than cross conjugation. There is limited effect of the size of the imine substituent on the basicity for the P_1 bases, while a steric bulk results in a slight increase in basicity in the P_2 bases (entry 5 vs. entry 6 compared to entry 8 vs. entry 9). Cyclic pyrrolidine groups enhance the basicity due to inductive effect (entry 13 vs. entry 14). The same effect is, however, not seen when incorporating a pair of amino groups into a six-membered ring (entry 9 vs. entry 10)[87,89].

An advantage of the phosphazene bases is the limited nucleophilicity, which is a consequence of the shielding effect by the imine alkyl groups. This can be seen in Table 4-2, where the increasing steric bulk of the P_4 bases efficiently controls the alkylation of the bases when reacting with MeI[89].

Table 4-2. Decrease in nucleophilicity due to steric shielding

Base	Structure	k_{MeI} (rel.)
P_4^{tBu}		1
P_4^{tOct}		0.22
P_4^{Hept}		0.001

In 1991 Schwezinger *et al.*[90] described the first attempt on synthesizing phosphazenium fluoride salt by reacting $P_2 \cdot BF_4$ with KF in MeOH (Scheme 4-5).
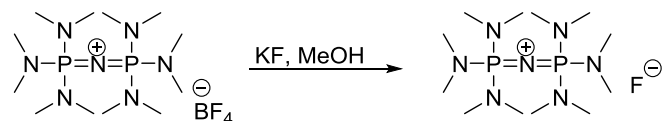
Scheme 4-5. Phosphazene fluoride salt formation

Through X-ray structure analysis, they found that in this salt, the cation-anion distance was 6.3 Å, which was the largest distance observed for any known fluoride salt. Six P-N bonds point to a fluoride ion (P-N-F = 178°) and one proton from each of the twelve methyl groups is positioned approximately icosahedral around it (Figure 4-1). The F-H distances (2.37 Å and 2.57 Å) are too large for hydrogen bonds, but can correspond to Van der Waals interactions. These findings indicated that the fluoride ion can be seen as "naked". The phosphazenium fluoride salt showed unique E2 reactivity as 1-alkenes were synthesized from 1-halides with good yields even at very low temperatures.
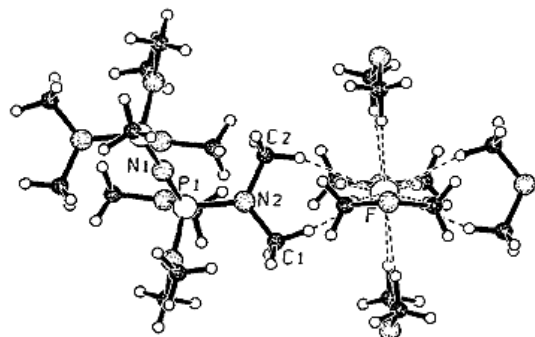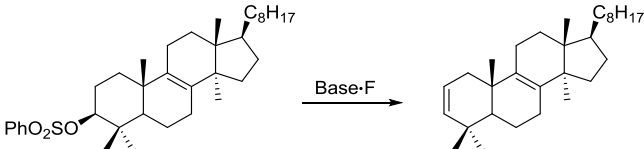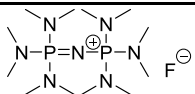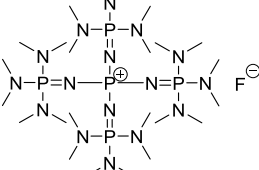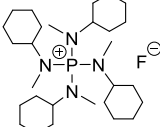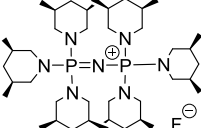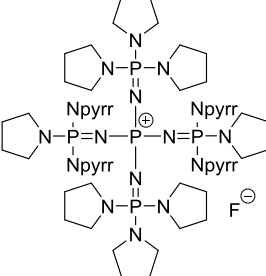
Figure 4-1. Crystal structure of $P_2 \cdot F$

Additional phosphazenium salts have been synthesized and analyzed with regard to reactivity[91]. Here it was demonstrated that phosphazenium fluoride salts are very reactive and extremely selective towards elimination. An example was the reaction between a sulfonated lanostenol derivative and the fluoride salts, where it with the exception of the P_1 fluoride salt, took between two to five minutes to achieve full conversion at 25°C with benzene as the solvent (Table 4-3).

Table 4-3. Elimination reaction with phosphazenium fluoride salts

Fluoride salt	Structure	t(min)
$P_2 \cdot F$		5
$P_5 \cdot F$, branched		2
$P_1 \cdot F$, R = Me; cyclohexane		1440
$P_2 \cdot F$, R = dimethylcyclohexane		5
$P_5 \cdot F$, branched, R = pyrr		3

The incredible anion reactivity was also demonstrated by Fruchard *et al.*[92]. The phosphazene base P_4^{tBu} was reacted with methyl phenylacetate where the first step was hydrogen abstraction by the base, resulting in a cation with its positive charge distributed over a volume of about 500 Å^3. The resulting anion-cation mismatch rendered the resulting "naked" enolate so reactive that subsequent alkylation using diemethyl sulphate was complete within one minute of reaction at -50°C in THF/hexane (8.4/1.6). Surprisingly, the study also showed that when changing the solvent ratio by adding just a little more hexane (THF/hexane 7.8/2.2) the ion pair formed was much more "tight" and with diminished delocalization of the negative charge into the phenyl ring. Subsequent alkylation was however only slightly slower than the one with the "naked" enolate (Scheme 4-6).
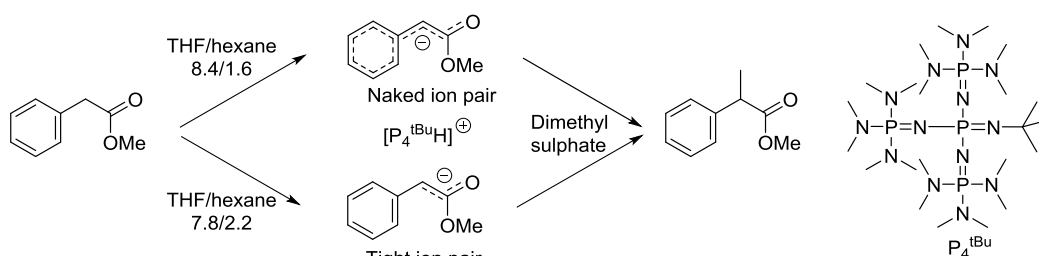
Scheme 4-6. Enolate formation by phosphazene base

In 2010[93] phosphazene bases were applied in radiofluorination as a mean to avoid the azeotropic evaporation by eluting $[^{18}F]F^-$ from the QMA cartridge with the use of strong bases, including phosphazene bases. It was hypothesized that the phosphazene base dissolved in MeCN would deprotonate the water present in MeCN and that the resulting hydroxide ion would be able to induce elution of $[^{18}F]F^-$ trapped on the QMA column as shown in Scheme 4-7.
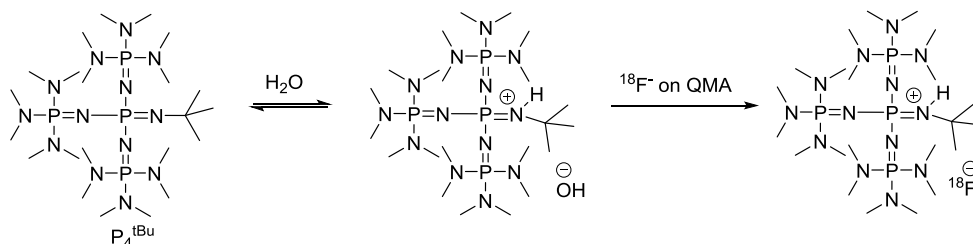
Scheme 4-7. Elution of $[^{18}F]F^-$ using a phosphazene base

It was initially analyzed whether P_2^{Et} would be able to elute $[^{18}F]F^-$ and if water content would influence on the elution efficiency. It was determined that dry acetonitrile resulted in no elution while water content between 3100 ppm to 25000 ppm gave almost quantitative elution (Figure 4-2 A). The needed elution volume was also smaller with eluents containing greater amounts of water. After establishing the necessity of water the relation between base strength and elution efficiency was investigated and it was concluded that pK_a values around 30 were required for quantitative elution of $[^{18}F]F^-$ when using an eluent containing 90 μmol base and 10900 ppm water in MeCN (Figure 4-2 B). The reactivity of the eluted $[^{18}F]F^-$ was evaluated through the labeling reaction of mannose triflate to $[^{18}F]FGD$. To the great surprise of the authors high and reproducible yields > 85% were only achieved with bases having a guadinine or phosphazene structure, no labile hydrogen atoms and a pK_a value

between 23 and 28 (BTMG, TMGN, MTBD, P_1^{tBu}, and BEMP). Stronger bases such as P_2^{Et} and P_4^{tBu} only resulted in RCY of 17% and 6%, respectively. The reason for the prerequisite features of these bases was unclear.
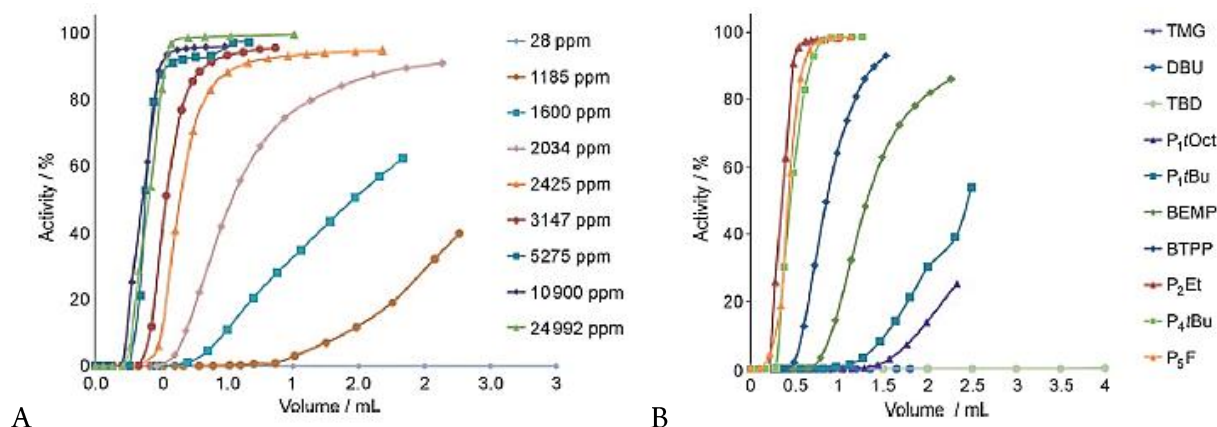
Figure 4-2. A: Water content dependence on P_2^{Et} elution of $[^{18}F]F^-$. B: Base strength dependence on elution of $[^{18}F]F^-$

4.3 Objective

The ability of phosphazenes to form strong complexes with fluoride was the reason why we chose them for the development of a one-step $[^{18}F]F^-$ recovery and nucleophilic activation procedure. But in light of the poor results previously described we decided another approach, which was to distill $[^{18}F]F^-$ from the $[^{18}F]F^-/[^{18}O]H_2O$ solution from the cyclotron as gaseous hydrogen fluoride. $[^{18}F]HF$ would then be trapped by a phosphazene base dissolved in the solvent intended for the subsequent radiofluorination step. The outcome would be chemical and radiochemical purification of $[^{18}F]F^-$ in addition to the nucleophilic activation. The radiofluorination step with the phosphazene hydrofluoride species were analyzed with respect to water tolerance and solvent as well as substrate scope. Simultaneously nonradioactive fluorination using phosphazene hydrofluorides was also investigated. This work is described in the following pages.

4.4 Article I - [^{18}F]Fluoride recovery via gaseous [^{18}F]HF

4.4.1 Introduction to the article

The conventional way for separating fluorine is by distillation from a solution of a strong mineral acid, from which it distils as hydrogen fluoride. Perchloric and sulphuric acid are the common choices, but due to explosion risks when working with perchloric acid, sulphuric acid is preferred[94,95].

Designing the setup for hydrogen fluoride distillation was guided by two main considerations. The first was the liberation efficiency of [^{18}F]HF gas, which was expected to be affected by three factors. Those were the significant energy of hydration, the low boiling point of hydrogen fluoride and finally the high viscosity of H_2SO_4 (1.84 g/cm^3). The second consideration was the corrosiveness and thereby the absorption of [^{18}F]HF to vessels and tubings, which meant that the material had to be chosen carefully.

The standard setup for the [^{18}F]HF generator (Figure 4-3) was three vessels connected by tubings, all made of polyethylene (PE). The first vessel was the reactor vessel, which contained sulphuric acid. To this vessel was added [^{18}F]F$^-$/[^{18}O]H$_2$O from the cyclotron. The second vessel was the receiving vessel and contained the phosphazene base dissolved in the solvent intended for the labeling step. The third vessel was a safety trap containing triethylamine in THF that could capture any [^{18}F]HF that had not been trapped in the receiving vessel. The receiving vessel and the safety trap were cooled to 0°C.
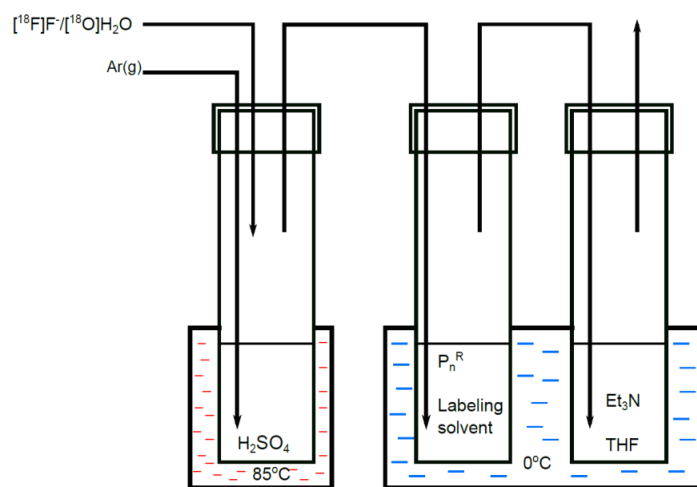
Figure 4-3. [^{18}F]HF distillation setup

Experiments clearly showed that vigorous Ar(g) purging (> 300 scc/min) of the reactor vessel was very beneficial for the [^{18}F]HF liberation efficiency. Further improvement of [^{18}F]HF liberation was achieved when ultrasound irradiation (240 W/35 kHz) of the reactor vessel was applied as well. We also analyzed the influence of the acid/water ratio. Those experiments showed that activity transfer worked very well despite a high water content in the reactor vessel (ratio of 4, 2 mL H_2SO_4:0.5 mL [^{18}F]F$^-$), while a ratio of 20 (4 mL H_2SO_4:0.2 mL [^{18}F]F$^-$) gave a marginally lower transfer efficiency. Experiments with other tubing material such as neoprene, natural rubber and PEEK (polyether ether ketone) showed that PE was preferable with regard to [^{18}F]HF absorption and chemical stability.

We analyzed the chemical purity of the distillate with regard to water as well as SO_3 and H_2SO_4 vapor. Water content increased from very few ppm to 5180 ppm as the highest after 30 minutes of distillation. As SO_3 and H_2SO_4 vapor would result in decrease in pH of the receiving vessel, pH was monitored during a 40 min distillation. The results showed that the change in pH is minimal within the 30 minutes that a standard distillation is carried out.

The work carried out regarding the development of a protocol for the [^{18}F]fluoride recovery via a gaseous [^{18}F]HF generator and subsequent trapping as phosphazene hydrofluorides is published[76] and presented on the following pages.

4.4.2 The article

[^{18}F]Fluoride recovery via gaseous [^{18}F]HF

Bente Mathiessen, Mikael Jensen, and Fedor Zhuravlev*

Acidification of target water with H_2SO_4 in a specially constructed glassy carbon/polyethylene apparatus allowed for recovery of up to 82% of [^{18}F]fluoride as [^{18}F]HF gas. The [^{18}F]HF distillate was found to be acid-free but moist; when passed through a solution of ^{t}BuPh$_2$SiOTf, it yielded [^{18}F]^{t}BuPh$_2$SiF. The multivariate design of experiment showed that the key to high yield of [^{18}F]HF was the efficient degassing of the reaction mixture.

Keywords: [^{18}F]fluoride; [^{18}F]HF

Introduction

^{18}F is the most commonly used positron emission tomography (PET) radionuclide because of its low positron energy (endpoint energy 0.6 MeV), optimal half-life (110 min), and favorable bioisosteric characteristics.[1] In the vast majority of cases, ^{18}F is introduced into organic molecules by reacting a suitably substituted substrate with [^{18}F]fluoride, produced by the ^{18}O(p,n)^{18}F reaction in a cyclotron. Although the ^{18}O(p,n)^{18}F reaction is inherently high-yielding, there is a caveat: obtained as a water solution, [^{18}F]fluoride is strongly hydrated and nucleophilically inert.[2] Its recovery and subsequent activation is usually achieved by the adsorption onto an ion-exchange resin, elution with a kryptand/base, and repeated azeotropic evaporation of water with acetonitrile. The latter step has been regarded as the bottleneck of the whole process. Consequently, significant efforts have been directed toward developing alternative approaches to [^{18}F]fluoride recovery and processing.[3] We have recently reported a new radiofluorination protocol where [^{18}F]fluoride, recovered as [^{18}F]HF gas, was trapped onto a phosphazene base and used to radiofluorinate a broad range of organic substrates.[4] In this note, we reveal the details of the [^{18}F]HF apparatus, analyze the distillate, describe the experimental conditions, and confirm the chemical identity of [^{18}F]HF.

Results and discussion

[^{18}F]HF could be produced by acidification of cyclotron-irradiated [^{18}O]-enriched target water with strong acid:

$$[^{18}F]F^-_{aq} + H^+ \rightarrow [^{18}F]HF$$
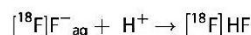
The resulting hydrogen fluoride (b.p. 19.5 °C), whose weak ionization[5] was expected to be further suppressed in the presence of a strong acid and elevated temperature,[6] could then be distilled as gas. This approach was reduced to practice in an apparatus consisting of two reaction vessels connected by a tube (Figure 1).

In the first vessel, the target water was mixed with 98% H_2SO_4, chosen for its nonvolatility, desiccating power, and thermal stability. The reaction with the acid produced gaseous [^{18}F]HF, which was driven into the second vessel by Ar flow. The second vessel contained an ice-cooled solution of triethylamine in THF and served as a trap. Because hydrogen fluoride is known to etch

glass, the initial experiments were conducted in high-density PE vessels equipped with PE tubing and stoppers. The preliminary runs at room temperature yielded no radioactivity in the trap. An increase in reaction temperature resulted in a gradual increase in the distillation rate of [^{18}F]HF, which leveled off at 85 °C. A 40-min [^{18}F]HF distillation allowed for recovery of $39 \pm 16\%$ (22 runs) of initial radioactivity found in the target water. We confirmed that the gaseous radioactive material was, indeed, [^{18}F]HF. In a control experiment, acidification of either the target water or the aqueous [^{19}F]HF, followed by the reaction of gas products with ^{t}BuPh$_2$SiOTf, yielded the corresponding isotopomers of ^{t}BuPh$_2$SiF[7], as measured by TLC and radio-TLC:

$$[^{18/19}F]HF + {}^tBuPh_2SiOTf \rightarrow [^{18/19}F]{}^tBuPh_2SiF$$

After establishing the basic process and the chemical identity of [^{18}F]HF, we analyzed the influence of apparatus material, amount of acid, and degassing efficiency on the yield of [^{18}F]HF. PE outperformed polyether ether ketone and natural rubber as reacting vessel and tubing material in terms of [^{18}F] absorption and chemical stability. Since the thermal stability of PE was a concern, we chose glassy carbon as a chemically and thermally resistant substitute. The preliminary experiments have also indicated that the yield of [^{18}F]HF was highly sensitive to Ar flow, which increased in magnitude and reproducibility when the reaction was run in an ultrasound bath. Therefore, all further experiments were carried out with the use of ultrasound.

To systematically explore the experimental space with minimal number of experiments, we employed the multivariate design of experiment (DoE), which served us well previously.[4] The reaction vessel material, temperature, amount of acid, and argon flow were set as experimental factors and were varied according to the DoE algorithm implemented in MODDE 9. The

Hevesy Laboratory, Technical University of Denmark, Risø National Laboratory, Frederiksborgvej 399, P.O. Box 494000 Roskilde, Denmark

*Correspondence to: Fedor Zhuravlev, Hevesy Laboratory, Technical University of Denmark, Risø National Laboratory, Frederiksborgvej 399, P.O. Box 49, 4000 Roskilde, Denmark.
E-mail: fezh@risoe.dtu.dk
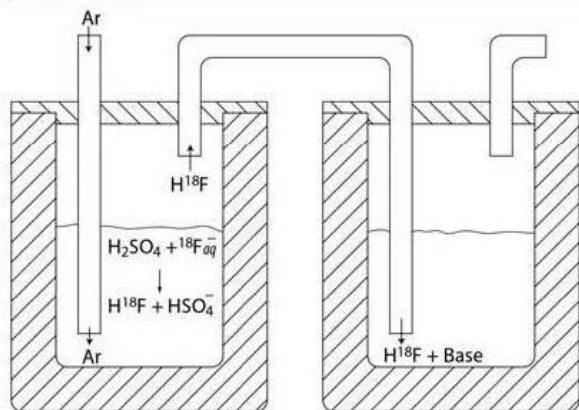
Figure 1. Schematics of the [^{18}F]HF apparatus.

Figure 2. Regression coefficients for the screening model: the effect of reaction parameters (X-axis) on [^{18}F]HF yield.

full factorial design resulted in a total of 11 experiments, 3 of which (entries 9–11) were replicated center points (Table 1).

For each experiment, we recorded the radiochemical yield of [^{18}F]HF. Fitting the results of the experiment with multiple linear regression implemented in MODDE yielded an excellent model (Figure 2, inset). The examination of the model coefficients revealed a strong and positive correlation of Ar flow with [^{18}F]HF yield. Surprisingly, neither the vessel material nor the amount of acid had any statistically significant effect on the yield (the error bars were larger than the coefficients and crossed the zero line, Figure 2), suggesting that it was the efficient degassing of the reaction mixture that controlled the yield of [^{18}F]HF. Consequently, running the reaction with ultrasound irradiation under a vigorous Ar flow (>300 ccm/min) allowed for recovery of up to 82% of initial [^{18}F]fluoride activity as [^{18}F]HF (average $62 \pm 11\%$, 15 runs).

Finally, we addressed the question of the chemical purity of the distillate. The distillation of gaseous material from hot aqueous sulfuric acid could potentially lead to a co-transfer of water vapor, SO_3, and H_2SO_4 vapor.[3] Indeed, a Karl Fischer titration of the acetonitrile solution in the trap indicated an increase of water content from 9 ppm to 5180 ppm after 30 min of distillation. The pH of the solution remained constant (7.5 ± 0.2) throughout the transfer.

In summary, [^{18}F]fluoride can be efficiently recovered from the target water as [^{18}F]HF gas. The key to high yield, reproducibility, and purity is efficient degassing of reaction mixture, which we achieved using vigorous Ar flow and ultrasound irradiation.

Experimental

Polyethylene (PE), glassy carbon (SIGRADUR) reaction vials, and glass pressure tubes were purchased from Kartell (Italy), HTW Hochtemperatur-Werkstoffe GmbH (Germany), and Aldrich, respectively. PE tubing (ID = 3 mm, OD = 4.5 mm) was purchased from Buch&Holm (Denmark); natural rubber (SUPRENE) tubing was obtained from New Age Industries. The ultrasound experiments were carried out using Sonorex DT52H, operating at 240 W/35 kHz. The aqueous solutions of [^{18}F]fluoride were prepared by the ^{18}O(p,n)^{18}F reaction in a GE PETtrace cyclotron using a 1.8-mL target of 95% enriched [^{18}O]water irradiated by a 14.1-MeV beam at 20–25 mA for 60–90 min. Thin layer chromatography (TLC) was run on precoated plates of silica gel 60 F254 (Merck). Radio-TLC was performed using a Raytest MiniGita TLC scanner. Karl Fischer titration was performed with a Metrohm 831 KF Coulometer. pH was determined using a calibrated WTW 330i pH meter. All solvents and reagents were purchased from Aldrich. Radiochemistry was performed without automation equipment.

Table 1. DoE screening studies for production of [^{18}F]HF

Entry	Vessel[a]	Acid/water[b]	Ar flow (cm/min)	[^{18}F]HF yield
1	PE	4	50	20
2	PE	20	50	16
3	PE	4	400	82
4	PE	20	400	51
5	GC	4	50	53
6	GC	20	50	20
7	GC	4	400	73
8	GC	20	400	76
9	PE	12	225	31
10	PE	12	225	48
11	PE	12	225	40

[a] PE, polyethylene; GC, glassy carbon.
[b] Volume ratio; total volume = 4.5 mL.

References

[1] S. M. Ametamey, M. Honer, P. A. Schubiger, *Chem. Rev.* **2008**, *108*, 1501–1516.
[2] C.-G. Zhan, D. A. Dixon, *J. Phys. Chem. A* **2004**, *108*, 2020–2029.

[3] (a) J. Aerts, S. Voccia, C. Lemaire, F. Giacomelli, D. Goblet, D. Thonon, A. Plenevaux, G. Warnock, A. Luxen, *Tet. Lett.* **2010**, *51*, 64–66; (b) D. W. Kim, Y. S. Choe, D. Y. Chi, *Nucl. Med. Biol.* **2003**, *30*, 345–350; (c) C. F. Lemaire, J. J. Aerts, S. Voccia, L. C. Libert, F. Mercier, D. Goblet, A. R. Plenevaux, A. J. Luxen, *Angew. Chem. Int. Edit.* **2010**, *49*, 3161–3164; (d) G. E. Smith, H. L. Sladen, S. C. G. Biagini, P. J. Blower, *Dalton Trans.* **2011**, *40h*, 6196–6205.

[4] B. Mathiessen, A. T. I. Jensen, F. Zhuravlev, *Chem. Eur. J.* **2011**, *17*, 7796–7805.

[5] (a) S. Re, *J. Phys. Chem. A*, **2001**, *105*, 9725–9735; (b) E. M. Cabaleiro-Lago, J. M. Hermida-Ramón, J. Rodríguez-Otero, *J. Chem. Phys.* **2002**, *117*, 3160.

[6] A. J. Ellis, *J. Chem. Soc.* **1963**, 4300–4304.

[7] R. Schirrmacher, G. Bradtmöller, E. Schirrmacher, O. Thews, J. Tillmanns, T. Siessmeier, H. G. Buchholz, P. Bartenstein, B. Wängler, C. M. Niemeyer, K. Jurkschat, *Angew. Chem. Int. Edit.* **2006**, *45*, 6047–6050.

[8] E. Verhoff, J. Banchero, *AIChE* **1972**, *18*, 1265–1268.

4.5 Article II – Homogeneous Nucleophilic Radiofluorination and Fluorination with Phosphazene Hydrofluorides

4.5.1 Introduction to the article

With a procedure for the synthesis of $P_n^R \cdot [^{18}F]HF$ in hand we turned to the development of the fluorination and radiofluorination methodology based on the phosphazene hydrofluorides. Octyl derivatives were used as model substrates for the fluorination study while naphthalene ethyl derivatives were used as model substrates for the radiofluorination study.
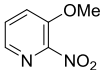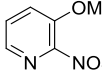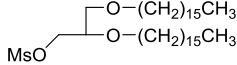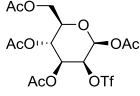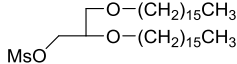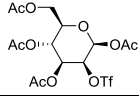
In addition to the $[^{18}F]$phosphazene hydrofluorides we also synthesized the ^{19}F isotopomers. The reason for the synthesis of "cold" phosphazene hydrofluorides was based on two considerations. The development of a fluorination strategy based on these would provide us with trackable products that could be isolated and analyzed and thereby provide us with insight into the underlying chemistry. Thereby we would have some basic guidelines from which we could develop a radiofluorination strategy. It was at the same time the expectation that this study would provide us with an efficient and versatile homogeneous fluorination methodology.

We were indeed able to carry out screening of the reaction conditions of the fluorination step using the "cold" phosphazene hydrofluorides, including solvent, vessel material and water content. The study resulted in a set of important factors influencing the outcome of the fluorination step. These were then optimized and the result was that the highest yield and selectivity of the labeling reaction would be achieved at 120°C and with a 46:54 tetramethylurea:mesitylene solvent mixture. These experimental conditions were also suitable for radiofluorination with the difference that toluene could replace the tmeu:Mes mixture without any loss in radiochemical yield.

These optimized reaction conditions were used to establish the substrate and base scope of the methodology (Table 4-4). The control reactions using $Et_3N \cdot 3HF$ or $Et_3N \cdot [^{18}F]HF$ resulted in no substrate conversion. Almost the same result did we get when using the P_1^R hydrofluorides, which was surprising considering the results from Lemaire[93] described previously. Further analysis showed that the reason was autofluorolysis of the P_1^R hydrofluorides. Pseudohalides and especially lipophilic substrates performed very well with the phosphazene $[^{18}F]$hydrofluorides and satisfyingly the FDG precursor was labeled with yields that outperform the $[^{18}F]$FDG synthesis strategy applied routinely. Also the

fluorination strategy was very efficient with regard to bromides and pseudohalides. The fluorination protocol also showed that this strategy was selective with regard to substitution compared to E2 elimination. However, the greatest feature of this fluorination and radiofluorination methodology was the tolerance of water, polar and nonpolar solvents as well as glass vessels as reaction vials.

Table 4-4. Results from the fluorination and radiofluorination strategies using phosphazene hydrofluorides

Reagent	Substrate^A	Time min	Yield %	Reagent	Substrate^B	Time min	Yield %
Et$_3$N·3HF	Octyl-Cl	60	0	Et$_3$N·[^{18}F]HF	NpEtOMs	20	0
P$_1^{tBu}$·HF	Octyl-Cl	60	Traces	P$_1^{tBu}$·[^{18}F]HF	NpEtOMs	20	0.6
P$_1^{tOct}$·HF	Octyl-Cl	60	Traces	P$_1^{tOct}$·[^{18}F]HF	NpEtOMs	20	0.4
P$_2^{Et}$·HF	Octyl-Cl	120	72	P$_2^{Et}$·[^{18}F]HF	NpEtCl	30	3
P$_2^{Et}$·HF	Octyl-Br	25	72	P$_2^{Et}$·[^{18}F]HF	NpEtBr	30	15
P$_2^{Et}$·HF	Octyl-I	10	59	P$_2^{Et}$·[^{18}F]HF	NpEtI	30	7
P$_2^{Et}$·HF	Octyl-OMs	<10	76	P$_2^{Et}$·[^{18}F]HF	NpEtOMs	30	91
P$_2^{Et}$·HF	Octyl-OTf	<5	95	P$_2^{Et}$·[^{18}F]HF	NpEtOTs	30	82
P$_2^{Et}$·HF	(pyridine OMe, NO$_2$)	180	47	P$_2^{Et}$·[^{18}F]HF	(pyridine OMe, NO$_2$)	30	11
P$_4^{tBu}$·HF	Octyl-Cl	60	38	P$_2^{Et}$·[^{18}F]HF	(MsO–, O–(CH$_2$)$_{15}$CH$_3$)	20	49
				P$_2^{Et}$·[^{18}F]HF	(AcO sugar OTf)	20	85
				P$_4^{tBu}$·[^{18}F]HF	NpEtOMs	20	70
				P$_4^{tBu}$·[^{18}F]HF	(MsO–, O–(CH$_2$)$_{15}$CH$_3$)	30	71
				P$_4^{tBu}$·[^{18}F]HF	(AcO sugar OTf)	30	82

A: 1.5 eq base·HF in toluene/DMF or tmeu/Mes (1:1), 120°C. B: 10 mg substrate, 52 μmol base·[^{18}F]HF, toluene, 120°C

The development of a fluorination and radiofluorination strategy based on phosphazene hydrofluorides is described in our second publication[96], which is presented on the following pages.

4.5.2 The article

Homogeneous Nucleophilic Radiofluorination and Fluorination with Phosphazene Hydrofluorides

Bente Mathiessen, Andreas T. I. Jensen, and Fedor Zhuravlev*[a]

70

FULL PAPER

Abstract: A series of phosphazenium hydrofluorides, $P_1^{tBu} \cdot [^{18/19}F]HF$, $P_1^{tOct} \cdot [^{18/19}F]HF$, $P_2^{Et} \cdot [^{18/19}F]HF$, and $P_4^{tBu} \cdot [^{18/19}F]HF$, was synthesized. The radioactive phosphazenium [18F]hydrofluorides were obtained by the one-step formation and trapping of gaseous [18F]HF with the respective phosphazene bases. The [19F] isotopomers were prepared from the corresponding phosphazene bases and $Et_3N \cdot 3HF$. Under the design of experiment (DoE)-optimized conditions, $P_2^{Et} \cdot HF$ and $P_4^{tBu} \cdot HF$ fluorinated alkyl chlorides, bromides, and pseudohalides in 76–98% yield, but gave lower yields with iodides and electron-deficient arenes. DoE models showed that fluorination can be performed in glass vessels, and that the reactivity of $P_2^{Et} \cdot HF$ and $P_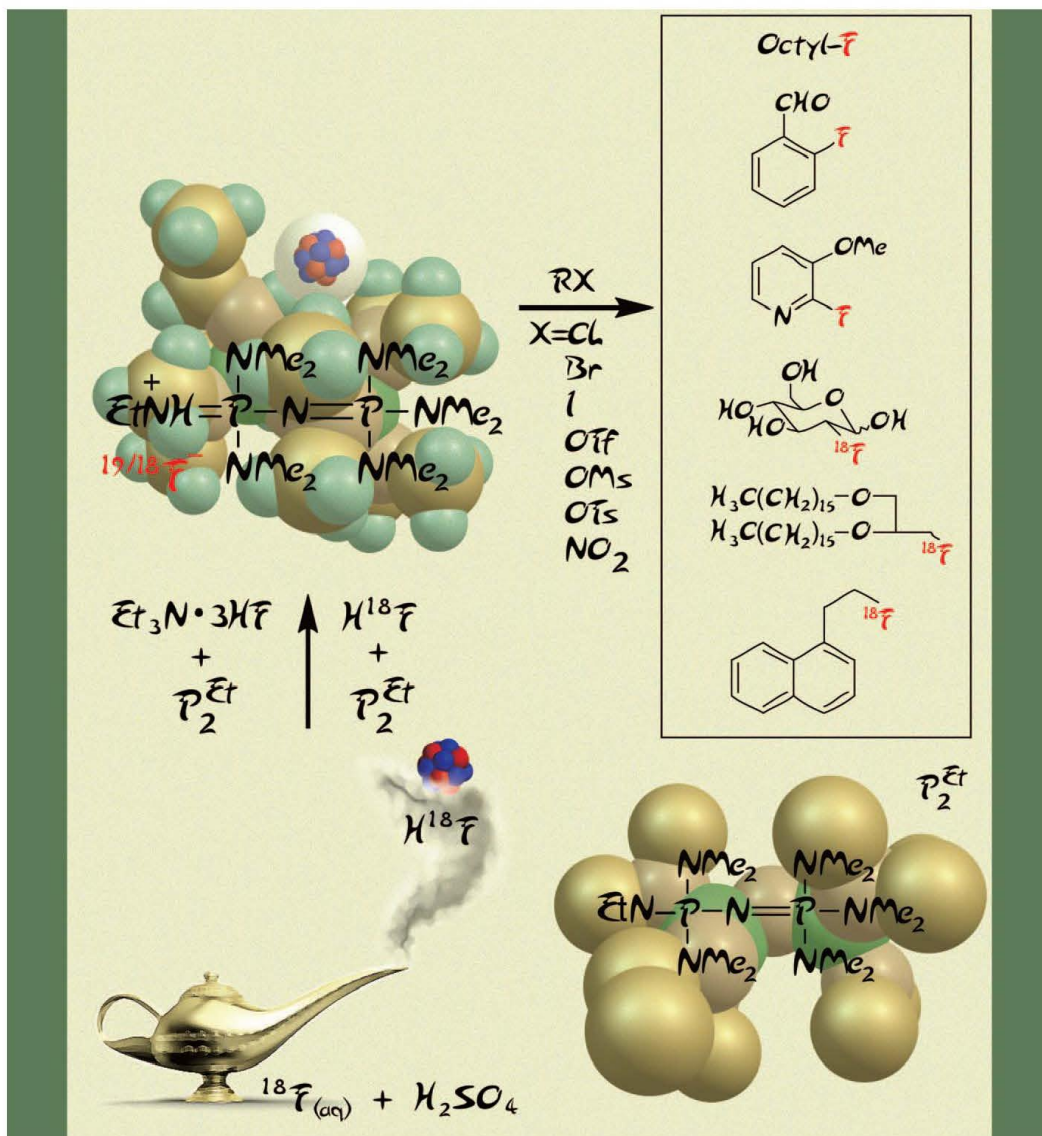4^{tBu} \cdot HF$ is dominated by solvent polarity but is insensitive to water to at least 2 equiv. In contrast, $P_1^{tBu} \cdot HF$ and $P_1^{tOct} \cdot HF$ were unstable towards autofluorolysis. DFT calculations were performed to rationalize this finding in terms of diminished steric bulk, higher Parr's electrophilicity, and chemical hardness of $P_1^R H^+$. The corresponding radiofluorination reaction gave no valid DoE model but displayed similar substrate scope. High specific activity and excellent radiochemical yields with various pseudohalides (81–91%) suggest that the proposed radiofluorination methodology can complement the current [18F]KF/Kryptofix methods, particularly in the areas for which nonpolar reaction conditions are required.

Keywords: fluorides · fluorination · nucleophilic substitution · phosphazenes · radiochemistry

Introduction

Over the years positron emission tomography (PET) has become an essential research and medical imaging modality.[1] Among different radioisotopes, biopharmaceutically[2] and PET friendly[3] [18F]fluorine is currently the most widely used. This drives the production of vintage[4] and the development of novel radiolabeled compounds.[5] As the 21st century technology of medical isotope production is gearing toward process automation[6] and device miniaturization,[7] one can anticipate that much of the future technical development will be shaped by the Procrustean bed of [18F]fluoride recovery and processing. In practice, if one wants to obtain [18F]fluorine in its highest specific activity one needs to run an $^{18}O(p,n)^{18}F$ reaction: the cyclotron-accelerated proton bombardment of [18O]-enriched H_2O, which yields [18F]fluoride as a water solution. At $-104\ kcal\,mol^{-1}$ of estimated free energy of hydration,[8] [18F]fluoride in water is nucleophilically inert. To restore its intrinsic nucleophilicity, water must be removed. In routine production, this is typically achieved by trapping [18F]fluoride on an ion-exchange column and subsequent elution with a kryptand, followed by repeated azeotropic evaporation of water. Due to the relatively short half-life of the radioisotope ($t_{1/2} = 110\ min$) and apparatus miniaturization requirements, simpler and more expeditious processes are sought after. The water evaporation step is often targeted for optimization,[9] and in some cases can be skipped altogether, for example: 1) by using ionic liquids;[10] 2) by eluting [18F]fluoride with strong organic base and protic additives;[11] 3) with polymer, loaded with alkylammonium carbonate;[12] 4) by radiofluorination performed directly on the resin;[13] and 5) by using a polydimethylsiloxane matrix for solvent exchange inside a microreactor.[7]

Our approach to [18F]fluoride recovery and radiofluorination was guided by the following considerations: 1) the recovery of [18F]fluoride and its intrinsic nucleophilicity must be achieved in no more than one step, physical or chemical; 2) to accommodate a wide range of biologically interesting substrates, including lipophilic, [18F]fluoride must be soluble in both polar and nonpolar solvents; and 3) the radiochemical yield must be at least 50% relative to target water. We became interested in alternative methods for a single-step [18F]fluoride recovery and nucleophilic activation. It occurred to us that instead of removing water from the radionuclide one can distill it as hydrogen fluoride gas.[14] This approach also has a corollary advantage as a chemical and radiochemical purification. Once liberated, [18F]HF can be trapped as N-onium hydrofluoride by using a strong organic base. Fluorination with organic base–hydrogen fluoride adducts, such as Olah's reagent (pyridine·nHF),[15] Franz reagent (Et_3N·3HF),[16] and ether-based HF adducts[17] is well precedented. Although readily available and moderately reactive, they have an unfortunate tendency to dissociate HF, thereby etching glass and causing side reactions. HF adducts of stronger bases, such as proton sponge, are less prone to dissociation, which allows for fluorination[18] and radiofluorination[19] of activated heterocycles. We hypothesized that stronger organic bases, such as Schwesinger's phosphazenes,[20b] would effectively suppress HF dissociation. Additionally, we believed that their bulk and globular shape would create a cation/anion mismatch, thus resulting in increased solubility and fluoride nucleophilicity. In tandem with radiofluorination we also investigated nonradioactive fluorination. This served two purposes: 1) fluorination would act as an isotopic "Sherpa" providing us with trackable or isolable products or intermediates and assisting in understanding the underlying chemistry; and 2) we also expected that this study would

[a] B. Mathiessen, A. T. I. Jensen, Dr. F. Zhuravlev
Hevesy Laboratory, Technical University of Denmark
Risø National Laboratory for Sustainable Energy
Frederiksborgvej 399, P.O. Box 49, 4000 Roskilde (Denmark)
Fax: (+45)46775347
E-mail: fezh@risoe.dtu.dk
Supporting information for this article is available on the WWW under http://dx.doi.org/10.1002/chem.201100458.

result in the development of a synthetically useful homogeneous fluorination methodology, applicable to a wide range of conditions and substrates.

Results and Discussion

Synthesis and characterization of P_n^R·HF: P_1^{tBu}·HF, P_1^{tOct}·HF, P_2^{Et}·HF, and P_4^{tBu}·HF were prepared by adding $1/3$ equiv of Et_3N·3HF to the solution of the corresponding phosphazene bases (Scheme 1) in diethyl ether [Eq. (1)]:

$$P_n^R + Et_3N \cdot 3HF \rightarrow P_n^R \cdot HF + Et_3N \cdot 2HF$$
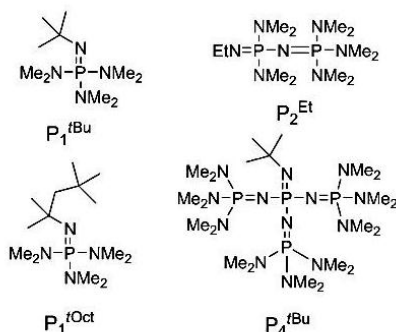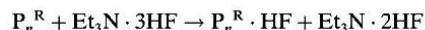
Scheme 1. Schwesinger's phosphazene bases P_n^R used in this study.

P_1^{tBu}·HF, P_1^{tOct}·HF, and P_4^{tBu}·HF precipitated out as very hygroscopic white solids; P_2^{Et}·HF separated as a mildly hygroscopic viscous oil. The compounds displayed prominent P_n^R·H$^+$ peaks in the positive mode of ESI-MS, and share many ^{1}H, ^{13}C, and ^{31}P NMR features with the reported earlier peralkyl phosphazenium cations. [20a] The ^{19}F chemical shifts for fluoride were found in the range of -150 to -153 ppm, which was consistent with the chemical shifts reported for other quaternary N-onium fluorides.[21] The synthesized P_n^R·HF were soluble in polar organic solvents, and also in benzene and toluene.

Synthesis of P_n^R·[18F]HF: We envisioned that the P_n^R·[18F]HF series of compounds could be obtained by reacting [18F]HF with the corresponding phosphazene bases [Eq. (2)]:

$$P_n^R + [^{18}F]HF \rightarrow P_n^R \cdot [^{18}F]HF$$
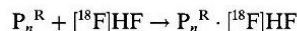
[18F]HF was generated by adding [18O]-enriched cyclotron-irradiated water to 98% sulfuric acid. The flow of Ar carried the liberated hydrogen fluoride to a trap containing a solution of P_n^R base in toluene. At the outset, we recognized that the large hydration energy of hydrogen fluoride,[22] its room-temperature boiling point (19.5°C), and the high viscosity of its H_2SO_4 solution would significantly affect the liberation efficiency of gaseous [18F]HF. Another con-

cern was the adsorption of [18F]HF to the reaction vessel and the tubing of the apparatus. The initial runs in polyethylene (PE) vials at room temperature yielded only traces of [18F]fluorine activity in the trap. Running the reaction at 85°C while vigorously (300 ccm min^{-1}) purging the solution with Ar improved radioactivity transfer to 39% (average of 22 runs). As a means to degas the bulk of the liquid and to reduce the adsorption of [18F]HF to the surface, we ran the [18F]HF synthesis in a glassy carbon vessel while applying constant ultrasound irradiation (240 W/35 kHz, 30 min). This proved successful: radioactivity transfer as high as 82% with an average of 71% could be achieved. Our attempts to characterize the synthesized P_n^R·[18F]HF by comparing their retention times with those of the stable isotope analogues using radio-TLC or radio-HPLC were stymied by extensive line broadening and decomposition on the sorbent.
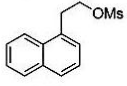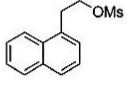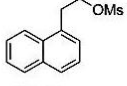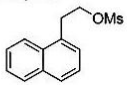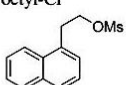
Initial P_n^R hydrofluoride screening: With P_n^R hydrofluorides in hand we turned to screening studies. Our objective was to identify a set of reaction conditions that had a statistically significant influence on the outcome of the fluorination. To simplify the screening we adopted a stepwise strategy. First, we ran both fluorination and radiofluorination with a set of P_n^R hydrofluorides under the same, albeit arbitrary, reaction conditions. The most active P_n^R hydrofluoride was then submitted to a series of experiments, in which we simultaneously varied a number of reaction parameters. The fluorination was performed in toluene at 100–120°C with 1-chlorooctane as substrate. 1-Naphthalenethyl methanesulfonate,[23] a substrate containing a UV chromophore, was chosen for radiofluorination under similar reaction conditions. The results of the P_n^R hydrofluoride screening are shown in Table 1.

A control experiment showed that the reference Et_3N·3HF and Et_3N·[18F]HF were inactive under the reaction conditions. Surprisingly, the P_1^R hydrofluorides also failed to give more than a trace level of products (Table 1, entries 3–6). On the other hand, P_2^{Et} and P_4^{tBu} hydrofluorides showed promising results in both fluorination (Table 1, entries 7 and 9) and radiofluorination (Table 1, entries 8 and 10). P_2^{Et} hydrofluoride, cheaper and less hygroscopic than its P_4^{tBu} congener, was chosen to enter the second stage of the screening process, in which we examined the influence of solvent, water content, and reaction vessel material.

Fluorination: screening the reaction conditions: The choice of reaction factors was guided by the following considerations. Fluoride is a powerful base[24] with enormous hydration energy.[8] Solvent polarity and hydration level are known to strongly affect fluoride's nucleophilicity and basicity.[25] The latter has another important ramification. In the majority of reported onium hydrofluorides, the fluoride anion successfully competes with the organic base for the proton, forming HF. Partial dissociation of HF, which leads to polyhydrofluorides, has been documented for pyridine,[15] triethylamine,[16b] and proton sponge hydrofluorides.[26] The dissociated HF is known to attack borosilicate glass.[16b] In our case, glass etching by [18F]HF would have a particularly

Table 1. Initial screening of P_n^R hydrofluorides for fluorination and radiofluorination efficiency.[a]

Entry	Reagent	Substrate	Yield [%][b]
1	Et₃N·3HF	octyl-Cl	NR[c]
2	Et₃N·[18F]HF	(naphthalene-CH₂CH₂-OMs)	NR
3	P_1^{tBu}·HF	octyl-Cl	traces
4	P_1^{tOct}·HF	octyl-Cl	traces
5	P_1^{tBu}·[18F]HF	(naphthalene-CH₂CH₂-OMs)	0.6
6	P_1^{tOct}·[18F]HF	(naphthalene-CH₂CH₂-OMs)	0.4
7	P_2^{Et}·HF	octyl-Cl	29
8	P_2^{Et}·[18F]HF	(naphthalene-CH₂CH₂-OMs)	85
9	P_4^{tBu}·HF	octyl-Cl	38
10	P_4^{tBu}·[18F]HF	(naphthalene-CH₂CH₂-OMs)	70

[a] Fluorination: 1-chlorooctane, P_n^R·HF (0.18 M), toluene, 100 °C, 1 h; radiofluorination: 1-naphthalenethyl methanesulfonate (52 μmol), 120 °C, 20 min. [b] Chemical or radiochemical yields as determined by GC or radio-TLC after purification on silica Sep-Pak. [c] NR: no reaction.

Table 2. Screening the reaction conditions: two-level full factorial design and results for fluorination of 1-chlorooctane with P_2^{Et}·HF[a].

Entry	Solvent	Reaction vessel	H₂O equiv.	Conversion [%][b]	1-Fluorooctane yield [%][b]	1-Octene yield [%][b]
1	toluene	steel	0	41	17	2
2	HMPA	steel	0	55	28	13
3	toluene	glass	0	40	28	3
4	HMPA	glass	0	67	17	10
5	toluene	steel	2	11	6	0
6	HMPA	steel	2	57	34	9
7	toluene	glass	2	34	29	3
8	HMPA	glass	2	69	29	10
9	toluene	steel	1	25	23	3
10	toluene	steel	1	17	18	2
11	toluene	steel	1	28	14	1

[a] Reaction conditions: 1-chlorooctane, P_2^{Et}·HF (0.18 M), 100 °C, 2 h. [b] Determined by GC.

detrimental effect as it would lead to trapping of [18F]fluoride in the walls of the reaction vessel. It was therefore important to consider the effect of the reaction vessel material. Because the underlying reason for the above-mentioned effects is ultimately rooted in the strength of the H−F bond, it was conceivable that the experimental factors we have just discussed are correlated. Therefore, a screening methodology that relies on the traditional "changing one separate factor at a time" (COST) approach would be a poor strategy, as it would fail to unravel a correlation if it existed. An unreasonably large number of experiments and the propensity to fall into local minima are other disadvantages of the COST method. A better approach was to use a multivariate statistical experimental design known as the design of experiment (DoE).[27] In DoE, the factors deemed important are systematically and simultaneously varied, thus allowing for statistically driven analysis of correlated data in a limited number of experiments. Changing the experimental conditions (factors) according to the DoE algorithm, and consequently measuring the results of the experiments (responses) would produce a model, typically in the polynomial form. The sign and the relative value of the coefficients define the contribution of the factor to the overall model. Table 2 describes our experimental design.

A reaction matrix, consisting of eight experiments plus three central point replicates (Table 2, entries 9–11) was generated by using a specialized DoE software

MODDE 9.0.[28] Three reaction factors were varied: the solvent polarity, the amount of water, and the reaction vessel material. We chose toluene as a nonpolar solvent ($E_T^N =$ 0.099) and hexamethylphosphoramide (HMPA; $E_T^N =$ 0.315)[29] as a polar aprotic solvent. The level of hydration was controlled by adding water to the reaction mixture. For each experiment we recorded three responses: the yield of the desired S_N2 product (1-fluorooctane), the yield of E2 byproduct (1-octene), and the conversion of the starting material. Fitting the data with partial least-squares (PLS) regression (MODDE) resulted in a statistically satisfactory model for all three responses (see the Supporting Information). The examination of the model coefficients revealed a number of interesting features. As expected, HMPA increased the reactivity of the substrate and promoted E2 elimination (Figure 1, red bars). The reaction vessel material was important: the conversion of the substrate was faster in a glass reaction vessel, but slower in a steel container (Figure 1, blue bars). There was also a small but statistically significant contribution to the yield from a correlated effect of reaction vessel material and the solvent. A combination of toluene in glass or HMPA in steel increased the yield, whereas the opposite combination decreased it (Figure 1, cyan bars). Surprisingly, water did not have any statistically significant effect on either the conversion or the yield (the confidence intervals for the corresponding coefficients cross the zero line).

Fluorination: optimizing the reaction conditions: The model resulting from the screening experiments identified the important factors to be used later in optimization studies. To minimize byproduct formation we optimized fluorination with respect to both the fluoride yield and substrate selectivity. The solvent polarity was chosen as a quantitative parameter for optimization as it affected the rates of both conversion and elimination. From a practical point of view, we also felt it was necessary to substitute toxic HMPA for a benign polar aprotic solvent. Unfortunately, the attempt to use DMSO led to oxidation of the substrate to 1-octanal in what
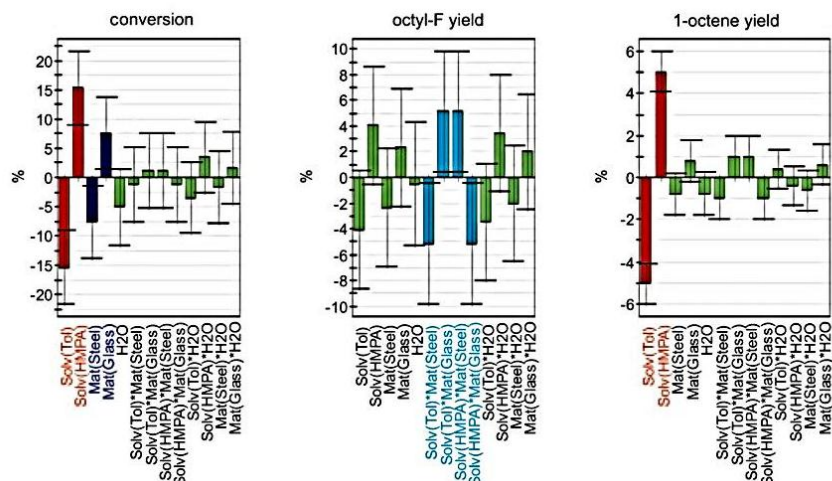
Figure 1. Regression coefficients for the screening model: the effect of reaction parameters (x axis) on 1-chlorooctane conversion (left), 1-fluorooctane yield (center), and 1-octene yield (right). Tol: toluene.

tures and polar solvent, whereas the corresponding selectivity is higher at the lower values of these parameters.

A so-called "sweet spot" graph shows the optimal operating region, which is located approximately in the center of the graph and corresponds to the median values of temperature and solvent polarity (Figure 3). A simplex-driven software optimizer included with MODDE predicted the highest yield and selectivity at 120 °C and 46:54 tmeu/Mes.

Fluorination: the substrate scope: The optimized reaction conditions were used to investi-

appears to be a Swern-like process,[30] driven by the basicity of fluoride (Scheme 2).
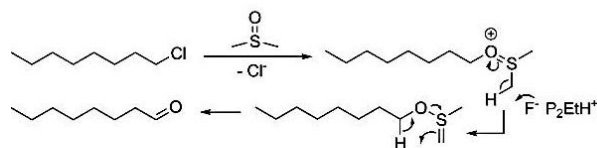
Scheme 2. Oxidation of 1-chlorooctane with DMSO in the presence of $P_2^{Et}HF$.

Table 3. Optimization: central composite face-centered design and results for fluorination of 1-chlorooctane with $P_2^{Et}\cdot HF$.[a]

Entry	Temp. [°C]	tmeu [vol %][b]	Yield [%][c]	Selectivity [%][d]
1	100	0	3	66
2	150	0	19	58
3	100	100	22	58
4	150	100	34	49
5	100	50	18	75
6	150	50	36	60
7	125	0	16	67
8	125	100	31	51
9	125	50	33	74
10	125	50	33	75
11	125	50	29	69

[a] Reaction conditions: 1-chlorooctane, $P_2^{Et}\cdot HF$ (0.18 M), 1 h. [b] Binary mixture of tetramethylurea (tmeu) and mesitylene (Mes). [c] Yield of 1-fluorooctane as determined by GC and/or quantitative NMR spectroscopy. [d] 1-Fluorooctane selectivity is defined as a ratio of 1-fluoroctane to spent 1-chlorooctane, as determined by GC.

DMF and tetramethylurea (tmeu) were found to be good alternatives to HMPA. Tmeu was subsequently chosen as solvent because its hexane miscibility was compatible with our GC protocol. Reaction temperature was chosen as another quantitative factor. Due to a wider range of reaction temperatures required for optimization runs, we used high-boiling mesitylene (Mes) instead of toluene. Because glass was well tolerated and the chemistry was insensitive to moisture, we ran the optimization in glass reaction vessels in HPLC-grade solvents. Once again, 1-chlorooctane was used as a substrate. A central composite face-centered design algorithm implemented in MODDE 9.0 was used to generate an experimental setup, consisting of nine experiments plus three replicated center points (Table 3). The results of 11 runs were fitted with multiple linear regression (MLR) producing a quadratic model of excellent statistical quality (see the Supporting Information).

The contour plot illustrates how 1-fluorooctane selectivity and yield change in response to the changes in temperature and solvent polarity (Figure 2). Both responses are nonlinear. The yield of 1-fluorooctane benefits from high tempera-

Figure 2. Response surfaces for 1-fluorooctane selectivity and yield as a function of solvent polarity and temperature (see Table 3).

74
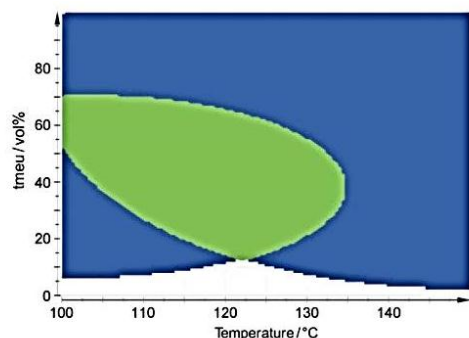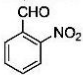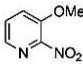
Figure 3. Sweet spot plot as a function of solvent polarity and temperature.

Table 4. Fluorination with P_2^{Et}·HF: the substrate scope.

Entry	Substrate[a]	Yield [%][b]	Alkene [%]	Selectivity [%][c]	Time [min][d]
1	octyl-Cl	72	8	88	180
2	octyl-Br	72	14	78	25
3	octyl-I	59	35	63	10
4	octyl-OMs	76	0	76	<10
5	octyl-OTf	95	0	95	<5
6	CHO / NO2	34	–	N/A	320
7	OMe / NO2	47	–	N/A	180

[a] Substrate (0.18 M), P_2^{Et}·HF (0.28 M, 1.5 equiv) in toluene/DMF or tmeu/Mes (1:1), 120°C. [b] Yield of the fluorides as determined by GC and/or quantitative NMR spectroscopy. [c] Fluoride selectivity defined as the ratio of fluorinated product to spent substrate. [d] Reactions were run to >90% conversion. Ms: methanesulfonyl, Tf: trifluoromethanesulfonyl, N/A: not applicable.

gate the scope of nucleophilic fluorination and access the relative reactivity and selectivity (Table 4). Alkyl halides were reactive and their reactivity followed the expected order: I > Br > Cl. Unfortunately, the E2 elimination also followed the same order; thus, the selectivity was opposite (Table 4, entries 1–3). Octyl triflate and mesylate reacted within several minutes giving high yields of 1-fluorooctane and no 1-octene. Overall, pseudohalides appear to be the best substrates for fluorination as they react quickly and cleanly.

When reacted with P_2^{Et}·HF, electron-deficient arenes undergo S_NAr fluorination. The nitro group can be substituted to give low-to-moderate yields of aryl fluorides (Table 4, entries 6 and 7).

Table 5 showcases the reactivity of homogeneous P_2^{Et}·HF-based fluorination by comparing it with several other popular nucleophilic fluorination systems. Although biased by the reagent-specific optimization, the results clearly indicate superior reactivity of P_2^{Et}·HF toward 1-chlorooctane.

Radiofluorination: A similar "screen–optimize–run" strategy was adapted for radiofluorination, this time including

Table 5. Comparative performance of different nucleophilic fluorination systems under the same reaction conditions.[a]

Entry	Reagent	Conversion [%]	1-Fluorooctane [%]
1	Et3N·3HF	5	0
2	proton sponge·HF	1	0
3	KF/Kryptofix 2.2.2	24	4
4	P_2^{Et}·HF	>95	72

[a] Reaction conditions: 1-chlorooctane (1 equiv, 0.18 M), fluorination reagent 1.5 equiv/F in tmeu/Mes (1:1), 120°C, 3 h.

reaction temperature as an additional reaction factor. Our software-generated screening reaction matrix now contained solvent, temperature, reaction vessel material, and H_2O as the reaction factors, and radiochemical yield as a single response. Table 6 lists the results of the 20 experiments that used 1-naphthalenethyl methanesulfonate as a substrate and the putative P_2^{Et}·[18F]HF as radiofluorination reagent.

Despite good reproducibility (Table 6, entries 9–11), no statistically valid model emerged from radiofluorination screening (see the Supporting Information). Visual inspection of Table 6 also revealed no discernable pattern. Although the insensitivity of radiofluorination to H_2O and reaction vessel material was not surprising given the results of fluorination screening, a solvent and temperature dependence was anticipated. Although at this stage of development the rationalization of these observations is largely speculative, we recognized that a "no model" outcome does not rigorously rule out the importance of the screened factors. Rather, it may indicate that these are masked by some dominant factor(s), which we have not yet been able to identify, for example the presence of impurities acting as an [18F]fluoride trap. Further experiments showed that the ex-

Table 6. Radiofluorination screening: fractional factorial resolution IV design and results for radiofluorination of 1-naphthalenethyl methanesulfonate with P_2^{Et}·[18F]HF.[a]

Entry	Solvent	Temp. [°C]	Reaction vessel	H_2O [μL]	Time [min]	RCY [%][b]
1	toluene	80	copper	10	45	0
2	DMF	80	copper	0	15	60±9
3	toluene	140	copper	0	45	39±7
4	DMF	140	copper	10	15	60±7
5	toluene	80	glass	10	15	42±6
6	DMF	80	glass	0	45	59±4
7	toluene	140	glass	0	15	86±5
8	DMF	140	glass	10	45	84±8
9	toluene	110	copper	5	30	42±6
10	toluene	110	copper	5	30	43±7
11	toluene	110	copper	5	30	45±8
12	toluene	80	copper	0	15	83±9
13	DMF	80	copper	10	45	29±3
14	toluene	140	copper	10	15	88±7
15	DMF	140	copper	0	45	57±5
16	toluene	80	glass	0	45	91±4
17	DMF	80	glass	10	15	28±2
18	toluene	140	glass	10	45	81±9
19	DMF	140	glass	0	15	83±4
20	toluene	110	copper	5	30	58±7

[a] Reaction conditions: 1-naphthalenethyl methanesulfonate (10 mg), solvent (2 mL). [b] Radiochemical yield, determined as an average of two runs.

perimental conditions, optimized for fluorination, are also suitable for radiofluorination. We also found that a tmeu/Mes mixture could be substituted for toluene without any noticeable loss in radiochemical yield. Consequently, the substrate scope was examined at 120°C in toluene (Table 7). In parallel with fluorination, alkyl pseudohalides proved to be excellent substrates, consistently giving high radiochemical yields (Table 7, entries 2–4). Importantly, mannose triflate can be converted into [18F]fluorodeoxyglucose ([18F]FDG) without any loss of stereochemical integrity (Table 7, entry 1). We were pleased to find that our new radiofluorination protocol was fully compatible with highly lipophilic substrates, such as the mesylate of glycerol ether (Table 7, entry 2). Although radiofluorination with a conventional [18F]KF/Kryptofix system has repeatedly failed to give more than 5% conversion, the reaction with $P_4^{tBu} \cdot [^{18}F]HF$ in toluene furnished the requested fluoride in 71% yield. In contrast to fluorination, alkyl halides did not perform well in radiofluorination: the highest yield of only 15% was obtained when the leaving group was a bromide (Table 7, entry 6). Nucleophilic substitution of a nitro group in pyridines also proceeded with lower yields. The amount of "cold" [19F]1-(2-fluoroethyl)naphthalene in radiofluorination was below the HPLC detection limit for this substrate

(156 ng mL^{-1}), corresponding to specific activity of at least 1.35 Ci µmol^{-1}.

Autofluorolysis of $P_1^R \cdot HF$: The success of $P_2^{Et} \cdot HF$ and $P_4^{tBu} \cdot HF$ as (radio)fluorination reagents raised the question as to why $P_1^{tBu} \cdot HF$ and $P_1^{tOct} \cdot HF$ gave no (radio)fluorination product. This was even more surprising because the reactivity pattern we described ($P_2^{Et} \cdot HF \approx P_4^{tBu} \cdot HF \gg P_1^R \cdot HF$) was at odds with the results reported by Lemaire et al.[11] The Belgian group used a number of strong bases including phosphazenes to elute [18F]fluoride from the ion-exchange resin, and performed radiofluorination directly in the eluent. Although the intermediacy of phosphazene hydrofluorides as fluorinating agents was not proven in the report, P_1^{tBu}-containing eluent significantly outperformed its P_2^{Et} analogue. We decided to revisit this issue by examining the reaction between $P_1^{tBu} \cdot HF$ and 1-chlorooctane. Heating the reaction mixture for one hour at 100°C in [D$_8$]toluene resulted in the formation of a white precipitate. ^{1}H NMR spectroscopy showed that the solution contained unreacted octyl chloride and no $P_1^{tBu} \cdot HF$, which suggested that the latter underwent thermal decomposition. This was confirmed by heating a solution of $P_1^{tBu} \cdot HF$ and observing the formation of a precipitate, which was spectroscopically identical to that obtained in the fluorination reaction with 1-chlorooctane. The ^{1}H and ^{13}C NMR spectra of the solid were similar to those of the parent $P_1^{tBu}HF$, which suggests the presence of $P_1^{tBu}H^+$. However, a peak at $m/z = 144$ (ESI, negative mode), a doublet at -70.4 ppm ($J_{P-F} = 711$ Hz) in the ^{19}F NMR spectrum, and a heptaplet at -143.3 in the ^{31}P NMR spectrum were characteristic of the PF_6^- anion. $P_1^{tBu}H^+PF_6^-$ was previously reported in the literature[20b] and its identity in our reaction was additionally confirmed by its independent synthesis from P_1^{tBu} and HPF$_6$. It was conceivable that the hexafluorophosphate PF_6^- resulted from the sequence of intra/intermolecular attacks of the fluoride anion on the phosphorus in $P_1^{tBu}H^+$, either via the intermediacy of known alkylamino fluorophosphoranes[31] **B** and **C** or by a direct substitution (Scheme 3).

Regardless of the particularities of the mechanism, a unique susceptibility of P_1^R phosphazene hydrofluorides to fluorolysis was most likely a combination of steric and electronic factors. To investigate the electronics of the system we ran density functional theory (DFT) calculations. Natural bond population analysis performed on $P_1^{tBu}H^+$, $P_2^{Et}H^+$, and $P_4^{tBu}H^+$ optimized at the B3LYP/6-31G* level showed that the positive charge resided mostly on the phosphorus atom and, on average, was the same per phosphorus (2.3–2.4) across the series. The electrophilicity index ω, introduced by Parr[32] and defined as $\omega = \mu^2/2\eta$ (μ is the chemical potential and η is the chemical hardness), was used to rank the phosphazenium cations $P_n^RH^+$ according to their strength as electrophiles.

Table 8 shows that $P_1^{tBu}H^+$ is the strongest electrophile in the series; its electrophilicity index ω is more than four times as high as that of $P_4^{tBu}H^+$ (0.61 vs. 0.14). Among the three phosphazene hydrofluorides $P_1^{tBu}H^+$ has the lowest-

Table 7. Radiofluorination with $P_2^{Et} \cdot [^{18}F]HF$.

Entry	Substrate[a]	Phosphazene + [18F]HF	RCY [%][b]
1	AcO, AcO''', OAc, AcO, OTf (mannose triflate structure)	P_4^{tBu}	82±5
2	H$_3$C(H$_2$C)$_{15}$-O, H$_3$C(H$_2$C)$_{15}$-O, OMs	P_4^{tBu}	71±6
3	naphthalene-CH$_2$OMs	P_2^{Et}	91±4 (81)[c]
4	naphthalene-CH$_2$OTs	P_2^{Et}	82±6
5	naphthalene-CH$_2$Cl	P_2^{Et}	3±1
6	naphthalene-CH$_2$CH$_2$Br	P_2^{Et}	15±2
7	naphthalene-CH$_2$CH$_2$I	P_2^{Et}	7±2
8	pyridine-OMe, NO$_2$	P_2^{Et}	11±3

[a] Substrate (10 mg), P_2^{Et} (10 µL), toluene (2 mL), 120°C, 30 min. [b] Radiochemical yield, as determined after silica Sep-Pak purification by radio-HPLC and radio-TLC, as an average of three runs. [c] Substrate (1.1 mg), P_2^{Et} (1 µL), toluene (1 mL), 120°C, 30 min.
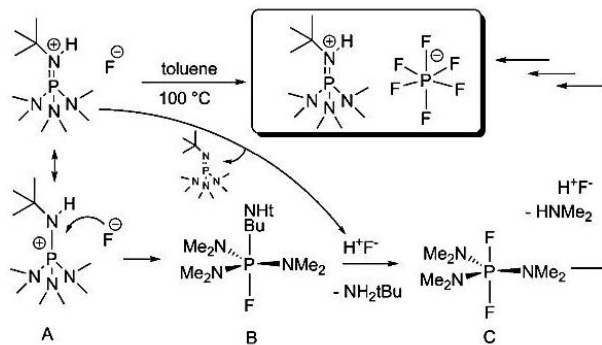
76

Scheme 3. Possible pathway for autofluorolysis of $P_1{}^{tBu}$·HF into $P_1{}^{tBu}$·HPF$_6$.

Table 8. HOMO and LUMO energies and reactivity indices μ, η, and ω for a series of phosphazenium cations calculated at the B3LYP/6-31G* level.

$P_n{}^R$HF	HOMO [a.u.]	LUMO [a.u.]	μ [a.u.][a]	η [a.u.][b]	ω [eV]
$P_1{}^{tBu}$H+	−0.4028	0.1003	−0.1513	0.5031	0.61
$P_2{}^{Et}$H+	−0.3630	0.1233	−0.1198	0.4863	0.40
$P_4{}^{tBu}$H+	−0.2945	0.1573	−0.0686	0.4518	0.14

[a] $\mu=$(HOMO+LUMO)/2. [b] $\eta=$LUMO−HOMO.

lying LUMO and the highest hardness η, thus making it the best HSAB (hard and soft acids and bases) match for the hard nucleophile, such as fluoride.[33] Furthermore, the LUMO in $P_1{}^{tBu}$H+ is predominantly a P−NMe$_2$ antibond, which suggests a ready trajectory for nucleophilic substitution of NMe$_2$ (Figure 4).
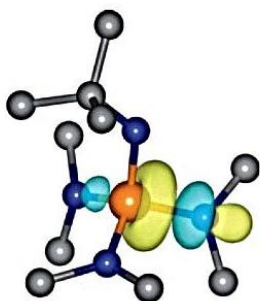
Figure 4. The lowest unoccupied molecular orbital (LUMO) for $P_1{}^{tBu}$H+ as calculated at the B3LYP/6-31G* level. Hydrogen atoms are omitted for clarity.

Investigation of space-filled models of the cations indicates that $P_2{}^R$H+ and $P_4{}^R$H+ are notably bulkier than $P_1{}^R$H+, thereby providing increased steric shielding against the nucleophilic attack by the fluoride. The analysis above suggests that the key to stability towards fluorolysis is the increase in steric bulk and electron density on the phosphazenium cation.

Conclusion

We have demonstrated the possibility of a one-step recovery and nucleophilic activation of [18F]fluoride$_{(aq)}$ as [18F]phosphazenium hydrofluorides via the intermediacy of gaseous [18F]HF. With alkyl pseudohalides, phosphazenium [18F]hydrofluorides perform on a par with the conventional [18F]KF/Kryptofix system but significantly outperform the latter if the substrate is lipophilic. The related nonradioactive $P_2{}^{Et}$·HF and $P_4{}^{tBu}$·HF, easily prepared from the corresponding phosphazene bases and Et$_3$N·3HF, are efficient reagents for homogeneous fluorination of bromides and pseudohalides. Under DoE optimized conditions, this system is also powerful enough to fluorinate alkyl chlorides in good yields. As revealed by the DoE screening, the system tolerates glass vessels and the presence of water, and can be performed in both polar and nonpolar solvents. In contrast, $P_1{}^{tBu}$·HF and $P_1{}^{tOct}$·HF are unstable towards autofluorolysis. This can be rationalized in terms of the diminished steric bulk and higher electrophilicity of $P_1{}^R$H+. Efforts to automate the radiofluorination process and to minimize [18F]HF recovery time are currently under way.

Experimental Section

General considerations: Unless otherwise noted, all operations were performed under an inert atmosphere of argon. Glassware and reaction vessels were dried in an oven at 160°C overnight or flame-dried on the Schlenk line prior to use. All fluorination and radiofluorination reactions were performed either in oven-dried screw-cap test tubes made of glass, copper, stainless steel, or glassy carbon, or in flame-sealed NMR tubes. Synthetic procedures for the phosphazenium hydrofluorides were optimized for purity. All solvents and reagents were purchased from Aldrich Co. Unless otherwise noted, diethyl ether, THF, and toluene were distilled from sodium benzophenone; acetonitrile, dichloromethane, DMF, HMPA, tmeu, and Mes were dried over activated molecular sieves (220°C, 0.1 mbar, 4 h) for at least 48 h prior to use; hexane was used as received. All radiochemical yields were decay-corrected.

Instrumentation: The ultrasound experiments were carried out using a Sonorex DT52H instrument operating at 240 W/35 kHz. ^{1}H, ^{13}C, and ^{31}P NMR spectra were recorded on a Bruker Avance II 500 instrument, at 500, 126, and 202 MHz, respectively. ^{19}F NMR spectra were recorded on a Bruker Avance DPX 250 instrument at 235 MHz. ^{1}H NMR spectra are reported in parts per million (ppm) downfield of TMS and were measured relative to residual protons in deuterated solvents. All ^{13}C NMR spectra are reported in ppm relative to carbon signals in deuterated solvents and were obtained with ^{1}H decoupling. All ^{19}F NMR spectra were obtained without ^{1}H decoupling and were referenced externally relative to C$_6$F$_6$. All ^{31}P NMR spectra were ^{1}H decoupled and referenced externally relative to 85% H$_3$PO$_4$. All coupling constants are reported in Hertz. Gas chromatography was performed on a Varian 3900 instrument equipped with a Factor Four capillary column (VF-200ms, 30 m × 0.32 mm I.D., DF=1.0) and a flame ionization detector. Mass spectrometry was performed on a Bruker Esquire 4000 ion-trap (IT) spectrometer equipped with an electrospray ionization (ESI) interface. Thin-layer chromatography (TLC) was run on precoated plates of silica gel 60 F254 (Merck). [18]F aqueous solutions were prepared by an [18]O(p,n)[18]F reaction in a GE PETrace cyclotron with a 1.8 mL target of 95% enriched [18O]water irradiated by a 14.1 MeV beam at 20–25 mA for 60–90 min. Radio-HPLC was performed by using a Knauer HPLC System K501, equipped with a Knauer RI detector K2301 and CRA radioactivity detector 105 S-1 on a Carbopac PA10 4×25 mm Dionex column eluted with

0.1 M NaOH at 1.0 mL min⁻¹. Radio-TLC was performed with a Raytest MiniGita TLC scanner.

Materials and apparatus for [¹⁸F]HF production and radiofluorination: The PE, glassy carbon (SIGRADUR) reaction vials, and glass pressure tubes were purchased from Kartell (Italy), HTW Hochtemperatur-Werkstoffe GmbH (Germany), and Aldrich, respectively. The PE tubing (I.D.=3 mm, O.D.=4.5 mm) was purchased from Buch & Holm and proved superior to natural rubber Suprene (New Age Industries) in terms of chemical resistance and [¹⁸F]fluoride absorption, and was used throughout. The stoppers were made of either PE or Teflon and fitted to the tubing via appropriately sized orifices; no valves were used. All radiochemistry was performed without automation equipment.

Computational methods: The DFT calculations were performed by using the Gaussian 09 suite of programs.[34] All structures were verified to be minima on the potential energy surfaces by vibrational analyses. The optimized structures are given in the Supporting Information as .xyz files. The electron densities were visualized by using VESTA.[35]

General procedure for the synthesis of phosphazene hydrofluorides, P_n^R·HF: A flame-dried 50 mL round-bottomed flask was charged with the corresponding phosphazene base P_n^R (19.69 mmol). The flask was connected to a vacuum line, evacuated, and Et₂O (20 mL) was vacuum-transferred onto the liquid. The flask was then backfilled with Ar, fitted with a rubber septum, and Et₃N·3HF (1.061 g, 6.581 mmol) was added. The reaction mixture was stirred for 1 h, and the product was either filtered under partial vacuum using a double-ended frit or removed by a syringe (P_2^{Et}·HF).

(*tert*-Butylimino)tris(dimethylamino)phosphonium hydrofluoride (P_1^{tBu}·HF): A white solid (54%). ¹H NMR (500 MHz, [D₆]benzene): δ= 2.47 (d, J=9.5 Hz, 18H), 1.25 ppm (s, 9H); ¹³C NMR (126 MHz, [D₆]benzene): δ=32.01 (s, 3C), 37.85 (d, J=3.6 Hz, 6C), 51.91 ppm (s, 1C); ³¹P NMR (202 MHz, [D₆]benzene): δ=35.40 ppm (s); ¹⁹F NMR (235 MHz, [D₆]benzene): δ= −151.18 ppm (br s); MS: m/z: ($P_1^{tBu}H^+$) 235.2 (100%), 236.0 (4%).

(1,1,3,3-Tetramethylbutylimino)tris(dimethylamino)phosphonium hydrofluoride (P_1^{tOct}·HF): A white solid (48%). ¹H NMR (500 MHz, [D₆]benzene): δ=1.04 (s, 9H), 1.28 (s, 6H), 1.64 (s, 2H), 2.50 ppm (d, J= 9.8 Hz, 18H); ¹³C NMR (126 MHz, [D₆]benzene): δ=30.69 (br s, 1C), 31.37 (s, 1C), 31.72 (s, 3C), 37.39 (d, J=4.5 Hz, 6C), 55.98 (brs, 2C), 56.68 ppm (br s, 1C); ³¹P NMR (202 MHz, [D₆]benzene): δ=34.87 ppm (s); ¹⁹F NMR (235 MHz, [D₆]benzene): δ=−152.61 ppm (brs); MS: m/z: ($P_1^{tOct}H^+$) 291.2 (100%), 292.2 (17%).

Tetramethyl[tris(dimethylamino)phosphoranylidene]phosphorictriamid-Et-iminium hydrofluoride (P_2^{Et}·HF): A yellowish viscous oil (77%). ¹H NMR (500 MHz, [D₆]benzene): δ=1.43 (td, J=7.2, 0.6 Hz, 3H), 2.41 (d, J=10.4 Hz, 18H), 2.59 (d, J=10.4 Hz, 12H), 2.89–2.98 ppm (m, 2H); ¹³C NMR (126 MHz, [D₆]benzene): δ=17.95 (d, J=9.1 Hz, 1C), 36.81 (s, 1C) 37.15 (d, J=4.5 Hz, 6C), 37.57 (d, J=4.5 Hz, 4C); ³¹P NMR (202 MHz, [D₆]benzene): δ=17.66, 18.42 ppm (AB quartet); ¹⁹F NMR (235 MHz, [D₆]benzene): δ=−150.38 ppm (brs); MS: m/z: ($P_2^{Et}H^+$) 340.3 (100%), 341.2 (18%).

1-*tert*-Butyl-4,4,4-tris(dimethylamino)-2,2-bis-[tris(dimethylamino)phosphoranylidenamino]-2λ^5,4λ^5-catenadiphosphazenium hydrofluoride (P_4^{tBu}·HF): A white solid (31%). ¹H NMR (500 MHz, [D₆]benzene): δ=1.34 (d, J=0.6 Hz, 9H), 2.53 ppm (d, J= 10.1 Hz, 54H); ¹³C NMR (126 MHz, [D₆]benzene): δ=32.27 (d, J= 5.5 Hz, 3C), 37.69 (d, J=4.5 Hz, 18C), 50.80 ppm (d, J=3.6 Hz, 1C); ³¹P NMR (202 MHz, [D₆]benzene): δ=−23.63 (q, J=49.8 Hz, 1P), 12.31 ppm (d, J=49.8 Hz, 1P); ¹⁹F NMR (235 MHz, [D₆]benzene): δ= −153.20 ppm (d, J=119.8 Hz); MS: m/z: ($P_4^{tBu}H^+$) 634.4 (100%), 635.3 (20%), 636.3 (4%).

Fluorination: GC response factor determination: The substrate (0.18 mmol) and naphthalene (internal GC standard, 15 mg) were added to a 1 mL volumetric flask and solvent (tmeu/Mes, 46:54) was added to the mark. A portion (100 μL) of the solution was withdrawn and transferred to a 1 mL volumetric flask. *n*-Hexane was added to the mark and the solution was filtered before injection. The experiment was carried out in triplicate.

Fluorination: general procedure: The substrate (0.18 mmol), P_2^{Et}·HF (1.5 equiv), and naphthalene (15 mg) were added to a 1 mL volumetric flask and the solvent (tmeu/Mes, 46:54) was added to the mark. The reaction mixture was transferred to a glass pressure tube and heated at 120°C. The initial and final concentrations were determined by GC following the GC response factor determination protocol.

General procedure for [¹⁸F]HF generation, transfer, and the synthesis of P_n^R·[¹⁸F]HF: [¹⁸F]Fluoride (cyclotron target wash, 1 mL, 15–1100 MBq) was added to a reaction vial (PE or glassy carbon) containing H₂SO₄ (98%, 5 mL). The vial was heated for 30 min at 80°C in an ultrasound bath while being irradiated at 35 kHz. [¹⁸F]HF was carried by an argon flow (300–400 sccm min⁻¹) to a receiving vial (glassy carbon) containing P_n^R (30 μmol) in toluene or MeCN (2 mL) at 0°C. The [¹⁸F]HF transfer yield was 16–82% measured by the dose calibrator.

Radiosynthesis of 2-[¹⁸F]fluoro-2-deoxyglucose ([¹⁸F]FDG): The content of the receiving vial (P_2^{Et}·[¹⁸F]HF in 2 mL MeCN) was transferred to a glass pressure tube containing mannose triflate (25 mg, 52 μmol) through a stainless steel cannula and the reaction was carried out at 120°C for 20 min. The reaction mixture was added to a C18 (Waters) cartridge preconditioned with EtOH and H₂O. NaOH (0.70 mL, 2N) was added to the column and the tetraacetate intermediate was hydrolyzed at room temperature for 5 min. The hydrolyzed product was eluted using H₂O (2 mL). The decay-corrected radiochemical yield was 82%; the radiochemical purity was 98%.

Radiosynthesis of [¹⁸F]NpEtF: The content of the receiving vial (P_2^{Et}·[¹⁸F]HF in 2 mL toluene) was transferred to a reaction vial (glassy carbon or a glass pressure tube) containing the substrate NpEtOMs (Np: naphthalene, Ms: methanesulfonyl), NpEtOTs (Ts: *p*-toluenesulfonyl), NpEtOTf, NpEtCl, NpEtBr, or NpEtI (52 μmol). [¹⁸F] fluorination was carried out at 120°C for 20 min and [¹⁸F] fluorinated product was purified by passing through a Silica Plus (Waters) cartridge. The corresponding radiochemical purities determined by radio-TLC were higher than 99%.

Automated radiochemical synthesis of 3-[¹⁸F]fluoro-1,2-di-hexadecylglycerol: [¹⁸F]fluoride was recovered from [¹⁸O]-enriched water on a QMA SepPak cartridge preconditioned with K₂CO₃. The activity was eluted with 50% acetonitrile in water (0.6 mL) containing K₂CO₃ (7.0 mg, 50.8 μmol) and Kryptofix 2.2.2 (22.0 mg, 58.5 μmol). The eluate was transferred to a ROTEM reactor vial and the acetonitrile/water solution was evaporated under reduced pressure (60 mbar) by using a series of temperature jumps and a helium stream (100 followed by 200 mL min⁻¹). Residual water was removed by azeotropic evaporation with acetonitrile (3×0.3 mL). MsO-1,2-di-hexadecylglycerol (5 mg, 8.0 μmol) was added in toluene (0.5 mL) and the solvent was evaporated. Dry DMSO (1 mL) was added and the mixture was allowed to react for 20 min at 165°C. The reaction mixture was analyzed by radio-TLC, which showed the target compound was obtained with a radiochemical conversion of 2.8%.

Acknowledgements

[1] S. M. Ametamey, M. Honer, P. A. Schubiger, *Chem. Rev.* **2008**, *108*, 1501–1516.

[2] S. Purser, P. R. Moore, S. Swallow, V. Gouverneur, *Chem. Soc. Rev.* **2008**, *37*, 320–330.

[3] O. Jacobson, X. Chen, *Curr. Top. Med. Chem.* **2010**, *10*, 1048–1059.

[4] J. Talbot, Y. Petegnief, K. Kerrou, F. Montravers, D. Grahek, N. Younsi, *Nucl. Instrum. Methods Phys. Res. Sect. A* **2003**, *504*, 129–138.

[5] a) L. Cai, S. Lu, V. W. Pike, *Eur. J. Org. Chem.* **2008**, 2843–2843; b) H. H. Coenen, P. H. Elsinga, R. Iwata, M. R. Kilbourn, M. R. A. Pillai, M. G. R. Rajan, H. N. Wagner, J. J. Zaknun, *Nucl. Med. Biol.* **2010**, *37*, 727–740.

[6] R. Krasikova, *PET Chem.* **2007**, *64*, 289–316.

78

New approaches to [18F]fluoride recovery and radiofluorination
Chapter 4 Homogeneous nucleophilic radiofluorination with phosphazene hydrofluorides

Nucleophilic Radiofluorination and Fluorination with Phosphazene Hydrofluorides

FULL PAPER

[7] C.-C. Lee, G. Sui, A. Elizarov, C. J. Shu, Y.-S. Shin, A. N. Dooley, J. Huang, A. Daridon, P. Wyatt, D. Stout, H. C. Kolb, O. N. Witte, N. Satyamurthy, J. R. Heath, M. E. Phelps, S. R. Quake, H.-R. Tseng, *Science* **2005**, *310*, 1793–1796.

[8] C.-G. Zhan, D. a. Dixon, *J. Phys. Chem. A* **2004**, *108*, 2020–2029.

[9] a) D. W. Kim, H.-j. Jeong, S. T. Lim, *Nucl. Med. Mol. Imaging* **2010**, *44*, 25–32; b) D. W. Kim, D.-S. Ahn, Y.-H. Oh, S. Lee, H. S. Kil, S. J. Oh, S. J. Lee, J. S. Kim, J. S. Ryu, D. H. Moon, D. Y. Chi, *J. Am. Chem. Soc.* **2006**, *128*, 16394–16397.

[10] D. W. Kim, Y. S. Choe, D. Y. Chi, *Nucl. Med. Biol.* **2003**, *30*, 345–350.

[11] C. F. Lemaire, J. J. Aerts, S. Voccia, L. C. Libert, F. Mercier, D. Goblet, A. R. Plenevaux, A. J. Luxen, *Angew. Chem.* **2010**, *122*, 3229–3232; *Angew. Chem. Int. Ed.* **2010**, *49*, 3161–3164.

[12] J. Aerts, S. Voccia, C. Lemaire, F. Giacomelli, D. Goblet, D. Thonon, A. Plenevaux, G. Warnock, A. Luxen, *Tetrahedron Lett.* **2010**, *51*, 64–66.

[13] S. A. Toorongian, G. K. Mulholland, D. M. Jewett, M. A. Bachelor, M. R. Kilbourn, *Int. J. Radiat. Appl. Instrum., B. Nucl. Med. Biol.* **1990**, *17*, 273–279.

[14] J. Simons, *Chem. Rev.* **1931**, *8*, 213–235.

[15] G. A. Olah, J. T. Welch, Y. D. Vankar, M. Nojima, I. Kerekes, J. A. Olah, *J. Org. Chem.* **1979**, *44*, 3872–3881.

[16] a) R. Franz, *J. Fluorine Chem.* **1980**, *15*, 423–434; b) J. M. Kremsner, M. Rack, C. Pilger, O. C. Kappe, *Tetrahedron Lett.* **2009**, *50*, 3665–3668; c) M. A. McClinton, *Aldrichimica Acta* **1995**, *28*, 31–35.

[17] a) I. Bucsi, B. Török, A. I. Marco, G. Rasul, G. K. S. Prakash, G. a. Olah, *J. Am. Chem. Soc.* **2002**, *124*, 7728–7736; b) N. Yoneda, *Tetrahedron* **1991**, *47*, 5329–5365.

[18] a) R. D. Chambers, S. R. Korn, G. Sandford, *J. Fluorine Chem.* **1994**, *69*, 103–108; b) R. D. Chambers, T. F. Holmes, S. R. Korn, G. Sandford, *J. Chem. Soc. Chem. Commun.* **1993**, 855–856; c) M. Darabantu, T. Lequeux, J.-C. Pommelet, N. Plé, A. Turck, L. Toupet, *Tetrahedron Lett.* **2000**, *41*, 6763–6767.

[19] G. Pascali, D. O. Kiesewetter, P. A. Salvadori, W. C. Eckelman, *J. Label. Compd. Radiopharm.* **2004**, *47*, 373–383.

[20] a) R. Schwesinger, R. Link, P. Wenzl, S. Kossek, M. Keller, *Chem. Eur. J.* **2006**, *12*, 429–437; b) R. Schwesinger, J. Willaredt, H. Schlemper, M. Keller, D. Schmitt, H. Fritz, *Chem. Ber.* **1994**, *127*, 2435–2454.

[21] R. Schwesinger, R. Link, P. Wenzl, S. Kossek, *Chem. Eur. J.* **2006**, *12*, 438–445.

[22] S. Re, *J. Phys. Chem. A* **2001**, *105*, 9725–9735.

[23] D. W. Kim, H.-J. Jeong, S. T. Lim, M.-H. Sohn, J. a. Katzenellenbogen, D. Y. Chi, *J. Org. Chem.* **2008**, *73*, 957–962.

[24] J. H. Clark, *Chem. Rev.* **1980**, *80*, 429–452.

[25] D. Landini, A. Maia, A. Rampoldi, *J. Org. Chem.* **1989**, *54*, 328–332.

[26] M. Darabantu, T. Lequeux, J.-C. Pommelet, N. Plé, A. Turck, *Tetrahedron* **2001**, *57*, 739–750.

[27] O. W. Gooding, *Curr. Opin. Chem. Biol.* **2004**, *8*, 297–304.

[28] MODDE 9.0, Umetrics, Umea, http://www.umetrics.com.

[29] C. Reichardt, *Solvent Effects in Organic Chemistry*, Verlag Chemie, Weinheim, **1979**.

[30] a) K. Omura, D. Swern, *Tetrahedron* **1978**, *34*, 1651–1660; b) T. Giagou, M. P. Meyer, *J. Org. Chem.* **2010**, *75*, 8088–8099.

[31] M. Kopp, B. Neumüller, *Z. Anorg. Allg. Chem.* **1999**, *625*, 363–367.

[32] R. Parr, L. Szentpály, S. Liu, *J. Am. Chem. Soc.* **1999**, *121*, 1922–1924.

[33] R. G. Pearson, J. Songstad, *J. Am. Chem. Soc.* **1967**, *89*, 1827–1836.

[34] Gaussian 09, Revision A.02, M. J. Frisch, G. W. Trucks, H. B. Schlegel, G. E. Scuseria, M. A. Robb, J. R. Cheeseman, G. Scalmani, V. Barone, B. Mennucci, G. A. Petersson, H. Nakatsuji, M. Caricato, X. Li, H. P. Hratchian, A. F. Izmaylov, J. Bloino, G. Zheng, J. L. Sonnenberg, M. Hada, M. Ehara, K. Toyota, R. Fukuda, J. Hasegawa, M. Ishida, T. Nakajima, Y. Honda, O. Kitao, H. Nakai, T. Vreven, J. A. Montgomery, Jr., J. E. Peralta, F. Ogliaro, M. Bearpark, J. J. Heyd, E. Brothers, K. N. Kudin, V. N. Staroverov, R. Kobayashi, J. Normand, K. Raghavachari, A. Rendell, J. C. Burant, S. S. Iyengar, J. Tomasi, M. Cossi, N. Rega, J. M. Millam, M. Klene, J. E. Knox, J. B. Cross, V. Bakken, C. Adamo, J. Jaramillo, R. Gomperts, R. E. Stratmann, O. Yazyev, A. J. Austin, R. Cammi, C. Pomelli, J. W. Ochterski, R. L. Martin, K. Morokuma, V. G. Zakrzewski, G. A. Voth, P. Salvador, J. J. Dannenberg, S. Dapprich, A. D. Daniels, Ö. Farkas, J. B. Foresman, J. V. Ortiz, J. Cioslowski, D. J. Fox, Gaussian, Inc., Wallingford CT, **2009**.

[35] K. Momma, F. Izumi, *J. Appl. Crystallogr.* **2008**, *41*, 653–658.

Received: February 10, 2011
Revised: April 5, 2011
Published online: May 30, 2011

Chem. Eur. J. **2011**, *17*, 7796–7805   © 2011 Wiley-VCH Verlag GmbH & Co. KGaA, Weinheim   www.chemeurj.org   7805

79

4.6 Conclusion to Chapter 4

As HF is the cheapest fluorination agent much research has been carried out regarding the development of a fluorination protocol that deals with the significant corrosivity and volatility of the compound. In this chapter I have described how HF in the form of phosphazene $[^{18/19}F]$hydrofluorides has been applied in the development of a homogeneous fluorination and radiofluorination strategy that is versatile with regard to both substrates and solvents and has a high water tolerance. The work has resulted in two publications.

4.7 Experimentals

Most of the experimental work carried out during this project has been included in the articles. Only the experiments not included in the articles are described here.
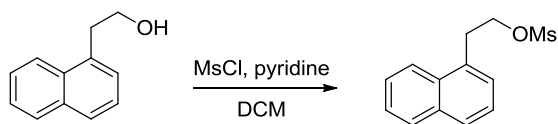
1-*O*-Ms-2-(naphtalen-1-yl)ethanol

1-naphtaleneethanol (888 mg, 5.23 mmol) was dissolved in anhydrous DCM (40 mL) and anhydrous pyridine (6 mL) under an argon atmosphere and cooled to 0 °C on an ice-bath. MsCl (1.0 mL, 2.5 eq) was added and the mixture was allowed to react at RT for 3 hours. The mixture was reduced by rotary evaporation and partitioned between water (100 mL) and hexane (100 mL). The organic phase was separated and washed with water (2 x 100 mL). The organic phase was reduced and the crude product was purified by flash chromatography in toluene:EtOAc (95:5), Rf = 0.26, yielding **1.092 g (85%)** of the title compound as a white solid.

^{1}H-NMR (500 MHz, CDCl$_3$): δ 8.03 (dd, *J* = 8.7, 0.8; 1H), 7.89 (m, 1H), 7.80 (m, 1H), 7.55 (m, 2H), 7.43 (m, 2H), 4.56 (t, *J* = 7.3; 2H), 3.56 (t, *J* = 7.3; 2H), 2.81 (s, 3H). **^{13}C-NMR** (125 MHz, CDCl$_3$): δ 133.89, 132.07, 131.76, 128.99, 127.97, 127.46, 126.51, 125.84, 125.49, 123.09, 69.54, 37.37, 32.81.
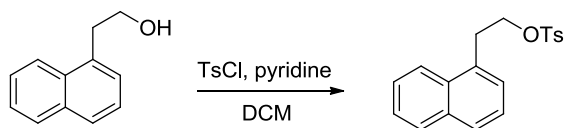
1-*O*-Ts-2-(naphtalen-1-yl)ethanol

1-naphtaleneethanol (535 mg, 5.23 mmol) was dissolved in anhydrous DCM (30 mL) and anhydrous pyridine (5 mL) under an argon atmosphere. TsCl (3118 mg, 5.3 eq) was added and the mixture was allowed to react at RT for 13 hours (overnight). The mixture was reduced by rotary evaporation and partitioned between water (100 mL) and hexane (100 mL). The organic phase was separated and washed with water (2 x 100 mL). The organic phase was reduced and the crude product

was purified by flash chromatography in toluene, Rf = 0.28, yielding **892 mg (84%)** of the title compound as a white solid.

¹H-NMR (250 MHz, CDCl₃): δ 7.84 (m, 2H), 7.75 (d, J = 8.1; 1H), 7.62 (m, 2H), 7.48 (m, 2H), 7.32 (m, 2H), 7.18 (m, 2H), 4.35 (t, J =7.3; 2H), 3.44 (t, J = 7.3; 2H), 2.39 (s, 3H). **¹³C-NMR** (62.5 MHz, CDCl₃): δ 144.43, 133.95, 133.17, 132.07 131.76, 129.61, 128.85, 127.75, 127.70, 127.36, 126.25, 125.64, 125.43, 123.04, 69.81, 32.59, 21.47.

R = -(CH₂)₁₅CH₃
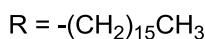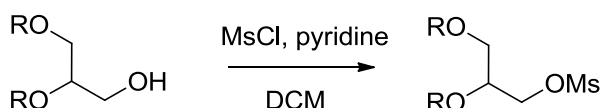
3-*O*-Ms-1,2-di-hexadecyl-glycerol

1,2-di-hexadecyl-glycerol (103 mg, 0.190 mmol) was dissolved in anhydrous DCM (9 mL) and anhydrous pyridine (6 mL). MsCl (59 μL, 4 eq) was added and the mixture was allowed to react for 4 hours at RT. The mixture was transferred to a separating funnel containing DCM (40 mL) and brine (30 mL). The organic phase was separated and washed with mL brine (2 x 40). The combined aqueous phases were extracted once with DCM (30 mL). The combined organic phases were rotary evaporated and the crude product was purified by flash chromatography in toluene:EtOAc (98:2), Rf = 0.34, yielding **100 mg (85%)** of the title compound as a white solid.

¹H-NMR (500 MHz, CDCl₃): δ 4.38 (dd, J = 10.3, 3.6; 1H), 4.25 (dd, J = 10.9, 5.8; 1H), 3.67 (m, 1H), 3.57 (t, J = 6.6; 2H), 3.48 (m, 4H), 3.04 (s, 3H), 1.56 (m, 4H), 1.36-1.20 (m, 52H), 0.89 (t, J = 6.9; 6H). **¹³C-NMR** (125 MHz, CDCl₃): δ 76.4, 71.9, 70.8, 69.7, 69.1, 37.4, 31.9-26.0 (*aliphatic*, 31.9 (2C), 29.9 (2C) 29.68 (2C), 29.67 (2C), 29.65 (2C), 29.64 (2C), 29.61 (2C), 29.59 (2C), 29.5 (2C), 29.4 (2C), 29.3 (2C), 26.1 (2C), 26.0 (2C)), 22.7 (2C), 14.1 (2C). m/z (MALDI-TOF, DHB-matrix - Na+-spiked, LP25%, 200 shots); Found: 641.38 (M+Na⁺), calculated: 618.53 + 22.99 = 641.92.

Chapter 5 Solid-phase radiofluorination using polymer-supported phosphazene bases

The next step in the development of methods for $[^{18}F]$fluoride recovery and radiofluorination was the implementation of our phosphazene base-driven radiofluorination strategy on a solid support in order to simplify the procedure. In this chapter the foundation of our ideas is described followed by a description the work carried out to achieve a polymer-supported methodology resulting in efficient $[^{18}F]$fluoride recovery and radiofluorination.

5.1 The impact of solid support on organic chemistry

Upon Bruce Merrifield's arrival at the Rockefeller Institute for Medical Research in 1949, one of his tasks was the synthesis of streptogenin peptides. His conclusion, after the solution phase synthesis of a pentapeptide was complete, was that the overall yield was 7% and it had taken him 11 months. There had to be a better way! In 1959 he formulated the concept of solid-phase peptide synthesis (SPPS) where the plan was to assemble a peptide chain in a stepwise manner while it was attached to a solid support. In this way, the peptide would be in suitable physical form to permit rapid filtration and washing in order to remove excess reactants and byproducts, and thereby he saved both time and effort. This concept was without chemical precedent and when Merrifield described the first successful synthesis of a tetrapeptide by SPPS at a conference in 1962 and in a full paper in 1963 the reactions were: "This is not the way to synthesize peptides" (professor Joseph Fruton) and, "Travestry,…not chemistry at all, a concept, which should be suppressed by the community" (one of the reviewers of the article). Today, however, that very article is the fifth most cited paper in JACS, and the general field of SPPS and solid-phase organic synthesis (SPOS) has grown enormously, rightfully earning Merrifield the Nobel Prize in chemistry in 1984[97–99].

The advantages of SPPS/SPOS are as mentioned primarily ease of purification together with selective product cleavage, recycling of precious catalyst and - last but not least - the fact that the strategy is amenable to automation, miniaturization and robotics.

5.2 Solid support and radiochemistry

The disadvantage of most radiofluorination strategies, both conventional and the alternative ones is that radiofluorination is not a stoichiometric reaction. The radionuclide is present in nanomolar scale and it is necessary to use millimolar amounts of precursor in order to achieve satisfyingly radiochemical yields. The result is a crude mixture of product, excess precursor, byproducts, solvent residues and additives that require purification before final formulation. If instead the principles of solid-phase synthesis were applied, the advantages could also be achieved. Thus, two strategies for the implementation of polymer-supported radiosynthesis have been explored. The first is the attachment of the precursor to the solid support and the other is to trap [18F]F- on the support. In both cases the labeling happens on the solid support and the product is eluted.

5.2.1 Radiofluorination of a polymer-supported precursor

Brown *et al.*[100,101] have described the synthesis of a solid-supported FDG precursor using a perfluoroalkylsulfonate linker to couple a D-mannose derivative to an aminomethyl polystyrene resin (Scheme 5-1).
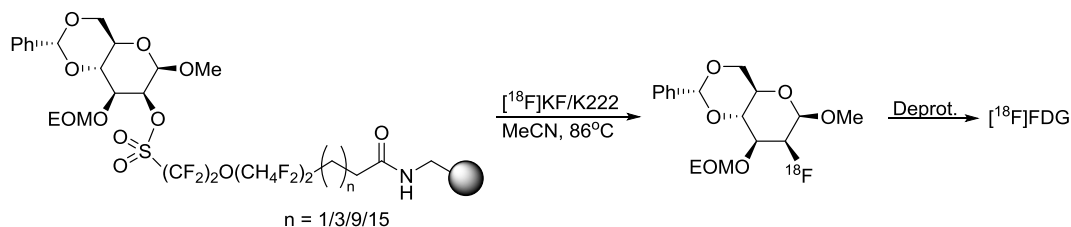
Scheme 5-1. Polymer-supported [18F]FDG synthesis

Radiofluorination was carried out by drying a solution of [18F]F-/[18O]H$_2$O, K222 and K$_2$CO$_3$ and redissolving the [18F]KF/K222 complex in MeCN. This was added to the resin contained in a vial and the mixture was heated. Labeling peaked after 3-4 minutes at 86°C with 18F incorporation between

70-91%. HPLC analysis of the crude products from the synthesis contained significantly reduced levels of impurities compared to those resulting from conventional solution phase [^{18}F]FDG synthesis. The effect of the linker chain length (Table 5-1) was also investigated and it was discovered that RCYs increased with chain length of up to four methylene groups, after which it leveled off and began to fall.

Table 5-1. Linker chain length effect on RCY

Entry	Linker length (n)	RCY %
1	0	45-50
2	1	75
3	3	92
4	9	85-90
5	15	77

A very interesting feature of this strategy was that the majority of the mannose derivative remained attached to the resin during the labeling experiment, which meant that one batch of resin could be used to generate multiple doses of the radiotracer.

Topley *et al.*[102] later described a further development of the methodology, where an arylsulfonate linker was used in the solid-supported synthesis of the glioma-imaging radiopharmaceutical [^{18}F]FET (Scheme 5-2). The dried [^{18}F]KF/K222 complex was mixed with the functionalized resin in MeCN at 110°C for 15 min with resulting 94% [^{18}F]fluoride incorporation. Again longer linkages (n = 3 and 5) proved to be more effective.
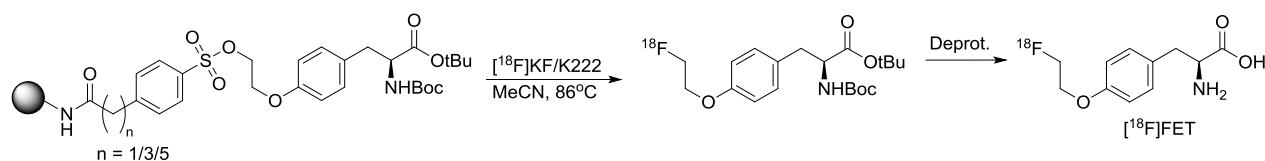
Scheme 5-2. Polymer-supported [^{18}F]FET synthesis

The major issue present in these and similar[103,104] protocols is the fact that [^{18}F]F$^-$ has to be dried before the labeling step, which results in a lengthy and comprehensive procedure. The alternative may be trapping and radiofluorination at the polymer support.

85

5.2.2 [^{18}F]F⁻ trapping and subsequent radiofluorination on solid support

In 1989 Mulholland *et al.*[105] were among the first to suggest a method to carry out polymer-supported trapping and radiofluorination. They used a polymeric quaternary ammonium hydroxide resin, which was synthesized by heating aminopyridines with Merrifield's resin (Scheme 5-3).
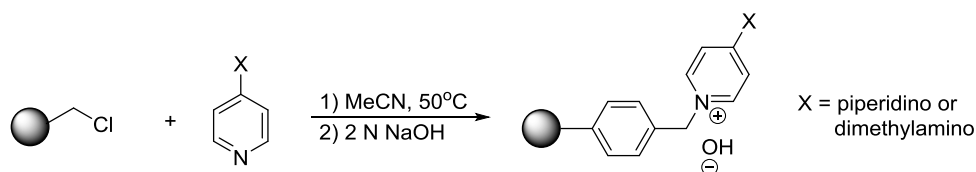
Scheme 5-3. Synthesis of quaternary ammonium hydroxide resin

[^{18}F]F⁻/[^{18}O]H$_2$O was passed directly through the resin, and the resin was able to trap 75-90% of the activity. Drying and reactivation of [^{18}F]F⁻ was achieved simply by passing dry MeCN or DMSO through the resin bed, no heating was required. Subsequent radiofluorination was carried out by passing the substrate dissolved in MeCN or DMSO back and forth through the resin bed at an elevated temperature. After 4 min at 130°C protected [^{18}F]FDG was synthesized with a 40-65% RCY. As stated by Mulholland, the advantages of this procedure included speed, simplicity and versatility as even base-sensitive substrates were radiofluorinated by this procedure, due to reduced contact time with base and heat. Also there was no need for separation of base or solubilizing agents from the labeled product, and target water was easily recovered. The work was further developed by Toorongian, Mulholland and coworkers[106] who achieved a routine production of [^{18}F]FDG based on trapping and labeling on the previously described 4-aminopyridinium resin. After trapping of [^{18}F]F⁻ on the resin it was dried by anhydrous MeCN while the temperature was gradually increased to 100°C. The FDG precursor (20 mg in 2 mL MeCN) was then passed through the column at 100°C over a period of 5-7 minutes. Subsequent acidic hydrolysis of the product gave [^{18}F]FDG (Scheme 5-4).
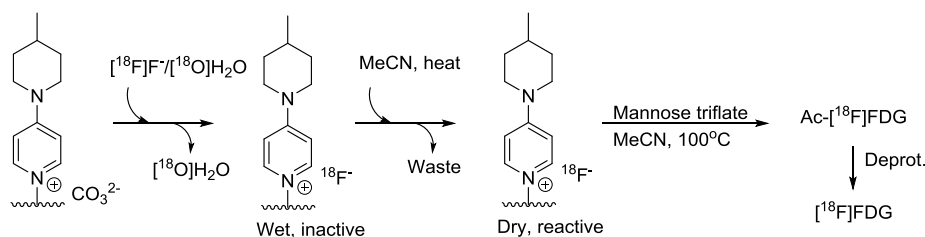
Scheme 5-4. On-column trapping and radiofluorination

The average RCY of $[^{18}F]FDG$ was 41% based on aqueous fluoride. The trapping efficiency depended on flow rate, packing defects, column geometry and the amount of resin in the bed. Slurry packing the column gave the most uniform resin beds, and thus the most consistent results. A TIN-100 cation exchange fiber resin was added in order to improve flow characteristics as liquid channeling and back pressure was prevented. A 6:1 aminopyridinium resin:TIN-100 resin ratio improved both $[^{18}F]F^-$ trapping efficiency and overall $[^{18}F]FDG$ RCY (Table 5-2).

Table 5-2. Trapping and labeling efficiency of mixed resin columns

	4:1 resin mix	6:1 resin mix
Trapping efficiency	66 %	95%
$[^{18}F]FDG$ RCY	36%	50%
Number of syntheses	69	35

Resin decomposition visible as strong discoloration of the resin during the labeling step rendered the resin useless after a complete synthesis and the columns had to be discarded. The mode of decomposition was not understood. The non-reacting portion of the trapped $[^{18}F]F^-$ after the radiofluorination step was investigated with regard to reactivity and it was discovered that it could be eluted using dilute aqueous K_2CO_3 and then used for classic solution-phase $[^{18}F]FDG$ synthesis. This suggests that the non-reacting portion was either physically inaccessible by the precursor within the polymer matrix, or was bound in some inert chemical complex that can be reversed by aqueous base treatment. A solution to this in order to enhance on-column radiofluorination efficiency was not found. The advantages of this solid-phase radiofluorination procedure were, however, numerous, as described previously. The methodology even formed the basis of a commercially available synthesis unit (PETtrace FDG Microlab™, GE Medical Systems)[31].

5.3 Objective

With the trapping and radiofluorination abilities of phosphazene bases established as well as the solid-phase method described above in mind, we began developing a solid-phase radiofluorination methodology based on polymer-supported phosphazene bases. In order to achieve satisfying and consistent radiochemical yields, both the drying step and the labeling step were analyzed and optimized. We aimed at a method that would allow for automation, and one thing that might be beneficial in that context was a reusable resin. We also worked with different bases and solid supports to establish the impact of those. The work is described in the following pages.

5.4 Development of the solid-phase radiofluorination methodology

The methodology was seen as consisting of two steps, first trapping of $[^{18}F]F^-$ on the polymer-supported phosphazene base, and secondly the labeling step on the resin as well, as seen in Figure 5-1.
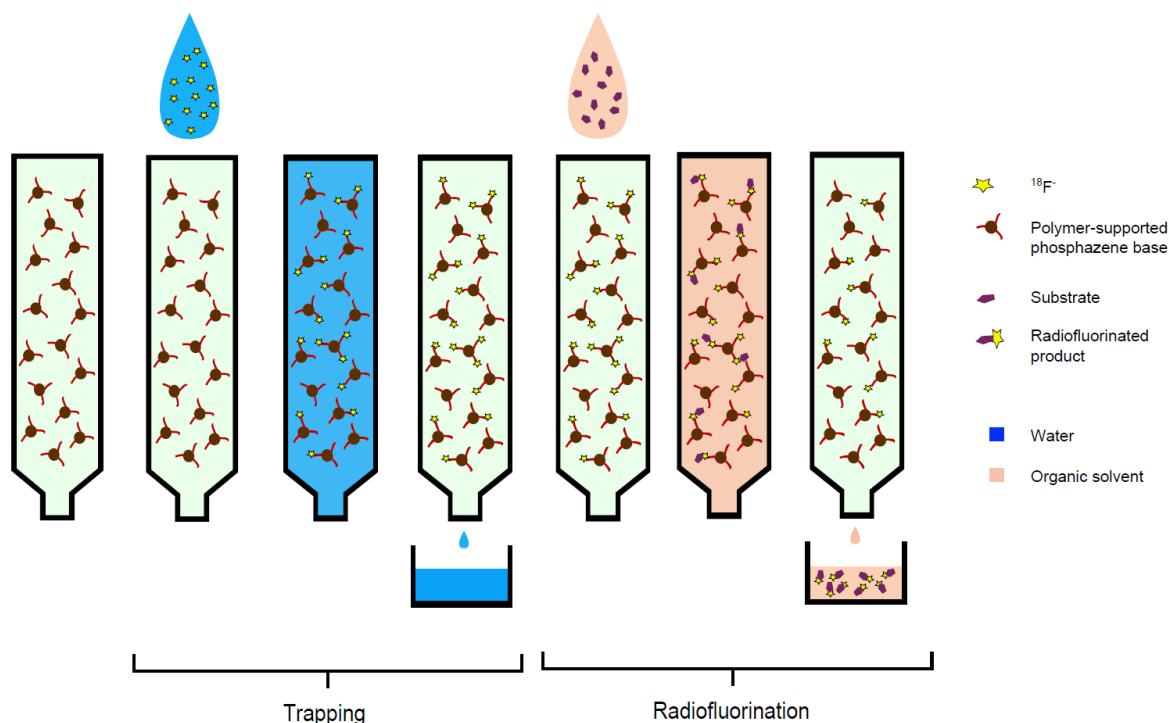
Figure 5-1. Schematics of the solid-phase radiofluorination methodology

The commercially available polymer-supported phosphazene base **PS**-P$_2$^{tBu} (**PS** = polymer-supported) was used for the preliminary experiments. A cold test experiment was carried out to evaluate the labeling ability of the base. **PS**-P$_2$^{tBu} was reacted with TREAT-HF in order to synthesize the polymer-supported phosphazene hydrofluoride **PS**-P$_2$^{tBu}·HF. This resin was then reacted with Oct-Cl according to our homogeneous fluorination protocol and the outcome was a fluorination yield at 12%. This result was not brilliant, but, nevertheless, encouraging enough for us to proceed with the methodology.

5.4.1 Column packing

In the preliminary experiments the columns were packed with a resin-glass bead mix in the entire length of a polyethylene tube (OD 6 mm), which resulted in difficulties in distributing the resin evenly on the column when only using smaller amounts. In order to analyze the distribution of the trapped activity on the column an experiment was performed where the [^{18}F]F$^-$/[^{18}O]H$_2$O solution (369 MBq) was passed through a 17 cm column packed with 148 mg resin mixed with 1 mm glass beads. The column was washed with MeCN, and residual solvent was removed by air purge. The activity of MeCN after the wash was only 2.75 MBq, which meant that trapping efficiency was 99%. An rTLC scan was then performed on the column, which clearly showed that the activity was trapped within the first 5 cm of the column (Figure 5-2). This meant that we could easily pack the column so that the resin was concentrated in a 5 cm middle section of the column.
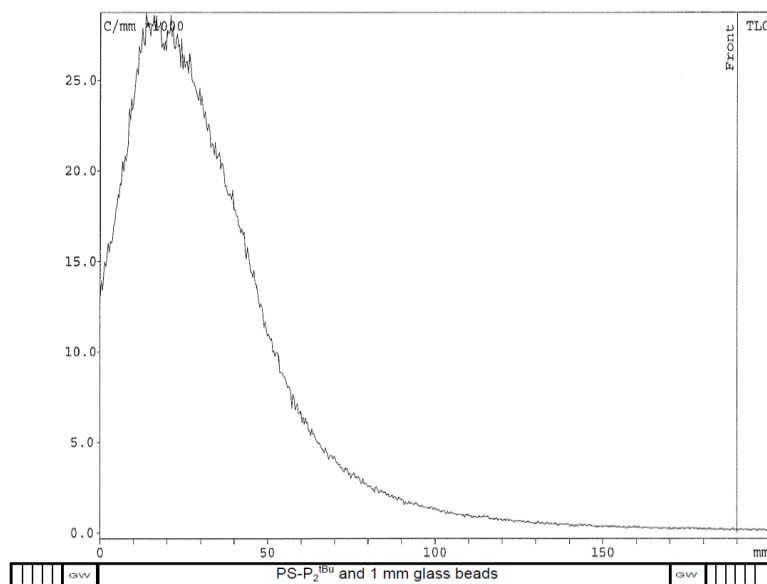
Figure 5-2. [^{18}F]F$^-$ trapping in the first part of the column

Based on the results from the column analysis the columns for manual experiments were packed in such a way that **PS**-$P_2{}^{tBu}$ was mixed with glass beads and packed in the middle 5 cm of a 17 cm tube (Figure 5-3).
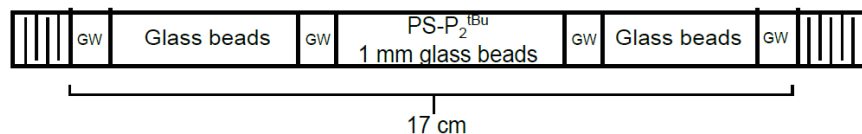
Figure 5-3. Column for manual radiofluorination experiments

Concerning the automated experiments, the polyethylene tubing was replaced with a 12 cm borosilicate glass tubing (OD 6 mm, ID 4 mm) and the glass beads used were 212-300 μm. The columns were otherwise packed in the same way.

5.4.2 Setups for the radiofluorination methodology

For the manually performed experiments a setup was made where the column was connected to a syringe pump in one end and waste/product vials in the other (Figure 5-4). The column was bent as much as the tubing would allow and placed in an oil bath when heating was required.
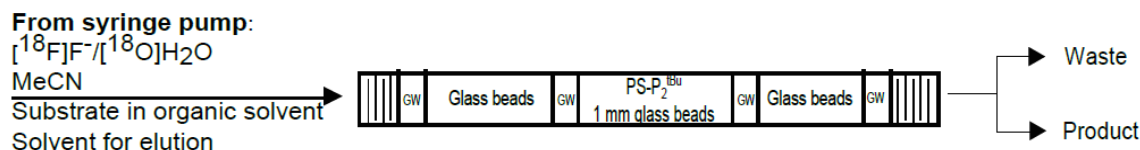
Figure 5-4. Setup for the manual experiments

As to the automated experiments, we used a home-made automation apparatus (Figure 5-5) controlled by LabView software. Solvents were driven by two syringe pumps and the column was placed in a column oven. Everything was connected by Teflon tubing (OD 1/16", ID 1 mm). The schematics of the machine, including the setup for both model substrate labeling and [18F]FDG synthesis and hydrolysis, is shown in Figure 5-6.

Figure 5-5. The radiofluorination apparatus with the column placed outside the column oven (yellow arrow)
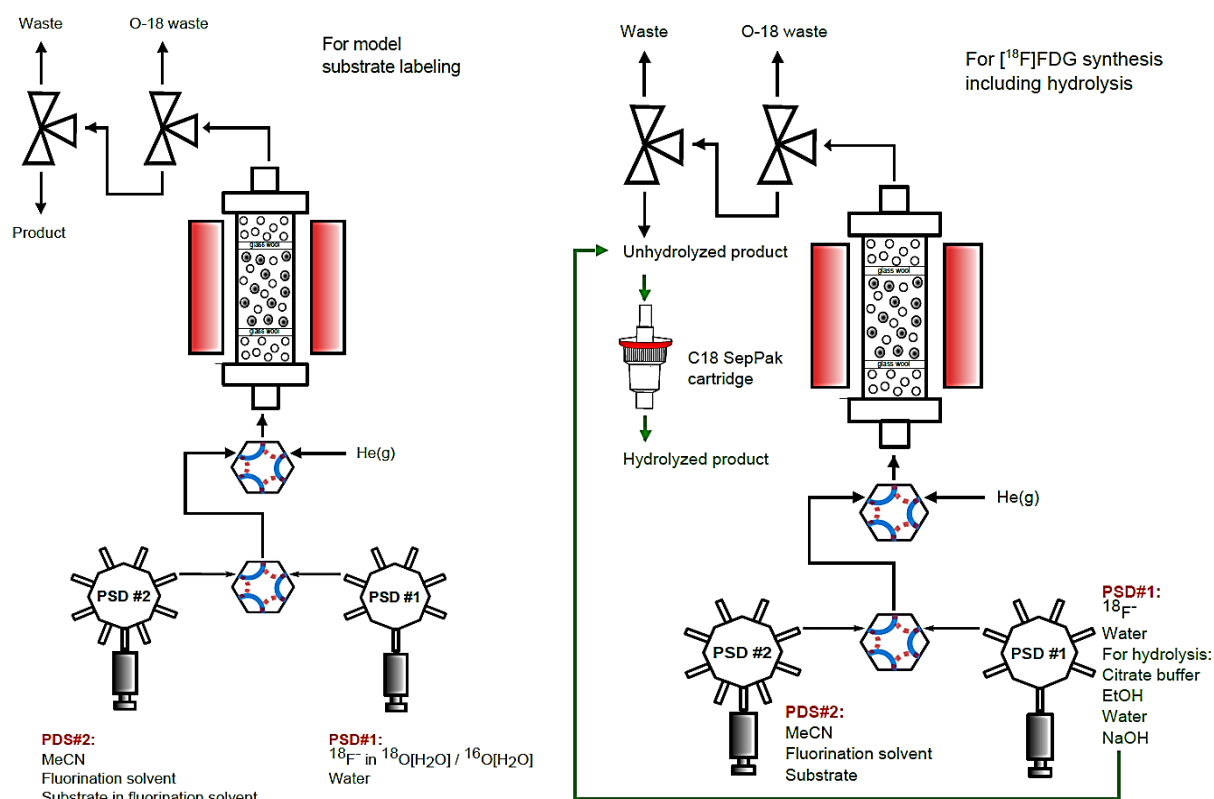
Figure 5-6. Schematics of the automated radiofluorination setups (PSD = Presition Syringe Drive)

Through LabView a program for each kind of experiment was made, and each parameter (solvent volume and flow speed, He flow time etc.) could be varied depending on the purpose of each experiment. An example of a standard radiofluorination of NpEtOMs is shown in Figure 5-7. Part A in

the program is the trapping step, where $[^{18}F]F^-/[^{18}O]H_2O$ is passed though the column and $[^{18}O]H_2O$ is recovered. Part B is the column drying step, where dry MeCN is passed though the column (in this case at 50°C) followed by a He(g) flush. Part C is priming of the column using the solvent for the labeling following the labeling step itself. The latter is done in six consecutive steps of 0.5 mL in order to get the flow of substrate though the column slowly enough (mechanical restrictions). To the left the level of activity on the column (top graph) as well as the product vial (bottom graph) can be seen. There it is possible to see both the trapping of activity on the column as well as removal of activity from the column to the product vial during the labeling step. In Appendix 2 more radiofluorination programs can be seen.
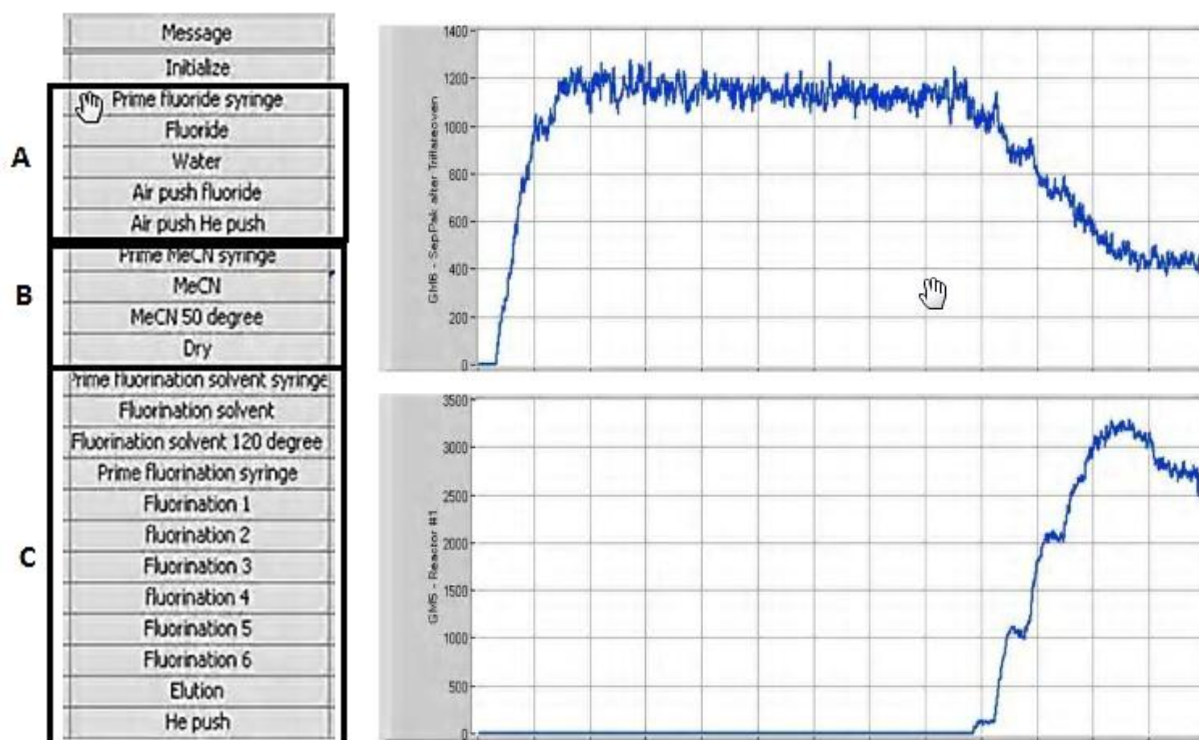
Figure 5-7. To the left: A LabView radiofluorination program. Top right: Activity on the column during the program. Bottom right: Activity in the product vial.

The work carried out to develop a solid-phase radiofluorination methodology is published[107] and the article is presented on the following pages.

5.5 Article III - Automated solid-Phase Radiofluorination Using Polymer-Supported Phosphazenes

5.5.1 Introduction to the article

Commercially available polymer supported phosphazene base **PS**-P_2^{tBu} was used for the first stage in the development of the solid-phase radiofluorination methodology. Preliminary experiments carried out manually showed that this resin was able to efficiently extract [18F]F- from the [18F]F-/[18O]H_2O solution from the cyclotron and the resulting **PS**-P_2^{tBu}.[18F]HF species could be used for the radiofluorination of both aliphatic and aromatic substrates, including [18F]FDG. The next step was an optimization of the reaction conditions. For this an automation apparatus was applied. In this way we could control the parameters in question and thereby establish which ones that were crucial for the trapping and labeling step, respectively. First the trapping parameters were analyzed, and it became very clear that the resin amount was crucial for the trapping efficiency compared to the amount of water, or the water flow rate. These experiments also showed that the same column could be used several times with little effect on the trapping efficiency. This was very encouraging as reusability is a crucial step towards simplification and miniaturization of the radiofluorination procedures. Optimization studies of the radiofluorination step provided us with the knowledge that the labeling temperature and the amount of resin in the column had a correlative effect on RCY and RCP. In other words, the effect of temperature on RCY and RCP depends on the amount of resin. Reusability of the column for the radiofluorination step was also possible and we could even conclude that the RCY increased for each experiment on the same column.

The RCYs achieved during the optimization studies were below 50% for the first experiment on a fresh column and consistently below 70% for any repetition on the same column (substrate NpEtOMs). It was thought that this was partly because of the very poor swelling properties of the **PS**-P_2^{tBu} resin and we turned to the investigation of the polymer matrix effect. The polymer-supported phosphazene base **PS**-P_2^{PEG} was synthesized, as it was expected that the highly swellable PEG-grafted (TentaGel) polystyrene matrix could influence positively on the RCYs. This high swelling actually complicated the radiofluorination protocol due to disruption of the uniform flow of substrate through the resin because of the trapping of air bubbles. This was partially rectified by adjusting the labeling

protocol, but RCY topped at 38% (substrate NpEtOMs). **PS**-P$_2^{PEG}$ could also be reused similarly to **PS**-P$_2^{tBu}$.

  PS-P$_2^{tBu}$ and **PS**-P$_2^{PEG}$ were analyzed with regard to the substrate scope, which showed that sulfonates were good substrates for on-column radiofluorination. Halides could be labeled with **PS**-P$_2^{tBu}$ only. [18F]FDG and [18F]FLT were both synthesized by our solidphase radiofluorination protocol. [18F]FDG was even synthesized on a 120 GBq scale with RCY at 40% and with a product that met the stringent GMP quality control requirements set for the release of commercial [18F]FDG produced in our laboratory.

5.5.2 The article

OPEN ACCESS

molecules

Article

Automated Solid-Phase Radiofluorination Using Polymer-Supported Phosphazenes

Bente Mathiessen and Fedor Zhuravlev *

Hevesy Laboratory, Center for Nuclear Technologies, Technical University of Denmark, Risø Campus, Frederiksborgvej 399, P.O. Box 49, 4000 Roskilde, Denmark; E-Mail: beem@dtu.dk

*   Author to whom correspondence should be addressed; E-Mail: fezh@dtu.dk;
    Tel.: +45-4677-5337; Fax: +45-4677-5347.

Abstract: The polymer supported phosphazene bases $PS-P_2^{tBu}$ and the novel $PS-P_2^{PEG}$ allowed for efficient extraction of $[^{18}F]F^-$ from proton irradiated $[^{18}O]H_2O$ and subsequent radiofluorination of a broad range of substrates directly on the resin. The highest radiochemical yields were obtained with aliphatic sulfonates (69%) and bromides (42%); the total radiosynthesis time was 35–45 min. The multivariate analysis showed that the radiochemical yields and purities were controlled by the resin load, reaction temperature, and column packing effects. The resins could be reused several times with the same or different substrates. The fully automated on-column radiofluorination methodology was applied to the radiosynthesis of the important PET radiotracers $[^{18}F]FLT$ and $[^{18}F]FDG$. The latter was produced with 40% yield on a 120 GBq scale and passed GMP-regulated quality control required for commercial production of $[^{18}F]FDG$. The combination of compact form factor, simplicity of $[^{18}F]F^-$ recovery and processing, and column reusability can make solid phase radiofluorination an attractive radiochemistry platform for the emerging dose-on-demand instruments for bedside production of PET radiotracers.

Keywords: solid phase radiofluorination; dose-on-demand; polymer-supported phosphazene; $[^{18}F]$; multivariate analysis

95

1. Introduction

Over the years positron emission tomography (PET) has developed into one of the most successful nuclear imaging modalities [1]. PET is a non-invasive, 10^{-12}M/cm^3-sensitive imaging method [2], able to provide quantitative biomolecular information regarding physiological processes in real time [3]. PET is currently finding applications in cardiology, neuroscience, oncology, gene therapy [4] and drug development [5]. Although more positron emitting radionuclides find their way into PET applications, fluorine-18 remains the most used PET radioisotope [6] due to its optimal half-life ($T_{1/2}$ = 109.8 min), high-yielding positron decay (97%, no γ-emission) and a low and narrow energy spectrum (E_{avg} = 249.3 keV, E_{max} = 633.5 keV), which translates into lower noise and higher image spatial resolution [7]. In a typical PET radiopharmacy setting, 200 GBq of cyclotron-produced [^{18}F]F$^-$ would be used to synthesize 15-20 doses of a given radiopharmaceutical and to ship it to a number of satellite PET centers. Due to high cost of establishing and maintaining the production facilities as well as difficulties associated with radiotracer development, the centralized PET radiopharmacies tend to have a lean and expensive radiotracer "menu". This limits the diversity of existing, and creates a barrier to adoption of new PET radiotracers [8]. Allowing researchers and clinicians to produce a tracer of their choice wherever and whenever there is a need for it, is a new paradigm often referred to as the "dose-on-demand" radiotracer production. Whether the tracer is produced from a radioisotope made at a centralized facility, or made on-site using the emerging compact cyclotron/radiosynthesis instruments [9], the dose-on-demand approach requires a significant change in current radiosynthesizer technology. The preferred embodiment of the dose-on-demand concept is an affordably priced, GMP-compliant, fully automated, compact (preferably table-top) instrument featuring: (1) single dose on demand tracer delivery via tracer-specific kits; (2) ability to run custom radiosyntheses; (3) execution of back-to-back production runs with minimal cassette replacement and radiation exposure to the operator; (4) integrated quality control (QC) module; (5) easy maintenance and operational simplicity. While some of these challenges can be met with new engineering approaches [10], the development of simpler and more efficient radiochemistry remains among the top priorities in radiochemical research.

In radiofluorination, the bottleneck is often considered to be the process of [^{18}F]F$^-$ recovery and activation. In routine production, the nanomolar amounts of cyclotron-produced [^{18}F]F$^-$ are recovered from several milliliters of its water solution by absorption onto an anion-exchange resin followed by elution with aqueous acetonitrile/ K$_2$CO$_3$ and Kryptofix. The subsequent azeotropic evaporations yield the [^{18}F]KF·Kryprofix complex in varying degrees of hydration and reactivity. The overall procedure requires multiple liquid and gas transfers resulting in lengthening of synthesis, diminished yields, and complex automation. Furthermore, the cartridge is not reusable and does not lend itself to efficient miniaturization. Significant efforts focused on eliminating the azeotropic evaporation step, for example, by using ionic liquids [11] or by eluting [^{18}F]F$^-$ with a strong organic base in the presence of protic additives [12]. In the light of potential applicability to dose-on-demand radiosynthesis, a more attractive approach would involve radiofluorination performed directly on the solid phase extraction (SPE) media. This would obviate the need for fluoride elution and azeotropic evaporation and allow for seamless integration of potentially reusable SPE resin into an automated dose-on-demand radiosynthesis module. The viability of radiofluorination at the point of fluoride capture was previously demonstrated [13,14], although the non-reusable aminopyridine-based resin suffered from

poor stability and inconsistent $[^{18}F]F^-$ trapping and radiofluorination. Herein, we report fully automated on-column radiofluorination of a wide variety of substrates using reusable polymer supported phosphazenes.

2. Results and Discussion

We have recently reported that phosphazenium hydrofluoride $[^{18}F]P_2^{Et}\cdot HF$ obtained by the reaction of P_2^{Et} (Scheme 1) with $[^{18}F]HF$ [15] is an efficient radiofluorination reagent (Scheme 2A) [16].

Scheme 1. Some phosphazene bases and substrates used in this study.
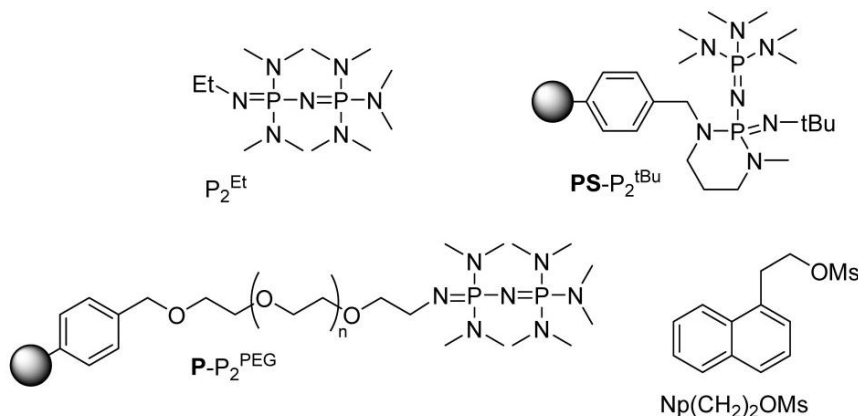
To access the radiolabeling ability of its polymer-supported analogue, we reacted the commercially available polystyrene-supported **PS**-P_2^{tBu} with $[^{18}F]HF_{(gas)}$ trapping 90% of activity as $[^{18}F]$**PS**-$P_2^{tBu}\cdot HF$. The subsequent reaction of the resin with the reference substrate $Np(CH_2)_2OMs$ [16,17] (Scheme 1) yielded the desired $[^{18}F]Np(CH_2)_2F$, albeit in only 5% radiochemical yield (RCY) (Scheme 2B).
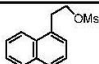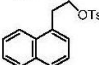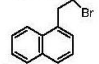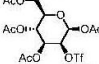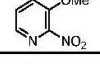
Scheme 2. Radiofluorination using phosphazene bases.
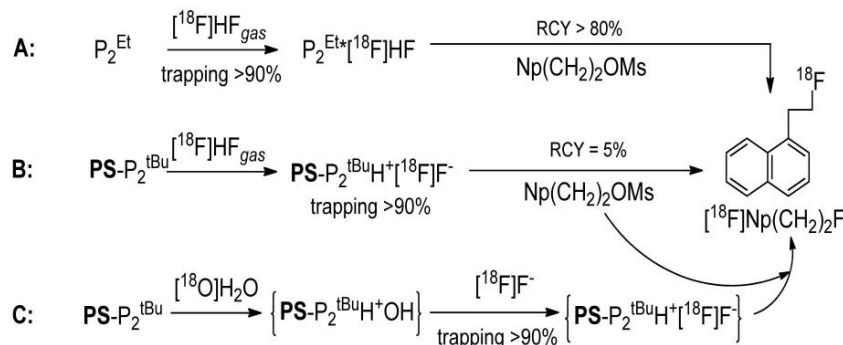
RCY aside, we were encouraged by these results: based on Lemaire's report,[12] one could expect the formation of $[^{18}F]$**PS**-$P_2^{tBu}H^+F^-$ from the putative **PS**-$P_2^{tBu}H^+OH^-$ via a $[^{18}F]F^-/OH^-$ anion exchange, whereas **PS**-$P_2^{tBu}H^+OH^-$ would result from the reaction of **PS**-P_2^{tBu} with water (Scheme 2C). Therefore, we decided to treat the resin with aqueous $[^{18}F]F^-$ and after drying, use the resulting $[^{18}F]F^-$-loaded resin for radiofluorination directly on the solid support. Indeed, this strategy proved

fruitful, as **PS-P$_2$**^{tBu} was able to extract the [^{18}F]F$^-$ from the cyclotron-irradiated target water and deliver it to a variety of substrates (Table 1).

Table 1. Manual on-column radiofluorination using **PS-P$_2$**^{tBu}: Preliminary experiments.

Entry [a]	Substrate	[^{18}F]F$^-$ trapping [%]	RCP [%] [b]	RCY [%] [c]
1	OMs	94	98	55
2	OTs	95	92	64
3	Br	99	61	16
4	AcO, O, OAc, AcO, OTf, OMe	84	76	25
5	N, NO$_2$	98	45	14

[a] New column for each experiment; Substrate: 0.2 mmol (52μmol for entry 4); **PS-P$_2$**^{tBu}: 100 mg; [^{18}F]F$^-$: 200–800 MBq; Column drying: MeCN, 7 mL at 30 mL/h, 60 °C; Radiofluorination: toluene, 5 mL at 10 mL/h, 90 °C; [b] RCP: radiochemical purity; [c] RCY: decay-corrected radiochemical yield based on [^{18}F]F$^-$$_{(aq)}$.

The preliminary experiments listed in Table 1 were performed manually, by sequential single passes of the target water, acetonitrile and the solution of a substrate through a flexible PTFE tube packed with the resin and immersed in an oil bath. We were pleased to see that both the aliphatic (entries 1–4) and the aromatic (entry 5) substrates could be radiofluorinated. On the other hand, the fluoride trapping, RCP and RCY varied significantly across the substrates/runs. While some variabilities were undoubtedly substrate-related, others could be due to operational variations, warranting systematic screening and optimization studies performed with automated equipment. To that end we prepared a column consisting of a short glass tube fitted with standard SwageLok fittings and packed with **PS-P$_2$**^{tBu} resin and glass beads to decrease back pressure. The column was connected to our home-made automated apparatus, where the necessary chemicals, solvents and gases could be remotely controlled and manipulated in a self-shielded and reproducible environment (Figure 1). Since the column could be as short as 5 cm, the size of the apparatus was limited only by the peripheral equipment, such as syringe pumps, valves and tubing.

In a typical automated experiment the target water was passed through the column, resulting in absorption of [^{18}F]F$^-$ on the resin. The residual water was then removed from the column by rinsing of the column with dry MeCN. Further drying could be assisted by passing a flow of He through the column at 60 °C. Finally, the solution of substrate was passed through the column at a suitable flow rate and temperature, effecting on-column radiofluorination. If necessary, the unreacted [^{18}F]F$^-$ could be removed from the product using a silica Sep-Pak cartridge (Figure 1). At the outset we recognized that the screening and optimization studies would require the exploration of the experimental domain defined by various physical and chemical parameters. While changing one variable at a time is a common strategy, a more efficient approach is the use of multivariate experimental design known as the design of experiments (DoE) [18]. In DoE the experimental conditions (factors) are varied systematically and simultaneously according to a DoE algorithm and the outcome of the experiments

(responses) are measured, thereby allowing for a statistically driven analysis of data in an optimal number of experiments. The final result is a model which describes the relationships between the factors and responses. The trapping efficiency of the resin was analysed first by varying the amount of resin (5–500 μmol), the volume of target water (0.5–3.5 mL), the flow rate (1.5–30 mL/min) and the number of times the column was used. The reaction matrix suggested by the DoE (Table 2) yielded an excellent single component partial least square (PLS) model ($R^2 = 0.91$, $Q^2 = 0.89$).

Figure 1. Automated radiosynthesis module for on-column radiofluorination.

Table 2. On-column [^{18}F]F$^-$ trapping using **PS**-P$_2$^{tBu}: trapping efficiency studies [a].

Number of times column was used [b]	Resin [μmol]	Water [mL]	Flow rate [mL/min]	[^{18}F]F$^-$ trapping [%]
1	5.8	0.5	1.5	77
4	5.8	0.5	1.5	67
1	509	0.5	1.5	100
4	509	0.5	1.5	100
1	5.5	3.5	1.5	57
4	5.5	3.5	1.5	58
1	499	3.5	1.5	100
4	499	3.5	1.5	100
1	5.1	30	30	56
4	5.1	30	30	52
1	501	30	30	100
4	501	30	30	99

[a] Full factorial design at two levels reduced to 12 experiments and analyzed by PLS; [b] after each trapping the column was washed with dry MeCN (50 mL, flow rate 1.5 mL/min, rt) and dried with a flow of He (flow rate: 100 mL/min, 20 min).

The variables important for the projection (VIP) plot indicated that the only factor controlling the trapping efficiency was the amount of resin (Figure 2). The column could be reused at least 3 times without any loss in $[^{18}F]F^-$ trapping efficiency and without resin degradation.

Figure 2. On-column $[^{18}F]F^-$ trapping using **PS**-P$_2^{tBu}$: variables important for the projection (VIP) plot.

We found that the minimal amount of resin necessary to obtain 99% trapping efficiency was 61 μmol (Figure 3).

Figure 3. On-column $[^{18}F]F^-$ trapping using PS-P$_2^{tBu}$: Correlation between resin amount and $[^{18}F]$fluoride trapping efficiency.

Although it is well known that hydration reduces fluoride nucleophilicity, some radiofluorination reactions show certain tolerance for water [11,12,16]. Since residual water entrapped in the resin could potentially influence both RCY and the radiochemical purity (RCP) we have attempted to optimize our drying protocol, varying the nature, the flow rate and the volume of the drying solvent, as well as the drying temperature (Table 3).

Table 3. Effect of column drying on radiofluorination of $Np(CH_2)_2OMs$ with **PS-P$_2^{tBu}$**.

Entry [a]	Drying solvent	Vol [mL]	Flow rate [mL/min]	Drying T [°C]	RCP [%] [b]	RCY [%] [c]
1	MeCN	1	1.5	25	88	32
2	Acetone	1	1.5	50	77	26
3	MeCN	10	1.5	50	77	18
4	Acetone	10	1.5	25	75	24
5	MeCN	1	20	50	74	20
6	Acetone	1	20	25	90	23
7	MeCN	10	20	25	85	32
8	Acetone	10	20	50	88	34
9	MeCN	5.5	10.75	38	85	25
10	MeCN	5.5	10.75	38	83	30
11	MeCN	5.5	10.75	38	91	31

[a] New column for each experiment; **PS-P$_2^{tBu}$**: 180 μmol; $[^{18}F]F^-$: 100-1000 MBq; Radiofluorination: $Np(CH_2)_2OMs$: 52 μmol; toluene, 3 mL, flow rate 0.55 mL/min, 90 °C; [b] RCP: radiochemical purity; [c] RCY: decay-corrected radiochemical yield based on $[^{18}F]F^-_{(aq)}$.

Despite good reproducibility (Table 3, entries 9–11), the analysis of the data showed little variability in RCY and did not result in a statistically valid model. No leaching of activity from the column was observed upon drying. For practical reasons, the drying protocol was adjusted to the use of MeCN (3–5 mL, 1.5 mL/min, 25 °C) for most of the following experiments.

The drying conditions established above were used to perform limited optimization studies where we looked at the influence of the amount of resin and the reaction temperature on RCP and RCY (Table 4). For consistency with our previous studies [16] the substrate loading was chosen at 52 μmol as the preliminary experiments showed that the high (150 μmol), medium (77.5 μmol) and low (5 μmol) substrate loading gave similar RCY.

Column packing effects, affecting the flow and likely to be responsible for some of the inter-column variability we have seen, were left out of optimization, as we did not find a reliable way to quantify them. It was also important to find out whether **PS-P$_2^{tBu}$** resin could be reused not only at the trapping stage (Table 2), but also after radiofluorination. To that end, the trapping and radiofluorination sequence was repeated several times on the same column (columns A, C, D, and E, Table 4).

The optimization studies yielded a 2-component PLS model ($R^2 = 0.99$, $Q^2 = 0.98$) which indicated a positive correlation for both the amount of resin and the reaction temperature. Higher amount of resin and higher temperature (T) led to higher RCP and RCY (Figure 4, left). Interestingly, the cross term *resin* * T was also important and positively correlated. The high covariance between the X-values (T, *resin*) and the Y values (RCY, RCP) can be clearly seen in the bi-plot (Figure 4, right) as the factors (X) and responses (Y) are grouped together. The RCP and RCY for columns A and B, and to a lesser extent C, are dominated by the *resin* and *resin* * T terms. The T variable overlaps with RCP and RCY, suggesting that the three are highly correlated. The cross term can be interpreted as interaction: the effect of T on RCY and RCP depends on the amount of resin.

Table 4. On-column radiofluorination of $Np(CH_2)_2OMs$ with $PS-P_2^{tBu}$: Optimization.

Entry [a]	Column/run [b]	$PS-P_2^{tBu}$, [μmol]	T [°C]	Trapping [%]	RCP [%] [c]	RCY [%] [d]
1	A/1	180	90	100	79	38
2	A/2	180	90	100	79	39
3	B	180	120	100	84	50
4	C/1	140	120	100	74	43
5	C/2	140	120	100	94	69
6	D/1	100	120	98	80	46
7	D/2	100	120	100	89	62
8	D/3	100	120	100	93	64
9	E/1	60	120	98	82	49
10	E/2	60	120	100	88	63

[a] Trapping: $[^{18}F]F^-/[^{18}O]H_2O$, 200–800 MBq, 3mL, 1.5mL/min; Drying: MeCN, 3mL, 1.5mL/min; Radiofluorination: $Np(CH_2)_2OMs$: 52 μmol; toluene, 3 mL, 0.55 mL/min, 90 °C; [b] Letter-coded columns A–E differed in $PS-P_2^{tBu}$ loading and reaction temperature, the Arabic numerals refer to the number of consecutive trapping and radiofluorination runs performed on that particular column; [c] RCP: radiochemical purity; [d] RCY: decay-corrected radiochemical yield based on $[^{18}F]F^-_{(aq)}$.

Importantly, Table 4 showed a consistent increase in the RCY and RCP when the columns were reused (columns A, C, D and E). The highest RCY and RCP (69% and 94%) were obtained on the second use of column C. Radio-TLC analysis showed that during radiosynthesis the only ^{18}F-containing materials found in the reaction mixture eluted from the column were $[^{18}F]Np(CH_2)_2F$ and $[^{18}F]fluoride$ (Figure 5). The formation of the latter was consistent with the substrate-dependent elimination of $[^{18}F]HF$ triggered by the basicity of $[^{18}F]$ F^-, as we have demonstrated for homogeneous fluorination with phosphazene hydrofluorides [16].

Figure 4. On-column radiofluorination of $Np(CH_2)_2OMs$ using $PS-P_2^{tBu}$: variables important for the projection (VIP) plot (**left**) and bi-plot of loadings and scores (t), (**right**).

Figure 5. On-column radiofluorination of Np(CH$_2$)$_2$OMs with **PS-P$_2$^{tBu}**: Radio-TLC.

The remaining activity was retained on the column and could be removed neither with the fresh portion of substrate nor with a variety of solvents, such as toluene, DMF or water. Increasing substrate's on-column residence time by recirculating the solution of Np(CH$_2$)$_2$OMs did not lead to any appreciable increase in RCY. The activity retained on the column after radiofluorination could indicate a physical entrapment of small fluoride anion within the polymer matrix, or a chemical deactivation due to reaction with the resin or impurities inside the resin.

Next, we turned to investigation of polymer matrix effects. The mobility of polymer chains and hence the accessibility of functional groups depends on polymer swelling. The highly cross-linked **PS-P$_2$^{tBu}** used in this study showed negligible swelling in MeCN, toluene and DMF. Therefore, swellable polymer matrix was sought after. The commercially available TentaGel-NH$_2$ resin, which is based on PEG-grafted polystyrene matrix offers a high and largely solvent-independent swelling. From the design point of view the TentaGel-NH$_2$ resin was also attractive as its alkyl-amino side chains could be easily functionalized with phosphazene residues. Consequently, the desired **PS-P$_2$^{PEG}** was synthesized by applying the Schwesinger's protocol [19] to the Tentagel –NH$_2$ resin (Scheme 3). Both **PS-P$_2$^{tBu}** and **PS-P$_2$^{PEG}** could be stored at room temperature indefinitely.

The resulting **PS-P$_2$^{PEG}** (95% phosphazene-functionalized) was reacted with Np(CH$_2$)$_2$OMs under the conditions optimized for **PS-P$_2$^{tBu}**. Unfortunately, due to its high swelling ability the microgel was prone to trapping air bubbles disrupting the uniform flow of the substrate through the column. Although this was partially rectified by careful degassing and recirculation of the starting material, the RCY topped at 38% (Table 5, entry 1). Similar to **PS-P$_2$^{tBu}**, the **PS-P$_2$^{PEG}** resin could be reused: the sequential radiofluorination of Np(CH$_2$)$_2$OMs and Np(CH$_2$)$_2$OTs performed on the same column gave the desired [^{18}F]Np(CH$_2$)$_2$F in 25% and 24% RCY correspondingly.

Scheme 3. Synthesis of **PS-P$_2^{PEG}$**.

Table 5 summarizes the scope of the polymer supported bases used for radiofluorination of Np(CH$_2$)$_2$OMs. **PS-P$_2^{tBu}$** gave the best RCY at 69% (entry 2) followed by **P-P$_2^{PEG}$** at 38% (entry 1). Both resins trapped 99% of [^{18}F]F$^-$. The polymer-supported DIPEA (entry 3) and BEMP (entry 4) failed to trap fluoride, consistent with their lower pKa (11.4 and 27.6, correspondingly).

Table 5. Radiofluorination of Np(CH$_2$)$_2$OMs: the scope of the polymer supported bases.

Entry [a]	Structure	[^{18}F]F$^-$ trapping [%]	RCY [%] [b]
1		99	38
2		99	69
3		— [c]	—
4		—	—

[a] New column for each experiment; Trapping: [^{18}F]F$^-$/[^{18}O]H$_2$O, 500–1100 MBq, 3 mL, flow rate 1.5 mL/min; Drying: MeCN, 3 mL, flow rate 1.5 mL/min; Radiofluorination: Np(CH$_2$)$_2$OMs: 52 μmol; toluene, 3 mL, 0.55 mL/min, 90 °C; [b] RCY: decay-corrected radiochemical yield based on [^{18}F]F$^-$$_{(aq)}$; [c] below detection limit.
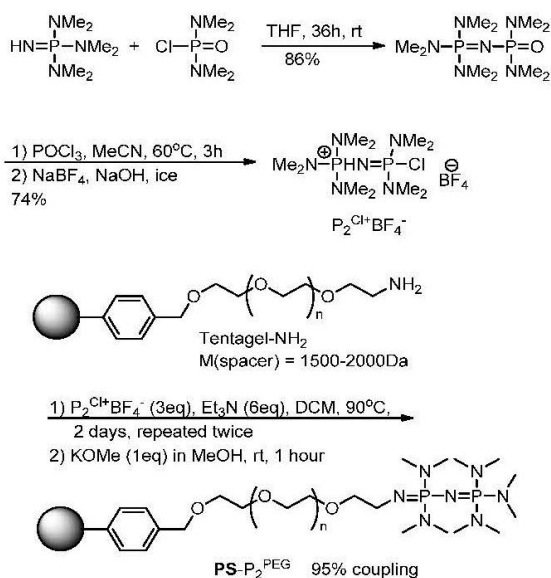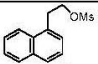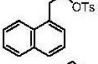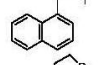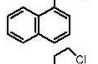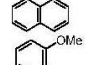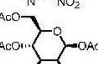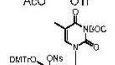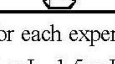
The optimized conditions established for $PS-P_2^{tBu}$ and $PS-P_2^{PEG}$ were used to investigate the substrate scope. The results are presented in Table 6. The reactivity profile of both resins was similar to that observed for homogeneous radiofluorination with $[^{18}F]P_2^{Et}HF$.[16] The sulfonates (Table 6, entries 1,2, and 7) were the best substrates for on-column radiofluorination with $PS-P_2^{tBu}$ and $PS-P_2^{PEG}$, delivering tetra-*O*-acetyl-$[^{18}F]FDG$ in 52% and 36% RCY, correspondingly (Table 5, entry 7). The halides could be radiofluorinated with $PS-P_2^{tBu}$, but not with $PS-P_2^{PEG}$ (Table 6, entries 3–5). The corresponding yields of FLT were only 7% and 5%, which is at the lower end of the currently reported homogeneous radiofluorination yields (8%–50%) [20]. The total radiosynthesis time for any substrate did not exceed 45 min.

Table 6. Radiofluorination with $P-P_2^{tBu}$ and $P-P_2^{PEG}$: The substrate scope.

Entry [a]	Substrate	Trapping $PS-P_2^{tBu}/PS-P_2^{PEG}$ [%]	RCP [b] $PS-P_2^{tBu}/PS-P_2^{PEG}$ [%]	RCY [c] $PS-P_2^{tBu}/PS-P_2^{PEG}$ [%]
1	OMs	99/99	97/96	51/38
2	OTs	94/100	86/96	34/24
3	I	94/100	73/-	18/-
4	Br	95/99	93/-	42/-
5	Cl	95/95	67/-	16/-
6	OMe / NO2	92/100	60/-	23/-
7	AcO... OAc / OTf	99/98	99/97	52/36
8	DMTrO ONs	100/100	65/92	7/5

[a] New column for each experiment; Trapping: $[^{18}F]F^-/[^{18}O]H_2O$, 500–5000 MBq, 3 mL, flow rate 1.5 mL/min; Drying: MeCN, 3 mL, 1.5 mL/min; Radiofluorination: Substrate: 100 μmol; in toluene at 120 °C (aromatic substrates), tBuOH: MeCN 5:1 at 100 °C (FLT) or MeCN at 85 °C (FDG), flow 0.55 mL/min; Total radiosynthesis time between 35 and 45 min. [b] RCP: radiochemical purity; [c] RCY: radiochemical yield based on $[^{18}F]F^-_{(aq)}$ as an average of two runs.

Finally, the on-column solid phase radiofluorination was applied to the automated radiosynthesis of $[^{18}F]FDG$ on a 120 GBq scale typically used for the commercial production of this radiotracer in our laboratory. The apparatus was adopted to accommodate the hydrolysis step (Figure 6).

Using $PS-P_2^{tBu}$ we achieved 98% of $[^{18}F]F^-$ trapping efficiency obtaining the desired $[^{18}F]FDG$ in 40% RCY and 96.7% RCP as measured by the radio-HPLC and radio-TLC. The specific activity was measured to be higher than 11 GBq/μmol, the limit of detection of cold FDG by our HPLC. Importantly, the resulting formulation of on-column produced $[^{18}F]FDG$ met the stringent GMP quality control requirements used in our laboratory to release the commercial $[^{18}F]FDG$ produced by the conventional methodology (Table 7).

Figure 6. Automated radiosynthesis module for on-column radiosynthesis of $[^{18}F]FDG$.
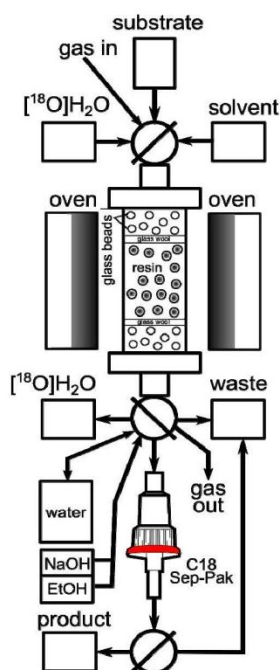
Table 7. Automated on-column radiosynthesis of $[^{18}F]FDG$ on 120 GBq scale: Quality Control.

Analysis	Result	Requirement (European Pharmacopoeia)
$[^{18}F]F^-$	0.5%	<5%
$[^{18}F]FDM$	ND	<10%
$[^{18}F]FDG$	97.8%	≥85%
Unhydrolyzed $[^{18}F]FDG$	1.0%	<5%
RCP	96.7%	≥95%
$[^{19}F]FDG$	<0.0167mg/mL	≤0.0167 mg/mL
Glucose	0.13mg/mL	No limit
Appearance	Clear, colorless	Clear, colorless or slightly yellow

3. Experimental

3.1. General

Unless otherwise noted, all synthetic steps were performed under an inert atmosphere of argon. Glassware and reaction vessels were dried in an oven at 160 °C overnight or flame-dried on the Schlenk line before use. All reagents were used as received without additional purification; toluene and THF were distilled from sodium benzophenone; other solvents were dried over activated molecular sieves. All radiochemical yields were decay-corrected. Polymer-supported P_2^{tBu} (loading: 1.6 mmol/g), 2-tert-Butylimino-2-diethylamino-1,3-dimethylperhydro-1,3,2-diazaphosphorine (BEMP, loading: 2.3 mmol/g) and diisopropylaminoethyl (DIPEA, loading: 3 mmol/g) were obtained from Sigma Aldrich; the amine-functionalized polystyrene resin with polyethylene glycol spacer (TentaGel HL, particle size 160 µm, loading: 0.4 mmol/g, PEG: 1500–2000 Da) was purchased from Rapp Polymere

10543

GmbH. Mannose triflate was purchased from Sigma Aldrich and 3-*N*-Boc-5'-*O*-dimethoxytrityl-3'-*O*-nosyl-thymidine (FLT precursor) was purchased from ABX. The naphthalene halides or pseudohalides were purchased from Sigma Aldrich or synthesized as described elsewhere.

3.2. Instrumentation

^{1}H, ^{13}C and ^{31}P-NMR spectra were recorded on a Bruker Avance II 500 instrument operating at 500, 126 and 202 MHz, respectively. ^{19}F-NMR was recorded on a Brucer Avance DPX 250 instrument at 235 MHz. Mass spectrometry was performed on a Bruker Esquire 4000 ion-trap (IT) spectrometer equipped with electrospray ionization (ESI) interface. Thin-layer chromatography (TLC) was run on pre-coated plates of silica gel 60, F254 (Merck). Radio-HPLC was performed by using a Knauer HPLC System K501, equipped with a Knauer RI detector K2301 and CRA radioactivity detector 105 S-1 on a Carbopac PA10 4_25 mm Dionex column eluted with 0.1M NaOH at 1.0 mL min^{-1}. Radio-TLC was performed with a Raytest MiniGita TLC scanner. The aqueous solutions of fluoride-18 were prepared by the ^{18}O(p,n)^{18}F reaction in a GE PETtrace cyclotron using a Ag or Nb target containing ~2.5 mL of 95%–98% enriched [^{18}O]H$_2$O irradiated by a 16.5 MeV proton beam at 55 μA. For automated radiosynthesis we used custom-made radiosynthesis robot controlled by LabView software.

3.3. Multivariate Analysis

Multivariate analysis was performed using MODDE 9.0 and SIMCA 13 software. The raw data were mean-centered and Pareto scaled; the Hotteling T2 values were below 95% for all models.

3.4. Synthesis of PS-P$_2^{PEG}$

TentaGel-NH$_2$ was reacted with P$_2^{Cl}$*BF$_4$[19] by mixing the resin (200–1000 mg) with P$_2^{Cl}$*BF$_4$ (3 eq. relative to the amine) and Et$_3$N (dry, 9 eq relative to the amine) in DCM (dry, 5 mL) in a sealed glass ampule. The reaction mixture was then heated and shaken at 90 °C for three days. The procedure was repeated one more time in order to ensure better coupling. The resulting resin was deprotonated by reacting the resin with a mixture of KOMe (1 eq to amine) in MeOH (dry, 5 mL) for one hour giving the desired **PS-P$_2^{PEG}$**. The degree of resin functionalization by the phosphazene residues was estimated using [^{19}F/^{18}F]fluoride trapping in the following way: an aqueous solution of [^{19}F]NaF (42.54 mg, 1.013 mmol) and [^{18}F]F$^-$ (82.85 MBq) in 3.4 mL, corresponding to 0.012 mmol [^{19}F]F$^-$ MBq^{-1} was passed through a column containing **PS-P$_2^{PEG}$** (204.58 mg, original amine content 0.4 mmol g^{-1}) at 1 mL/min; the column was then washed with water (4 mL, flow 1 mL/min). The activity retained on the column was measured at 6.49 MBq [^{18}F]F$^-$, which corresponded to 0.078 mmol [^{19}F]F$^-$, and consequently, to 0.38 mmol of phosphazene residues per gram of resin (95% of the original amine functionalization).

3.5. [^{18}F]Fluoride Trapping, RCP and RCY

[^{18}F]fluoride trapping [%] was based on target water and calculated as: Trapping = 100%* (Activity $^{\text{added to the column}}$ − Activity $^{\text{eluted from the column}}$)/Activity $^{\text{added to the column}}$. The RCP was determined by

radio-TLC or radio-HPLC and calculated as: RCP = (Area^{product}/Total Area)*100%. The RCY was determined by the dose calibrator and calculated as RCY=Activity^{product}*RCP/Activity$^{[18F]F^-\ added\ to\ the\ column}$.

3.6. Manual Radiofluorination of [^{18}F]Np(CH$_2$)$_2$OMs with [^{18}F]HF and PS-P$_2^{tBu}$ (Scheme 2, B)

A PTFE tube (OD = 0.64 cm) was packed with **PS-P$_2^{tBu}$** (100–200 mg) and 1200 mg of glass beads and connected to a PE vial containing 4 mL of 98% H$_2$SO$_4$. The PE vial was connected to an Ar inlet and Ar was bubbled through sulphuric acid at a rate of 150–300 scc/min. [^{18}F]F$^-$$_{(aq)}$ (1 mL, 200–500 MBq) was added and the vial was heated for 30 min at 80 °C in an ultrasound bath while being irradiated at 35 kHz under the flow of Ar. The resulting [^{18}F]HF was carried by argon flow to the column. After 30 min the column was placed in an oil bath at 100 °C and a solution of NpEtOMs (200 μmol) in toluene (dry, 5 mL) was passed through the column using a syringe pump (flow rate 10 mL/h). Toluene (dry, 5 mL) was passed through the column to elute the residual product. The fluorinated product was analyzed by radio-TLC (eluent heptane:EtOAc 80:20). Trapping = 95%, RCP = 73%, RCY = 5%. Total time of radiosynthesis was up to 90 min.

3.7. General Procedure for Manual Solid-Phase Radiofluorination (Scheme 2 C and Table 1)

An aliquot of [^{18}F]F$^-$$_{(aq)}$ (1.0 ml, 200–800 MBq) was mixed with water (3 mL) and passed through the column (PTFE tube, **PS-P$_2^{tBu}$**: 100 mg; glass beads: 1200 mg). MeCN (dry, 7 mL) was then passed through the column (flow rate: 30 mL/h, duration 10 min, rt to 60 °C) followed by Ar until excess of solvent was removed. A substrate (52–200 μmol) was dissolved in toluene (dry, 5 mL) and the solution was passed through the column (flow rate 10 mL/h, duration 30 min) while heating the column at 90 °C. Thereafter, toluene (dry, 5 mL) was passed through the column (flow rate 20 mL/h, duration 15 min) at 90 °C to elute the remaining product. The fluorinated products were analyzed by radio-TLC (eluent heptane:EtOAc 80:20 for the naphthalene derivatives, MeCN:H$_2$O 95:5 for Ac$_4$-FDG, DCM:MeOH 9:1 for hydrolyzed FLT, petroleum ether:EtOAc 3:1 for the pyridine derivative) Total time of radiosynthesis was 60–90 min.

3.8. General Procedure for Automated Solid-Phase Radiofluorination Using PS-P$_2^{tBu}$

An aqueous solution of [^{18}F]F$^-$ (0.5–3.5 mL, flow rate 0.5–30 mL/min) was passed through the column (borosilicate glass tubing, ID 4 mm, OD 0.6 cm, length 12 cm) packed with the resin (5–500 μmol; glass beads to fill the remaining volume). To remove the bulk of water, the column was flushed with He$_{(gas)}$ (flow rate 100 mL/min, 3 min). The column was dried by passing MeCN or acetone (1–10 mL, flow rate 1.5–20 mL/min) through, followed by a helium flush (100 mL/min, 2–5 min). The column was primed by passing the radiofluorination solvent (MeCN for mannose triflate, MeCN/tBuOH 1:5 for FLT-ONs, toluene for the naphthalene derivatives and 2-nitro-3-methoxypyridine, dry, 4 mL, flow rate 2 mL/min) through the column at room temperature followed by the substrate (50–100 μmol) dissolved in the radiofluorination solvent (dry, 3 mL) at 60–120 °C (flow rate 0.55 mL/min). The radiofluorination solvent (dry, 2 mL, flow rate 0.55 mL/min) was then passed through the column again to elute the remaining product. The reaction mixture was analyzed by radio-TLC (eluent heptane:EtOAc 80:20 for the naphthalene derivatives, MeCN:H$_2$O 95:5 for FDG,

Molecules **2013**, *18*   **10545**

DCM:MeOH 9:1 for hydrolyzed FLT, petroleum ether:EtOAc 3:1 for the pyridine derivative. Total time of radiosynthesis was 35–45 min.

3.9. General Procedure for Automated Solid-Phase Radiofluorination Using PS-P₂^{PEG}

The apparatus and column was degassed before use by passing through MeCN (5 mL, 1.5 mL/h) followed by water (5 mL, 1.5 mL/h). An aqueous solution of [^{18}F]F⁻ (3.5 mL, flow rate 1.5 mL/min) was passed through the column (borosilicate glass tubing, I.D. 4 mm, OD 0.6 cm, length 12 cm) packed with the resin (200–500 µmol). Residual water was removed by passing through MeCN (5 mL, flow rate 1.5 mL/min). The column was primed by passing the radiofluorination solvent (MeCN for mannose triflate, MeCN/tBuOH 1:5 for FLT-ONs, toluene for the naphthalene derivatives and 2-nitro-3-methoxypyridine, dry, 4 mL, flow rate 1.5 mL/min) through the column at room temperature followed by the substrate (50-100 µmol) dissolved in the radiofluorination solvent (dry, 3 mL) at 60–120 °C (flow rate 0.55 mL/min). The radiofluorination solvent (dry, 2 mL, flow 0.55 mL/min) was then passed through the column again to elute the remaining product. The reaction mixture was analyzed by radio-TLC (eluent heptane:EtOAc 80:20 for the naphthalene derivatives, MeCN:H₂O 95:5 for FDG, DCM:MeOH 9:1 for hydrolyzed FLT, petroleum ether:EtOAc 3:1 for the pyridine derivative. Total time of radiosynthesis was up to 45 min.

3.10. Washing Procedure for Back-to-Back Radiofluorination

After each trapping-radiofluorination sequence the column was washed with dry MeCN (50 mL, flow rate 1.5 mL/min, rt) and dried with a flow of He (flow rate: 100 mL/min, 20 min).

3.11. Large Scale Automated [^{18}F]FDG Synthesis using P-P₂^{tBu} Column

Mannose triflate together with the solvents and reagents used for hydrolysis of the product was acquired from ABX Advanced Biochemical Compounds (Radeberg, Germany) and are of pharmaceutical grade quality manufactured according to GMP standards. The cyclotron irradiated target water containing [^{18}F]F⁻ (3.0 mL, flow rate 1.5 mL/min, 119 GBq) was passed through the column (borosilicate glass, **PS-P₂^{tBu}**: 100 µmol; glass beads to fill the remaining volume) followed by He$_{(gas)}$ (flow rate 100 mL/min, 2 min). MeCN (dry, 5 mL, flow 1.5 mL/min) was passed through the column followed by He$_{(gas)}$ (100 mL/min, 3 min) in order to dry the column completely (trapped 117 GBq of [^{18}F]F⁻, 98% trapping efficiency). MeCN (dry, 4 mL, flow 2 mL/min) was passed through the column at room temperature followed by mannose triflate (25 mg, 52 µmol) dissolved in MeCN (dry, 3 mL) at 85 °C (flow 0.55 mL/min). MeCN (dry, 2 mL, flow 0.55 mL/min) was then passed through the column to elute the remaining product. The two fractions were mixed with water (total volume 50 mL) and passed through a tC C-18 Sep Pak cartridge (preconditioned using 5.0 mL EtOH and 5.0 mL water) to trap the unhydrolyzed [^{18}F]FDG. The cartridge was washed with water (5 mL). NaOH (2.0 M, 0.5 mL) was added to the cartridge in order to hydrolyze the compound (duration 5 min) and the hydrolyzed product was eluted with water (5 mL) to a product vial containing saline (9 mg/mL NaCl, 0.64% EtOH, total volume 14 mL) and a buffer solution (citrate buffer, 6 mL, pH 1.3). Full QC analysis confirmed that the product was [^{18}F]FDG (49 GBq, RCP 97%, RCY 41%).

10546

4. Conclusions

In conclusion, we have demonstrated that polymer supported phosphazenes **PS-P$_2$^{tBu}** and the novel **PS-P$_2$^{PEG}** allowed for efficient extraction of [^{18}F]F$^-$ from the target water and subsequent radiofluorination of a broad range of substrates directly on the resin, thus simplifying radiosynthesis and QC by avoiding [^{18}F]F$^-$ elution, azeotropic evaporation and kryptand addition. The highest radiochemical yields were obtained with aliphatic sulfonates (69%) and bromides (42%); the total radiosynthesis time for any substrate did not exceed 45 min. We found that the RCY and RCP were controlled by the amount of resin, reaction temperature, and column packing effects. The same resin could be used at least 3 times with the same substrate and at least two times with two different substrates. The incorporation of the compact phosphazene resin column into a remotely controlled programmable dispensing system resulted in a solid phase radiosynthesis module which was used for automated radiosyntheses, including FLT and a large scale production of [^{18}F]FDG. Although at this stage of development the solid phase RCY are generally ~10%–30% behind those obtained homogeneously, the large scale production of GMP-quality [^{18}F]FDG with 40% RCY and 97% RCP clearly demonstrates the potential of solid phase radiofluorination methodology. We believe that the combination of compact form factor, streamlined [^{18}F]F$^-$ recovery and processing, and column reusability will make the solid phase radiofluorination an attractive radiochemistry platform for the emerging dose-on-demand instruments for bedside production of PET radiotracers.

Supplementary Materials

Supplementary materials can be accessed at: http://www.mdpi.com/1420-3049/18/9/10531/s1.

Acknowledgments

Conflicts of Interest

The authors declare no conflict of interest.

References

1. Paans, A.M. J.; van Waarde, A.; Elsinga, P.H.; Willemsen, A.T.M.; Vaalburg, W. Positron emission tomography: The conceptual idea using a multidisciplinary approach. *Methods* **2002**, *27*, 195–207.
2. Skotland, T. Molecular imaging: Challenges of bringing imaging of intracellular targets into common clinical use. *Contrast Media Mol. Imaging* **2012**, *7*, 1–6.
3. Ametamey, S.M.; Honer, M.; Schubiger, P.A. Molecular imaging with PET. *Chem. Rev.* **2008**, *108*, 1501–1516.
4. Collins, S.A.; Hiraoka, K.; Inagaki, A.; Kasahara, N.; Tangney, M. PET Imaging for gene cell therapy. *Curr. Gene Ther.* **2012**, *12*, 20–32.
5. Marik, J.; Bohorquez, S.M.S.; Williams, S.-P.; van Bruggen, N. New imaging paradigms in drug development: The PET imaging approach. *Drug Discovery Today* **2011**, *8*, e63–e69.

6. Coenen, H.H.; Elsinga, P.H.; Iwata, R.; Kilbourn, M.R.; Pillai, M.R.A.; Rajan, M.G.R.; Wagner, H.N., Jr.; Zaknun, J.J. Fluorine-18 radiopharmaceuticals beyond [18F]FDG for use in oncology and neurosciences. *Nucl. Med. Biol.* **2010**, *37*, 727–740.

7. Sanchez-Crespo, A. Comparison of Gallium-68 and Fluorine-18 imaging characteristics in positron emission tomography. *Appl. Radiat. Isotopes* **2013**, *76*, 55–62.

8. Keng, P.Y.; Esterby, M.; van Dam, R.M. Emerging technologies for decentralized production of PET tracers. *Positron Emiss. Tomogr. Clin. Res. Asp.* **2012**, 153–182.

9. Nutt, R.; Vento, L.; Ridinger, M. *In Vivo* molecular imaging biomarkers: Clinical pharmacology's new "PET"? *Clin. Pharmacol. Ther.* **2007**, *81*, 792–795.

10. Ming-Wei W. Wei-Yu L.; Kan L.; Masterman-Smith, M.; Kwang-Fu S.C. Microfluidics for positron emission tomography probe development. *Mol. Imaging* **2010**, *9*, 175–191.

11. Kim, D.W.; Choe, Y.S.; Chi, D.Y. A new nucleophilic fluorine-18 labeling method for aliphatic mesylates: Reaction in ionic liquids shows tolerance for water. *Nucl. Med. Biol.* **2003**, *30*, 345–350.

12. Lemaire, C.F.; Aerts, J.J.; Voccia, S.; Libert, L.C.; Mercier, F.; Goblet, D.; Plenevaux, A.R.; Luxen, A.J. Fast production of highly reactive no-carrier-added [18F]fluoride for the labeling of radiopharmaceuticals. *Angew. Chem. Int. Ed.* **2010**, *49*, 3161–3164.

13. Mulholland, G.K.; Mangner, T.J.; Jewett, D.M.; Kilbourn, M. R. Polymer-supported nucleophilic radiolabeling reactions with [18F]fluoride and [11C]cyanide ion on quaternary ammonium resins. *J. Label. Compound. Radiopharm.* **1989**, *26*, 378–380.

14. Toorongian, S.A.; Mulholland, G.K.; Jewett, D.M.; Bachelor, M.A.; Kilbourn, M.R. Routine production of 2-deoxy-2-[18F]fluoro-d-glucose by direct nucleophilic exchange on a quaternary 4-aminopyridinium resin. *Int. J. Rad. Appl. Instrum. B* **1990**, *17*, 273–279.

15. Mathiessen, B.; Jensen, M.; Zhuravlev, F. [18F]Fluoride recovery via gaseous [18F]HF. *J. Label. Compound. Radiopharm.* **2011**, *54*, 816–818.

16. Mathiessen, B.; Jensen, A.T.I.; Zhuravlev, F. Homogeneous nucleophilic radiofluorination and fluorination with phosphazene hydrofluorides. *Chem-Eur. J.* **2011**, *17*, 7796–7805.

17. Jadhav, V.H.; Jang, S.H.; Jeong, H.-J.; Lim, S.T.; Sohn, M.-H.; Chi, D.Y.; Kim, D.W. Polymer-supported pentaethylene glycol as a facile heterogeneous catalyst for nucleophilic fluorination. *Org. Lett.* **2010**, *12*, 3740–3743.

18. Wold, S.; Sjöström, M.; Carlson, R.; Lundstedt, T.; Hellberg, S.; Skagerberg, B.; Wikström, C.; Öhman, J. Multivariate design. *Anal. Chim. Acta* **1986**, *191*, 17–32.

19. Schwesinger, R.; Schlemper, H.; Hasenfratz, C.; Willaredt, J.; Dambacher, T.; Breuer, T.; Ottaway, C.; Fletschinger, M.; Boele, J.; Fritz, H.; *et al.* Extremely strong, Uncharged auxiliary bases; Monomeric and polymer-supported polyaminophosphazenes (P2–P5). *Liebigs Ann.* **1996**, *1996*, 1055–1081.

20. Niedermoser, S.; Pape, M.; Gildehaus, F.J.; Wängler, C.; Hartenbach, M.; Schirrmacher, R.; Bartenstein, P.; Wängler, B. Evaluation of an automated double-synthesis module: Efficiency and reliability of subsequent radiosyntheses of FHBG and FLT. *Nucl. Med. Biol.* **2012**, *39*, 586–592.

Sample Availability: Not available.

5.5.3 Impurities in the product from solid-phase radiofluorination

Kuge *et al.*[108] have described the analysis of chemical impurities resulting from the production of [^{18}F]FDG with the application of Toorongians 4-aminopyridinium resin. It was done by ion chromatography and the impurities found were D-glucose, FDG, 2-deoxy-2-chloro-D-glucose (ClDG), and D-mannose. The non-radioactive fluoride and chloride are assumed either to originate from the [^{18}F]F$^-$/[^{18}O]H$_2$O cyclotron solution or, for chloride, from either the additives or the hydrolysis step. ClDG and FDG are a result of the nucleophile attack of these ions on mannose triflate. They assumed that D-mannose and D-glucose were a result of hydrolysis of mannose triflate (Figure 5-8). The amounts of these impurities were similar to those found in [^{18}F]FDG productions based on conventional methods. FDM and [^{18}F]FDM were not detected. Nor was contamination of the 4-methylpiperidine, which could be suspected to leach from the resin.
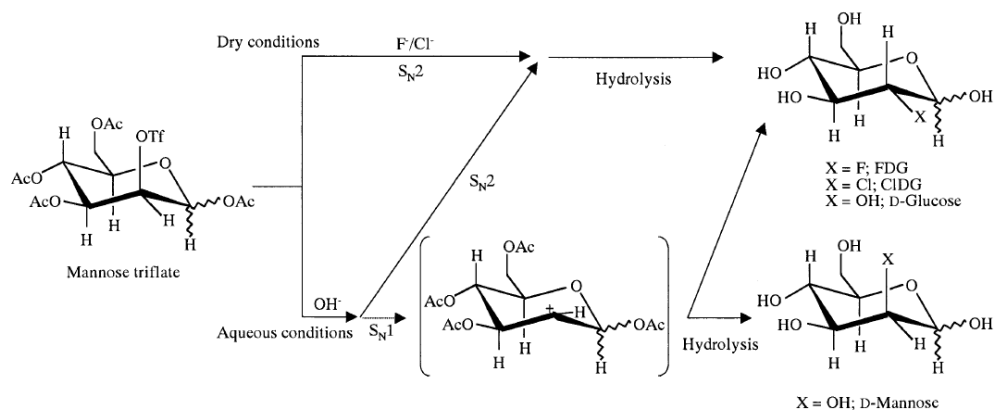
Figure 5-8. Formation of impurities during the [^{18}F]FDG synthesis

Based on this work we decided to take a closer look at the HPLC results from the 120 GBq production of [^{18}F]FDG described in article III in order to see if the product showed the same or other impurities that could indicate that the phosphazene-base mediated solid-phase labeling method was not stereospecific, or that impurities leached from the resin. The refractive index (RI) and radio detector (RD) chromatograms as well as an overlay are shown in Figure 5-9.
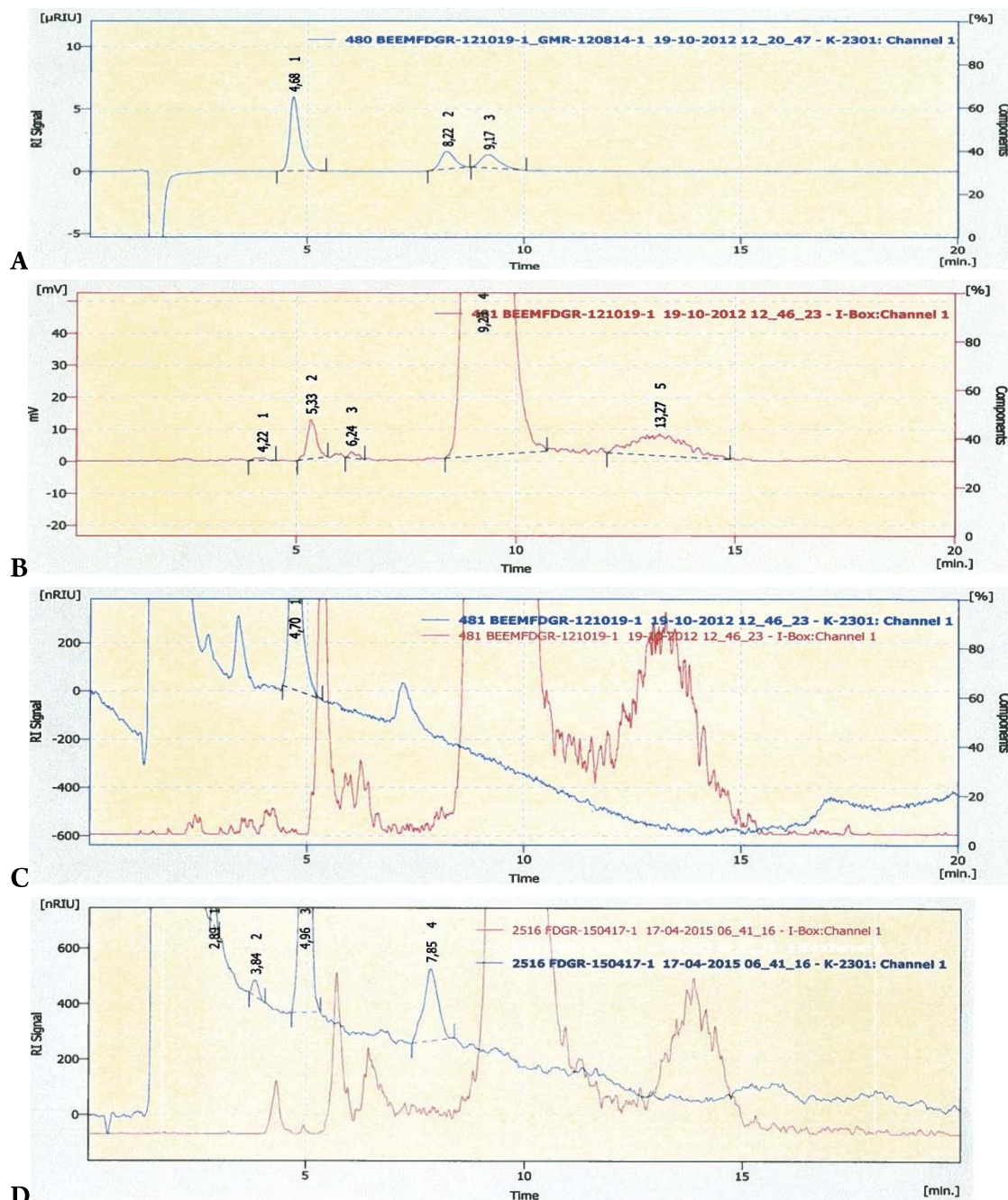
Figure 5-9. HPLC analysis of 120 GBq solid-phase production of [^{18}F]FDG
A: Reference trace of glucose (4.68 min), FDM (8.22 min) and FDG (9.17 min)
B: Radiotrace of the product showing [^{18}F]F$^-$ (5.33 min) and [^{18}F]FDG (9.23 min)
C: Overlay of RD and RI trace of the product showing glucose (4.70 min) and acetate (~ 7.8 min)
D: Comparative overlay from [^{18}F]FDG produced at Hevesy and released for human administration

The HPLC analysis showed no [^{18}F]FDM, which would have been seen as a peak right before the [^{18}F]FDG peak as shown by the reference trace (A). FDG was not detected either as in the overlay there are no RI peaks in the area of the [^{18}F]FDG peak. Glucose was detected, but the amount was on

level with conventionally produced [^{18}F]FDG at Hevesy Laboratory. A comparison of the two overlays showed that the other peaks were corresponding to what was normally seen in the product of the GMP-compliant [^{18}F]FDG. We also did a ^{31}P NMR analysis of the product of a [^{18}F]NpEtF synthesis that showed that no phosphorous-containing compounds leached from the resin despite the 120°C synthesis. The conclusion based on these analyses was that polymer-supported phosphazene base mediated radiofluorination is a feasible method for routine production of radiofluorinated compounds.

5.6 Further work on the solid-phase radiofluorination methodology

5.6.1 Synthesis of the novel polymer-supported phosphazene base **PS**-P$_2$^{Bz}

The lack of other commercially available polymer-supported phosphazene bases than **PS**-P$_2$^{tBu} made it necessary to strive against the synthesis of novel analogues. A successful outcome of this was the synthesis of **PS**-P$_2$^{PEG} as described in Article III.

It was conceived that the polymer-supported analogue **PS**-P$_2$^{Bz} would have similarly trapping and fluorination abilities compared to **PS**-P$_2$^{tBu}. The advantage of the base P$_2$^{Bz} is that the benzyl group can be functionalized in a way that makes coupling to a polymer support possible. We envisioned two ways of synthesizing **PS**-P$_2$^{tBu}. The first one was through the reaction between P$_2$^{Cl}·BF$_4$ and aminomethyl polystyrene (AMPS). The other was through the polymerization of the monomer P$_2$^{VBz} (VBz = vinylbenzyl). The different compounds are shown in Scheme 5-5.
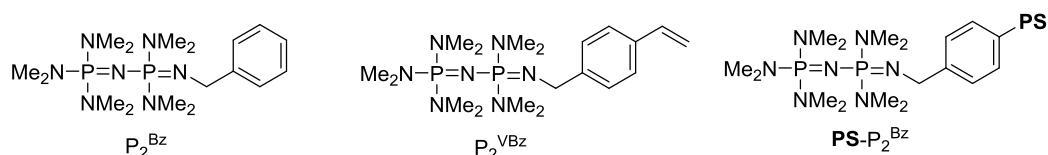
Scheme 5-5. The novel phosphazene base P$_2$^{Bz} and the polymer-supported analogue

The development of **PS**-P$_2$^{Bz} consists of four steps.

1. Synthesis of the phosphazene base P$_2$^{Bz} based on Schwesinger's work[109]. Subsequent synthesis of the corresponding hydrofluoride P$_2$^{Bz}·[$^{18/19}$F]HF followed by (radio)fluorination studies in order to establish (radio)fluorination abilities.

2. Synthesis of the polymer-supported version **PS**-P$_2^{Bz}$ by P$_2$ coupling to AMPS and subsequent [^{18}F]fluoride trapping and radiofluorination in order to establish trapping and radiofluorination abilities.

3. Synthesis of the P$_2^{VBz}$ monomer

4. Polymerization of the P$_2^{VBz}$ monomer with styrene and divinylbenzene in order to establish a relationship between the polymer matrix and trapping/radiofluorination ability

5.6.1.1 Synthesis of P$_2^{Bz}$

The synthesis of P$_2^{tBu}$ is shown in Scheme 5-6, including reaction conditions and yields.
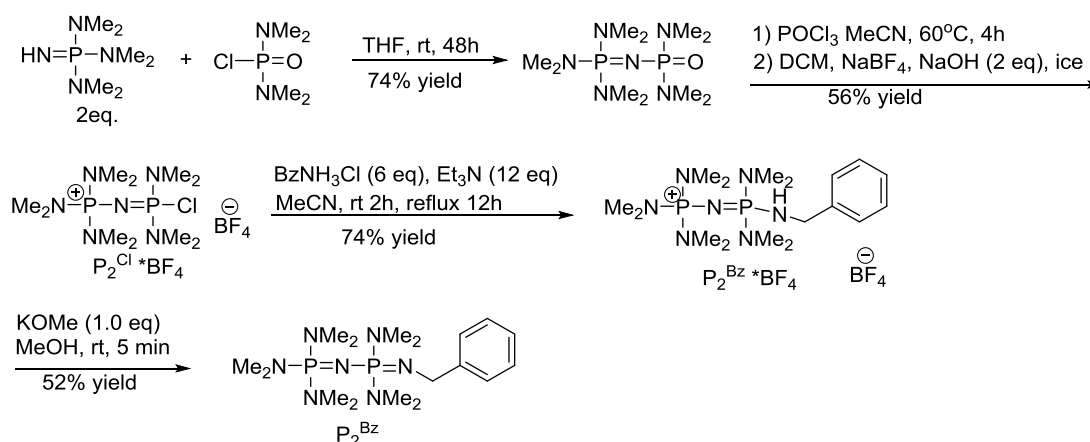
Scheme 5-6. Synthesis of P$_2^{Bz}$

P$_2^{Bz}$·HF was prepared using TREAT-HF (Scheme 5-7). Full conversion to the hydrofluoride was achieved after 1.5 hours, which was confirmed by NMR.
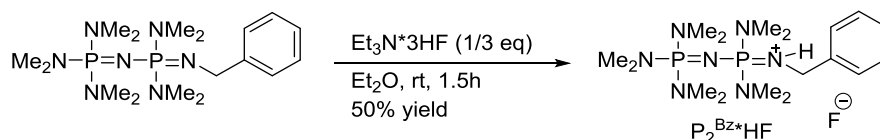
Scheme 5-7. P$_2^{Bz}$·HF synthesis

Subsequent fluorination using $P_2^{Bz}\cdot HF$ was carried out with 1-octylchloride as substrate and application of the optimized reaction conditions established for our homogeneous radiofluorination protocol (Scheme 5-8).
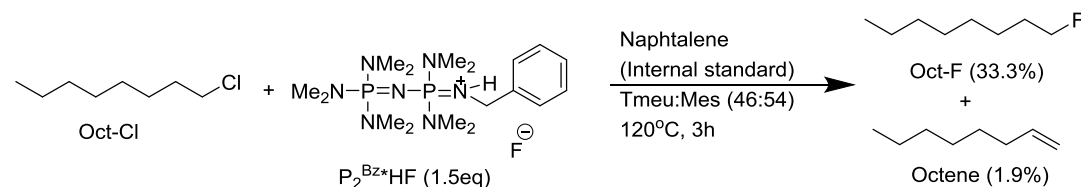
Scheme 5-8. Fluorination using $P_2^{Bz}\cdot HF$

GC analysis with naphthalene as internal standard showed a 33.3% conversion of 1-octylchloride to 1-octylfluoride while only 1.9% conversion to 1-octene. This meant that the fluorination ability of this base was satisfying. $P_2^{Bz}\cdot[^{18}F]HF$ was then prepared by our $[^{18}F]HF$ generator protocol and NpEtOMs was used as substrate. The trapping efficiency was 64%, RCP was 71% and RCY was 45% (Scheme 5-9). These results were not completely on par with the results achieved with P_2^{Et}, but sufficient enough for us to proceed to the synthesis of the polymer supported analogue.
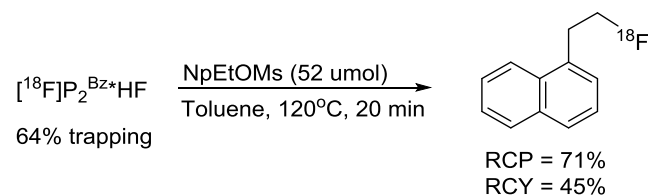
Scheme 5-9. Radiofluorination using P_2^{Bz}

5.6.1.2 Synthesis of PS-P_2^{Bz} and subsequent radiofluorination

PS-P_2^{Bz} was synthesized in the same way as **PS**-P_2^{PEG} with the only exception that the resin used was aminomethyl polystyrene (AMPS) (Scheme 5-10).
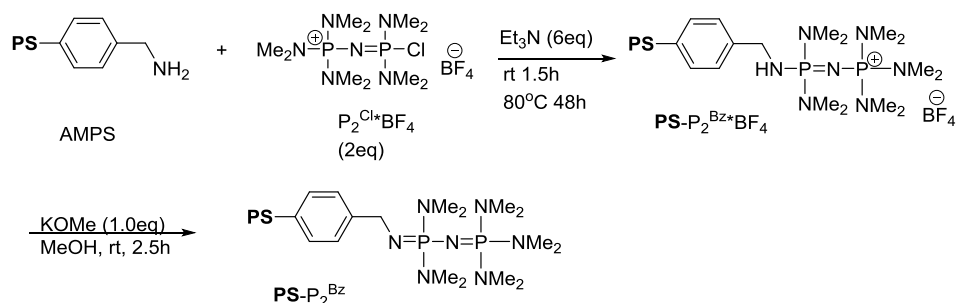
Scheme 5-10. Synthesis of PS-P$_2$^{Bz} by coupling to AMPS

Regrettably, radiofluorination using this polymer-supported phosphazene base only resulted in 48% trapping and less than 1% radiofluorination. Change of base to DIPEA and solvent to DMF for the coupling step resulted in a resin with no trapping ability at all. It was then decided to turn to the polymerization of P$_2$^{VBz} instead.

5.6.1.3 Synthesis of the phosphazene base P$_2$^{VBz}

In order to synthesize **PS**-P$_2$^{Bz}, the plan was to synthesize vinylbenzylamine hydrochloride (VBAH), use this for the synthesis of the monomer P$_2$^{VBz} and then establish a polymerization method, which would produce a polymer-supported phosphazene base useful for [^{18}F]fluoride trapping and radiofluorination. The synthesis of VBAH is shown in Scheme 5-11.
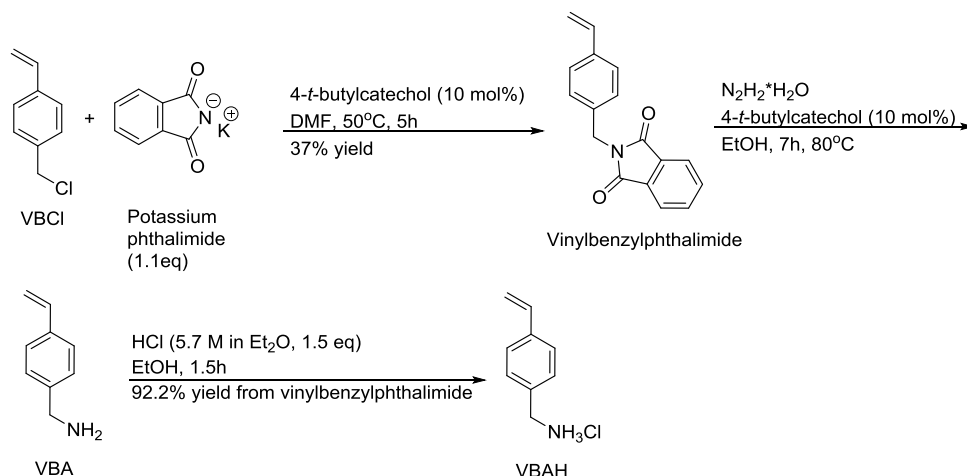
Scheme 5-11. Synthesis of VBAH

The Gabriel synthesis of the monomer VBAH was based on the combination of two procedures described in literature[110,111] and gave the product in a good yield. The radical scavenger 4-*t*-butylcatechol was added to minimize the risk of polymerization, which was indeed avoided. VBAH was then reacted with $P_2^{Cl}\cdot BF_4$ in order to synthesize the salt $P_2^{VBz}\cdot BF_4$. The final step was liberation of the base from the BF_4 salt (Scheme 5-12) in order to achieve P_2^{VBz}. The same procedure as with the synthesis of P_2^{Bz} was applied.
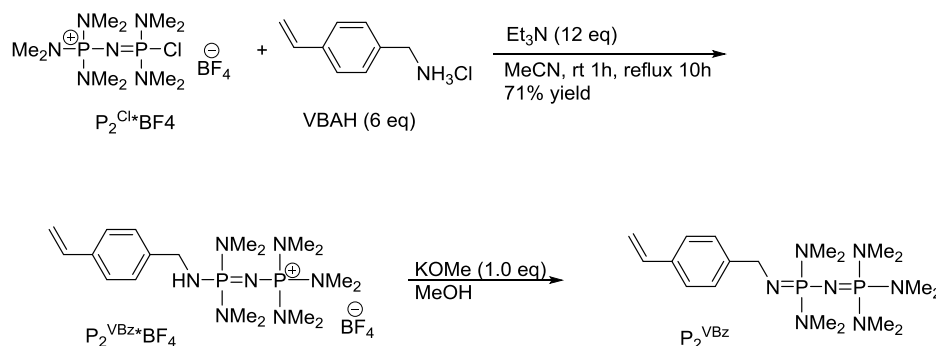
Scheme 5-12. Synthesis of P_2^{VBz}

Two polymerization strategies for the synthesis **PS**-P_2^{Bz} from P_2^{VBz} were then tested. The first was with AIBN as radical initiator (Scheme 5-13, A) while the second was with benzophenone as photoinitiator (Scheme 5-13, B).
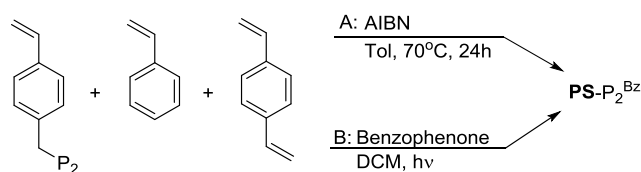
Scheme 5-13. PS-P_2^{Bz} synthesis from polymerization (carried out by supervisor Fedor Zhuravlev)

The resulting particles were packed in two columns and radiofluorination was carried out as shown in Table 5-3. The polymer resulting from method A seemed to dissolve during the labeling step, which resulted in a blocking of the tubing leading from the column. Despite the relatively acceptable trapping ability of the polymer resulting from method B, it was decided that the work needed to achieve a completely controlled polymerization method resulting in a well-defined resin was more comprehensive than the interest in the polymer could justify and this plan was dropped.

Table 5-3. [^{18}F]FDG synthesis using polymerized PS-P$_2$^{Bz}

Method	m(resin) mg	Substrate	n(substrate) μmol	Solvent	Temp °C	Trapping %	RCP %	RCY %
A	61	Mannose triflate	57	MeCN	85	22	-	-
B	100	Mannose triflate	104	MeCN	85	44	14	8

5.6.2 Synthesis of the novel polymer-supported phosphazene base **PS**-P$_2$$^{Et+}Cl^-$

As it has been demonstrated that P$_2$^{Et} has excellent trapping and radiofluorination abilities, it is conceivable that a polymer-supported version would possess similar abilities. For that reason a setup was made where a solution of P$_2$^{Et} was circulated through a column containing Merrifield's resin at room temperature for 12 hours in order to couple the base to the resin. The reaction is shown in Scheme 5-14.

Scheme 5-14. PS-P$_2$$^{Et+}Cl^-$ synthesis (carried out by supervisor Fedor Zhuravlev)
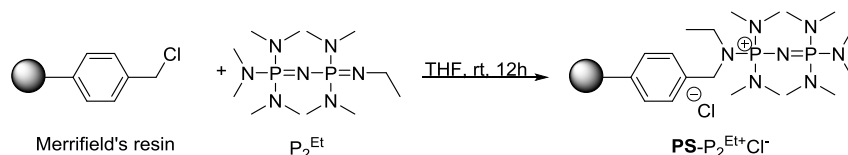
The resulting resin was used for the synthesis of [^{18}F]FDG (Table 5-4). The trapping efficiency of **PS**-P$_2$$^{Et+}Cl^-$ was very good, while the labeling ability was poor. Optimization of the coupling reaction between Merrifield's resin and P$_2$^{Et} could possibly improve the labeling efficiency, but this has not yet been carried out.

Table 5-4. [^{18}F]FDG synthesis using PS-P$_2$$^{Et+}Cl^-$

n(PS-P$_2$$^{Et+}Cl^-$) μmol	Substrate	n(substrate) μmol	Solvent	Temp °C	Trapping %	RCP %	RCY %
400	Mannose triflate	105	MeCN	85	100	99	5

5.7 Work to improve solid-phase radiofluorination yields

Despite numerous efforts to optimize and improve the radiochemical yields of the solid-phase radiofluorination methodology we always seemed to hit a dead end at about 60%. The reason for this was further analyzed, in order to see what kind of obstacle we were dealing with.

5.7.1 Analysis of metal impurity effect

It was thought that cationic metal impurities in the cyclotron-irradiated water could work as a fluoride trap and thereby render the [^{18}F]fluoride useless for the fluorination step. As the solubility product K_{sp} of for instance CaF_2 and MgF_2 is very low ($3.9 \ast 10^{-11}$ and $5.16 \ast 10^{-11}$, respectively), addition of organic solvent to the column after the trapping step will result in precipitation and thereby entrapment of [^{18}F]fluoride in an inert state.

To avoid this, a small column containing AG 50W-X4 cation exchange resin (H^+ form) to trap the cationic metal impurities was made and attached to the radiofluorination column. Three experiments were carried out - one control experiment without exchange resin, and two with the resin - but otherwise the same reaction conditions were applied. The experimental results are shown in Table 5-5. These experiments clearly show that this cation exchange column has a negative impact on the outcome of the reaction and the use of this was dropped without further analysis.

Table 5-5. Experiments with cation exchange resin

Entry	Cation exchange resin	n(P_2^{tBu}) mmol	n(NpEtOMs) μmol	Trapping %	RCP %	RCY %
0	-	0.18	54	100	88	32
1	+	0.18	56	95	96	19
2	+	0.12	52	98	97	8

5.7.2 Article IV - Towards automated solid phase radiofluorination for dose-on-demand PET: retention of activity by solid support

5.7.2.1 Introduction to the article

It was conceivable that the retained activity may be trapped physically either as free or loosely bound [^{18}F]F$^-$ in the polymer matrix, or chemically bound to impurities in the polymer support.

Toorongian and Mulhollan[106] faced a very similar problem. They were able to elute the retained activity using dilute aqueous K_2CO_3, and the eluted activity was still applicable towards solution-phase nucleophilic radiofluorination with the use of K222. Based on this result, they concluded that $[^{18}F]F^-$ was either physically inaccessible within the polymer matrix for the precursor, or it was bound in some inert chemical complex that is disrupted by base/catalyst treatment. We decided to do a similar test to see if we faced the same kind of entrapment.

First we carried out standard on-column radiofluorination experiments. After that we passed a solution of $K222/K_2CO_3$ through the column and used the eluted activity for standard solution-phase radiofluorination. We were indeed able to elute most of the retained activity from the column and use the eluted activity for the labeling of our model substrate NpEtOTs. This meant that the physical entrapment theory was confirmed.

The article is published[112] and presented on the following pages.

5.7.2.2   The article

Bente Mathiessen, Gregory Severin, and Fedor Zhuravlev*

Towards automated solid phase radiofluorination for dose-on-demand PET: retention of activity by solid support

Abstract: On-column [^{18}F]fluoride trapping and radiofluorination of 2-(naphthalen-1-yl)ethyl-4-methyl-benzenesulfonate ($C_{10}H_7(CH_2)_2OTs$), performed on polystyrene supported phosphazene base PS-P$_2^{tBu}$ yielded [^{18}F]1-(2-fluoroethyl)naphthalene ([^{18}F]$C_{10}H_7(CH_2)_2F$) in 50% radiochemical yield but left up to 43% of activity unreacted on the resin. This activity could be eluted with Kryptofix/K_2CO_3 and then used for conventional radiofluorination of the same substrate, suggesting that the column-retained activity was present in the form of [^{18}F]fluoride entrapped in polymer matrix. An approach to minimize the amount of entrapped [^{18}F]fluoride by use of glass beads functionalized with alkylsilane-derivatized phosphazene residues was attempted but was stymied by fluorolysis/hydrolysis of the alkylsilane spacer. The results suggest that the key to high yield of on-column radiofluorination is to minimize the residual [^{18}F]fluoride absorption in the matrix by the judicious choice of solid support.

Keywords: Dose-on-demand PET, [^{18}F], radiofluorination, on-column, solid phase.

1 Introduction

The worldwide demand for PET scans is increasing at a dramatic rate. Over the time period from 2010 to 2012, the number of scans performed in Western Europe increased by 19.6%, with over one million scans performed annually in the region [1]. The supply of radioisotopes, partic-ularly fluorine-18, has appropriately grown to meet the increasing demand. The most cost effective supply chain for fluorine-18 has been through daily, high activity, single-batch radiopharmaceutical production at a regional facility with distribution to several PET centers within a reasonable distance. While this model has effectively provided the population with PET tracers, it has led to a one-size-fits-all clinical implementation, where 95% of all PET scans performed use [^{18}F]FDG. [^{18}F]FDG is an important general purpose tracer, and its value should not be ignored. But, with the development of disease specific tracers, the important opportunity for personalized medicine is presented in dose-on-demand (DoD) PET.

The basic aims of DoD PET are to consider the needs of a given patient, and produce the tracer that is best suited for them as necessary. One way to implement DoD PET is to shift radiopharmaceutical production from the large regional centers, which depend upon large batches matching large patient populations, to small hospital based radiopharmacies. These laboratories would have to be equipped with robust multi-use, single-platform, automated radiochemistry systems that could be supplied with fluorine-18, for example, either from a small in-house cyclotron or from [^{18}O]H$_2$O that was irradiated at regional facility. Any such radiochemical system should involve rapid chemical processes, eliminate or simplify time-consuming steps like solvent evaporations, and be capable of producing many tracers from the same platform. One way to realize these improvements to current procedure, and thereby make DoD PET more tenable, is through use of on-column, solid-supported radiofluorination methodology.

Practically, the majority of radionuclide extractions and purifications are now performed on solid phase anion exchange cartridges. Conventional solvent-related operations such as solvent wash and solvent exchange, which could be rather difficult to perform on radioactive samples, become straightforward and amenable to automation when on-column radionuclide recovery is used. However, the incorporation of PET radionuclides into PET tracers also requires desorption of the radionuclide from the solid support followed by the conventional liquid

*Corresponding author: Fedor Zhuravlev, Hevesy Laboratory, Center for Nuclear Technologies, Technical University of Denmark, Risø Campus, Frederiksborgvej 399, P.O. Box 49, 4000 Roskilde, Denmark, e-mail: fezh@dtu.dk
Bente Mathiessen, Gregory Severin: Hevesy Laboratory, Center for Nuclear Technologies, Technical University of Denmark, Risø Campus, Frederiksborgvej 399, P.O. Box 49, 4000 Roskilde, Denmark

New approaches to [18F]fluoride recovery and radiofluorination
Chapter 5 Solid-phase radiofluorination using polymer-supported phosphazene bases

228 —— B. Mathiessen et al., Towards automated solid phase radiofluorination for dose-on-demand PET   **DE GRUYTER**

phase radiochemistry. This approach is implemented in emerging microfluidic radiofluorination devices. While taking advantage of microreactor-based chemistry the microfluidics still requires the use of "macro-sized" pre-concentration and solid phase extraction modules [2]. We believe that combining isotope recovery and radiosynthesis into one inexpensive and robust on-column process can be especially attractive for the emerging DoD PET technology if implemented as a tracer-specific self-shielded compact cartridge module. The possibility of direct on-column [18F]fluoride recovery and radiofluorination has been demonstrated by Toorongian, Mulholland and co-workers as early as in 1989 [3, 4]. Unfortunately, their aminopyridinium-based resin suffered from low stability, inconsistent trapping and poor synthetic reproducibility. We have recently reported a new method which allowed for solid phase extraction of [18F]fluoride from [18O]H2O on a polystyrene-based phosphazene resin followed by radiofluorination of a wide variety of substrates on the same resin [5]. The method is characterized by uniformly high trapping efficiency (>98%), moderate yields (40%–69%, substrate dependent) and column re-usability. However, numerous on-column radiofluorination runs indicated a persistent deficiency of the method: up to 43% of activity remained absorbed on the column after reaction. In this work we further investigated the nature of the activity retained on the solid phase.

2 Experimental

2.1 General

Unless otherwise noted, all synthetic steps were performed under an inert atmosphere of argon or helium. Glassware and reaction vessels were dried in an oven at 160 °C overnight or flame-dried on the Schlenk line before use. All reagents were used as received without additional purification; solvents were dried over activated molecular sieves. All radiochemical yields were decay-corrected. Polystyrene-supported P_2^{tBu} **PS-P_2^{tBu}** (loading: 1.6 mmol/g), was obtained from Sigma Aldrich; the aminoalkylsilane-functionalized glass beads were purchased from Polysciences Inc. The 2-(naphthalen-1-yl)ethyl-4-methylbenzenesulfonate ($C_{10}H_7(CH_2)_2OTs$) was synthesized as described elsewhere.

2.2 Instrumentation

^{1}H, ^{13}C and ^{31}P-NMR spectra were recorded on a Bruker Avance II 500 instrument operating at 500, 126 and 202 MHz, respectively. ^{19}F-NMR was recorded on a Bruker Avance DPX 250 instrument at 235 MHz. The mass spectrometry was performed on a Bruker Esquire 4000 ion-trap (IT) spectrometer equipped with electrospray ionization (ESI) interface. Thin-layer chromatography (TLC) was run on pre-coated plates of silica gel 60, F254 (Merck). Radio-TLC was performed with a Raytest MiniGita TLC scanner. The aqueous solutions of [18F]fluoride were prepared by the ^{18}O(p,n)^{18}F reaction in a GE PETtrace cyclotron using a Ag or Nb target containing 2.5 mL of 95%–98% enriched [^{18}O]H$_2$O irradiated by a 16.5 MeV proton beam at 55 μA for around 100 min. A small fraction of the irradiated water was diluted with unenriched water, and used as the source of fluorine-18 for radiochemistry. For automated radiosynthesis we used custom-made module controlled by LabView software.

2.3 Column preparation and on-column radiofluorination followed by Kryptofix/K$_2$CO$_3$/[^{18}F]fluoride labeling

The representative procedures are as follows:

2.3.1 Column preparation

A borosilicate glass tube (OD 0.6 mm, length 12 cm) was packed with **PS**-supported P_2^{tBu} (150 μmol base, loading 1.6 mmol/g, 93.75 mg) mixed with glass beads (212–300 μm, 100–500 mg) and placed in a column oven in a LabView controlled automation apparatus.

2.3.2 [^{18}F]fluoride trapping and column drying

[^{18}F]fluoride (in water, 2.5 mL, 684 MBq, flow rate 1 mL/min) was passed through the column followed by acetonitrile (MeCN) : water (1 : 1, 1 mL, flow rate 1 mL/min). MeCN (dry, 1 mL) was passed through the column at room temperature followed by MeCN (dry, 5 mL, flow rate 1 mL/min) while heating the column at 50 °C. Then He was passed through the column until excess of solvent was removed. [^{18}F]Fluoride trapping was 100%.

New approaches to [18F]fluoride recovery and radiofluorination
Chapter 5 Solid-phase radiofluorination using polymer-supported phosphazene bases

DE GRUYTER   B. Mathiessen et al., Towards automated solid phase radiofluorination for dose-on-demand PET ⸻ **229**

2.3.3 On-column radiofluorination followed by Kryptofix/K$_2$CO$_3$ elution and radiofluorinaton

MeCN (dry, 5 mL) was passed through the column (flow rate 1 mL/min) at 80 °C followed by C$_{10}$H$_7$(CH$_2$)$_2$OTs (19.64 mg, 58 µmol) dissolved in MeCN (dry, 3 mL, flow 0.55 mL/min) at 80 °C. Then MeCN (dry, 2 mL, flow rate 0.55 mL/min) was passed through the column to elute the remaining product. The fluorinated product was analyzed by radio-TLC (eluent heptane : EtOAc 80 : 20). The conversion to the desired product [^{18}F]C$_{10}$H$_7$(CH$_2$)$_2$F was 91%. 43% of the [^{18}F]fluoride (291 MBq) was retained on the column at this point. The column was then washed using MeCN (dry, 12 mL, flow rate 750 µL/min) and dried using He while cooling from 80 °C to 50 °C. Kryptofix (K$_{2.2.2}$) solution (1.0 mL solution of a mixture containing 22.0 mg of Kryptofix, 7.0 mg K$_2$CO$_3$, 3.0 mL MeCN and 3.0 mL H$_2$O) was passed through the washed and dried column (flow rate 0.55 mL/min) at room temperature in order to elute the remaining [^{18}F]fluoride still trapped on the column after the previous on-column radiofluorination. Only 6%–7% [^{18}F]fluoride (48 MBq) was retained on the column at this point. The resulting Kryptofix/K$_2$CO$_3$/[^{18}F]fluoride mixture was collected in a glass reactor vial and the solvents were removed by repeated azeotropic evaporation steps (vacuum and He applied, 1st time at 60 °C for 3 min, 2nd to 4th time at 90 °C at 3–4 min, 0.5–1.0 mL dry MeCN added between each evaporation step). C$_{10}$H$_7$(CH$_2$)$_2$OTs (18.60 mg, 57 µmol) dissolved in MeCN (dry, 3 mL) was added to the reactor vial and radiofluorination was carried out at 80 °C for 10 min. After cooling to room temperature the product was analyzed by radio-TLC (eluent heptane : EtOAc, 80 : 20); conversion to the desired product [^{18}F]C$_{10}$H$_7$(CH$_2$)$_2$F was 66%.

2.3.4 Phosphazene-functionalized glass beads G-P_2

The aminoalkylsilane-functionalized glass beads were reacted with P$_2^{Cl}$ · BF$_4$ (1-chloro-1,1,3,3,3-pentakis(dimethyl-amino)-1λ^5-diphosphazen-3-ium tetrafluorborate) by mixing the beads (200–1000 mg) with P$_2^{Cl}$ · BF$_4$ (3 eq to amine) and Et$_3$N (dry, 9 eq to amine) in dichloromethane (DCM, dry, 5 mL) in a glass vial, which was sealed under vacuum. The reaction mixture was then heated with slight agitation at 90 °C for three days. This coupling procedure was repeated two times in order to ensure good coupling. The resulting functionalized glass beads were treated with a mixture of KOMe (1 eq to amine) in MeOH (dry, 5 mL) for one hour at room temperature in order to give the desired glass bead-supported phosphazene base.

3 Results and discussion

The on-column [^{18}F]fluoride recovery and radiofluorination was performed in the following way (Figure 1a). First,
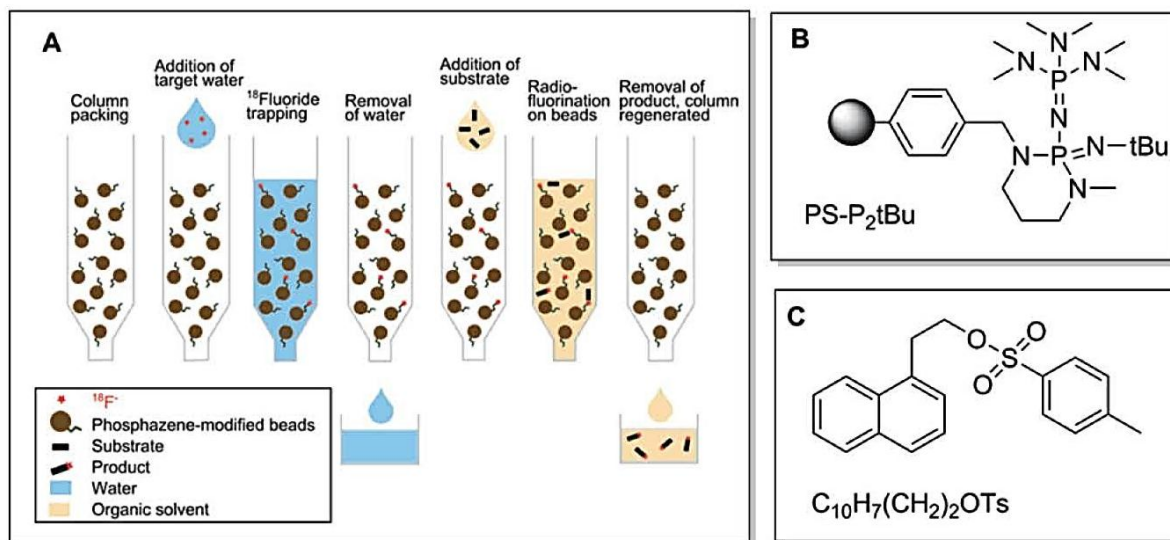
Fig. 1: (A) Conceptual representation of on-column [^{18}F]fluoride recovery and radiofluorination; (B) the structure of polystyrene-based phosphazene base **PS**-P$_2^{tBu}$, and (C) the structure of model substrates 2-(naphthalen-1-yl)ethyl alkylsulfonate C$_{10}$H$_7$(CH$_2$)$_2$OTs used in this study.

New approaches to [18F]fluoride recovery and radiofluorination
Chapter 5 Solid-phase radiofluorination using polymer-supported phosphazene bases

230 —— B. Mathiessen et al., Towards automated solid phase radiofluorination for dose-on-demand PET   **DE GRUYTER**

the cyclotron target water, containing [^{18}F]fluoride was passed through the column containing **PS-P$_2^{tBu}$** beads (Figure 1b). The [^{18}F]fluoride was retained on the column, most likely as a counter anion to phosphazenium cation initially formed by deprotonation of water with highly basic **PS-P$_2^{tBu}$**. The target water was then released from the column and the column was dried by rinsing with dry acetonitrile. Then, a solution of $C_{10}H_7(CH_2)_2OTs$ (Figure 1c), a model substrate used previously by us[6] and others[7], in acetonitrile was slowly (10–15 min) passed through the column while the column was heated at 80 °C. This resulted in radiofluorination of the substrate directly on the phosphazene-modified polymer beads. The solution containing the radiolabeled substrate was then released from the column. Regardless of radiofluorination conditions (flow rate, temperature, substrate concentration), a substantial amount of radioactivity (up to 43%) remained trapped on the column.

Conceivably, the retained activity can be either physically entrapped in the polymer matrix in form of free or loosely bound [^{18}F]fluoride, or chemically bound to the impurities in the polymer support. In the first case, [^{18}F]fluoride encapsulated in the cavernous pockets of cross-linked polymer matrix might not be accessible to the larger molecules of the substrate. However, smaller ions, such as hydroxide or carbonate might still be able to substitute fluoride and release the entrapped activity. Interestingly, the absorption of activity was also reported in case of on-column radiofluorination of mannose triflate on aminopyridinium resin in an earlier work by Toorongian and Mulholland[3]. The authors were able to elute the retained activity with aqueous solution of potassium carbonate and use the eluate for radiofluorination. To test the entrapment hypothesis, we modified our automatic radiofluorination apparatus to include a module for elution of retained activity and subsequent radiofluorination (Figure 2).
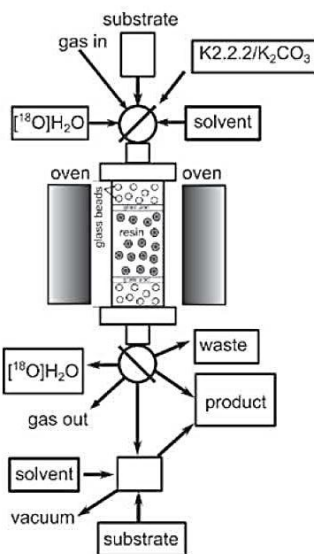
Fig. 2: The schematics of apparatus for automatic on-column radiofluorination of $C_{10}H_7(CH_2)_2OTs$. The apparatus is equipped with a module for elution of column-retained activity with Kryptofix/K_2CO_3 and subsequent radiofluorination of the same substrate in the liquid phase.

After on-column radiofluorination of $C_{10}H_7(CH_2)_2OTs$ a solution of Kryptofix/K_2CO_3 in acetonitrile-water was passed through the column containing **PS-P$_2^{tBu}$** and the resulting activity was dried by azeotropic evaporation of water. The radiofluorination ability of the eluted [^{18}F]fluoride activity was accessed by reacting it with the model substrate $C_{10}H_7(CH_2)_2OTs$ in acetonitrile at 80 °C. The results are presented in Table 1.

The results show that approximately half of the activity loaded on the column as target water reacted with the substrate directly on the column (51%–56%, Table 1, column 4). The rest (41%–43% of activity, column 3) remained attached to the resin. The subsequent elution with

Table 1: Automated on-column radiofluorination of $C_{10}H_7(CH_2)_2OTs$ and subsequent elution/radiofluorination of the same substrate with the column-retained activity using Kryptofix/K_2CO_3 elution. All activities and radiochemical yields (RCY) were calculated relative to the initial radioactivity of [^{18}F]fluoride loaded onto the column. Radiochemical conversion (RCC) was calculated relative to the total activity in a given solution.[1]

Entry	Activity trapped on column (%)	Activity remaining on column after on-column radio-fluorination (%)	On-column radio-fluorination RCC (%)/RCY(%)	Activity remaining on column after K$_{2.2.2}$/ K$_2CO_3$ wash (%)	Radio-fluorination with K$_{2.2.2}$/[^{18}F]KF, RCC (%)/RCY (%)	Combined RCY from on-column and K$_{2.2.2}$/[^{18}F]KF radio-fluorinations (%)
1	99	42	97/56	6	42/14	70
2	100	43	91/51	7	66/21	72
3	100	41	92/52	6	41/13	65

[1] For details on the reaction conditions see Section 2.

New approaches to [18F]fluoride recovery and radiofluorination
Chapter 5 Solid-phase radiofluorination using polymer-supported phosphazene bases

DE GRUYTER   B. Mathiessen et al., Towards automated solid phase radiofluorination for dose-on-demand PET ⸺ **231**
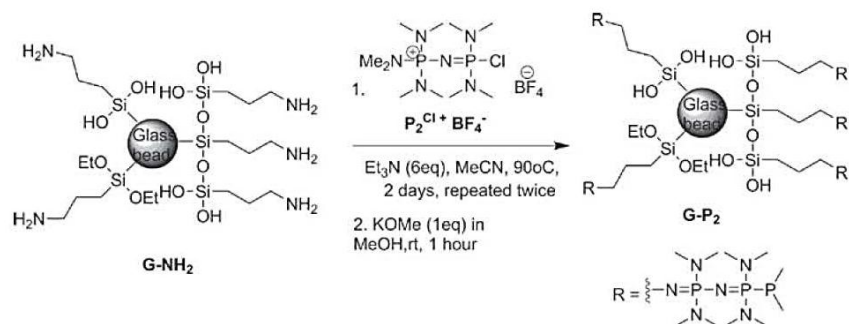
Scheme 1: Synthesis of phosphazene-functionalized glass beads G-P$_2$.
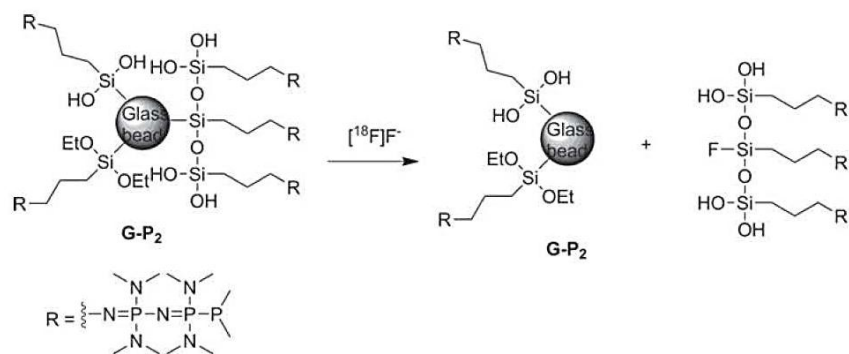
Scheme 2: Possible pathway for fluorolysis of G-P$_2$ in the presence of [^{18}F]fluoride.

the solution of Kryptofix/K$_2$CO$_3$ does remove most of this activity leaving behind only 6%–7% (column 5). Based on the consistency of retained values across different runs and resins, and on the control experiment, where the resin was pre-treated with cold fluoride and yielded the same column activity retention value after on-column radiofluorination, we believe that the 6%–7% we are seeing is due to the system's dead volume. The Kryptofix/K$_2$CO$_3$ wash/radiofluorination experiment demonstrated that after on-column radiofluorination 30%–35% of fluorine-18 activity is retained on the column in the form of nucleophilically active, but latent [^{18}F]fluoride. Thus, the results of these experiments appear to be in line with the entrapment hypothesis.

One way to minimize the influence of solid support on [^{18}F]fluoride retention and reactivity is to substitute the polymer-based matrix for a non-porous solid support, such as glass beads. To that end, aminoalkylsilane functionalized glass beads were treated with P$_2^{Cl}$ · BF$_4$ giving the glass-supported **G**-P$_2$ (Scheme 1).

Unfortunately, the column containing glass-supported **G**-P$_2$ trapped no activity upon passing the target water. Instead, all activity came through the column in a cloudy aqueous solution. This can be explained by instability of Si–O$_{glass}$ bond with respect to fluorolysis

(Scheme 2) and/or hydrolysis (not shown). Therefore, at present, glass appears to be an unlikely candidate for solid support compatible with on-column radiofluorination.

4 Conclusions

In our effort to develop an automated, solid phase based radiofluorination method for dose-on-demand PET we have investigated and quantified the fluorine-18 activity retained on the polystyrene supported phosphazene base **PS**-P$_2^{tBu}$ after reaction with the model substrate C$_{10}$H$_7$(CH$_2$)$_2$OTs. After on-column radiofluorination, proceeding with up to 56% yield, as much as 43% of fluorine-18 activity was retained on the resin. All of it (less 5%–6%, corresponding to the dead volume of the apparatus) could be eluted with Kryptofix/K$_2$CO$_3$ and then used for conventional radiofluorination of the same substrate, suggesting the activity was present in the form of [^{18}F]fluoride entrapped in polymer matrix. An approach to minimize the amount of entrapped [^{18}F]fluoride by use of glass beads functionalized with alkylsilane-derivatized phosphazene residues was attempted but was stymied by fluorolysis and/or hydrolysis of the alkylsilane spacer. The results suggest that the key to high yield of

126

on-column radiofluorination is to minimize the residual $[^{18}F]$fluoride absorption by the judicious choice of solid support. The future directions include development of stable, low fluoride-absorbing phosphazene-functionalized solid support.

On-column synthesis of fluorine-18 radiotracers could represent a major step forward in the development of DoD PET. This method for rapid, general-purpose, nucleophilic radiofluorination allows production of many different tracers from the same hot cell. Coupling this with the abundance of available radioactivity from small proton accelerators brings a wide variety of tracers closer to the patient population. Ideally this platform will eventually provide single patient doses, as needed, in the new era of personalized medicine.

References

1. Stevens, A.: Molecular and Multimodality Imaging: Hybrid Imaging – Image Processing and Quantitation. Annual Congress of the European Association of Nuclear Medicine, OP104 (2013).

2. Arima, V., Pascali, G., Lade, O., Kretschmer, H. R., Bernsdorf, I., Hammond, V., *et al.*: Radiochemistry on chip: towards dose-on-demand synthesis of PET radiopharmaceuticals. Lab Chip **13**, 2328–2336 (2013).

3. Toorongian, S. A., Mulholland, C. K., Jewett, D. M, Bachelor, M. A., Kilbourn, M. R.: Routine production of 2-deoxy-2-$[^{18}F]$fluoro-D-glucose by direct nucleophilic exchange on a quaternary 4-aminopyridinium resin. Int. J. Radiat. Appl. Instrum. B **17**, 273–279 (1990).

4. Mulholland, C. K, Mangner, T. J., Jewett, D. M., Kilbourn, M. R.: Polymer-supported nucleophilic radiolabeling reactions with $[^{18}F]$fluoride and $[^{11}C]$cyanide ion on quaternary ammonium resins. J. Lab. Comp. Radiopharm. **26**, 378–380 (1989).

5. Mathiessen, B., Zhuravlev, F.: Automated solid-phase radiofluorination using polymer-supported phosphazenes. Molecules **18**, 10531–10547 (2013).

6. Mathiessen, B., Jensen, A. T. I., Zhuravlev, F.: Homogeneous nucleophilic radiofluorination and fluorination with phosphazene hydrofluorides. Chemistry Eur. J., **17**, 7796–7805 (2011).

7. Jadhav, V. H., Jang, S. H., Jeong, H. J., Lim, S. T., Sohn, M.-H., Chi, D. Y., Kim, D. W.: Polymer-supported pentaethylene glycol as a facile heterogeneous catalyst for nucleophilic fluorination. Org. Lett. **12**, 3740–3743 (2010).

5.7.3 Addition of "cold" KF to [18F]F-

With the fact established that $[^{18}F]F^-$ was physically trapped in a nucleophilically active state within the polymer matrix, we looked for a way to "saturate" these cavities. It was decided to attempt this by adding potassium fluoride to the $[^{18}F]F^-/[^{18}O]H_2O$ solution from the cyclotron before passing it through the column. It was expected that to some degree it would have a negative effect on the trapping efficiency, as many more base sites would be saturated. It was hoped, however, that due to a partly cold fluoride saturation of the cavities inaccessible by the substrate, the overall effect would be a higher radiochemical yield. This procedure would have a negative effect on the specific activity of the resulting product. It was, however, not a concern at that point, because it would not be a procedure that would be implemented, if this methodology in the future is used for PET tracer production for human administration. It was just a means to establish a strategy, with which a higher yield may be achieved.

The results from a series of experiments with KF used as an additive are shown in Table 5-6. They show that with about 4 μmol added KF, a positive effect is seen on the RCY. However, the outcome was not as significant as we had hoped for. We had expected to see a larger difference between the ratio of RCY to added activity and the ratio RCY to trapped activity, because that would correspond to the cold saturation of the inaccessible sites. A larger difference is first observed with addition of more than 40 μmol KF, as this is where trapping is significantly affected. At this point, however, the resulting RCYs are too low.

Table 5-6. Solid radiofluorination with addition of KF

Entry	KF μmol	$n(P_2^{tBu})$ μmol	Trapping %	n(subst) μmol	Retained/ added act %	Retained/ trapped act %	RCP %	RCY/ added act %	RCY/ trapped act %
1	0	167	99	61	53	54	79	31	31
2	0	165	99	62	50	50	83	38	38
3	2	164	100	59	50	50	96	48	48
5	4	165	100	62	47	47	98	51	51
6	4	161	100	61	40	40	97	53	53
8	9	165	100	61	49	49	98	47	47
9	9	160	100	61	52	52	98	45	46
10	20	161	98	62	59	60	94	34	35
11	20	156	84	62	47	55	88	31	36
12	26	161	88	60	59	68	97	24	27
13	26	162	80	58	51	64	97	26	32
14	40	166	74	61	52	70	94	16	22

Entry	KF µmol	n(P$_2^{tBu}$) µmol	Trapping %	n(subst) µmol	Retained/ added act %	Retained/ trapped act %	RCP %	RCY/ added act %	RCY/ trapped act %
15	40	160	88	59	68	78	94	16	18
16	160	160	42	62	33	79	96	5	13
17	479	158	25	61	20	79	96	2	7

5.8 Our patent

Much of our work regarding solid-phase radiofluorination has laid the foundation for a PCT patent application[113], which is presented in Appendix 1.

5.9 Conclusion to Chapter 5

The development of the homogeneous radiofluorination methodology based on phosphazene hydrofluorides described in chapter 4 fostered the idea of solid-phase radiofluorination based on the same complex. We started out with the commercially available polymer supported phosphazene base **PS**-P$_2^{tBu}$. With this base we were able to develop a method that resulted in very efficient extraction of [^{18}F]F$^-$ from aqueous solution and subsequent radiofluorination of a variety of substrates, including aliphatic sulphonates with RCYs up to 69% and bromides with RCY up to 42%. [^{18}F]FDG was also synthesized in good yields, even when working on a large scale (120 GBq). We have synthesized the novel polymer-supported phosphazene base **PS**-P$_2^{PEG}$, which showed excellent trapping efficiency, while the radiofluorination abilities were a bit lower than **PS**-P$_2^{tBu}$. The solid-phase radiofluorination methodology resulted in simplification of the synthetic procedure as [^{18}F]F$^-$ elution and azeotropic evaporation are avoided. Kryptand addition likewise. The same resin could be reused up to 3 times and the method is applicable for automation. Work in order to achieve even higher RCYs is still in process.

5.10 Experimental

Most of the experimental work carried out during this project has been included in the articles. Only the experiments not included in the articles are described here.
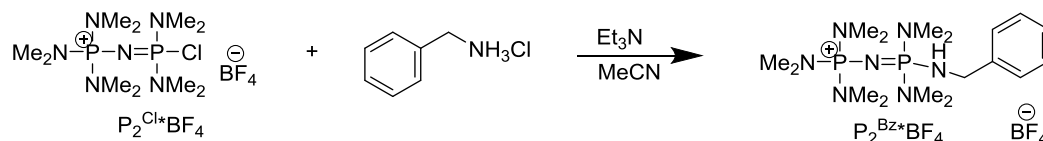
1,1,1,3,3-pentakis(dimethylamino)-3-(benzylamino)-1λ^5-diphosphazen-3-ium tetrafluoroborate P$_2^{Bz}$·HBF$_4$

P$_2^{Cl}$*BF$_4$ (1141mg, 2.73mmol) and MeCN (dry, 10mL) was added to a two-neck round-bottom flask (flame-dried, backfilled with Ar(g)) followed by BzNH$_3$Cl (13.38mmol, 2318.70mg) and Et$_3$N (dry, 32.76mmol, 4560μL). The flask was fitted with a condenser and drying tube and the reaction mixture was stirred at rt under Ar(g) atmosphere for one hour. After that the reaction mixture (yellow with white precipitate) was stirred at 85°C for 10hours. Et$_3$N*HCl was removed by filtration, solvent removed by rotavap and the resulting residue was dissolved in DCM (8.0mL). Water (2x10mL) was added for extraction and the organic phase was concentrated by rotavap and dried under high vacuum. Yield = 981.2mg (74%, about 95% pure) of a yellow solid. This was used for the next step without further purification.

^{1}H NMR (500MHz, CDCl$_3$): δ = 2.64 (d, J=10Hz, 12H), 2,68 (d, J=10Hz, 18H), 4.07 (dd, J=10HZ; 15Hz, 2H), 7.25 (m, 1H), 7.35 (m, 4H). ^{1}H NMR (500MHz, CD$_3$OD + D$_2$O): δ = 2.69 (d, J=10Hz, 12H), 2.71 (d, J=10Hz, 18H), 4.10 (d, J=15Hz, 2H), 7.29 (m, 1H), 7.38 (m, 4H). ^{13}C NMR (126MHz, CDCl$_3$): δ = 36.84 (d, J=5.0Hz), 36.90 (d, J=3.8Hz), 44.97, 127.18, 127.59, 128.49, 139.87 (d, J=5.0). ^{31}P NMR (202MHz, CDCl$_3$): δ = 14.95 (d, J=67Hz), 18.70 (d, J=67Hz). ^{19}F NMR (235MHz, CDCl$_3$): δ = -153 (s with a shoulder)
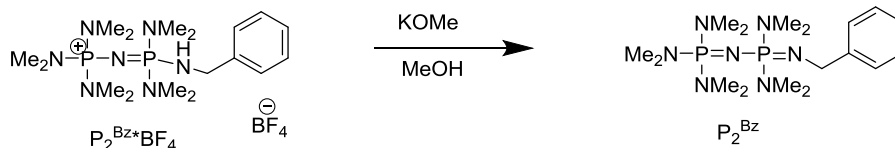
1,1,1,3,3-pentakis(dimethylamino)-3-(benzylimino)-1λ^5,3λ^5-diphosphazene

P$_2^{Bz}$·BF$_4$ (663.80mg, 1.36mmol) was added to a pear-shaped flask (5mL, flame-dried and backfilled with Ar(g)) and dissolved in a minimal amount of MeOH (dry, 0.6mL). KOMe (1,36mmol, 95.71mg, has to be exactly 1eq.) was dissolved in MeOH (dry, 2mL) and added to the solution. The reaction was stirred at rt under Ar(g) for 5 min. KBF$_4$ precipitated instantly and after the precipitate had settled the supernatant was syringed out and filtered by frit. The solvent was removed by rotevap and the resulting oil was dried under high vacuum. Yield = 283.9mg (52%) of a yellow oil.

^{1}H NMR (500MHz, CDCl$_3$): δ = 2.64 (d, J=10Hz, 12H), 2,68 (d, J=10Hz, 18H), 4.11 (d, J=15HZ, 2H), 7.19 (dt, J=10Hz, 1H), 7.29 (dt, J=10Hz, 2H), 7.52 (dd, J=10Hz, 2H). ^{31}P NMR (202MHz, CDCl$_3$): δ = 16.47 (d, J=71Hz), 28.19 (d, J=69Hz). Chem.Ion MS 402.2 (M+1)
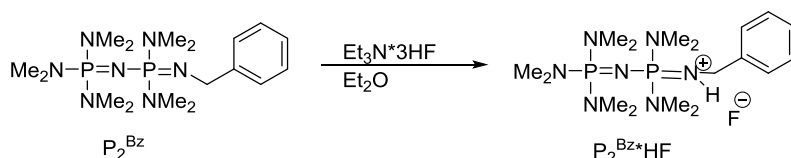
1,1,1,3,3-pentakis(dimethylamino)-3-(benzylamino)-1λ^5-diphosphazen-3-ium hydrofluoride P$_2^{Bz}$·HF

A 10 mL round-bottom flask (dried, backfilled with Ar) was charged with P$_2^{Bz}$ (1.66 mmol, 666.77 mg) followed by Et$_2$O (dry, 3 mL) and Et$_3$N·3HF (1/3 eq, 90 μL). The two-phase solution was stirred under slight vacuum at rt for 1.5 hours. The top phase was syringed out and the base was rotavap'ed and dried under high vacuum. Yield = 348.94 mg (50%) of a yellow oil.

^{1}H NMR (500 MHz, Benzene-d_6) δ = 2.32 (d, J=9.93 Hz, 18 H) 2.47 (d, J=10.09 Hz, 12 H) 4.11 (d, J=14.74 Hz, 2 H) 7.13 (t, J=7.60 Hz, 1 H) 7.29 (t, J=7.68 Hz, 2 H) 7.77 (d, J=7.49 Hz, 2 H). ^{13}C NMR (126 MHz, Benzene-d_6) δ = 36.46 (d, J=4.54 Hz) 36.78 (d, J=4.54 Hz), 44.98, 126.60, 128.22,

128.26, 142.05 (d, J=4.54 Hz). ^{31}P NMR (202MHz, Benzene-d_6): δ = 17.74 (d, J=64Hz), 18.97 (d, J=65Hz). ^{19}F NMR (235MHz, Benzene-d_6): δ = -152.29.
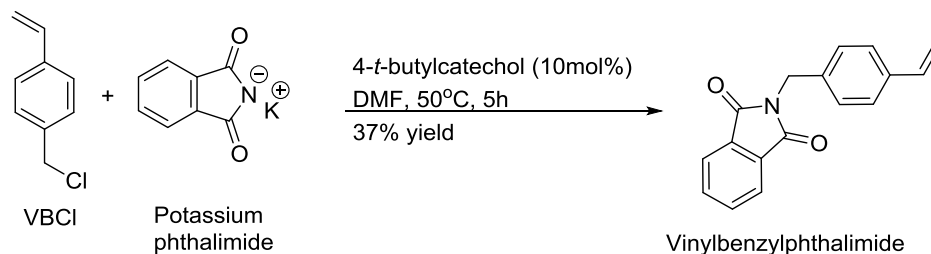
p-vinylbenzylphthalimide

Potassium phthalimide (20.35 g, 110 mmol) was added to a 250mL roundbottom flask containing DMF (dry, 50mL). To this white suspension was added 4-vinylbenzylchloride (14.0 mL, 100 mmol), which resulted in a yellow suspension. The stirred suspension was heated to 50°C under Ar(g) atmosphere. 4-*t*butylcatechol (1.6252 g, 10mmol) was dissolved in DMF (dry, 5 mL) and added to the reaction mixture, which was then stirred at 50°C for 5 hours. The cooled solution was added to NaOH (1.7 M, 1000 mL) and the formed precipitate was collected with filtration under vacuum, dissolved in EtOAc (100 mL) to give a cloudy white solution. The solvent was removed under reduced pressure and the product was twice recrystallised from MeOH to give *p*-vinylbenzylphthalimide as a white solid. Yield = 9.64 g (37%).

^{1}H NMR (500 MHz, CDCl$_3$) δ = 4.84 (s, 2 H), 5.23 (d, *J*=10.88 Hz, 1 H), 5.72 (d, *J*=17.58 Hz, 1 H), 6.68 (dd, *J*=17.58, 10.88 Hz, 1 H), 7.38 (dd, *J*=22.78, 8.12 Hz, 4 H), 7.71 (dd, *J*=5.52, 3.07 Hz, 2 H), 7.85 (dd, *J*=5.36, 3.15 Hz, 2 H).
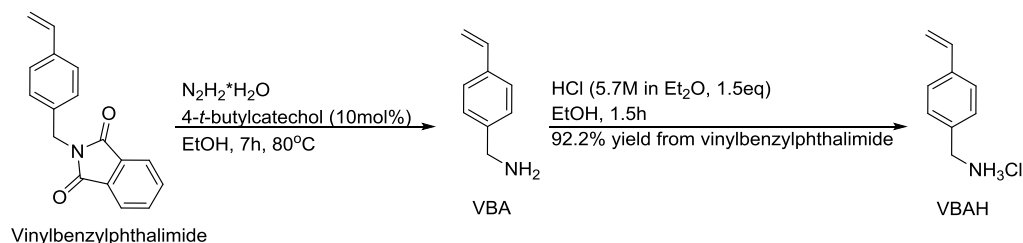
Vinylbenzylamine hydrochloride VBAH

4-Vinylbenzylphthalimide (1.0123 g, 3.85 mmol) was dissolved in argon-flushed ethanol (50 mL) in a 100 mL 3-neck round-bottom flask (dried, backfilled with Ar) and heated under reflux until dissolution of the starting material. Hydrazine hydrate (480 μL, 7.7 mmol, 2 eq.) and 4-$t$butylcatechol (62.5 mg, 0.4 mmol) were added and the reaction mixture was stirred for 7 h. The solution was filtered and washed twice with EtOH (10 mL). The filtrate was concentrated on rotevap to give a white solid, which was treated with KOH (3 M, 200 mL) and extracted with Et2O (3 × 100 mL). The combined organic phases were washed with K_2CO_3 (5 %, 95 mL), dried over $MgSO_4$, and concentrated on rotevap to give a yellow oil. This was destilled using kugelrohr (75°C, 0.74 mbar), giving a clear oil. This oil was dissolved in MeOH (30 mL) and cooled to 0°C. HCl in Et2O (~5.7 M, 1.5mL) was added dropwise over 1.5 hours. Et2O (~150 mL) was slowly added while the reaction mixture heated to rt - duration about 1 hour. As Et2O was added white precipitate was formed which was recovered by filtration and dried under high vacuum. Yield = 606.30 mg (92.7% from the phthalimide).

^{1}H NMR (500 MHz, Methanol-d_4) δ = 4.08 (s, 2 H), 5.30 (dd, J=10.96, 0.79 Hz, 1 H), 5.84 (dd, J=17.62, 0.83 Hz, 1 H), 6.76 (dd, J=17.65, 10.96 Hz, 1 H), 7.41 (d, J=8.20 Hz, 2 H), 7.51 (d, J=8.20 Hz, 2 H).
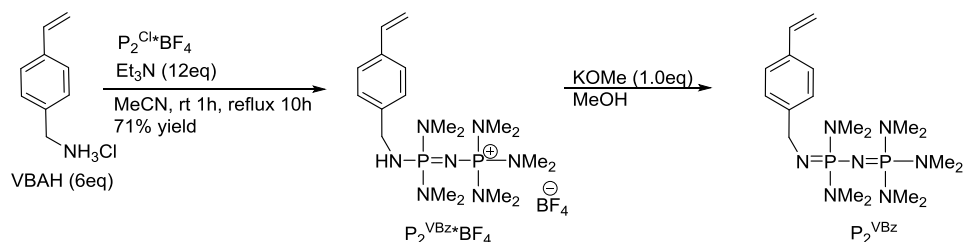
1,1,1,3,3-pentakis(dimethylamino)-3-(vinylbenzylimino)-1λ⁵,3λ⁵-diphosphazene

Synthesized in the same way as P_2^{Bz}.

^{1}H NMR (500 MHz, Benzene-d_6) δ = 2.37 (d, J=10.09 Hz, 18 H), 2.78 (d, J=9.69 Hz, 12 H), 4.61 (d, J=16.63 Hz, 2 H), 5.08 (dd, J=10.88, 1.10 Hz, 1 H), 5.69 (dd, J=17.62, 1.14 Hz, 1 H), 6.74 (dd, J=17.58, 10.88 Hz, 1 H), 7.45 (d, J=8.04 Hz, 2 H), 7.84 (d, J=8.04 Hz, 2 H). ^{31}P NMR (202 MHz, Benzene-d_6) δ = 15.29 (d, J=47.27 Hz), 16.78 (d, J=47.27 Hz).

Addition of cold KF to $[^{18}F]F^-$

A solution of KF (0.5mL, desired concentration) was added to the $[^{18}F]F^-/[^{18}O]H_2O$ solution (maximum 2.5 mL, $[^{16}O]H_2O$ was added to total volume of 3.0 mL). This was used for automated solid-phase radiofluorination according to the general procedure described in Article III.

Chapter 6   General conclusion and perspectives

PET has become a very prominent imaging modality in diagnostic medicine and is routinely used to locate and assess physiological abnormalities in oncology, neurology and cardiology. The use of PET is growing rapidly, as new applications are found almost constantly. This has led to a concomitant demand in the availability of tracers to cover these new areas. As ^{18}F is the most widely used radioisotope for PET imaging, due to the combination of a suitable half-life and low positron energy, the primary demand is within the production of radiofluorinated tracers. Unfortunately, current chemical and radiochemical methodologies lack the efficiency and versatility needed to meet these demands. In particular, the recovery of $[^{18}F]F^-$ from the aqueous solution, in which it is produced by the cyclotron, and subsequent regeneration of its intrinsic nucleophilicity is seen as the Achilles' heel of modern radiofluorination. The reason is that the conventional method applied is very comprehensive and time-consuming and results in limited options for the subsequent labeling step with regard to solvents and substrates. Many alternative methods for the $[^{18}F]F^-$ harvesting and nucleophilic activation including procedures involving ionic liquids, tertiary alcohols, electrochemical separation, and transition metals have been developed.

Our approach was to develop a single-step $[^{18}F]F^-$ recovery and nucleophilic activation by distilling it from the aqueous solution as hydrogen fluoride gas and then trap it using phosphazene bases, resulting in phosphazene $[^{18}F]$hydrofluorides. Schwesinger's phosphazene bases are among the strongest uncharged organic bases available and it was conceivable that they would suppress HF dissociation otherwise seen from other base-HF adducts. At the same time the great size of the bases should result in a cation/anion mismatch and thereby create an almost "naked" and thereby very nucleophilically reactive fluoride ion that could be used for the labeling of various substrates. This was indeed the case and we were able to develop a fluorination and radiofluorination methodology based on phosphazene hydrofluorides. The methodology resulted in the radiofluorination of alkyl pseudohalides, halogens and lipophilic substrates with high yields. The advantages are that glass vessels as well as the

presence of water are tolerated and the labeling procedure can be performed in both polar and nonpolar solvents. This means that the methodology is significantly more versatile than conventional methods.

Another obstacle in the process of developing new radiotracers is the limitations set by the radiopharmaceutical production facilities as most are aimed at large scale productions with specialized synthetic modules optimized for each radiotracer. In an ideal world the synthetic modules should be able to accommodate multiple tracers and different settings in order to meet both the clinical and the research demand for PET tracers.

Drawing on our knowledge of the labeling potential of phosphazene hydrofluorides we envisioned a reusable "coffee machine" like $[^{18}F]$HF generator based on polymer-supported phosphazene bases. $[^{18}F]$F$^-$ extraction from the aqueous solution by the resin as polymer-supported phoaphazene $[^{18}F]$hydrofluoride could be seen as the grinded coffee and the addition of the substrate to the resin and pressing the start button would result in a "cup" of freshly prepared radiotracer in no time. A huge advantage of this approach is that it draws on the advantages of solid-phase synthesis, where the chemical process is simplified by simple washing and filtration of the resin. Thereby the need for extensive purification of the final product is eliminated. We started working with the commercially available polymer-supported phosphazene base **PS**-P$_2^{tBu}$, which showed to have excellent trapping abilities and we were able to carry out radiofluorination of a wide variety of substrates directly on the resin with radiochemical yields up to around 60% within 45 minutes. The resin could be reused up to three times without any significant impact on radiochemical yield, which was a much desired ability in order for this methodology to be applicable for the envisioned reusable "coffee machine" setup. **PS**-P$_2^{tBu}$ had very poor swelling ability and as it was conceivable that increased swelling could result in higher radiochemical yield due to the accessibility of more labeling sites we started developing novel polymer-supported phosphazene bases. **PS**-P$_2^{PEG}$ turned out to have equally excellent trapping abilities as **PS**-P$_2^{tBu}$, while the labeling abilities were less good despite very good swelling ability due to the PEG functionalization of the resin matrix. We then analyzed why we were unable to achieve radiochemical yields higher than about 60% and it turned out that the residual activity was physically trapped within the resin matrix in a nucleophilically active state. The attempt to solve this issue by coupling a phosphazene base to functionalized glass beads and thereby avoiding the tight matrix regrettably failed due to fluorolysis of the Si-O$_{glass}$ bond.

The procedure could be automated and the setup for this strategy was very simple with a column containing the resin that was in a column oven. The column was connected to syringe pumps that pushed the solvents through the column to the product/waste vial.

It is believed that this methodology due to the compact setup, very simple procedure with efficient [^{18}F]F$^-$ recovery and processing together with the column reusability will be an attractive platform for a minimalistic synthesis module that would make PET tracer production available at any radiochemistry lab or hospital. Ideally the platform could even accommodate the emerging dose-on-demand concept where PET tracers are produced in patient-size doses whenever needed.

The next step in the development of the polymer-supported radiofluorination methodology will be the use of non-porous solid support other than glass beads in order to eliminate the issue of matrix entrapment of [^{18}F]F$^-$. Right now work is also done at the Hevesy Laboratory to implement the methodology on a robotic synthesizer in order to optimize the radiofluorination procedure even further. When this is in place the routine production of PET tracers by the solid-phase strategy is only a few steps away.

Chapter 7   Reference list

(1)   Nutt, R. The History of Positron Emission Tomography. *Mol. Imaging Biol.* **2002**, *4* (1), 11–26.

(2)   Maisey, M. N. Positron Emission Tomography in Clinical Medicine. In *Positron Emission Tomography Basic Sciences*; Bailey, D. L., Townsend, D. W., Valk, P. E., Maisey, M. N., Eds.; Springer-Verlag, 2005; pp 1–12.

(3)   Ametamey, S. M.; Honer, M.; Schubiger, P. A. Molecular Imaging with PET. *Chem. Rev.* **2008**, *108* (5), 1501–1516.

(4)   Phelps, M. E. The Molecular Basis Of Disease. In *PET: Molecular Imaging an Its Biological Applications*; Springer-Verlag New York, 2004; pp 270–320.

(5)   Cherry, S. R. Fundamentals of Positron Emission Tomography and Applications in Preclinical Drug Development. *J. Clin. Pharmacol.* **2001**, *41* (5), 482–491.

(6)   Wadsak, W.; Mitterhauser, M. Basics and Principles of Radiopharmaceuticals for PET/CT. *Eur. J. Radiol.* **2010**, *73* (3), 461–469.

(7)   Herance, J. R.; Gispert, J. D.; Abad, S.; Victor, V. M.; Pareto, D.; Torrent, È.; Rojas, S. Erythrocytes Labeled with [(18) F]SFB as an Alternative to Radioactive CO for Quantification of Blood Volume with PET. *Contrast Media Mol. Imaging* **2013**, *8* (4), 375–381.

(8)   Machac, J. Radiopharmaceuticals for Clinical Cardiac PET Imaging. In *Cardiac PET and PET/CT Imaging*; Di Carli, M. F., Lipton, M. J., Eds.; Springer New York: New York, NY, 2007; pp 73–82.

(9)   Young, H.; Carnochan, P.; Zweit, J.; Babich, J.; Cherry, S.; Ott, R. Evaluation of copper(II)-Pyruvaldehyde Bis (N-4-Methylthiosemicarbazone) for Tissue Blood Flow Measurement Using a Trapped Tracer Model. *Eur. J. Nucl. Med.* **1994**, *21* (4), 336–341.

(10)   Chitneni, S. K.; Palmer, G. M.; Zalutsky, M. R.; Dewhirst, M. W. Molecular Imaging of Hypoxia. *J. Nucl. Med.* **2011**, *52* (2), 165–168.

(11)   Bastawrous, S.; Bhargava, P.; Behnia, F.; Djang, D. S. W.; Haseley, D. R. Newer PET Application with an Old Tracer: Role of 18F-NaF Skeletal PET/CT in Oncologic Practice. **2014**.

(12) Grassi, I.; Nanni, C.; Allegri, V.; Morigi, J. J.; Montini, G. C.; Castellucci, P.; Fanti, S. The Clinical Use of PET with (11)C-Acetate. *Am. J. Nucl. Med. Mol. Imaging* **2012**, *2* (1), 33–47.

(13) Bading, J. R.; Shields, A. F. Imaging of Cell Proliferation: Status and Prospects. *J. Nucl. Med.* **2008**, *49 Suppl 2* (Suppl_2), 64S – 80S.

(14) Krause, B. J.; Souvatzoglou, M.; Treiber, U. Imaging of Prostate Cancer with PET/CT and Radioactively Labeled Choline Derivates. *Urol. Oncol.* **2013**, *31* (4), 427–435.

(15) Fueger, B. J.; Czernin, J.; Cloughesy, T.; Silverman, D. H.; Geist, C. L.; Walter, M. A.; Schiepers, C.; Nghiemphu, P.; Lai, A.; Phelps, M. E.; et al. Correlation of 6-18F-Fluoro-L-Dopa PET Uptake with Proliferation and Tumor Grade in Newly Diagnosed and Recurrent Gliomas. *J. Nucl. Med.* **2010**, *51* (10), 1532–1538.

(16) Hanaoka, H.; Tominaga, H.; Yamada, K.; Paudyal, P.; Iida, Y.; Watanabe, S.; Paudyal, B.; Higuchi, T.; Oriuchi, N.; Endo, K. Evaluation of (64)Cu-Labeled DOTA-D-Phe(1)-Tyr (3)-Octreotide ((64)Cu-DOTA-TOC) for Imaging Somatostatin Receptor-Expressing Tumors. *Ann. Nucl. Med.* **2009**, *23* (6), 559–567.

(17) Chen, X.; Park, R.; Shahinian, A. H.; Tohme, M.; Khankaldyyan, V.; Bozorgzadeh, M. H.; Bading, J. R.; Moats, R.; Laug, W. E.; Conti, P. S. 18F-Labeled RGD Peptide: Initial Evaluation for Imaging Brain Tumor Angiogenesis. *Nucl. Med. Biol.* **2004**, *31* (2), 179–189.

(18) Van Kruchten, M.; Glaudemans, A. W. J. M.; de Vries, E. F. J.; Beets-Tan, R. G. H.; Schröder, C. P.; Dierckx, R. A.; de Vries, E. G. E.; Hospers, G. A. P. PET Imaging of Estrogen Receptors as a Diagnostic Tool for Breast Cancer Patients Presenting with a Clinical Dilemma. *J. Nucl. Med.* **2012**, *53* (2), 182–190.

(19) Slifstein, M.; Hwang, D.-R.; Martinez, D.; Ekelund, J.; Huang, Y.; Hackett, E.; Abi-Dargham, A.; Laruelle, M. Biodistribution and Radiation Dosimetry of the Dopamine D2 Ligand 11C-Raclopride Determined from Human Whole-Body PET. *J. Nucl. Med.* **2006**, *47* (2), 313–319.

(20) Lemaire, C.; Cantineau, Robert Guillaume, M.; Plenevaux, A.; Christiaens, L. Luorine- 18-Altanserin: A Radioligand for the Study of Serotonin Receptors with PET: Radiolabeling and In Vivo Biologic Behavior in Rats. *J. Nucl. Med.* **1991**, *32* (12), 2266–2272.

(21) Cherry, S. R.; Sorenson, J. A.; Phelps, M. E. Modes of Radioactive Decay. In *Physics in Nuclear Medicine*; Elsevier, 2012; pp 19–30.

(22) Phelps, M. E. MOLECULAR IMAGING WITH POSITRON EMISSION TOMOGRAPHY. *Annu. Rev. Nucl. Part. Sci.* **2002**, *52* (1), 303–338.

(23)   Phelps, M. E. PET: Physics, Instrumentation and Scanners. In *PET: Molecular Imaging an Its Biological Applications*; 2004; pp 1–124.

(24)   Cherry, S. R.; Sorenson, J. A.; Phelps, M. E. Radionuclide and Radiopharmaceutical Production. In *Physics in Nuclear Medicine*; Elsevier, 2012; pp 43–61.

(25)   Phelps, M. E.; Hoffman, E. J.; Huang, S. C.; Ter-Pogossian, M. M. Effect of Positron Range on Spatial Resolution. *J. Nucl. Med.* **1975**, *16* (7), 649–652.

(26)   Li, Z.; Conti, P. S. Radiopharmaceutical Chemistry for Positron Emission Tomography. *Adv. Drug Deliv. Rev.* **2010**, *62* (11), 1031–1051.

(27)   Banerjee, S. R.; Pomper, M. G. Clinical Applications of Gallium-68. *Appl. Radiat. Isot.* **2013**, *76*, 2–13.

(28)   Sadeghi, M.; Kakavand, T.; Rajabifar, S.; Mokhtari, L.; Rahimi-Nezhad, A. Cyclotron Production of 68Ga via Proton-Induced Reaction on 68Zn Target. *NUKLEONIKA* **2009**, *54* (1), 25–28.

(29)   Choppin, G.; Liljenzin, J.-O.; Rydberg, J.; Ekberg, C. Particle Accelerators. In *Radiochemistry and Nuclear Chemistry*; Elsevier, 2013; pp 493–512.

(30)   International Atomic Energy Agency (IAEA); Technical Reports Series No. 465. *Cyclotron Produced Radionuclides: Principles and Practice*; Vienna, Austria, 2008.

(31)   Mason, N. S.; Mathis, C. A. Radiohalogens for PET Imaging. In *Positron Emission Tomography Basic Sciences*; Bailey, D. L., Townsend, D. W., Valk, P. E., Maisey, M. N., Eds.; Springer-Verlag, 2005; pp 203–222.

(32)   Casella, V.; Ido, T.; Wolf, A. P.; Fowler, Jowrna S. MacGegor, R. R.; Ruth, T. J. Anhydrous F-18 Labeled Elemental Fluorine for Radiopharmaceutical Preparation. *J. Nucl. Med.* **1980**, *21* (8), 750–757.

(33)   Nickles, R. J.; Daube, M. E.; Ruth, T. J. An 18O2 Target for the Production of [18F]F2. *Int. J. Appl. Radiat. Isot.* **1984**, *35* (2), 117–122.

(34)   Dolle, F.; Roeda, D.; Kuhnast, B.; Lasne, M.-C. Fluorine-18 Chemistry for Molecular Imaging with Positron Emission Tomography. In *FLUORINE AND HEALTH Molecular Imaging, Biomedical Materials and Pharmaceuticals*; Tressaud, A., Haufe, G., Eds.; Elsevier, 2008; pp 3–66.

(35)   Schirrmacher, R.; Wängler, C.; Schirrmacher, E. Fluorine-18 Radiochemistry: Theory and Practice. In *Pharmaceutical Radiochemistry (I)*; Wester, H.-J., Ed.; Scintomics, 2010; pp 5–74.

(36) Fimau, G.; Chirakal, R.; Garnett, E. S. Aromatic Radiofluorination with [18F]Fluorine Gas: 6-[18F]Fluoro-L-Dopa. *J. Nucl. Med.* **1984**, *25* (11), 1228–1233.

(37) Dolle, F.; Demphel, S.; Hinnen, F.; Fournier, D.; Vaufrey, F.; Crouzel, C. 6-[18F]Fluoro-L-DOPA by Radiofluorodestannylation: A Short and Simple Synthesis of a New Labelling Precursor. *J. Label. Compd. Radiopharm.* **1998**, *41* (2), 105–114.

(38) Luxen, A.; Perlmutter, M.; Bida, G. T.; Moffaert, G. Van; Cook, J. S.; Satyamurthy, N.; Phelps, M. E.; Barrio, J. R. Remote, Semiautomated Production of 6-[18F]fluoro-L-Dopa for Human Studies with PET. *Int. J. Radiat. Appl. Instrumentation. Part A. Appl. Radiat. Isot.* **1990**, *41* (3), 275–281.

(39) Bergman, J.; Solin, O. Fluorine-18-Labeled Fluorine Gas for Synthesis of Tracer Molecules. *Nucl. Med. Biol.* **1997**, *24* (7), 677–683.

(40) Zhan, C.-G.; Dixon, D. a. Hydration of the Fluoride Anion: Structures and Absolute Hydration Free Energy from First-Principles Electronic Structure Calculations. *J. Phys. Chem. A* **2004**, *108* (11), 2020–2029.

(41) Kemp, D. D.; Gordon, M. S. Theoretical Study of the Solvation of Fluorine and Chlorine Anions by Water. *J. Phys. Chem. A* **2005**, *109* (34), 7688–7699.

(42) Bowden, L.; León Vintró, L.; Mitchell, P. I.; O'Donnell, R. G.; Seymour, A. M.; Duffy, G. J. Radionuclide Impurities in Proton-Irradiated [18O]H2O for the Production of 18F–: Activities and Distribution in the [18F]FDG Synthesis Process. *Appl. Radiat. Isot.* **2009**, *67* (2), 248–255.

(43) Cai, L.; Lu, S.; Pike, V. W. Chemistry with [18F]Fluoride Ion. *European J. Org. Chem.* **2008**, *2008* (17), 2853–2873.

(44) Noyce, D. S.; Virgilio, J. A. Synthesis and Solvolysis of 1-Phenylethyl Disubstituted Phosphinates. *J. Org. Chem.* **1972**, *37* (17), 2643–2647.

(45) Ross, T. L.; Ametamey, S. M. PET Chemistry: An Introduction. In *Basic Sciences of Nuclear Medicine*; Khalil, M. M., Ed.; Springer-Verlag Berlin Heidelberg, 2011; pp 65–102.

(46) Masumoto, K.; Iiduka, H.; Sato, S.; Kuga, K.; Fujibuchi, T.; Sasaki, M.; Fukumura, T.; Nakamura, H.; Toyoda, A. Effectiveness of Self-Shielding Type Cyclotrons. *Prog. Nucl. Sci. Technol.* **2014**, *4*, 223–227.

(47) Saha, G. B. Design and Cost of PET Center. In *Basics of PET Imaging Physics, Chemistry, and Regulations*; Springer, 2010; pp 191–204.

(48)   Keng, P. Y.; Esterby, M.; van Dam, R. M. Emerging Technologies for Decentralized Production
         of PET Tracers. In *Positron Emission Tomography - Current Clinical and Research Aspects*; Hsieh,
         C.-H., Ed.; InTech, 2012; pp 153–182.

(49)   Arima, V.; Pascali, G.; Lade, O.; Kretschmer, H. R.; Bernsdorf, I.; Hammond, V.; Watts, P.; De
         Leonardis, F.; Tarn, M. D.; Pamme, N.; et al. Radiochemistry on Chip: Towards Dose-on-
         Demand Synthesis of PET Radiopharmaceuticals. *Lab Chip* **2013**, *13* (12), 2328–2336.

(50)   Lu, S.; Pike, V. W. Micro-Reactors for PET Tracer Labeling. In *PET Chemistry The Driving Force
         in Molecular Imaging*; Schubiger, P. A., Lehmann, L., Friebe, M., Eds.; Springer-Verlag Berlin
         Heidelberg, 2007; pp 271–288.

(51)   Rensch, C.; Jackson, A.; Lindner, S.; Salvamoser, R.; Samper, V.; Riese, S.; Bartenstein, P.;
         Wängler, C.; Wängler, B. Microfluidics: A Groundbreaking Technology for PET Tracer
         Production? *Molecules* **2013**, *18* (7), 7930–7956.

(52)   Elizarov, A. M. Microreactors for Radiopharmaceutical Synthesis. *Lab Chip* **2009**, *9* (10), 1326–
         1333.

(53)   Welton, T. Room-Temperature Ionic Liquids. Solvents for Synthesis and Catalysis. *Chem. Rev.*
         1999, *99* (8), 2071–2084.

(54)   Kim, H. W.; Jeong, J. M.; Lee, Y.-S.; Chi, D. Y.; Chung, K.-H.; Lee, D. S.; Chung, J.-K.; Lee, M. C.
         Rapid Synthesis of [18F]FDG without an Evaporation Step Using an Ionic Liquid. *Appl. Radiat.
         Isot.* **2004**, *61* (6), 1241–1246.

(55)   Moon, B. S.; Lee, K. C.; An, G. Il; Chi, D. Y.; Yang, S. D.; Choi, C. W.; Lim, S. M.; Chun, K. S.
         Preparation of 3'-Deoxy-3'-[18F]fluorothymidine ([18F]FLT) in Ionic Liquid, [bmim][OTf]. *J.
         Label. Compd. Radiopharm.* **2006**, *49* (3), 287–293.

(56)   Yun, M.; Oh, S. J.; Ha, H.-J.; Ryu, J. S.; Moon, D. H. High Radiochemical Yield Synthesis of 3'-
         Deoxy-3'-[18F]fluorothymidine Using (5'-O-Dimethoxytrityl-2'-Deoxy-3'-O-Nosyl-B-D-Threo
         Pentofuranosyl)thymine and Its 3-N-BOC-Protected Analogue as a Labeling Precursor. *Nucl.
         Med. Biol.* **2003**, *30* (2), 151–157.

(57)   Kim, D. W.; Ahn, D.-S.; Oh, Y.-H.; Lee, S.; Kil, H. S.; Oh, S. J.; Lee, S. J.; Kim, J. S.; Ryu, J. S.;
         Moon, D. H.; et al. A New Class of SN2 Reactions Catalyzed by Protic Solvents: Facile
         Fluorination for Isotopic Labeling of Diagnostic Molecules. *J. Am. Chem. Soc.* **2006**, *128* (50),
         16394–16397.

(58)   Kim, D. W.; Jeong, H.-J.; Lim, S. T.; Sohn, M.-H.; Katzenellenbogen, J. A.; Chi, D. Y. Facile
         Nucleophilic Fluorination Reactions Using Tert-Alcohols as a Reaction Medium: Significantly

Enhanced Reactivity of Alkali Metal Fluorides and Improved Selectivity. *J. Org. Chem.* **2008**, *73* (3), 957–962.

(59)   Voccia, S.; Aerts, J.; Lemaire, C.; Luxen, A.; Morelle, J.-L.; Philippart, G. Method for the Preparation of Reactive 18F Fluoride, and for the Labeling of Radiotracers, Using a Modified Non-Ionic Solid Support and without Any Evaporation Step EP 1 990 310 A1, 2008.

(60)   Aerts, J.; Lemaire, C.; Lignon, S.; Luxen, A.; Morelle, J.-L.; Philippart, G.; Voccia, S. Method for the Elution of 18f Fluoride Trapped on an Anion-Exchange Phase in a Form Suitable for Efficient Radiolabeling without Any Evaporation Step. US20110006011 A1, January 13, 2011.

(61)   Aerts, J.; Voccia, S.; Lemaire, C.; Giacomelli, F.; Goblet, D.; Thonon, D.; Plenevaux, A.; Warnock, G.; Luxen, A. Fast Production of Highly Concentrated Reactive [18F] Fluoride for Aliphatic and Aromatic Nucleophilic Radiolabelling. *Tetrahedron Lett.* **2010**, *51* (1), 64–66.

(62)   Schottelius, M.; Wester, H.-J. Fluorine-18 Labeling of Peptides and Proteins. In *PET Chemistry The Driving Force in Molecular Imaging*; Schubinger, P. A., Lehmann, L., Friebe, M., Eds.; Springer-Verlag Berlin Heidelberg, 2007; pp 79–112.

(63)   Bruce Martin, R. Ternary Complexes of Al3+ and F− with a Third Ligand. *Coord. Chem. Rev.* **1996**, *149*, 23–32.

(64)   McBride, W. J.; Sharkey, R. M.; Karacay, H.; D'Souza, C. A.; Rossi, E. A.; Laverman, P.; Chang, C.-H.; Boerman, O. C.; Goldenberg, D. M. A Novel Method of 18F Radiolabeling for PET. *J. Nucl. Med.* **2009**, *50* (6), 991–998.

(65)   Laverman, P.; McBride, W. J.; Sharkey, R. M.; Eek, A.; Joosten, L.; Oyen, W. J. G.; Goldenberg, D. M.; Boerman, O. C. A Novel Facile Method of Labeling Octreotide with (18)F-Fluorine. *J. Nucl. Med.* **2010**, *51* (3), 454–461.

(66)   D'Souza, C. A.; McBride, W. J.; Sharkey, R. M.; Todaro, L. J.; Goldenberg, D. M. High-Yielding Aqueous 18F-Labeling of Peptides via Al18F Chelation. *Bioconjug. Chem.* **2011**, *22* (9), 1793–1803.

(67)   Dean, J. A. *LANGE'S HANDBOOK OF CHEMISTRY*, 15th ed.; McGraw-Hill, Inc, 1999.

(68)   Ting, R.; Adam, M. J.; Ruth, T. J.; Perrin, D. M. Arylfluoroborates and Alkylfluorosilicates as Potential PET Imaging Agents: High-Yielding Aqueous Biomolecular 18F-Labeling. *J. Am. Chem. Soc.* **2005**, *127* (38), 13094–13095.

(69)   Ting, R.; Harwig, C.; auf dem Keller, U.; McCormick, S.; Austin, P.; Overall, C. M.; Adam, M. J.; Ruth, T. J.; Perrin, D. M. Toward [18F]-Labeled Aryltrifluoroborate Radiotracers: In Vivo

Positron Emission Tomography Imaging of Stable Aryltrifluoroborate Clearance in Mice. *J. Am. Chem. Soc.* **2008**, *130* (36), 12045–12055.

(70)   Saiki, H.; Iwata, R.; Nakanishi, H.; Wong, R.; Ishikawa, Y.; Furumoto, S.; Yamahara, R.; Sakamoto, K.; Ozeki, E. Electrochemical Concentration of No-Carrier-Added [(18)F]fluoride from [(18)O]water in a Disposable Microfluidic Cell for Radiosynthesis of (18)F-Labeled Radiopharmaceuticals. *Appl. Radiat. Isot.* **2010**, *68* (9), 1703–1708.

(71)   He, P.; Haswell, S. J.; Pamme, N.; Archibald, S. J. Advances in Processes for PET Radiotracer Synthesis: Separation of [^{18}F]fluoride from Enriched [^{18}O]water. *Appl. Radiat. Isot.* **2014**, *91*, 64–70.

(72)   Campbell, M. G.; Ritter, T. Modern Carbon-Fluorine Bond Forming Reactions for Aryl Fluoride Synthesis. *Chem. Rev.* **2015**, *115* (2), 612–633.

(73)   Lee, E.; Hooker, J. M.; Ritter, T. Nickel-Mediated Oxidative Fluorination for PET with Aqueous [18F] Fluoride. *J. Am. Chem. Soc.* **2012**, *134* (42), 17456–17458.

(74)   Huang, X.; Liu, W.; Ren, H.; Neelamegam, R.; Hooker, J. M.; Groves, J. T. Late Stage Benzylic C-H Fluorination with [^{18}F]fluoride for PET Imaging. *J. Am. Chem. Soc.* **2014**, *136* (19), 6842–6845.

(75)   Revunov, E.; Zhuravlev, F. Co(salen)-Mediated Enantioselective Radiofluorination of Epoxides. Radiosynthesis of Enantiomerically Enriched [18F]F-MISO via Kinetic Resolution. *J. Fluor. Chem.* **2013**, *156*, 130–135.

(76)   Mathiessen, B.; Jensen, M.; Zhuravlev, F. [18F]Fluoride Recovery via Gaseous [18F]HF. *J. Label. Compd. Radiopharm.* **2011**, *54* (13), 816–818.

(77)   Hirschmann, R. F.; Miller, R.; Wood, J.; Jones, R. E. The Reaction of Epoxides with Anhydrous Hydrogen Fluoride in the Presence of Organic Bases. The Preparation of 9α-Fluoro-4-Pregnene-11β,17α,21-Triol 3,20-Dione 21-Acetate and Its 1-Dehydro Analog. *J. Am. Chem. Soc.* **1956**, *78* (19), 4956–4959.

(78)   Olah, G. A.; Welch, J. T.; Vankar, Y. D.; Nojima, M.; Kerekes, I.; Olah, J. A. Synthetic Methods and Reactions. 63. Pyridinium Poly(hydrogen Fluoride) (30% Pyridine-70% Hydrogen Fluoride): A Convenient Reagent for Organic Fluorination Reactions. *J. Org. Chem.* **1979**, *44* (22), 3872–3881.

(79)   McClinton, M. A. Triethylamine Tris(hydrogen Fluoride): Applications in Synthesis. *Aldrichimica Acta* **1995**, *28* (2), 31–35.

(80) Kremsner, J. M.; Rack, M.; Pilger, C.; Oliver Kappe, C. Microwave-Assisted Aliphatic Fluorine–
chlorine Exchange Using Triethylamine Trihydrofluoride (TREAT-HF). *Tetrahedron Lett.* **2009**,
50 (26), 3665–3668.

(81) Staab, H. A.; Saupe, T. ?Proton Sponges? And the Geometry of Hydrogen Bonds: Aromatic
Nitrogen Bases with Exceptional Basicities. *Angew. Chemie Int. Ed. English* **1988**, *27* (7), 865–
879.

(82) Chambers, R. D.; Holmes, T. F.; Korn, S. R.; Sandford, G. Proton Sponge Hydrofluoride as a
Soluble Fluoride Ion Source. *J. Chem. Soc. Chem. Commun.* **1993**, No. 10, 855.

(83) Chambers, R. D.; Korn, S. R.; Sandford, G. Reactions Involving Fluoride Ion. Part 37. "Proton
Sponge" Hydrofluoride as a Fluoride Ion Donor. *J. Fluor. Chem.* **1994**, *69* (1), 103–108.

(84) Darabantu, M.; Lequeux, T.; Pommelet, J.-C.; Plé, N.; Turck, A.; Toupet, L. The Proton
Sponge–triethylamine Tris(hydrogen Fluoride) System as a Selective Nucleophilic Fluorinating
Reagent for Chlorodiazines. *Tetrahedron Lett.* **2000**, *41* (35), 6763–6767.

(85) Pascali, G.; Kiesewetter, D. O.; Salvadori, P. A.; Eckelman, W. C. Use of 1,8-Bis-
(dimethylamino)-naphthalene/H18F Complex as New Radiofluorinating Agent. *J. Label.
Compd. Radiopharm.* **2004**, *47* (6), 373–383.

(86) Schwesinger, R.; Schlemper, H. Peralkylated Polyaminophosphazenes— Extremely Strong,
Neutral Nitrogen Bases. *Angew. Chemie Int. Ed. English* **1987**, *26* (11), 1167–1169.

(87) Margetic, D. Physico-Chemical Properties of Organosuperbases. In *Superbases for Organic
Synthesis*; ISHIKAWA, T., Ed.; John Wiley & Sons, Ltd., 2009; pp 9–48.

(88) Schwesinger, R.; Willaredt, J.; Schlemper, H.; Keller, M.; Schmitt, D.; Fritz, H. Novel, Very
Strong, Uncharged Auxiliary Bases; Design and Synthesis of Monomeric and Polymer-Bound
Triaminoiminophosphorane Bases of Broadly Varied Steric Demand. *Chem. Ber.* **1994**, *127* (12),
2435–2454.

(89) Schwesinger, R.; Hasenfratz, C.; Schlemper, H.; Walz, L.; Peters, E.-M.; Peters, K.; von
Schnering, H. G. How Strong and How Hindered Can Uncharged Phosphazene Bases Be?
Angew. Chemie Int. Ed. English **1993**, *32* (9), 1361–1363.

(90) Schwesinger, R.; Link, R.; Thiele, G.; Rotter, H.; Honert, D.; Limbach, H.-H.; Männle, F. Stable
Phosphazenium Ions in Synthesis—an Easily Accessible, Extremely Reactive"Naked" Fluoride
Salt. *Angew. Chemie Int. Ed. English* **1991**, *30* (10), 1372–1375.

(91) Schwesinger, R.; Link, R.; Wenzl, P.; Kossek, S. Anhydrous Phosphazenium Fluorides as Sources
for Extremely Reactive Fluoride Ions in Solution. *Chemistry* **2005**, *12* (2), 438–445.

(92) Fruchart, J.-S.; Gras-Masse, H.; Melnyk, O. Methyl Phenylacetate Enolate Generated with the P4-tBu Schwesinger Base: "naked" or Not? *Tetrahedron Lett.* **2001**, *42* (52), 9153–9155.

(93) Lemaire, C. F.; Aerts, J. J.; Voccia, S.; Libert, L. C.; Mercier, F.; Goblet, D.; Plenevaux, A. R.; Luxen, A. J. Fast Production of Highly Reactive No-Carrier-Added [18F]fluoride for the Labeling of Radiopharmaceuticals. *Angew. Chem. Int. Ed. Engl.* **2010**, *49* (18), 3161–3164.

(94) Simons, J. H. Hydrogen Fluoride and Its Solutions. *Chem. Rev.* **1931**, *8* (2), 213–235.

(95) Marczenko, Z.; Balcerzak, M. Separation, Preconcentration and Spectrophotometry in Inorganic Analysis. In *Analytical Spectroscopy Library*; Analytical Spectroscopy Library; Elsevier, 2000; Vol. 10, pp 189–197.

(96) Mathiessen, B.; Jensen, A. T. I.; Zhuravlev, F. Homogeneous Nucleophilic Radiofluorination and Fluorination with Phosphazene Hydrofluorides. *Chem. A Eur. J.* **2011**, *17* (28), 7796–7805.

(97) Mitchell, A. R. Bruce Merrifield and Solid-Phase Peptide Synthesis: A Historical Assessment. *Biopolymers* **2008**, *90* (3), 175–184.

(98) Truran, G. A.; Aiken, K. S.; Fleming, T. R.; Webb, P. J.; Markgraf, J. H. Solid-Phase Organic Synthesis and Combinatorial Chemistry: A Laboratory Preparation of Oligopeptides. *J. Chem. Educ.* **2002**, *79* (1), 85.

(99) Merrifield, B. Bruce Merrifield - Nobel Lecture: Solid Phase Synthesis. *Nobel Lect. Chem. 1981-1990* **1984**.

(100) Brown, L. J.; Bouvet, D. R.; Champion, S.; Gibson, A. M.; Hu, Y.; Jackson, A.; Khan, I.; Ma, N.; Millot, N.; Wadsworth, H.; et al. A Solid-Phase Route to 18F-Labeled Tracers, Exemplified by the Synthesis of [18F]2-Fluoro-2-Deoxy-D-Glucose. *Angew. Chem. Int. Ed. Engl.* **2007**, *46* (6), 941–944.

(101) Brown, L. J.; Ma, N.; Bouvet, D. R.; Champion, S.; Gibson, A. M.; Hu, Y.; Jackson, A.; Khan, I.; Millot, N.; Topley, A. C.; et al. Synthesis of the Positron-Emitting Radiotracer [(18)F]-2-Fluoro-2-Deoxy-D-Glucose from Resin-Bound Perfluoroalkylsulfonates. *Org. Biomol. Chem.* **2009**, *7* (3), 564–575.

(102) Topley, A. C.; Isoni, V.; Logothetis, T. A.; Wynn, D.; Wadsworth, H.; Gibson, A. M. R.; Khan, I.; Wells, N. J.; Perrio, C.; Brown, R. C. D. A Resin-Linker-Vector Approach to Radiopharmaceuticals Containing 18F: Application in the Synthesis of O-(2-[18F]-Fluoroethyl)-L-Tyrosine. *Chemistry* **2013**, *19* (5), 1720–1725.

(103) Brady, F.; Luthra, S. K.; Robins, E. G. Solid-Phase Fluorination of Uracil and Cytocine (WO2004/056400A1), 2004.

(104) Riss, P. J.; Kuschel, S.; Aigbirhio, F. I. No Carrier-Added Nucleophilic Aromatic Radiofluorination Using Solid Phase Supported Arenediazonium Sulfonates and 1-(aryldiazenyl)piperazines. *Tetrahedron Lett.* **2012**, *53* (14), 1717–1719.

(105) Mulholland, G. K.; Mangner, T. J.; Jewett, D. M.; Kilbourn, M. R. Polymer-Supported Nucleophilic Radiolabeling Reactions with [18F]fluoride and [11C]cyanide Ion on Quaternary Ammonium Resins. *J. Label. Compd. Radiopharm.* **1989**, *26* (1-12), 378–380.

(106) Toorongian, S. A.; Mulholland, G. K.; Jewett, D. M.; Bachelor, M. A.; Kilbourn, M. R. Routine Production of 2-Deoxy-2-[18F]fluoro-D-Glucose by Direct Nucleophilic Exchange on a Quaternary 4-Aminopyridinium Resin. *Int. J. Rad. Appl. Instrum. B.* **1990**, *17* (3), 273–279.

(107) Mathiessen, B.; Zhuravlev, F. Automated Solid-Phase Radiofluorination Using Polymer-Supported Phosphazenes. *Molecules* **2013**, *18* (9), 10531–10547.

(108) Kuge, Y.; Nishijima, K.; Nagatsu, K.; Seki, K.; Ohkura, K.; Tanaka, A.; Sasaki, M.; Tsukamoto, E.; Tamaki, N. Chemical Impurities in [18F]FDG Preparations Produced by Solid-Phase 18F-Fluorination. *Nucl. Med. Biol.* **2002**, *29* (2), 275–279.

(109) Schwesinger, R.; Schlemper, H.; Hasenfratz, C.; Willaredt, J.; Dambacher, T.; Breuer, T.; Ottaway, C.; Fletschinger, M.; Boele, J.; Fritz, H.; et al. Extremely Strong, Uncharged Auxiliary Bases; Monomeric and Polymer-Supported Polyaminophosphazenes (P2-P5). *Liebigs Ann.* **2006**, *1996* (7), 1055–1081.

(110) Thielbeer, F.; Donaldson, K.; Bradley, M. Zeta Potential Mediated Reaction Monitoring on Nano and Microparticles. *Bioconjug. Chem.* **2011**, *22* (2), 144–150.

(111) Miraballes-Mart�nez, I.; Forcada, J. Synthesis of Latex Particles with Surface Amino Groups. *J. Polym. Sci. Part A Polym. Chem.* **2000**, *38* (23), 4230–4237.

(112) Mathiessen, B.; Severin, G.; Zhuravlev, F. Towards Automated Solid Phase Radiofluorination for Dose-on-Demand PET: Retention of Activity by Solid Support. *Radiochim. Acta* **2015**, *103* (3), 227–232.

(113) ZHURAVLEV, F.; MATHIESSEN, B. WO2014020035A1 RADIOFLUORINATION METHOD, February 7, 2014.

Appendix 1 - The patent

Patent: Zhuravlev, F.; Mathiessen, B. Radiofluorination Method. PCT Patent application: WO2014020035A1, pp. 39, 16 claims, 3 drawings.

(12) INTERNATIONAL APPLICATION PUBLISHED UNDER THE PATENT COOPERATION TREATY (PCT)

(19) World Intellectual Property Organization
International Bureau

(43) International Publication Date
6 February 2014 (06.02.2014)

WIPO | PCT

(10) International Publication Number
WO 2014/020035 A1

(51) **International Patent Classification:**
C07B 59/00 (2006.01)   *B01D 15/36* (2006.01)

(21) **International Application Number:**
PCT/EP2013/066025

(22) **International Filing Date:**
30 July 2013 (30.07.2013)

(25) **Filing Language:**   English

(26) **Publication Language:**   English

(30) **Priority Data:**
PA 2012 00482   30 July 2012 (30.07.2012)   DK
PA 2013 00319   24 May 2013 (24.05.2013)   DK

(71) **Applicant: TECHNICAL UNIVERSITY OF DEN-MARK** [DK/DK]; Anker Engelunds Vej 1, building 101 A, DK-2800 Kgs. Lyngby (DK).

(72) **Inventors: ZHURAVLEV, Fedor**; Vibevej 13, DK-4000 Roskilde (DK). **MATHIESSEN, Bente**; Tjærebyvej 107, DK-4000 Roskilde (DK).

(74) **Agent: SELDEN, Deborah A.**; Beck Greener, Fulwood House, 12 Fulwood Place, London London WC1V 6HR (GB).

(81) **Designated States** *(unless otherwise indicated, for every kind of national protection available)*: AE, AG, AL, AM, AO, AT, AU, AZ, BA, BB, BG, BH, BN, BR, BW, BY, BZ, CA, CH, CL, CN, CO, CR, CU, CZ, DE, DK, DM, DO, DZ, EC, EE, EG, ES, FI, GB, GD, GE, GH, GM, GT, HN, HR, HU, ID, IL, IN, IS, JP, KE, KG, KN, KP, KR, KZ, LA, LC, LK, LR, LS, LT, LU, LY, MA, MD, ME, MG, MK, MN, MW, MX, MY, MZ, NA, NG, NI, NO, NZ, OM, PA, PE, PG, PH, PL, PT, QA, RO, RS, RU, RW, SC, SD, SE, SG, SK, SL, SM, ST, SV, SY, TH, TJ, TM, TN, TR, TT, TZ, UA, UG, US, UZ, VC, VN, ZA, ZM, ZW.

(84) **Designated States** *(unless otherwise indicated, for every kind of regional protection available)*: ARIPO (BW, GH, GM, KE, LR, LS, MW, MZ, NA, RW, SD, SL, SZ, TZ, UG, ZM, ZW), Eurasian (AM, AZ, BY, KG, KZ, RU, TJ, TM), European (AL, AT, BE, BG, CH, CY, CZ, DE, DK, EE, ES, FI, FR, GB, GR, HR, HU, IE, IS, IT, LT, LU, LV, MC, MK, MT, NL, NO, PL, PT, RO, RS, SE, SI, SK, SM, TR), OAPI (BF, BJ, CF, CG, CI, CM, GA, GN, GQ, GW, KM, ML, MR, NE, SN, TD, TG).

Published:
— *with international search report (Art. 21(3))*

(54) **Title:** RADIOFLUORINATION METHOD
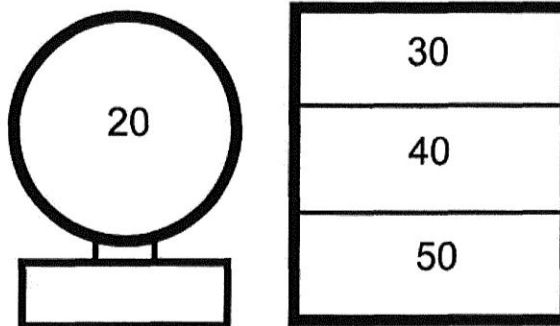
Figure 1

(57) **Abstract:** A method of conducting radiofluorination of a substrate, comprising the steps of: (a) contacting an aqueous solution of [18F] fluoride with a polymer supported phosphazene base for sufficient time for trapping of [18F] fluoride on the polymer supported phosphazene base; and (b) contacting a solution of the substrate with the polymer supported phosphazene base having [18F] fluoride trapped thereon obtained in step (a) for sufficient time for a radiofluorination reaction to take place; an apparatus for conducting radiofluorination; use of the apparatus; and an apparatus for production of a dose of a radiotracer for administration to a patient.

-1-

Radiofluorination Method

The present invention relates to a method of
radiofluorination, in particular that can be used for dose-on-
demand and/or bedside production of ^{18}F PET radiotracers.

5   Positron emission tomography (PET) is an imaging method
used to obtain quantitative molecular and biochemical
information regarding physiological processes in the human body.
The most common PET radiotracer in use is ^{18}F-fluorodeoxyglucose
(^{18}F-FDG), a radiolabelled glucose molecule. PET imaging with
10   ^{18}F-FDG allows the visualisation of glucose metabolism and has a
broad range of clinical uses. ^{18}F is the most widely used
positron emitter in the clinical environment.

^{18}F fluoride is produced by the irradiation of water
containing $H_2^{18}O$ with protons, resulting in the reaction
15     $^{18}O(p,n)^{18}F$. Only a minor fraction of the ^{18}O is converted. For
production efficiency and radiochemical purity, it is desirable
to use water that is as highly enriched as possible. The ^{18}F
isotope is then separated from the water and processed for
reaction to produce a radiochemical agent, as, due to the high
20   free energy of hydration of $^{18}F^-$, this species is
nucleophilically inert in aqueous solution. Routinely, the
removal of water is achieved by trapping $^{18}F^-$ on an ion exchange
resin, eluting the trapped $^{18}F^-$ from the resin using a cryptand
ligand and a base (for example Kryptofix 222-K_2CO_3) dissolved in
25   organic solvent, and removal of the water by repeated and time
consuming azeotropic distillations, which process is unsuitable
for miniaturisation.

Improvement of the production of $^{18}F^-$ has been attempted.
WO2008/128306 (Voccia et al) describes a method of removing
30   water from the $^{18}F^-$ and providing it in an organic solvent
suitable for conducting fluorination reactions, which method is
conducted without the need for azeotropic distillation of water.

150

-2-

This document teaches the use of a non-ionic solid support
modified with a trapping agent which is a metal salt complex of
a positively charged base such as a cryptand or polydentate
amine ligand, which trapping agent is able to remain bound to
5   the solid support in aqueous solution, but is released from the
solid support when exposed to a polar aprotic solvent suitable
for radiolabelling. Thus, the $^{18}F^-$ is bound to the solid support
as a complex with the trapping agent, and is subsequently eluted
in the chosen polar aprotic organic solvent in the form of an
10   $^{18}F^-$-trapping agent complex. An intermediate elution step can
eliminate the majority of the water while allowing the $^{18}F^-$ and
trapping agent to remain bound to the solid support, if a
suitable organic solvent is selected. The eluted $^{18}F^-$-trapping
agent complex in solution in the polar aprotic solvent is
15   suitable for conducting radiolabelling.

Similarly, Lemaire et al (Angewandte Chemie Int Ed 2010,
49, 3161-3164) describe the elution of $^{18}F^-$ from a solid support
using acetonitrile and a variety of bases such as BEMP, BTMG,
P_2^{Et} and P_4^{tBu}, followed by use of the eluted solution in the
20   radiofluorination of a number of precursors of PET radiotracers.

US2011/0006011 (Aerts et al) describes the trapping of $^{18}F^-$
on an anion exchange column, rinsing with organic solvent to
remove water, and elution with an organic solution containing a
tertiary alcohol and/or a phase transfer agent. The resulting
25   solution can be used for radiolabelling reactions.

KR20080078233 (Yoon et al) describes a method in which $^{18}F^-$
is trapped on a quaternary ammonium salt supported on a polymer
support, the $^{18}F^-$ is eluted by a solution comprising a metal
ammonium salt in an alcoholic solvent, and subsequently the
30   eluted solution is reacted with an alkyl halide or alkyl
sulphonate.

-3-

US6190637 (Ino et al) describes a method of isolating $^{18}F^-$ from $H_2{}^{18}O$ by trapping it on a weakly basic anion exchange resin, and subsequently eluting it in the form of a complex with a phase transfer catalyst such as a cryptand. The eluted solution

5   is an aqueous solution, and so the $^{18}F^-$ complex must be dried and redissolved in a suitable organic solvent before a radiolabelling reaction can be carried out.

Schlyer et al (Appl Radiat Isot 1990, 41, 6, 531-533) also describes a method in which $^{18}F^-$ is isolated from $H_2{}^{18}O$ by binding

10 to an anion exchange resin. The trapped $^{18}F^-$ is eluted from the resin using a dilute solution of caesium carbonate or potassium carbonate in water.

US2006/0083677 (Brady et al) describes a method in which a precursor molecule for radiolabelling, in particular a

15 benzothiazole compound, is bound to a solid support, and $^{18}F^-$ is contacted with the solid support and reacts with the precursor molecule by displacing the support to result in a labelled tracer molecule.

WO2011/110994 describes a method of producing a radio

20 tracer by nucleophilic displacement by $^{18}F^-$ of a labelled leaving group, and subsequent removal of unreacted precursor by use of an adsorbent recognising the labelled leaving group.

Toorongian et al (Nucl Med Biol 1990, 17, 3, 273-279) describes the use of $^{18}F^-$ supported on a quaternary 4-(N,N-

25 dialkylamino)-pyridinium functionalised polystyrene anion exchange resin for conducting radiofluorination reactions to produce radiolabelled ^{18}F-FDG. The $^{18}F^-$ is captured directly by the resin from $H_2{}^{18}O$, acetonitrile is passed through the column to remove water from the resin, and an acetonitrile solution of

30 the precursor compound for the radiofluorination passed through the column while heating in order to conduct the radiofluorination reaction. The resin columns are stated not to

-4-

be reusable as the resin becomes strongly discoloured during
normal reaction conditions, although the mechanism of
decomposition of the resin is not known.

5   Mathiessen et al (Chem Eur J 2011, 17, 7796-7805)
describes the formation of phosphazenium hydrofluorides by
trapping of gaseous HF, and $H^{18}F$, by phosphazene bases. These
phosphazenium hydrofluorides, in particular P_2^{Et} and P_4^{tBu}
hydrofluorides, were used to carry out solution phase
fluorination and radiofluorination reactions on alkyl halides
10 and pseudohalides, and optimisation of the conditions for
conducting the fluorination reactions was carried out.

It is an aim of the present invention to provide an
efficient method of trapping $^{18}F^-$ from aqueous solution and
delivering it to a target molecule as a nucleophile.

15 An aim of certain embodiments of the present invention is
to provide such a method for preparation of radiotracers for PET
imaging.

An aim of certain embodiments of the present invention is
to provide such a method that is suitable for bedside production
20 of radiotracers, or other applications in which miniaturisation
of the apparatus is desirable.

An aim of certain embodiments of the present invention is
to provide a method in which the apparatus can be re-used.

An aim of certain embodiments of the present invention is
25 to provide apparatus which is stable at room temperature.

An aim of certain embodiments of the present invention is
to remove the need for purification steps and/or the use of
solution phase complexing agents in the generation and use of
$^{18}F^-$.

-5-

An aim of the present invention is to provide a method in which $^{18}F^{-}$ recovery and radiofluorination can take place within the same vessel or column.

5   An aim of certain embodiments of the present invention is to provide more rapid methods of trapping $^{18}F^{-}$ and subsequent radiolabelling reactions, in particular to provide rapid on demand synthesis of radiotracers.

An aim of certain embodiments of the present invention is to provide a disposable cartridge that can be used in the
10   production of radiotracers.

Accordingly, in a first aspect, the present invention provides a method of conducting radiofluorination of a substrate, comprising the steps of:

(a) contacting an aqueous solution of [^{18}F]fluoride with a
15   polymer supported phosphazene base selected from a phosphazene

R=alkyl

of the general formula   supported on polystyrene (P_{PS}-P_2^R), and a phosphazene of the formula
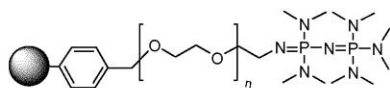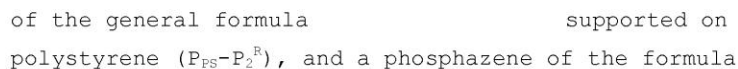
                  supported on PEG-coated polystyrene (P_{PS-PEG}-P_2^{Bz}), for sufficient time for trapping of the
20   [^{18}F]fluoride by the polymer-supported phosphazene base; and

(b) contacting a solution of the substrate with the polymer

154

-6-

supported phosphazene base having [^{18}F] fluoride trapped thereon
obtained in step (a) for sufficient time for a radiofluorination
reaction to take place.

Preferably, the radiofluorination method further comprises
5   a step of preparing an aqueous solution of ^{18}F^{-} by ^{18}O(p,n)^{18}F
reaction in a cyclotron using enriched H$_2$^{18}O water.

Preferably, following step (a) and before step (b),
residual water is removed from the polymer supported phosphazene
base having [^{18}F] fluoride trapped thereon by contacting it with
10 a water-miscible solvent. The removal step may suitably be
carried out by flowing the water miscible solvent over the
polymer supported phosphazene base having [^{18}F] fluoride trapped
thereon, or by one or more iterations of immersing the polymer
supported base having [^{18}F] fluoride trapped thereon in the water
15 miscible solvent and then removing the water miscible solvent.
Preferably, the water miscible solvent is selected from
acetonitrile, THF, DMF and acetone. Suitably, the polymer
supported phosphazene base having [^{18}F] fluoride trapped thereon
can be further dried by passing a flow of dry gas over it.

20 Suitably, following step (a) and any drying steps, and
prior to step (b), the polymer supported phosphazene base having
[^{18}F] fluoride trapped thereon can be contacted with organic
solvent to allow for swelling of the polymer support.
Preferably, the organic solvent is the same as the solvent used
25 to prepare the substrate solution to be used in step (b).

Preferably, the substrate solution is prepared using
toluene, acetonitrile, dichloromethane or DMF as solvent.

The substrate used in step (b) is an aliphatic or aromatic
compound comprising a leaving group. The leaving group is
30 suitably selected from the group consisting of fluorosulfonates,
perfluoroalkysulfonates, alkanesulfonates, arenesulfonates,
alkyl, perfluoroalkyl or arene esters, phosphate, sulphate or

-7-

nitrate esters, alkyl or aryl diazonium salts, ammonium,
tetraalkylammonium or pyridinium salts, ethers or thioethers,
halogens (other than fluoride), nitro groups and
diiodoaryliodonium salts. Preferably, the leaving group is
5 selected from the group consisting of triflate, nosylate,
mesylate, tosylate, chloride, bromide, iodide and nitro.
Preferably, the compound comprising the leaving group is
selected from naphthylethyl compounds, mannose, optionally
substituted pyridine compounds and glycols.

10   Preferably, the polymer supported phosphazene base is
contained in a column. Suitably, the column can be re-used in
more than one iteration of the method of the invention.
Suitably, the column can be sealed and disposed of after a
chosen number of iterations of the method of the invention.

15   Preferably, where the polymer supported phosphazene base
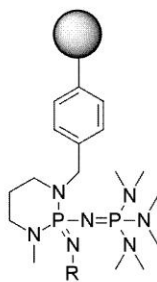

R=alkyl

is of the formula   supported on polystyrene, R
is selected from the group consisting of methyl, ethyl, propyl,
butyl, isopropyl, isobutyl, tert-butyl, pentyl, isopentyl, tert-
pentyl, tert-octyl, and more preferably is selected from the
20 group consisting of ethyl, tert-butyl and tert-octyl.

156

-8-

Preferably, the polymer supported phosphazene base is

selected from $P_{PS}\text{-}P_2^{tBu}$ (   ) and $P_{PS\text{-}PEG}\text{-}P_2^{Bz}$

( ).
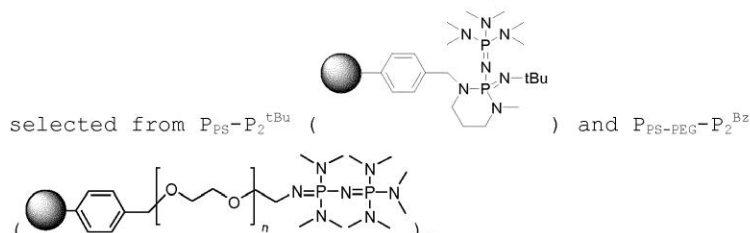
Preferably, step (b) comprises heating the polymer
5   supported phosphazene base having [^{18}F] fluoride trapped thereon
in contact with the substrate solution to a temperature of from
50 °C to 120 °C.

Preferably, the product of the reaction in step (b) is
isolated from the polymer supported phosphazene base. Where the
10   polymer supported phosphazene base is contained in a column,
this can be done by passing a suitable organic solvent, such as
the solvent in which the substrate was dissolved, through the
column.

Preferably, following step (b), a purification step is
15   conducted, in which the product of the reaction between the
polymer supported phosphazene base having [^{18}F] fluoride trapped
thereon and the substrate solution is contacted with a solid
phase adsorbent. The solid phase adsorbent may conveniently be
provided in a column or cartridge, in a known manner.

20   Suitably, following step (b), the polymer supported
phosphazene base can be cleaned for re-use by contact with an
organic solvent, preferably the same solvent as that in which
the substrate was dissolved, and optionally also by heating the
polymer supported phosphazene base and solvent to a temperature
25   of from 50 °C to 120 °C.

Suitably, more than one iteration of the steps (a) and
(b), and, if desired, of one or more of the optional steps
described above, may be carried out.

157

-9-

In a second aspect, the present invention provides a method of preparation of a radiotracer for administration to a patient, comprising the radiofluorination method according to the first aspect of the invention, followed by a step of

5   formulation of the product of step (b) for administration to the patient. Suitably, the formulation step comprises removal of the solvent from the product of step (b), which product may optionally have been purified as described in the first aspect of the invention, dissolution of the product in saline solution,

10   and filtration of the saline solution through a sterile filter.

In a third aspect, the present invention provides an apparatus for conducting radiofluorination reactions, such as those according to the first aspect of the invention, comprising a polymer supported phosphazene base selected from a phosphazene
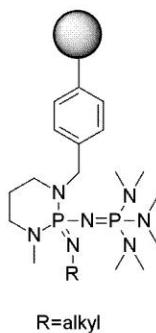
R=alkyl

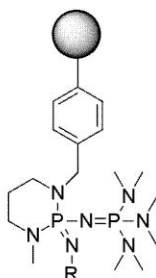15   of the general formula   supported on polystyrene (P_{PS}-P_2^R), and a phosphazene of the formula
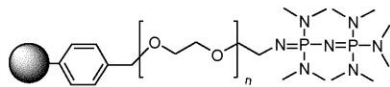
supported on PEG-coated polystyrene (P_{PS-PEG}-P_2^{Bz}) contained in a column.

-10-

Preferably, where the polymer supported phosphazene base


R=alkyl

is of the formula   supported on PEG-coated
polystyrene, R is selected from the group consisting of methyl,
ethyl, propyl, butyl, isopropyl, isobutyl, tert-butyl, pentyl,
5   isopentyl, tert-pentyl, tert-octyl, and more preferably is
selected from the group consisting of ethyl, tert-butyl and
tert-octyl.

        Preferably, the polymer supported phosphazene base is
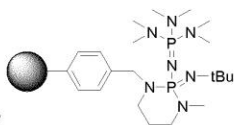
selected from $P_{PS}\text{-}P_2^{tBu}$ (   ) and $P_{PS\text{-}PEG}\text{-}P_2^{Bz}$

10   (   ).
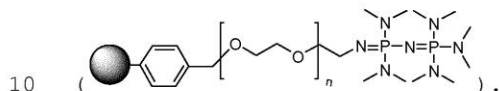
        Preferably, the apparatus further comprises one or more
elements selected from: means, such as tubing, for connection of
the column to other apparatus, such as a cyclotron, vessels
containing solvents, substrate solutions, aqueous solutions of
15   $^{18}F^-$; means, such as tubing, for connection of the column to a
gas line; one or more vessels for supply of solvent, substrate
solution, aqueous solution of $^{18}F^-$ to the column, and for the
collection of waste from the column; a second column containing
solid phase adsorbent for purification of the product of the

-11-

radiofluorination reaction; sealing means for isolating the
column prior to disposal.

Preferably, the column is for use in production of
radiotracers, such as those according to the second aspect of
5   the invention.

In a fourth aspect, the present invention provides the use
of a column according to the third aspect of the invention in
conducting radiofluorination reactions, such as those according
to the first aspect of the invention.

10   Preferably, the use is in the production of radiotracers,
such as those according to the second aspect of the invention.

In a fifth aspect, the present invention provides an
apparatus for production of a dose of a radiotracer for
administration to a patient, which apparatus comprises:
15   (a) a cyclotron;
(b) a radiosynthesis module, comprising a column according to
the third aspect of the invention; and
(c) a formulation module.

Preferably, the apparatus is shielded to prevent exposure
20   of an operator to radiation. Preferably, the apparatus is
arranged such that it can be operated remotely.

Preferably, the cyclotron can operate at 7.8 MeV and is
able to produce ^{18}F, ^{13}N and ^{11}C isotopes. However, any known
cyclotron able to produce ^{18}F may suitably be used.

25   Preferably, the radiosynthesis module further comprises
one or more of: a heating element, a gas supply, syringe pumps,
valve systems for control of the supply of gases and solutions
to the column, and a second column containing solid phase
adsorbent.

30   Preferably, the formulation module comprises [apparatus
for evaporation of solvent], such as a heating element and a

-12-

supply of inert gas, provided in order that the solution can be heated under a flow of the inert gas; a vessel containing saline solution, [means for introducing the saline solution to the radiotracer], and a sterile filter.

5   Suitably, the apparatus further comprises a quality control module, which suitably comprises a radio-HPLC, a gas chromatograph, and a pH meter.

It is envisaged that preferred features described for one aspect of the invention may be combined with any other aspect of 10 the invention.

Brief Description of the Figures

Figure 1 shows a schematic representation of a dose-on-demand radiofluorination apparatus;

15   Figure 2 shows the apparatus for on-column $^{18}F^-$ recovery and radiofluorination;

Figure 3 shows a conceptual representation of on-column $^{18}F^-$ recovery and radiofluorination.

20   Detailed Description

Referring to Figure 1, the dose-on-demand instrument 10 is a self-shielded, remotely operated instrument consisting of

(1)   a compact cyclotron 20 operating at 7.8 MeV and able to produce 18F, 13N, and 11C radioisotopes,

25   (2)   a radiosynthesis module 30, connected to the compact cyclotron and consisting of heating elements, gas line, syringe pumps, and a disposable radiochemical cartridge,

(3)   A formulation module 40,

-13-

(4)   A quality control module 50.

Referring to Figure 2, the apparatus (100), ie the radiochemical cartridge included in the radiosynthesis module 30 of the dose-on-demand instrument 10, comprises the following
5   elements: the column (110), which performs [^{18}F]fluoride trapping and on-column radiofluorination, an optional solid phase extraction cartridge (120) for product purification, vessels to hold the substrate (130), [^{18}O]water (target water) (140), solvents (150), waste (160), waste [^{18}O] water (170) and the
10   product (180), and the gas line (190+195). These elements are interconnected by tubing (arrows) and valves (135, 175, 185).

The column (110) can be made of glass, such as borosilicate glass, or plastic, such as PTFE. The column is packed with appropriate polymer supported phosphazene base
15   (113). Unreactive fillers, such as glass beads (111) and/or glass wool (112) can be optionally added to minimize the dead volume of the column.
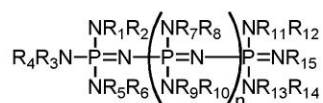
The said polymer supported phosphazene base (113) comprises a phosphazene base residue covalently bound to a solid
20   phase support, which is insoluble in any solvents to be used in the process. Examples of suitable polymer support include, but are not limited to, polymers such as polyethylene, polystyrene, poly(ethylene terephthalate), polycaprolactam, poly(p-phenylene), polybenzimidazole, polyimide, poly(phenylene oxide),
25   polyfluoroethylene, or any co-polymers or polyethylene glycol (PEG) derivatives of these. These polymers may be block grafted, and/or crosslinked with crosslinking agents, such as ethylene glycol diacrylate, N,N'-methylenebisacrylamide, divinylbenzene or any combination of these. The said polymer support may also
30   comprise glass or silicon coated with such a polymer. Furthermore, said polymer support may also be in the form of small discrete particles such as beads, or as a coating on the inner surface of a cartridge or on a microfabricated vessel.

-14-

A general structure for phosphazene bases is given below. The phosphazene residue can be optionally substituted with alkyl, aryl, benzyl or PEG groups, and/or any fluorinated derivatives thereof. The R_1-R_{15} groups can be a part of the same
5   polymer or can be linked to the same or different polymers.

$$R_4R_3N-P=N\left(\begin{array}{c}NR_1R_2\\ \\NR_5R_6\end{array}\right.\left.\begin{array}{c}NR_7R_8\\ \\P=N\\ \\NR_9R_{10}\end{array}\right)_n\left.\begin{array}{c}NR_{11}R_{12}\\ \\P=NR_{15}\\ \\NR_{13}R_{14}\end{array}\right.$$

The polymer supported phosphazene base residue used in the present invention comprises a phosphazene with two or more
10   phosphazene units (n≥0).

The inventors have found that attempting fluoride trapping and subsequent fluorination of a substrate with a number of different polymer and glass supported bases occurs in good yield only with P_{PS}-P_2^{tBu} and P_{PS-PEG}-P_2^{Bz}. Compounds such as P_{PS}-$P_2^{Et^+}Cl^-$
15   and P_{PS}-P_2^{Bz} are able to trap $^{18}F^-$, but are then unreactive towards the fluorination substrate. Bases such as diisopropylaminomethylbenzene supported on polystyrene, P-BEMP and G-P_2^{Bz} were found to be unreactive towards trapping of $^{18}F^-$ from aqueous solution. These results differ from those that
20   might be expected from the prior art: for example, BEMP is disclosed by Lemaire et al to trap and elute $^{18}F^-$ from aqueous solution; and P_2^{Et} and P_2^{tBu} hydrofluorides are taught to have similar reactivity towards fluorination reactions in solution. It is clear that the solid support has a significant effect on
25   the reactivity of the supported base, as can be seen from the difference in reactivity between glass-supported (G-) P_2^{Bz}, polystyrene-supported (P_{PS}-) P_2^{Bz} and the same base supported on PEG-coated polystyrene (P_{PS-PEG}-P_2^{Bz}). These results are not predictable based on the teachings of the prior art.

-15-

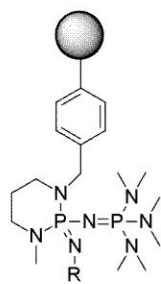It is expected that polymer supported phosphazene bases having a structure closely related to P_{PS}-$P_2{}^{tBu}$ will also be useful in the present invention, as it is taught in Schwesinger et al that phosphazene bases of the following general formula
5   have similar reactivity:

R=alkyl

In use, the cartridge is unsealed and inserted into the radiosynthesis module 30 of the dose on demand apparatus 10. It is then prepared for use by connecting its parts to the valves
10   135, 175, and 185, hosted by the dose on demand instrument. The connections use standard fittings, Luer locks and flanged PTFE tubing used in modern HPLC systems. The tubing is 1/16" (1.59 mm) in diameter for liquid transfer and 1/8" (3.18 mm) for gas transfer. The vessels 130, 140, 150, 160, 170 and 180 for
15   reagents, solvents, starting materials and products are regular 10-100 mL vials made of borosilicate glass and fitted with rubber septa. These are connected to the valves 135, 175 and 185 via flanged tubing fitted with regular needles. The purification cartridge or cartridges 120 can be chosen from any commercially
20   available solid phase extraction (SPE) cartridges based on silica, alumina, C18 or molecularly imprinted polymers and available from commercial vendors, such as Waters, Supelco, and Polyintell. A solution of substrate is loaded into vessel 130,

-16-

and solvent into vessel 150. Gas line 195 is connected to a
suitable gas supply. The aqueous solution of $^{18}F^-$ is then
transferred from the cyclotron 20 in which it has been prepared
in a known manner, and is introduced into the appropriate vessel
5   140. As shown in step 220 of Figure 3, valves 135 and 175 are
then opened to allow the aqueous solution of [^{18}F]fluoride to
flow to the said column 110, containing phosphazene base bound
to polymer support. The aqueous solution of $^{18}F^-$ can be allowed
to flow through the column 110 at various flow rates, or
10   alternatively, left on the column for a period of time enough to
ensure sufficient absorption of [^{18}F]fluoride on to the
phosphazene base.

     As shown in step 240 of Figure 3, the residual water can
then be removed from the column by a single-time or repeated
15   rinsing of the column with dry organic solvent miscible with
water, such as acetonitrile, THF, DMF or acetone, by opening
valve 135 such that solvent can flow from vessel 150 and opening
valve 175 such that the residual water can pass to waste vessel
170.

20   Further drying can be achieved by passing a flow of dry
gas, such as air, nitrogen, argon or helium through the column.
This can be achieved by opening valve 135 to permit gas flow
from gas line 195 to the column, and opening valve 175 to permit
gas flow from the column to pass to the gas exit line 190.

25   Once the column has been satisfactorily dried, valve 135
is opened to permit flow of the substrate solution from vessel
130 to the column. This is shown at step 250 of Figure 3. The
solution of substrate is then passed through the column at a
suitable flow rate by opening valve 175 to permit the solution
30   to flow from the column 110 towards the product vessel 180, or
alternatively, left on the column for a period of time
previously determined to be enough to ensure a sufficient degree
of substitution of the leaving group in the substrate by the

-17-

[^{18}F]fluoride , by closing valve 175 once the desired quantity of substrate solution has entered column 110. This reaction can be further assisted by heating the column to 50-120 $^{\circ}$C. The reaction step is shown at step 260 of Figure 3.

5   Prior to permitting flow of the substrate the column containing phosphazene base bound to polymer support may be optionally treated with an organic solvent to allow for swelling of the resin. This can be achieved by opening valve 135 so as to permit flow of solvent from vessel 150 to the column, and
10   opening valve 175 to permit solvent leaving the column to pass to waste vessel 160.

       A suitably substituted substrate is an aliphatic or aromatic compound comprising a leaving group. This leaving group may comprise, but is not limited to, fluorosulfate,
15   perfluoroalkanesulfonates, such as triflate or nonaflate, alkane sulfonates, such as mesylate or tresylate, arenesulfonates, such as benzenesulfonate, tosylate, brosylate, nosylate, and trinosylate, the derivatives of alkyl and perfluoroalkyl esters, such as acetate and trifluoroacetate, the derivatives of arene
20   esters, such as benzoate and p-nitrobenzoate, the derivatives of phosphate, sulphate and nitrate esters, alkyl or aryldiazonium salts, ammonium, tetralkylammonium and pyridinium salts, the derivatives of ethers and thioethers, such as phenolates, nitrophenolates, and thiophenolates, diiodoaryliodonium salts,
25   nitro groups and halogens other than fluoride.

       The substrate can be dissolved in a suitable organic solvent, such as toluene, acetonitrile, dichloromethane, or DMF before applying to the column.

       After the reaction is taken to the desired degree of
30   conversion, the reaction mixture is pushed from the column with a new portion of solvent, as shown in step 270 of Figure 3. This is achieved by opening the valve 135 to allow solvent to

-18-

flow from vessel 150 to column 110, and opening valve 175 to allow the solution on the column to flow towards solid phase purification cartridge 120. The cartridge 120 contains a solid phase suitable to adsorb any side products, starting material

5   and other contaminants from the solution obtained from the column that must be removed prior to administration of the radiofluorinated product to a patient. The radiofluorinated product is eluted from cartridge 120 by continuing to pass solvent from vessel 150 through the system, and valve 185 is

10   opened to permit flow of the product solution to product vessel 180. When contaminants are eluted from the cartridge 120, valve 185 is opened to permit flow of the eluted solution to waste vessel 160.

     The purified product is then transferred to the
15   formulation module where the organic solvent is evaporated, suitably by heating the solution and flowing an inert gas over it, and the product is dissolved in a saline solution and filtered through a sterile filter. The saline solution of the product is then passed to the quality control module, where it

20   is analysed to determine that it is in a suitable condition to be administered to a patient, by analysis by radio-HPLC, gas chromatography and a pH meter.

     The column can be optionally cleaned in between the doses by opening the valves 150 and 175 and allowing the solvent from

25   vial 150 to flow towards waste vessel 160. The column 110 can be heated to 50 – 120 °C to assist desorption of impurities from the column. The column is then dried with a stream of gas.

     Once the apparatus has been used for the preparation of the desired number of doses of radiotracer, the disposable

30   cartridge, consisting of the column and all the vessels and tubing described above are sealed and disconnected from the dose-on-demand apparatus 10 and are disposed of in a suitable manner.

-19-

<u>Examples</u>

Materials and Equipment

All solvents and reagents were purchased from Aldrich.
Unless otherwise noted, diethyl ether, THF and toluene were
5   distilled from sodium benzophenone; acetonitrile,
dichloromethane, DMF, HMPA, tetramethylurea and mesitylene were
dried over activated molecular sieves (220 °C, 0.1 mbar, 4
hours) for at least 48 hours prior to use; hexane was used as
received. Phosphazene base P_2^{Et}, phosphazene base P_2-^tBu on
10   polystyrene, polymer bound BEMP and diisopropylaminomethyl
benzene supported on polystyrene were obtained from Aldrich.

The columns were prepared using PTFE tubing (OD 0.25 inch
(0.64 cm)) purchased from Aldrich. The glass beads (212-300
µm), used as neutral filler, were also purchased from Aldrich.
15   All radiochemical yields were decay corrected. ^{18}F aqueous
solutions were prepared by a $^{18}O(p,n)^{18}F$ reaction in a GE
PETtrace cyclotron using a 2.5 ml target of 95-98% enriched ^{18}O
water irradiated by a 16.5 MeV proton beam at 55 µA for 60-90
min. RadioTLC was performed using Raytest MiniGita TLC-scanner.
20   Column preparation

Polymer-P_2^tBu (100 mg, P_2^tBu loading 1.6 mmol/g resin) was
mixed with glass beads (1200 mg) and packed in a PTFE tube.

Example 1: $^{18}F^-$ trapping and radiofluorination of an
aliphatic mesylate
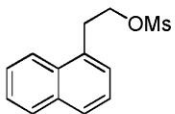
25
$^{18}F^-$ trapping: $^{18}F^-$ (target water, 1.0 ml, 105 MBq) was mixed
with water (3 ml) and passed through the column. MeCN (dry, 5
ml) was passed through the column at room temperature followed
by MeCN (dry, 5 ml) by syringe pump (flow 30 ml/h, duration 10

-20-

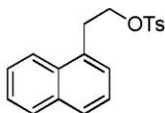min) while heating the column at 60 °C. Argon gas was flushed
through the column while heating at 60 °C until excess of
solvent was removed. The $^{18}F^-$ trapping was 98%.

5   Radiofluorination: 1-(2-(methylsulfonyl)ethyl)naphthalene
(56.0 mg, 224 μmol) was dissolved in toluene (dry, 5 ml) and
passed through the column by syringe pump (flow 10 ml/h,
duration 30 min) while heating at 90 °C. Toluene (dry, 5 ml)
was passed through the column by syringe pump (flow 20 ml/h,
duration 15 min) while heating at 90 °C to elute the remaining
10   product. The fluorinated product was analyzed by radio-TLC
(eluent heptane:EtOAc 80:20). Radiochemical yield was 66% and
radiochemical purity was 98%.

       Example 2: $^{18}F^-$ trapping and radiofluorination of an
aliphatic tosylate

15

       $^{18}F^-$ trapping: $^{18}F^-$ (fraction of target water, 1.0 ml, 311
MBq) was added to the column followed by water (5 ml). MeCN
(dry, 5 ml) was passed through the column at room temperature
followed by MeCN (dry, 5 ml) by syringe pump (flow 30 ml/h,
20   duration 10 min) while heating the column at 60 °C. Argon gas
was flushed through the column while heating at 60 °C until
excess of solvent was removed. The $^{18}F^-$ trapping was 95%.

       Radiofluorination: 1-(2-tosylethyl)naphthalene (68.0 mg,
208 μmol) was dissolved in toluene (dry, 5 ml) and passed
25   through the column by syringe pump (flow 10 ml/h, duration 30
min) while heating at 90 °C. Toluene (dry, 5 ml) was passed
through the column by syringe pump (flow 20 ml/h, duration 15
min) while heating at 90 °C to elute the remaining product. The
fluorinated product was analyzed by radio-TLC (eluent

-21-

heptane:EtOAc 80:20). Radiochemical yield was 64% and
radiochemical purity was 92%.

Example 3: $^{18}F^-$ trapping and radiofluorination of an
aliphatic triflate (mannose triflate, FDG precursor)

5
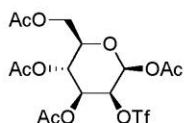
$^{18}F^-$ trapping: $^{18}F^-$ (target water, 1.5 ml, 460 MBq) was mixed
with water (2 ml) and passed through the column. MeCN (dry, 2
ml) was passed through the column at room temperature followed
by MeCN (dry, 8 ml) while heating the column at 60 °C. Argon gas

10 was flushed through the column while heating at 60 °C until
excess of solvent was removed. The $^{18}F^-$ trapping was 84%.

Radiofluorination: Mannose triflate (50 mg, 100 μmol) was
dissolved in toluene (dry, 4 ml) and passed through the column
by syringe pump (flow 8 ml/h, duration 30 min) while heating at

15 90 °C. Toluene (dry, 2 ml) was passed through the column by
syringe pump (flow 10 ml/h, duration 12 min) while heating at 90
°C to elute the remaining product. The fluorinated product was
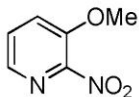analyzed by radio-TLC (eluent benzene:MeCN 2:1). Radiochemical
yield was 25% and radiochemical purity of acetylated ^{18}F FDG was

20 76%.

Example 4: $^{18}F^-$ trapping and radiofluorination of a
nitrated aromatic compound

$^{18}F^-$ trapping: $^{18}F^-$ (target water, 0.5 ml, 201 MBq) was added

25 to the column followed by water (5 ml). MeCN (dry, 5 ml) was
passed through the column at room temperature followed by MeCN
(dry, 5 ml) by syringe pump (flow 30 ml/h, duration 10 min)

-22-

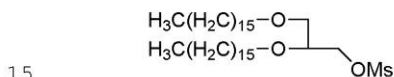while heating the column at 60 °C. Argon gas was flushed through
the column while heating at 60 °C until excess of solvent was
removed. The ^{18}F$^-$ trapping was 98%.

5   Radiofluorination: 3-methoxy-2-nitropyridine (63.0 mg, 408
μmol) was dissolved in toluene (dry, 5 ml) and passed through
the column by syringe pump (flow 10 ml/h, duration 30 min) while
heating at 90 °C. Toluene (dry, 5 ml) was passed through the
column by syringe pump (flow 20 ml/h, duration 15 min) while
heating at 90 °C to elute the remaining product. The
10   fluorinated product was analyzed by radio-TLC (eluent petroleum
ether:EtOAc 3:1). Radiochemical yield was 14% and radiochemical
purity was 45%.

Example 5: ^{18}F$^-$ trapping and radiofluorination of a
lipophilic aliphatic mesylate

15

^{18}F$^-$ trapping: ^{18}F$^-$ (target water, 1.2 ml, 752 MBq) was mixed
with water (5 ml) and passed through the column using a syringe
pump (flow 20 ml/h, duration 9 min). MeCN (dry, 5 ml) was
passed through the column at room temperature followed by
20   another portion of MeCN (dry, 5 ml) by syringe pump (flow 30
ml/h, duration 10 min) while heating the column at 60 °C. Argon
gas was flushed through the column while heating at 60 °C until
excess of solvent was removed. The ^{18}F$^-$ trapping was 92%.

Radiofluorination: 2,3-bis(hexadecyloxy)propyl
25   methanesulfonate (MsDHG, 63 mg, 101 μmol) was dissolved in
toluene (dry, 5 ml) and passed through the column by syringe
pump (flow 10 ml/h, duration 30 min) while heating at 90 °C.
Toluene (dry, 5 ml) was passed through the column by syringe
pump (flow 20 ml/h, duration 15 min) while heating at 90 °C to
30   elute the remaining product. The fluorinated product was

171

-23-

analyzed by radio-TLC (eluent heptane:EtOAc 95:5).
Radiochemical yield was 1% and radiochemical purity was 5%.

Example 6: $^{18}F^-$ trapping and radiofluorination of an
aliphatic bromide

5
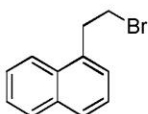
$^{18}F^-$ trapping: $^{18}F^-$ (target water, 0.5 ml, 721 MBq) was mixed
with water (4.5 ml) and passed through the column at room
temperature by syringe pump (flow 20 ml/h, duration 15 min).
MeCN (dry, 5 ml) was passed through the column at 60 °C followed
10 by another portion of MeCN (dry, 5 ml) by syringe pump (flow 20
ml/h, duration 15 min) while heating the column at 60 °C. Argon
gas was flushed through the column while heating at 60 °C until
excess of solvent was removed. The $^{18}F^-$ trapping was 94%.

Radiofluorination: NpEtBr (47.73 mg, 203 μmol) was
15 dissolved in toluene (dry, 5 ml) and passed through the column
by syringe pump (flow 10 ml/h, duration 30 min) while heating at
90 °C. Toluene (dry, 2 ml) was passed through the column by
syringe pump (flow 20 ml/h, duration 6 min) while heating at 90
°C to elute the remaining product. The fluorinated product was
20 analyzed by radio-TLC (eluent heptane:EtOAc 80:20).
Radiochemical yield was 16% and radiochemical purity was 61%.

Example 7: Investigation of polymer supported bases in on-
column $^{18}F^-$ trapping and radiofluorination

General procedure:
25 A borosilicate glass tube (OD 0.6 mm, length 12 cm) was
packed with the polymer-supported base (100 μmol base) mixed
with glass beads (212-300 μm, 100-500 mg) and placed in a column
oven in a LabView controlled automation apparatus.

-24-

$^{18}F^-$ trapping: $^{18}F^-$ (target water, 3.5 mL, 500-5000 MBq) passed through the column at room temperature (flow 1.5 mL/min). MeCN (dry, 4 ml, flow 2 mL/min) was passed through the column at room temperature followed by a helium gas flush through the

5   column until excess of solvent was removed.

Radiofluorination: Toluene (dry, 4 mL, flow 2 mL/min) was passed through the column at room temperature followed by 1-naphthaleneethyl methanesulfonate (100 µmol, 25.03 mg) dissolved in toluene (dry, 3 mL) and passed through the column at 120°C

10   (flow 0.55 mL/min). Toluene (dry, 2 mL, flow 0.55 mL/min) was then passed through the column to elute the remaining product. The fluorinated product was analyzed by radio-TLC (eluent heptane:EtOAc 80:20)

15   Synthesis of polymer supported bases:

Polymer-supported P_2^{tBu} (1.6 mmol/g loading), BEMP (2.3 mmol/g loading) and diisopropylaminomethyl (3 mmol/g loading) were obtained from Sigma Aldrich. Amine-functionalized glass beads (30-50 micron, loading unknown) were obtained from

20   Polysciences Europe GmbH. Benzylamine-functionalized polystyrene (0.8-1.2 mmol/g loading), and Merrifield resin (0.8-1.4 mmol/g) were purchased from Bachem. The amine-functionalized polystyrene resin with polyethylene glycol (PEG, 1500-2000 Da) spacer (TentaGel HL, particle size 160 µm, 0.4 mmol/g loading) was

25   obtained from Rapp Polymere.

The amine-functionalized resins/glass beads were reacted with $P_2^{Cl}*BF_4$ (1-chloro-1,1,3,3,3-pentakis(dimethylamino)-$1\lambda^5$-diphosphazen-3-ium tetrafluoroborate) by mixing the support (200-1000 mg) with $P_2^{Cl}*BF_4$ (3 eq to amine) and Et_3N (dry, 9 eq to

30   amine) in DCM (dry, 5mL) in a glass vial, which was sealed under vacuum. The reaction mixture was then heated with slight agitation at 90°C for up to three days. This coupling procedure
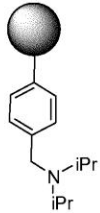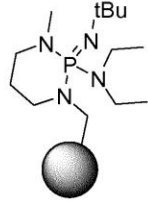
-25-

was repeated up to two times in order to ensure good coupling. The resulting resin was deprotonated by reacting the resin with a mixture of KOMe (1 eq to amine) in MeOH (dry, 5 mL) for one hour at room temperature in order to give the desired solid-supported phosphazene base.

Alkylation of the Merrifield resin was done by mixing Merrifield resin with P_2^{Et} (4 eq to chloride) in THF and shaking at room temperature for five days.

	Structure	Name	Chemical class	On-column $^{18}F^-$ trapping	On-column radio-fluorin-ation
1		Diisopropyl-aminomethyl benzene supported on polystyrene	Non-ionic strong organic base	0%	0%
2		P-BEMP (2-^{t}Butylimino-2-diethyl-amino-1,3-dimethyl-perhydro-1,3,2-diaza-phosphorine on polystyrene	Non-ionic phosphazene supported on propylene-diamine modified polystyrene	0%	0%

3		$P_{PS}\text{-}P_2^{Bz}$ (from benzylamine-functional-ized polystyrene)	Non-ionic phosphazene supported on polystyrene	50%	0%
4		$G\text{-}P_2^{Bz}$ (from amine-functionalized glass beads)	Non-ionic phosphazene supported on glass beads	0%	0%
5		$P_{PS}\text{-}P_2^{Et+}Cl^-$ (from Merrifield resin)	Ionic phosphazene supported on polystyrene	99%	Trace
6		$P_{PS}\text{-}P_2^{tBu}$ (Aldrich resin)	Non-ionic phosphazene supported on polystyrene	99%	Good
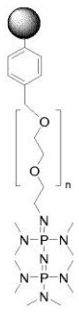
7		$P_{PS-PEG}-P_2^{Bz}$ (from PEG-coated polystyrene)	Non-ionic phosphazene supported on polystyrene	99%	Good

Table 1

Example 8: Investigation of radiofluorination of different substrates using polystyrene-supported P_2^{tBu}

General procedure:

5   A borosilicate glass tube (OD 0.6 mm, length 12 cm) was packed with PS-supported P_2^{tBu} (150 µmol base, loading 1.6 mmol/g, 93.75 mg) mixed with glass beads (212-300 µm, 100-500 mg) and placed in a column oven in a LabView controlled automation apparatus.

10      $^{18}F^-$ trapping: $^{18}F^-$ (target water, 3.5 mL, 500-5000 MBq) passed through the column at room temperature (flow 1.5 mL/min). MeCN (dry, 4 ml, flow 2 mL/min) was passed through the column at room temperature followed by a helium gas flush through the column until excess of solvent was removed.

15   Radiofluorination: Radiofluorination solvent (MeCN for mannose triflate, MeCN/tBuOH 1:5 for FLT-ONs, toluene for the naphthalene analogues and 2-nitro-3-methoxypyridine, dry, 4 mL, flow 2 mL/min) was passed through the column at room temperature followed by the substrate (50-100 µmol) dissolved in

20   radiofluorination solvent (dry, 3 mL) and passed through the column at 120°C (flow 0.55 mL/min). Radiofluorination solvent (dry, 2 mL, flow 0.55 mL/min) was then passed through the column to elute the remaining product. The fluorinated product was

-28-

analyzed by radio-TLC (eluent heptane:EtOAc 80:20 for the naphthalene analogues, MeCN:H_2O 95:5 for hydrolyzed FDG, DCM:MeOH 9:1 for hydrolyzed FLT, petroleum ether:EtOAc for the pyridine analogue).

5

Entry	Substrate	Product	Radiochemical Yield (%)
1	Mannose triflate	^{18}F FDG	40
2	FLT-ONs	^{18}F FLT	7
3	Naphthylethyl mesylate	^{18}F NpEtF	51
4	Naphthylethyl tosylate	^{18}F NpEtF	34
5	Naphthylethyl chloride	^{18}F NpEtF	16
6	Naphthylethyl bromide	^{18}F NpEtF	42
7	Naphthylethyl iodide	^{18}F NpEtF	18
8	2-nitro-3-methoxypyridine	^{18}F 2-fluoro-3-methoxypyridine	23

Table 2

Example 9: Investigation of radiofluorination of different substrates using $P_{PS-PEG}-P_2^{Bz}$

General procedure:

10   A borosilicate glass tube (OD 0.6 mm, length 12 cm) was packed with $P_{PS-PEG}-P_2^{Bz}$ (150 μmol base, loading 0.4 mmol/g, 375

-29-

mg) and placed in a column oven in a LabView controlled
automation apparatus.

$^{18}F^-$ trapping: $^{18}F^-$ (target water, 3.5 mL, 500-5000 MBq)
passed through the column at room temperature (flow 1.5 mL/min).
5   MeCN (dry, 2 ml, flow 2 mL/min) was passed through the column at
room temperature followed by MeCN (dry, 2 ml, flow 2 mL/min) at
50°C.

Radiofluorination: Radiofluorination solvent (MeCN for
mannose triflate, toluene for FLT-ONs, the naphthalene analogues
10   and 2-nitro-3-methoxypyridine, dry, 4 mL, flow 2 mL/min) was
passed through the column at 50°C followed by the substrate (50-
100 µmol) dissolved in radiofluorination solvent (dry, 3 mL) and
passed through the column at 120°C (85°C for mannose triflate,
flow 0.55 mL/min). Radiofluorination solvent (dry, 2 mL, flow
15   0.55 mL/min) was then passed through the column to elute the
remaining product. The fluorinated product was analyzed by
radio-TLC (eluent heptane:EtOAc 80:20 for the naphthalene
analogues, benzene:MeCN 2:1 for unhydrolyzed FDG, EtOH:EtOAc 1:1
for unhydrolyzed FLT, petroleum ether:EtOAc for the pyridine
20   analogue)

Entry	Substrate	Product	Radiochemical Yield (%)
1	Mannose triflate	^{18}F FDG	36
2	FLT-ONs	^{18}F FLT	5
3	Naphthylethyl mesylate	^{18}F NpEtF	38
4	Naphthylethyl tosylate	^{18}F NpEtF	24

-30-

Entry	Substrate	Product	Radiochemical Yield (%)
5	Naphthylethyl chloride	^{18}F NpEtF	Trace
6	Naphthylethyl bromide	^{18}F NpEtF	Trace
7	Naphthylethyl iodide	^{18}F NpEtF	Trace
8	2-nitro-3-methoxypyridine	^{18}F 2-fluoro-3-methoxypyridine	Trace

Table 3

Example 10: Investigation of reusability of the polystyrene-supported P_2^{tBu} radiofluorination approach

5   General procedure:

A borosilicate glass tube (OD 0.6 mm, length 12 cm) was packed with PS-supported P_2^{tBu} (100-140 µmol base, loading 1.6 mmol/g) mixed with glass beads (212-300 µm, 100-500 mg) and placed in a column oven in a LabView controlled automation

10   apparatus. Two columns, A and B, were prepared in this manner, and each was used for assessing reusability of the column.

^{18}F$^-$ trapping: ^{18}F$^-$ (target water, 3.5 mL, 500-5000 MBq) passed through the column at room temperature (flow 1.5 mL/min). MeCN (dry, 4 ml, flow 2 mL/min) was passed through the column at

15   room temperature followed by a helium gas flush through the column until excess of solvent was removed.

Radiofluorination: Toluene, dry, 4 mL, flow 2 mL/min) was passed through the column at room temperature followed by the

-31-

substrate (50 μmol) dissolved in toluene (dry, 3 mL) at 120°C
(flow 0.55 mL/min). Toluene (dry, 2 mL, flow 0.55 mL/min) was
then passed through the column to elute the remaining product.
The fluorinated product was analyzed by radio-TLC (eluent
5   heptane:EtOAc 80:20).

These procedures were repeated up to two times.

Exp. No.	Column	$\mathbf{P}$-P$_2^{tBu}$ μmol	Trapping %	RCP %	RCY %
First use	A	140	100	74	43
Second use	A	140	100	94	69
Third use	A	140	100	92	61
First use	B	100	98	80	46
Second use	B	100	100	89	62
Third use	B	100	100	93	64

Table 4
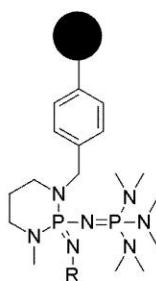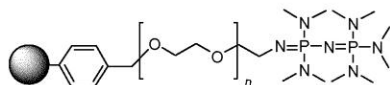
-32-

Claims

1. A method of conducting radiofluorination of a
substrate, comprising the steps of:

5   (a) contacting an aqueous solution of [^{18}F] fluoride with a
polymer supported phosphazene base selected from a phosphazene

R=alkyl

of the general formula   supported on
polystyrene (P_{PS}-P_2^{R}), and a phosphazene of the formula

                 supported on PEG-coated

10 polystyrene ($P_{PS\text{-}PEG}$-P_2^{Bz}), for sufficient time for trapping of
[^{18}F] fluoride on the polymer supported phosphazene base; and
(b) contacting a solution of the substrate with the polymer
supported phosphazene base having [^{18}F] fluoride trapped thereon
obtained in step (a) for sufficient time for a radiofluorination

15 reaction to take place.

2. The method according to claim 1, wherein the substrate
used in step (b) is an aliphatic or aromatic compound comprising
a leaving group.

3. The method according to claim 2, wherein the leaving

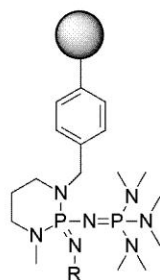20 group is selected from the group consisting of triflate,

-33-

nosylate, mesylate, tosylate, chloride, bromide, iodide and
nitro.

   4. The method according to claim 2 or claim 3, wherein the
compound comprising the leaving group is selected from
5   naphthylethyl compounds, mannose, optionally substituted
pyridine compounds and glycols.

   5. The method according to any preceding claim, wherein
the polymer supported phosphazene base is contained in a column.

   6. The method according to any preceding claim, wherein
10   the polymer supported phosphazene base is of the general formula

R=alkyl

            supported on polystyrene ($P_{PS}-P_2^R$), and R is
selected from the group consisting of methyl, ethyl, propyl,
butyl, isopropyl, isobutyl, tert-butyl, pentyl, isopentyl, tert-
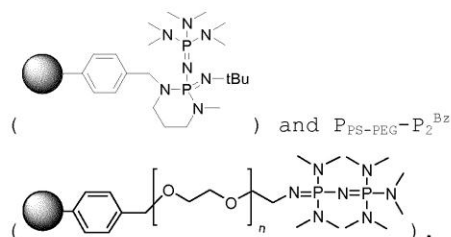pentyl, and tert-octyl.

15   7. The method according to claim 6, wherein R is selected
from the group consisting of ethyl, tert-butyl and tert-octyl.

   8. The method according to any preceding claim, wherein
the polymer supported phosphazene base is selected from $P_{PS}-P_2^{tBu}$

-34-

( ) and $P_{PS-PEG}-P_2^{Bz}$

( ).

9. The method according to any preceding claim, wherein step (b) comprises heating the polymer supported phosphazene base having [^{18}F] fluoride trapped thereon in contact with the substrate solution to a temperature of from 50 °C to 120 °C.

10. A method of preparation of a radiotracer for administration to a patient, comprising the radiofluorination method according to any one of claims 1-9, followed by a step of formulation of the product of step (b) for administration to the patient.

11. An apparatus for conducting radiofluorination reactions, comprising a polymer supported phosphazene base selected from a phosphazene of the general formula
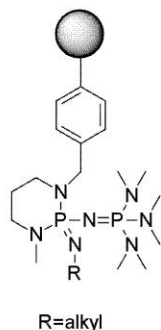
R=alkyl

supported on polystyrene ($P_{PS}-P_2^R$), and a

phosphazene of the formula

-35-

supported on PEG-coated polystyrene ($P_{PS\text{-}PEG}\text{-}P_2{}^{Bz}$) contained in a column.

    12. The apparatus of claim 11, wherein R is selected from the group consisting of methyl, ethyl, propyl, butyl, isopropyl, isobutyl, tert-butyl, pentyl, isopentyl, tert-pentyl, and tert-octyl.

    13. The apparatus of claim 12, wherein R is selected from the group consisting of ethyl, tert-butyl and tert-octyl.

    14. The apparatus of claim 11, wherein the polymer supported phosphazene base is selected from $P_{PS}\text{-}P_2{}^{tBu}$

( ) and $P_{PS\text{-}PEG}\text{-}P_2{}^{Bz}$

( ).
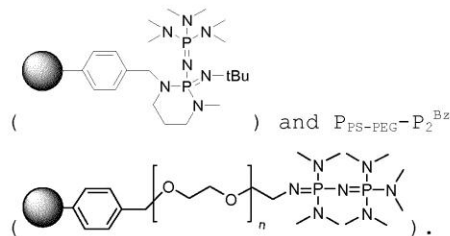
    15. Use of a column according to any one of claims 11 to 14 in conducting radiofluorination reactions.

    16. An apparatus for production of a dose of a radiotracer for administration to a patient, which apparatus comprises:
(a) a cyclotron;
(b) a radiosynthesis module, comprising a column according to and one of claims 11 to 14; and
(c) a formulation module.

1/3

Figure 1

Figure 2

Figure 3

INTERNATIONAL SEARCH REPORT

International application No
PCT/EP2013/066025

A. CLASSIFICATION OF SUBJECT MATTER
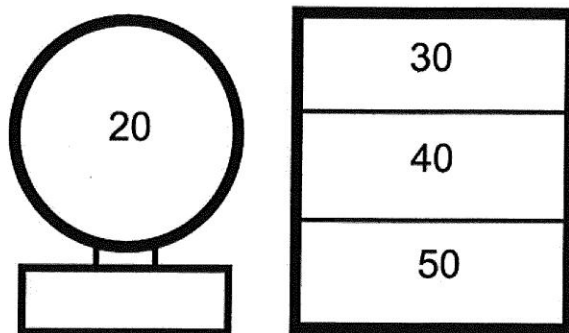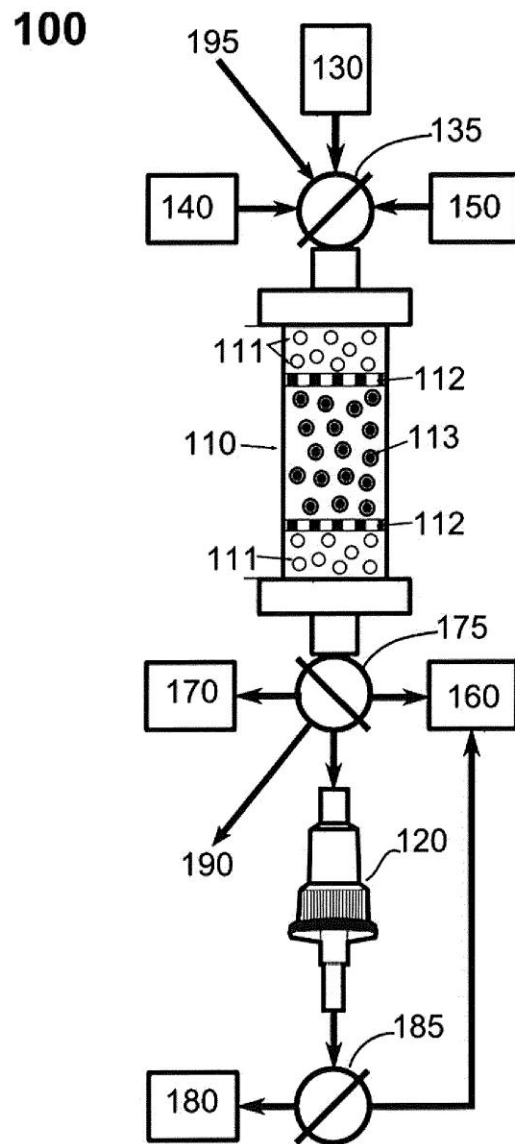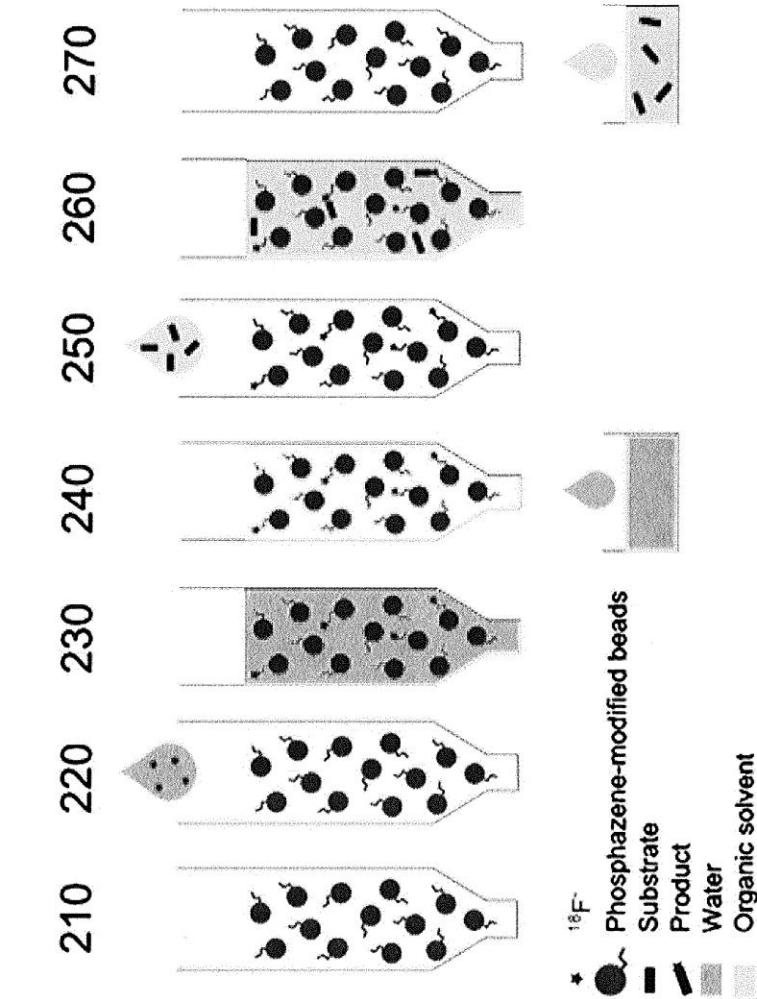
INV. C07B59/00   B01D15/36
ADD.

According to International Patent Classification (IPC) or to both national classification and IPC

B. FIELDS SEARCHED

Minimum documentation searched (classification system followed by classification symbols)

C07B B01D

Documentation searched other than minimum documentation to the extent that such documents are included in the fields searched

Electronic data base consulted during the international search (name of data base and, where practicable, search terms used)

EPO-Internal, CHEM ABS Data, WPI Data

C. DOCUMENTS CONSIDERED TO BE RELEVANT

Category*	Citation of document, with indication, where appropriate, of the relevant passages	Relevant to claim No.
A	WO 2009/003251 A1 (TRASIS S A [BE]; UNIV LIEGE [BE]; LEMAIRE CHRISTIAN [BE]; VOCCIA SAMUE) 8 January 2009 (2009-01-08) the whole document -----	1-16

☐ Further documents are listed in the continuation of Box C.   ☒ See patent family annex.

```
*  Special categories of cited documents :

"A"  document defining the general state of the art which is not considered
     to be of particular relevance
"E"  earlier application or patent but published on or after the international
     filing date
"L"  document which may throw doubts on priority claim(s) or which is
     cited to establish the publication date of another citation or other
     special reason (as specified)
"O"  document referring to an oral disclosure, use, exhibition or other
     means
"P"  document published prior to the international filing date but later than
     the priority date claimed
```

```
"T"  later document published after the international filing date or priority
     date and not in conflict with the application but cited to understand
     the principle or theory underlying the invention
"X"  document of particular relevance; the claimed invention cannot be
     considered novel or cannot be considered to involve an inventive
     step when the document is taken alone
"Y"  document of particular relevance; the claimed invention cannot be
     considered to involve an inventive step when the document is
     combined with one or more other such documents, such combination
     being obvious to a person skilled in the art
"&"  document member of the same patent family
```

Date of the actual completion of the international search	Date of mailing of the international search report
3 October 2013	17/10/2013

Name and mailing address of the ISA/	Authorized officer
European Patent Office, P.B. 5818 Patentlaan 2 NL - 2280 HV Rijswijk Tel. (+31-70) 340-2040, Fax: (+31-70) 340-3016	Diederen, Jeroen

1

Form PCT/ISA/210 (second sheet) (April 2005)

INTERNATIONAL SEARCH REPORT

Information on patent family members

International application No
PCT/EP2013/066025

Patent document cited in search report	Publication date	Patent family member(s)		Publication date
WO 2009003251 A1	08-01-2009	CN	101687120 A	31-03-2010
		EP	2062630 A1	27-05-2009
		EP	2164590 A1	24-03-2010
		US	2010196254 A1	05-08-2010
		WO	2009003251 A1	08-01-2009

Form PCT/ISA/210 (patent family annex) (April 2005)

Appendix 2 - LabView radiofluorination programs
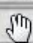
Program for the radiofluorination of model substrates

Message	Vol (ml)	Valve p.u.	Valve disp	Speed p.u.	Speed disp
Initialize	0	1	1	0	0
Prime fluoride syringe	1	6	6	2000	20000
Fluoride	3	6	3	20000	5000
Water	2	4	3	20000	5000
Air push fluoride	3	5	3	20000	20000
Air push He push	3	5	6	20000	20000
Prime MeCN syringe	2	4	1	20000	20000
MeCN	1	4	3	20000	5000
MeCN 50 degree	5	4	3	20000	1000
Dry	0	1	1	0	0
Prime fluorination solvent syringe	2	5	1	20000	20000
Fluorination solvent	1	5	3	20000	5000
Fluorination solvent 120 degree	5	5	3	20000	1000
Prime fluorination syringe	0	6	6	20000	20000
Fluorination 1	0	6	3	20000	550
fluorination 2	0	6	3	550	550
Fluorination 3	0	6	3	550	550
fluorination 4	0	6	3	550	550
Fluorination 5	0	6	3	550	550
Fluorination 6	0	6	3	550	550
Elution	2	5	3	20000	550
He push	0	1	1	0	0

Program for radiofluorination and hydrolysis of mannose triflate ($[^{18}F]$FDG synthesis)

Message	Vol (mul)	Valve p.u.	Valve disp	Speed p.u.	Speed disp
Initialize	0	1	1	0	0
Prime fluoride syringe	1000	4	4	25000000	25000000
Fluoride trapping	3000	4	6	25000000	550000
Air push	1000	2	6	30000000	550000
Air push fluoride vial	500	2	4	25000000	25000000
Prime MeCN syringe	2000	8	1	25000000	25000000
Column wash MeCN	4000	8	6	25000000	2000000
Dry	0	1	1	0	0
Prime fluorination solvent syringe	2000	7	1	25000000	25000000
Heating column oven	0	1	1	0	0
Fluorination solvent	2000	7	6	25000000	1000000
Fluorination 1	500	5	6	550000	550000
Fluorination 2	500	5	6	550000	550000
Fluorination 3	500	5	6	550000	550000
Fluorination 4	500	5	6	550000	550000
Fluorination 5	500	5	6	550000	550000
Fluorination 6	500	5	6	550000	550000
Elution column	1500	7	6	1500000	550000
He push	0	1	1	0	0
Precond C18 EtOH	5000	6	4	30000000	5000000
Wait	0	1	1	0	0
Prime water syringe	5000	5	2	30000000	30000000
Precond C18 water	5000	5	4	30000000	20000000
Trapping product	50000	1	4	30000000	20000000
Wash product vial	5000	5	1	30000000	30000000
Trap product wash	5000	1	4	30000000	20000000
Air push	5000	1	4	30000000	20000000
Prime NaOH syringe	400	3	2	30000000	30000000
Hydrolysis	500	3	4	30000000	20000000
Wait	0	1	1	0	0
Prime water syringe	5000	5	2	30000000	30000000
Elution product	8000	5	4	30000000	20000000
Air push	10000	2	4	30000000	20000000
Finish	0	1	1	0	0

Program for fluoride trapping followed by K222 elution, azeotropic evaporation and solution-phase radiofluorination of either a model substrate or mannose triflate. This program was used to develop a functioning sequence for the on-column labeling followed by solution-phase labeling described in Article IV.

Message	Vol (ml)	Valve p.u.	Valve disp	Speed p.u.	Speed disp
Initialize	0	1		0	0
Prime fluoride syringe	1	6	6	20000	20000
Fluoride	3	6	3	20000	5000
Water	2	4	3	20000	5000
Air push fluoride	3	5	3	20000	20000
Air push He push	3	5	6	20000	20000
Kryptofix	1	2	3	20000	1000
Air push	2	5	3	20000	1000
Prime MeCN syringe	2	4	1	20000	20000
MeCN 1	1	4	3	20000	1000
He push evap 1	0	1	1	0	0
MeCN 2	0	4	3	20000	1000
Evap 2	0	1	1	0	0
MeCN 2	0	4	3	20000	1000
Evap 3	0	1	1	0	0
He Prime mesylate syringe	0	6	6	20000	20000
Add mesylate	2	6	7	20000	20000
Air push	2	2	7	20000	20000
Fluorination	0	1	1	0	0
Cooling	0	1	1	0	0
Finish	0	1	1	0	0